

**Paleoclimatology of Upper Triassic  
Playa Cycles:  
New Insights Into an  
Orbital Controlled Monsoon System  
(Norian, German Basin)**

Inaugural-Dissertation

Zur

Erlangung des Doktorgrades

der Mathematisch-Naturwissenschaftlichen Fakultät

der Universität zu Köln

vorgelegt von

**Thorsten Vollmer**

aus Leichlingen

Universität Köln  
2005

## **Vollmer, Thorsten**

Paleoclimatology of Upper Triassic Playa Cycles:  
New Insights Into an Orbital Controlled Monsoon System  
(Norian, German Basin)

Dissertation an der Mathematisch-Naturwissenschaftlichen  
Fakultät der Universität zu Köln.

Berichterstatter: Prof. Dr. Werner Ricken  
Prof. Dr. Klaus Krumsiek

Tag der mündlichen Prüfung: 07. Dez. 2005

Pour Caroline et Annabel

Don't Hurry: Enjoy the Present Moment (Thich Nhat Hanh)

---

## Table of Content

<b>Kurzfassung</b>	<b>1</b>
<b>Abstract</b>	<b>2</b>
<b>1 Introduction</b>	<b>3</b>
1.1 Goals and Perspectives of the Project	3
1.1.1 Goals	4
1.2 Geological Overview	5
1.2.1 Paleogeography	7
1.2.2 Tectonic Evolution	8
1.3 Stratigraphy	12
1.4 Paleoclimatology	14
<b>2 Methods</b>	<b>17</b>
2.1 Sampling Strategy	17
2.2 Geochemical and Geophysical Methods	17
2.3 Frequency Analysis	23
2.4 Milankovitch Theory	24
<b>3 Playa Facies</b>	<b>26</b>
3.1 Introduction	26
3.1.1 Definition and Setting of Playa Systems	26
3.1.2 Classification and Evolution of Playa Systems	27
3.1.3 Depositional Environments	30
3.2 Clay Mineralogy	32
3.3 Stratified Lake Facies	39
3.4 Dolomite Beds	42
3.5 Gypsum Facies	48
3.6 Red Mudstone Facies	50
3.7 Dolocrête Facies	57
3.8 Erosional Channels and Sandstones	61
3.9 The Steinmergel Keuper Facies Model	64



---

<b>4</b>	<b>Geochemistry and Geophysics</b>	<b>72</b>
4.1	XRF Analysis	72
4.1.1	The Basic Cycles	73
4.1.2	Bundles of Cycles	86
4.1.3	Long Term Trends: example core MorsDp52a	101
4.2	Stable Oxygen and Carbon Isotopes	105
4.2.1	The Basic Cycles	106
4.2.2	Bundles of Cycles	108
4.2.3	Long Term Trends	110
4.3	Magnetic Susceptibility	113
4.4	Colour Logging	115
4.4.1	The Basic Cycles	115
4.4.2	Hierarchical Bundling of Colour Cycles and Long Term Trends Example Core MorsDp52a	117
4.4.3	Origin of the Colours of the Steinmergel Keuper Playa system	124
<b>5</b>	<b>Controlling Processes of the Cyclicity</b>	<b>127</b>
5.1	Frequency Analysis	127
5.1.1	Example 1: Core MorsDp52a, Saxony Anhalt, N Germany	127
5.1.2	Example 2: Core Malschenberg, Baden Württemberg, S Germany	132
5.1.3	Example 3: Outcrop Mönchberg, Baden Württemberg, S Germany	134
5.1.4	Example 4: Composit of the outcrops Gleichenburg and Wachsenburg from the Drei Gleichen area, Thuringia	135
<b>6</b>	<b>A Basin-Wide Correlation</b>	<b>137</b>
<b>7</b>	<b>Conclusion</b>	<b>141</b>
<b>8</b>	<b>Outlook</b>	<b>143</b>
<b>9</b>	<b>References</b>	<b>144</b>
	<b>Appendix</b>	<b>155</b>
	<b>Danksagung</b>	<b>161</b>
	<b>Lebenslauf</b>	<b>162</b>
	<b>Erklärung</b>	<b>164</b>

## Kurzfassung

Das Hauptanliegen der vorliegenden Arbeit war die Charakterisierung rhythmischer Sedimente des Steinmergelkeuper Playa Systems im nord sowie im südgermanischen Becken um die Hypothese einer möglichen orbitalen Steuerung der Sedimentation im Becken zu überprüfen. Weiterhin sollte im Falle einer orbitalen Steuerung ein hochauflösendes zyklustratigraphisches Modell sowie eine Nord-Süd-Korrelation durchgeführt werden.

Dazu war eine detaillierte Fazies Analyse unter Berücksichtigung paläogeographischer und paläoklimatischer Aspekte notwendig. Des Weiteren wurden geophysikalische, sowie geochemische Proxyparameter benutzt. Zeitreihen-Analysen lieferten die notwendigen Informationen über eine orbitale Steuerung der zyklischen Sedimentation im Becken.

Farbmessungen liefern einen sehr hochauflösenden paläoklimatischen Proxyparameter, da Änderungen der Farbe sehr gut wechselnde Redox-Bedingungen, besonders Wechsel von rot nach grün, in kontinentalen Milieus widerspiegeln. Periodische Änderungen der Helligkeit reflektieren unterschiedliche Karbonatgehalte. Die stabilen Sauerstoff und Kohlenstoff Isotope sind als paläoklimatische und paläohydrologische Indikatoren geeignet. Die Kovarianz zwischen den Isotopen zeigt, dass das Steinmergelkeuper-Playa-System ein hydrologisch geschlossenes System war. Außerdem deutet einen Trend zu leichteren Isotopenwerten ein Wechsel zu humideren Zeiten im Becken an. Weitere paläoklimatische Proxyparameter werden durch die RFA geliefert. So zeigt z.B. das K/Al Verhältnis die Witterungsbedingungen des Hinterlandes an, d.h. wechselnde Intensität der Monsunaktivität. Niedrige Verhältnisse im Playa-System deuten auf eine erhöhte chemische Verwitterung des Hinterlandes hin. Hohe Verhältnisse hingegen weisen auf erhöhte physikalische Verwitterung des Hinterlandes hin. Suszeptibilitätsdaten wurden ebenso wie Farbdaten für die Spektralanalysen benutzt. RDF-Analysen, Dünnschliffe und Kathodenlumineszenz gaben weitere wichtige petrographische Informationen.

Eine integrierte Analyse von Bohrkernen, Aufschlüsse aus dem gesamten germanischen Becken in Deutschland, sowie die Analyse von Proben führten zu einem detaillierten Faziesmodell des Steinmergelkeupers. Es konnten drei basale Zyklentypen unterschieden werden. Im zentralen Playabereich (d.h. im See) herrscht eine zyklische Wechsellagerung von dunkelgrauen Tonmergeln, Dolomitmergelbänken, sowie displaziver Gips in den Dolomiten vor. In etwas randlicheren Bereichen (See bis nasse Schlammebene) liegt eine Wechsellagerung von dunkelgrauen Tonmergeln, Dolomitmergelbänken gefolgt von intensiv rotgefärbten Tonmergeln vor. Der marginale Bereich ist durch eine zyklische Wiederholung von pedogenetischen Dolocrête Horizonten gekennzeichnet. Der enge Zusammenhang zwischen den Ablagerungsbedingungen und der Monsunaktivität legt eine orbitale Steuerung, d.h. Milankovitch-Zyklen, der Sedimentation im Becken nahe. Trockene Phasen wechseln regelmäßig mit feuchten Phasen (in ein allgemein semiarides Klimasystem) ab.

Die klimagesteuerte Sedimentation sowie die Spektralanalyse deuten auf Milankovitch-Zyklen hin:

- Der basale Zyklus wird durch die Präzession (20kyr) verursacht. Dieser Zyklus besteht aus zwei Subzyklen, die durch die Hemipräzession (10kyr) verursacht werden.
- Die Präzessionszyklen sind zu Exzentrizitätszyklen (100Kyr, E1-E2) gebündelt, die wiederum zu Exzentrizitätszyklen von 400kyr (E3) gebündelt sind.
- Der niederfrequente Exzentrizitätszyklus E4 (~2Myr) besteht seinerseits aus Bündeln von E3 Zyklen.

---

## Abstract

The main purpose of the project was to study the rhythmic sediments of the Steinmergel Keuper playa system in the North and South German basin in order to test the hypothesis of possible climate control on sedimentation. Furthermore, in case of there being orbital control on sedimentation, the North/South correlation was tested based on high-resolution cyclostratigraphy.

This needed a detailed facies study taking into account paleogeography and paleoclimatology. Moreover, additional geophysical and geochemical parameters were used as proxy parameters for paleoclimatology. Time series analysis provided the necessary information about the orbital controlling factors on cyclicity.

Colour logging provided a very high-resolution paleoclimatic proxy parameter as it is a good indicator of changes of the reduction/oxidation conditions and especially cyclic changes from green/grey to red are shown well by colour logging. Cyclic changes in the lightness give reliable information about dolomite formation in the playa lake. Therefore, changes in lightness reflect lake level changes. Stable oxygen and carbon isotopes furnished indications about paleoclimatology and paleohydrology of the playa system. Covariance of the isotopes suggests a hydrological closed basin. Trends of lightening of the isotopes show the climatic trends toward more humid periods. Further climatic proxy parameters were given by XRF-analysis. The K/Al ratio, for example, provides information on the weathering pattern of the hinterlands. Thus, low K/Al ratios suggest an increased chemical weathering of the hinterlands and high K/Al ratios an increased physical weathering of the hinterlands. Susceptibility data were used besides colour data for frequency analysis. Petrographic data were provided by XRD, thin section and cathode luminescence.

The integrated study of drill cores, outcrops distributed all over the German basin and samples results in a detailed facies model of the playa system. Three different main cycle types were recognized depending on their position within the playa. The most central part of the playa system (i.e. playa lake) is characterized by repeated successions of dark grey mudstones, dolomite beds and displacive gypsum within the dolomite. A more marginal (playa lake to wet mudflat) cyclic facies is a succession of dark grey mudstones, dolomite beds followed by red mudstones. The most marginal facies (mudflat) is a cyclic pedogenetic dolocrête facies. Because of the close relationship between the sediments and cyclic changes in the monsoonal activity the cyclicity within the sediments is interpreted to be initiated by changes in the orbital parameters, i.e. Milankovitch cycles. Playa mudflats change cyclically with playa lakes reflecting cyclic changes between drier and wetter periods in an overall semi-arid setting.

The overall climate control on sedimentation and the results of evolutionary spectral analysis allow an interpretation in terms of Milankovitch cycles:

- A basic wet dry cycle is interpreted as having its origin in the precession (20kyr). The very high-resolution of the colour logging show further that this cycle is composed of two sub-cycles, which are most likely hemi-precessional cycles (10kyr).
- Five basic cycles are bundled into a lower frequent cycle representing the eccentricity of 100 kyr (E1-E2).
- These cycles are bundled again to form the eccentricity of 400kyr (E3).
- The lowest-frequency cycle is the 2Myr cycle formed by bundling of E3 cycles.

# 1 Introduction

*Keywords: Triassic, Carnian, Norian, Keuper, Steinmergel-Keuper, Germanic Basin, Playa, Paleoclimatology, Cyclicality, Milankovitch - Cycles, Colors, XRF, XRD, Stable Isotopes, Dolomite.*

## 1.1 Goals and Perspectives of the Project

This PhD-project, financed by the German Research Foundation, is the succeeding project of REINHARDT'S doctoral thesis: "Dynamic stratigraphy and geochemistry of the Steinmergel-Keuper playa system: a record of Pangaeian monsoon cyclicality (Triassic, Middle Keuper, Southern Germany)" published in 2002. His studies focused on the marginal basin of the continental playa system of the Carnian/Norian Steinmergel Keuper. The present study is focused mainly on the central part of the Steinmergel Keuper basin in Northern Germany, but the southern margin is also taken into consideration (fig. 1). The results are compared with REINHARDT'S results and a correlation of the northern basin with the southern basin is put forward.

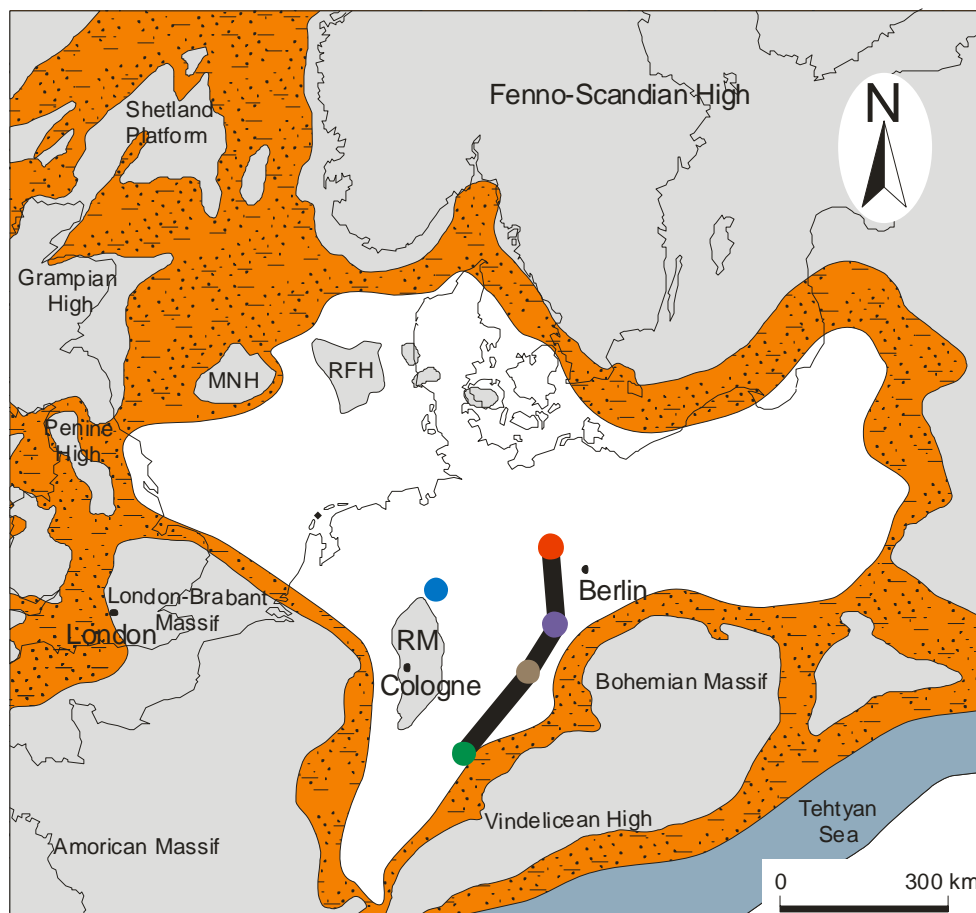


Fig. 1: Simplified paleogeographic map (after ZIEGLER, 1990). Insets = working areas; green: Baden Württemberg; brown: Hassberge, Bavaria; violet: Creuzburg and Drei Gleichen, Thuringia; red: Allertal, Saxony Anhalt; blue: Osnabrücker Bergland, Lower Saxony. Black line = major transect through the basin.

### 1.1.1 Goals

The results of REINHARDT'S (1998, 2000a and b, 2002) studies suggests an orbital control on sedimentation of the Steinmergel Keuper playa system. Reinhardt put forward a model with precessional (20 kyr) and eccentricity (100 kyr and 400 kyr) cycles. His model is based on geochemical and geophysical proxy parameters as well as high-resolution stratigraphy and the obvious bundling of dolomitic marl beds. These dolomite/marl cycles were formed by the alternation of wet and dry periods (fig. 2). Additionally, the orbital cyclicity influenced the seasonal variations through a year. During dry periods the playa dried out seasonally after rainfall and dolomite was not formed. On the other hand during wet periods despite extensive evaporation the playa did not dry out completely and dolomite precipitated within a persisting playa lake. For reasons of simplification the dolomitic marls are referred as dolomites throughout this work.

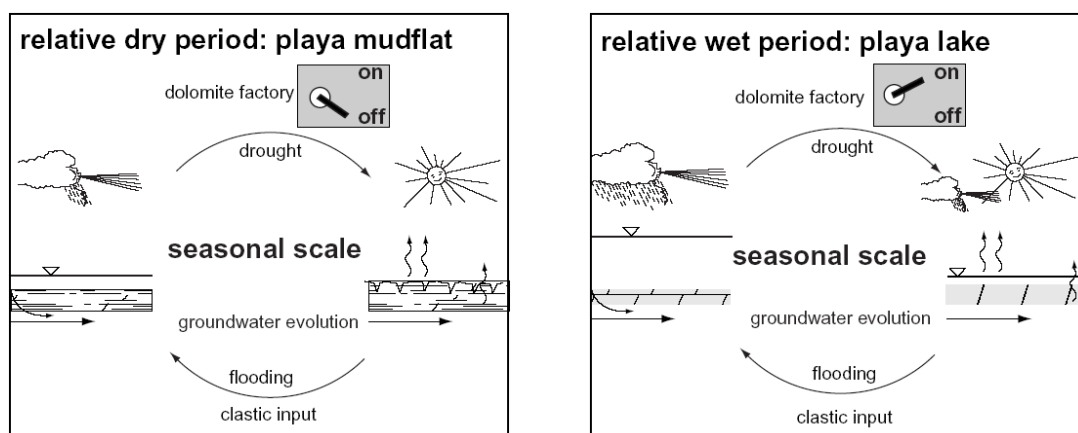


Fig. 2: Effects of orbital control and major climate variation on sedimentation within the Steinmergel Keuper playa system with the dolomite factory turned off or on. A: seasonal processes during a relative dry period. Only an ephemeral lake was formed and dolomite was not formed. B: seasonal processes during a relative wet period. A persisting lake with standing waters was formed and dolomite could precipitate (from REINHARDT, 2002).

One goal of the present study was to apply the hypothesis of orbital control on cyclic stratification to the whole basin, i.e. also to the central playa system. Beside a very high-resolution stratigraphy a detailed facies analysis of the central playa was necessary. This led to new facies model of the central playa system. The stratigraphy is mainly based on the excellent works of BRENNER (1973, 1978a, b, 1981) DUCHROW (1984), NITSCH (2005a), ETZOLD & SCHWEIZER (2005) and BEUTLER (1998, 2005). Geochemical and geophysical analysis and the facies analysis were carried out at core MorsDp52a (Morsleben, Allertal; with the kind permission of the Bundesamt für Strahlenschutz) and at several outcrops in Lower Saxony, Thuringia, Bavaria and Baden Württemberg. A completely new parameter for paleoclimatic and cyclic studies in continental sedimentology is the use of colour logging. Furthermore, pre-existing geochemical and geophysical data (REINHARDT, 2002) from core Malschenberg compared with colour measurements. The results were analysed and interpreted in terms of paleoclimatology. The different parameters were also interpreted with evolutionary spectral analysis to establish a cyclic model and a high-resolution cyclostratigraphy. Then the central basin (N German Basin) could be correlated with the marginal basin (S German Basin). Based on orbital tuning a model for minimum time content for the playa system was established. Furthermore, low frequent climate cycles of about 2Myr (E4) were identified. Moreover, the high resolution of colour logging revealed the presence of hemi-precessional cycles.

## 1.2 Geological Overview

The work presented here is based on two cores and several outcrops distributed all over the German Basin. It is essential for the hypothesis of an orbital control on sedimentation to have a record of outcrops, which is as complete as possible, to work out the evolution from the marginal basin to the central basin i.e. from South to North Germany. Because of the great number of outcrops and the great distances only the best-exposed and best-preserved outcrops were chosen. For location overview see fig. 1 and a detailed listing of outcrops on which this work is based is given in the following tables.

Well preserved outcrops studied, including core Malschenberg in Baden Württemberg (tab. 1):

Nr.	TK 25	Sheet	R/H	Location / core	Stratigraphy	remark
1	6718	Wiesloch	34 78 060 / 54 57 360	Malschenberg 1	km4.1-km5	core, Geolog. Survey
2	7419	Herrenberg	34 92 869 / 53 84 980	E Herrenberg	km4ms2	loc. typ. H/R
3	7419	Herrenberg	34 94 275 / 53 83 175	NNE Mönchberg	km3t-km3sF	BRENNER 1978
4	7419	Herrenberg	34 95 350 / 53 82 575	ENE Kayh	km2-sc2	BRENNER 1978
5	7419	Herrenberg	34 98 875 / 53 78 275	N Unterjesingen	km3t-km4us1	BRENNER 1978
6	7419	Herrenberg	34 99 750 / 53 78 275	Rechtesteige	km3s-km4.2	SCHAUER 1994
7	7420	Tübingen	35 07 000 / 53 80 250	Geol. Lehrpfad	km2-km4.4	BRENNER 1978
8	7420	Tübingen	35 03 200 / 53 80 100	Geschl. Brunnen	km3t-km4.1	BRENNER 1978
9	7420	Tübingen	35 04 650 / 53 76 850	Tübingen	km2-km4.1	REINHARDT 2002
10	7519	Rottenburg	34 97 920 / 53 67 600	Bodelshausen	km3t-km3sF	REINHARDT 2002
11	7618	Haigerloch	34 79 225 / 53 57 850	W Haigerloch	km2-km4.2	BRENNER 1978
12	7619	Hechingen	34 95 180 / 53 59 220	W Stein	km3-km4ms2	BRENNER 1978

Tab. 1: List of the core outcrops locations in Tübingen and surroundings.

The outcrop Funkenloch and two other outcrops nearby were studied in the Hassberge Region of Bavaria (tab. 2).

Nr.	TK 25	Sheet	R/H	Location	Stratigraphy	remark
1	5728	Oberlauringen	36 02 700 / 55 70 700	ENE Sulzfeld, Funkenloch	km3sA-km4.2	SCHROEDER & WELZER 1966
2	5728	Oberlauringen	36 00 900 / 56 71 250	Anadenkmal near Sulzfeld		Courtesy Mr. JAEGER (Forstamt of Bavaria)
3	5728	Oberlauringen	36 00 500 / 56 71 000	2km from Sportplatz Sulzfeld		Courtesy Mr. JAEGER (Forstamt of Bavaria)

Tab. 2: Outcrop list from Bavaria.

The field trips in Thuringia concentrated on very well-documented outcrops of the Drei Gleichen area (NAUMANN, 1911, HOPF AND MARTENS 1992, SEIDEL 1995, SCHULZ 1996, KELLNER 1997) and the Creuzburg area (tab.3).

Nr.	TK 25	Sheet	R/H	Location	Stratigraphy	Remark
1	5131	Arnstadt	44 21 000 / 56 36 400	SW side of Wachsenburg	Arnstadt Formation	NAUMANN 1911
2	5131	Arnstadt	44 18 400 / 56 38 800	S side of Gleichenburg near Wandersleben	Arnstadt Formation	NAUMANN 1911
3	5131	Arnstadt	44 17 800 / 56 38 800	W side below of Mühlenburg	Arnstadt Formation	NAUMANN 1911
4	5131	Arnstadt	44 15 400 / 56 43 400	Seebergen / centre of village	Arnstadt Formation	KELLNER 1997
5	5131	Arnstadt	44 15 600 / 56 43 700	N Seebergen	Arnstadt Formation	KELLNER 1997
6	4827	Treffurt	35 82 400 / 56 59 520	W Ifta	Arnstadt Formation	KELLNER 1997
7	4927	Creuzburg	35 90 420 / 56 55 600	Between Ütteroda and Madelungen ~ 500m SW from Ütteroda	Arnstadt Formation	KELLNER 1997

Tab. 3: List of outcrops in Thuringia.

Within the Osnabrücker Bergland are some well described (DUCHROW, 1984) profiles (tab 4).

Nr.	TK 25	Sheet	R/H	Location	Stratigraphy	Remark
1	3819	Vlotho	34 89 160 / 54 80 720	SW Vlotho	km4b1-koQS	DUCHROW 1984
2	3819	Vlotho	34 91 300 / 54 84 070	N Uffeln	km4a3b-km4b2	DUCHROW 1984
3	3819	Vlotho	34 89 700 / 54 77 400	S Valdorf	km4a2-km4b1	DUCHROW 1984
4	3819	Vlotho	34 09 580 / 54 81 700	Vlotho	km4a1-km4a3a	DUCHROW 1984
5	3819	Vlotho	34 92 450 / 54 79 660	Valdorf-Ost	km3b-km4a3b	DUCHROW 1984
6	4121	Shieder – Schwalenberg	35 13 650 / 57 47 100	Route B 239 S Schwalenberg	Arnstadt Formation	Courtesy BEUTLER

Tab. 4: List of outcrops in the Osnabrücker Bergland.

Core MorsDp52a (courtesy of the Bundesamt für Strahlenschutz) was drilled in Morsleben, Allertal, Saxony Anhalt.

### 1.2.1 Paleogeography

Due to the collision between Gondwana and Laurussia in Permian times the supercontinent Pangaea was formed. This continent had persisted for over 40 Myr until latest Triassic period when it started breaking up. At this time Pangaea was surrounded by the global ocean Panthalassa (fig. 3). Eastwards of the continent was according to the map the Thetyan Ocean which incised the huge landmasses of Pangaea.

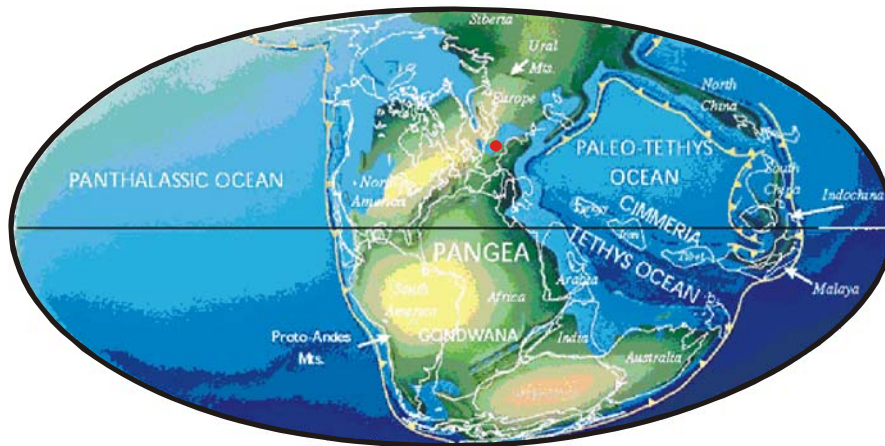


Fig. 3: Paleogeographic map of Pangaea at early Triassic. Red point: Steinmergel Keuper basin. After SCOTSESE, 2001.

The Steinmergel Keuper basin was situated between 20° and 30°N. It developed from a shallow marine environment into a purely continental playa system at the middle Keuper. The basin was surrounded by crystalline landmasses as the Vindelicean High southwards and the Bohemian massif at the east. America, the London Brabant massif and the Grampian High formed the western border of the basin. North of the basin was located Fenno Scandia. Some smaller highs such as the Rheinisch massif and Ringkøbing – Fyn – High were located within the playa lake (fig. 1).



## 1.2.2 Tectonic Evolution

More than 80Myrs after the origin of the supercontinent Pangaea, it started breaking up during late Triassic times, and a complex rift system developed (see fig. 4).

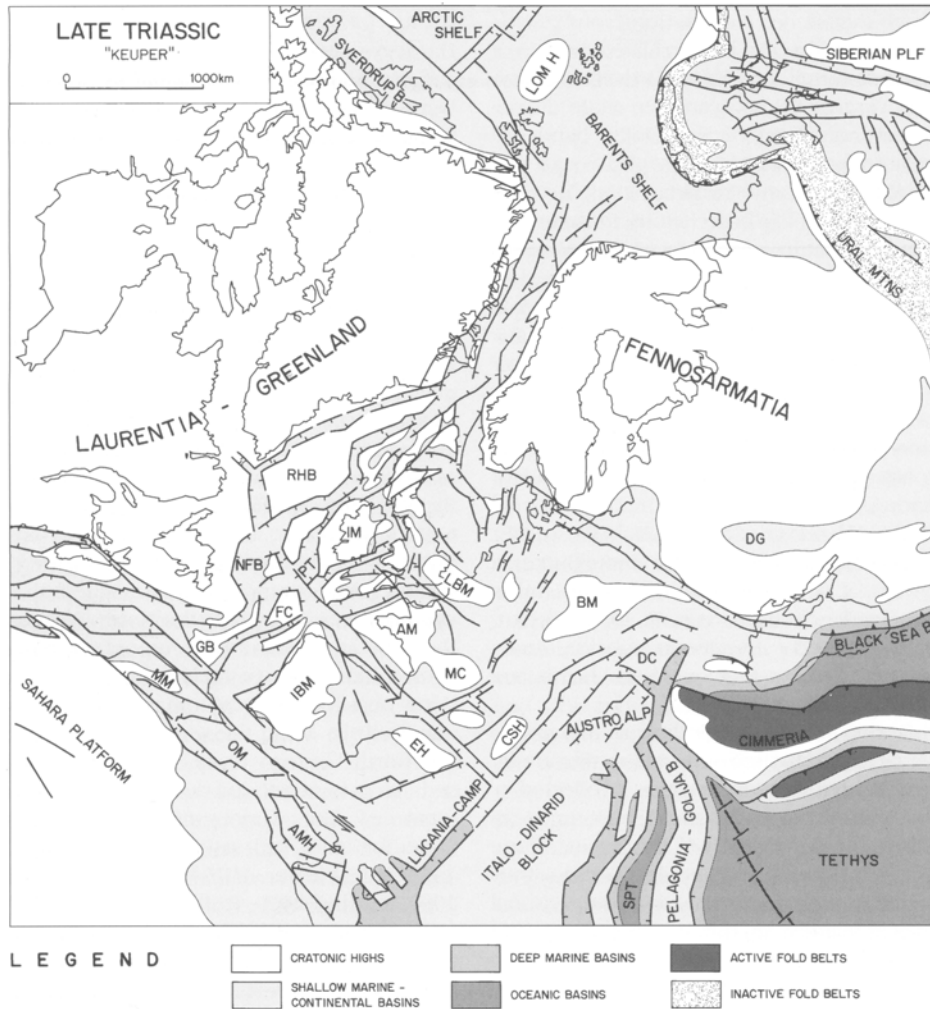
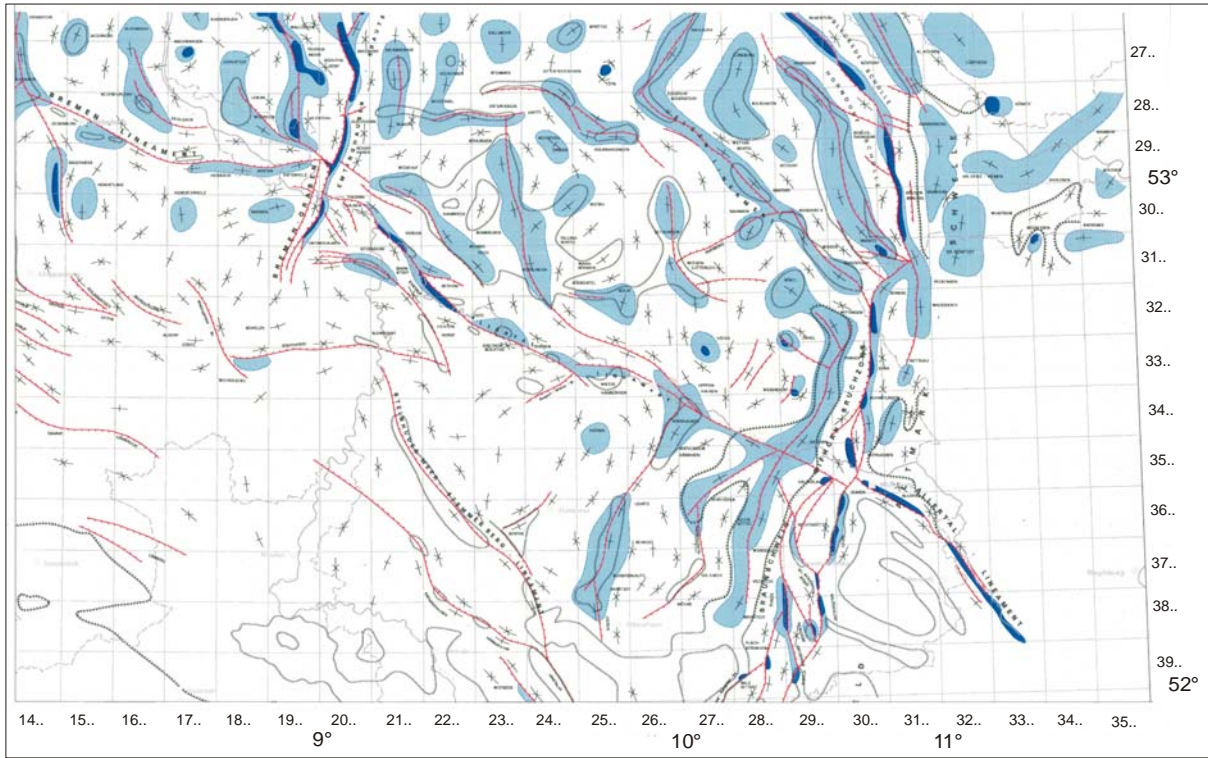


Fig. 4: Rift system during the late Triassic period for the northern part of Pangaea. Abbreviations: AM = Armorican Massif, AMH = Ain-M'lila High, BM = Bohemian Massif, CSH = Corsica-Sardinia High, DC = Dacides Block, DG = Donets Graben, EH = Ebro High, FC = Flemish Cap, GB = Grand Banks, IM = Irish Massif, IBM = Iberian Meseta, LBM = London Brabant Massif, LOM H = Lomonosov High, MC = Massif Central High, MM = Morocco Meseta, NFB = East Newfoundland Basin, OM = Oran meseta, PLF = Platform, PT = Porcupine Trough, RHB = Rockall-Hatton Bank, SPT = Sub-Pelagonia Trough. From ZIEGLER, 1990.

During the breakup of Pangaea older inherited structures and fracture systems in the German basin were reactivated, leading to a complex structure of synsedimentary faulting with graben, halfgraben structures, uplifting and halokinetic overprints (fig. 5), especially in the northern part of the German basin. In any case, the tectonic activity increased northwards leading to lowered subsidence rates in the South German basin, but higher rates in the North German basin. Therefore, halokinesis of Permian (Zechstein and Rotliegend) salts became more important towards the north. This must be considered as halokinesis can lead to more extensive local depressions related to salt diapirism. Sedimentation within these depressions might be controlled by local factors rather than by climate.



Legend:

- |  |   |  |   |
|--|---|--|---|
|  | Salt structure in pillow stage with axis of minimum sedimentary thickness   |  | Synsedimentary active normal fault or half graben (down throw >500m)                              |
|  | Salt structure in diapiric stage  |  | Synsedimentary active graben  |
|  | Salt dome in late stage with axis of minimum sedimentary thickness  |  | Present day distribution of Schilfsandstein + Upper Gipskeuper (subcrop, fault, salt dome margin) |
|  | Axis of maximum sedimentary thickness (rim sink, graben, half graben, regional trough, subsrosion sink)                       |  | Subcrop of formations within the units displayed:   |
|  | Axis of minimum sedimentary thickness (i.e. salt pillow, salt dome, horst, graben shoulder, turtle structure, regional ridge) |  | Subcrop beneath Steinmergel-unconformity (km4)  |
|  | Synsedimentary active normal fault or half graben (down throw <500m)  |  | Subcrop beneath Rhaetian discordance (ko)   |
|  |   |  | Name of structure   |
|  |   |  | Name of principle structure   |

Fig. 5: Tectonic evolution during Schilfsandstein and Upper Gipskeuper times (Carnian, Norian). Extract from the paleotectonic map 1:500.000. After BALDSCHUHN, R. et al (1999).

BEUTLER (1998) pointed out a series of basin-wide unconformities (Fig. 6) through Keuper times, which may serve as marker horizons for correlations. These unconformities reflect not only hiatuses but also rifting, faulting, uplifting and halokinetic movements within the German basin. The unconformity D3 divides the Steinmergel Keuper (km<sup>3</sup>) in the southern German basin and divides the Upper Gipskeuper in the northern basin. Unconformity D4 separates the Arnstadt Formation (Steinmergel Keuper) from the Weser Formation (Upper Gipskeuper) in the northern basin, whereas in the southern basin D4 is at the base of the Stubensandstein. Halokinetic movements ceased during times of the Arnstadt Formation. The Steinmergel Keuper is separated from Rhaetian sediments by another basin-wide unconformity (D5), which defines the end of the Steinmergel Keuper playa system.

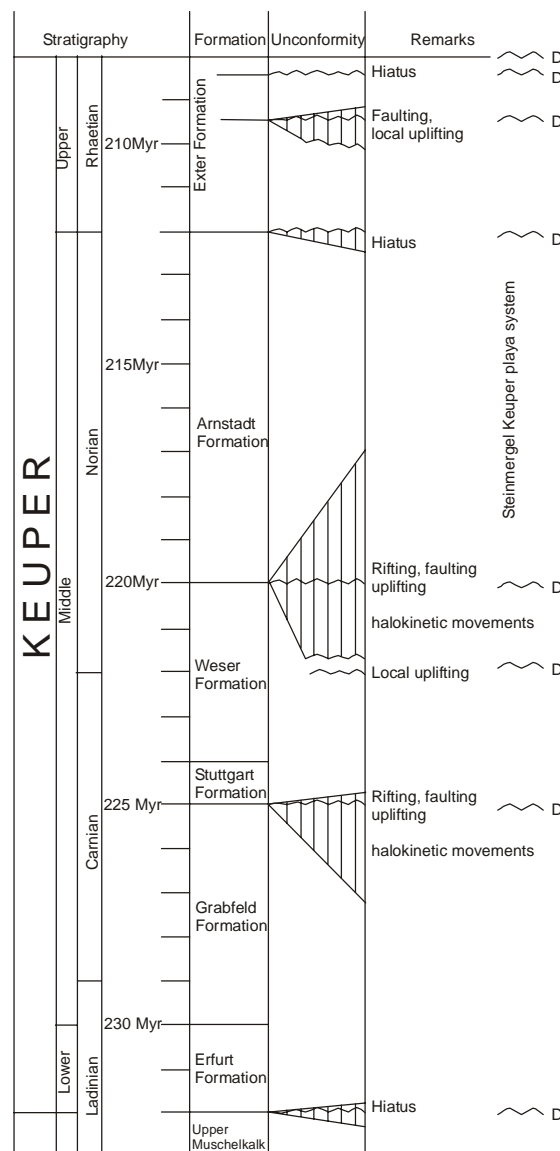


Fig. 6: Lithostratigraphic time chart of the Keuper. After BEUTLER 1998.

The Arnstadt Formation evolved from a marine-influenced sabkha (Weser Formation) into a completely closed continental playa system. The facies is characterized by multicoloured and

grey shales alternating with grey dolomites (fig. 7). The colour is dominantly red, red-brown and red-violet in the marginal parts and green-grey in the central part of the basin.

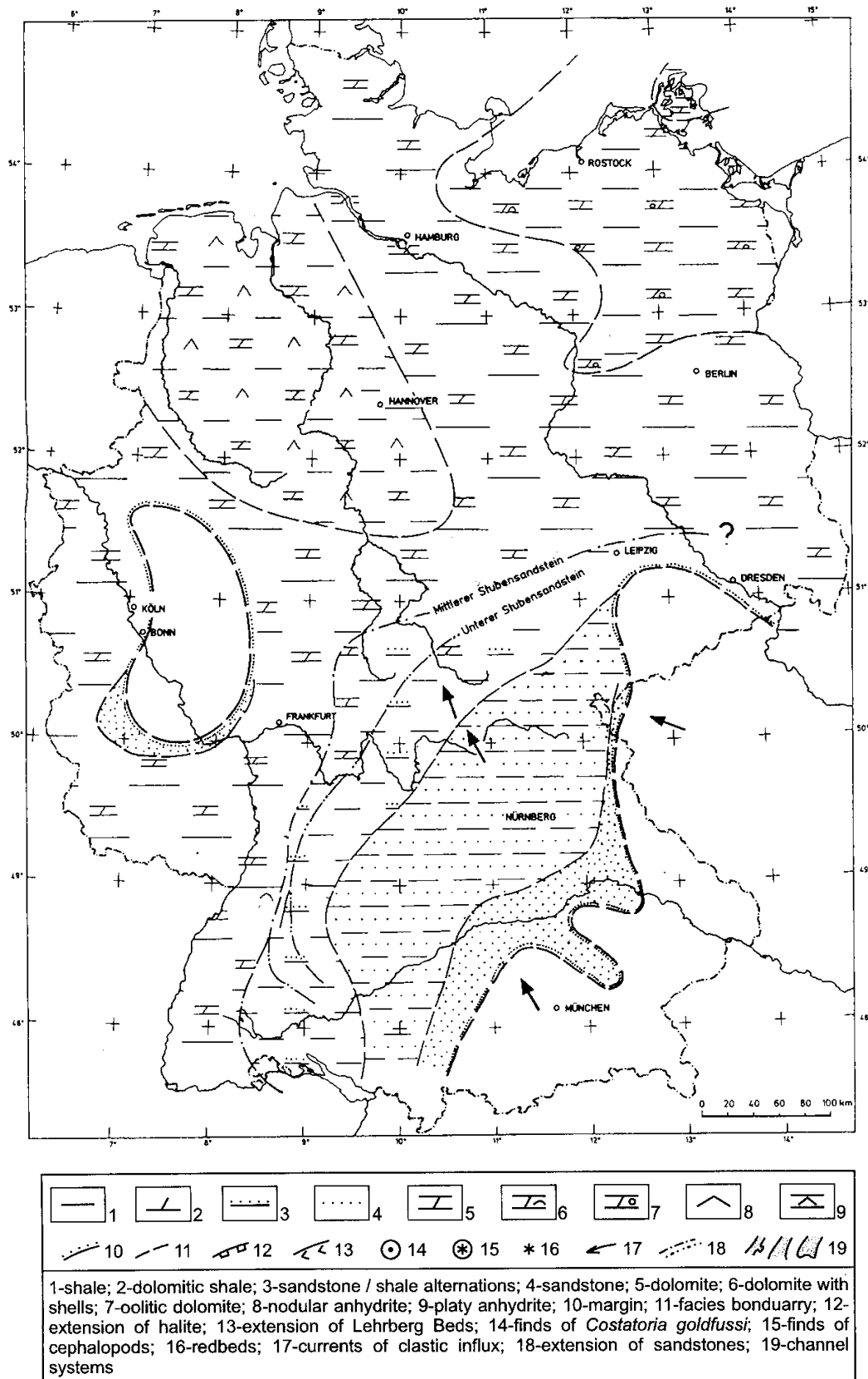


Fig. 7: Generalized facies map of the Arnstadt Formation (Steinmergel Keuper); from BEUTLER (1998).

### 1.3 Stratigraphy

The Triassic is divided into seven international stages: Indusian, Olenekian, Anisian, Ladinian, Carnian, Norian and Rhaetian. Sedimentation within the Steinmergel Keuper playa system took place in Upper Triassic times, which comprises the stages Carnian and Norian. Sedimentation within the playa system started after deposition of the Schilfsandstein (Stuttgart-Fm.) with the onset of a deltaic/fluviatile sedimentation at the marginal basin (Steigerwald-Fm., Hassberge-Fm., and Mainhardt-Fm.) and a shallow restricted marine-influenced sedimentation in the central basin (Upper Gipskeuper, Weser-Fm., Northern Germany). Then it passed progressively to a purely continental playa system: the Steinmergel Keuper. Finally in Rhaetian times an open marine system dominated in the German Basin.

The Keuper nowadays is divided into 6 sequences: k1 to k6 (LUTZ 2005) comprising the time slices Ladinian, Carnian, Norian and Rhaetian. Sequence k5 represents Steinmergel Keuper (=Arnstadt Formation). The time covered by the Arnstadt Formation is about 15Myr (LUTZ, 2005).

A major problem one is faced with is the differing nomenclature in older literature and the time covered by the Arnstadt Formation in southern Germany and northern Germany. Important aids for correlating the units in southern Germany with the units in northern Germany are provided by basin-wide discordances numerated D1 to D5 (BEUTLER, 1998) and basin-wide marker horizons. A recent correlation based on cyclostratigraphy between Thuringia and SW Germany is provided by NITSCH (2005).

In southern Germany several works from BRENNER (1973, 1978), BRENNER AND VILLINGER (1981) and SEEGIS (1997) lead to accurate and precise lithostratigraphy. The Keuper of Southern Germany is subdivided into 5 units: km1 to km5. The Steinmergel Keuper comprises the time slices km3 to km5 and starts with the onset of the Ansbacher Sandstein. The further subdivision of the Steinmergel Keuper (km3 to km5) is based on the subdivision of the sandstones which represents distal sheet flows. At the base of the playa is situated the Ansbacher Sandstein (km3u). At the top of this unit is a basin-wide marker, a fossil-bearing horizon composed of three dolomite beds called Lehrberg beds (km3L, SEEGIS, 1997). At the base of the third Lehrberg bed is the discordance D3, which separates the Ansbacher Sandstein from the Kieselsandstein (= Coburgsandstein in Bavaria) that has been differentiated into km3s1 and km3s2. The Kieselsandstein was further divided by BRENNER (1973) using a six-fold distinction from km3sA to km3sF. Km3sA, km3sB and km3sC form the unit km3s1 whereas the other three build the unit km3s2. Sedimentation of the Kieselsandstein ends after deposition of the Heldburggips with the discordance D4. The Heldburggips is a marker horizon throughout the whole basin. Then follows the Stubensandstein (= Burgsandstein in Bavaria) with its classification into km4us1, km4ms2, km4os3 and km4os4. The Ochsenbach horizon at the base of km4os1 provides an important marker horizon in southern Germany. This horizon is cut off by an erosive discordance at the top. Another important horizon within km4os2 is the so-called Rottweiler bed. Afterwards follow km4os3 and km4os4. Sedimentation in the Steinmergel Keuper playa system finishes with the Knollenmergel (km5). Then separated by discordance D5, follow the Rhaetian sandstones.

The situation in northern Germany is somewhat different as it corresponds to a more central position in the playa system than southern Germany. The huge deltaic/fluviatile sandstones of southern Germany, i.e. the Ansbacher Sandstone, the Kiesel Sandstone are replaced by the

Upper Gipskeuper and they are grouped together within the Weser Formation. The stratigraphic equivalent of the Stubensandstein (nowadays: Löwenstein Formation) is the Arnstadt Formation (Steinmergel Keuper s. str.). The Knollenmergel (Trossingen Formation) that follows the Löwenstein Formation reaches into the Rhaetian.

A stratigraphic subdivision of the Arnstadt Formation is given by KELLNER (1997). In Thuringia the Arnstadt Formation is divided into three main units: the Untere Bunte Mergel (UBM), the Mittlere Graue Mergel (MGM) and the Obere Bunte Mergel (OBM). The UBM is further subdivided by the marker horizon *alpha* into UBM1 and UBM2 (fig. 7). The marker horizon beta separates the UBM and the MGM. Another Marker Horizon (horizon gamma) separates the MGM from the OBM. The transition from the MGM to the OBM is characterized by the presence of pedogenetic horizons (Untere Pedogene Folge, OPF). Then follow the OBM with dolomarl beds, followed by the Obere Pedogene Folge (OPF), which shows an intensive pedogenetic overprint. Horizon delta separates the OPF from the OBM without dolomarl beds.

The time slices of the different sections studied are given in the tables 1 to 4 (see chapter Geological Overview).

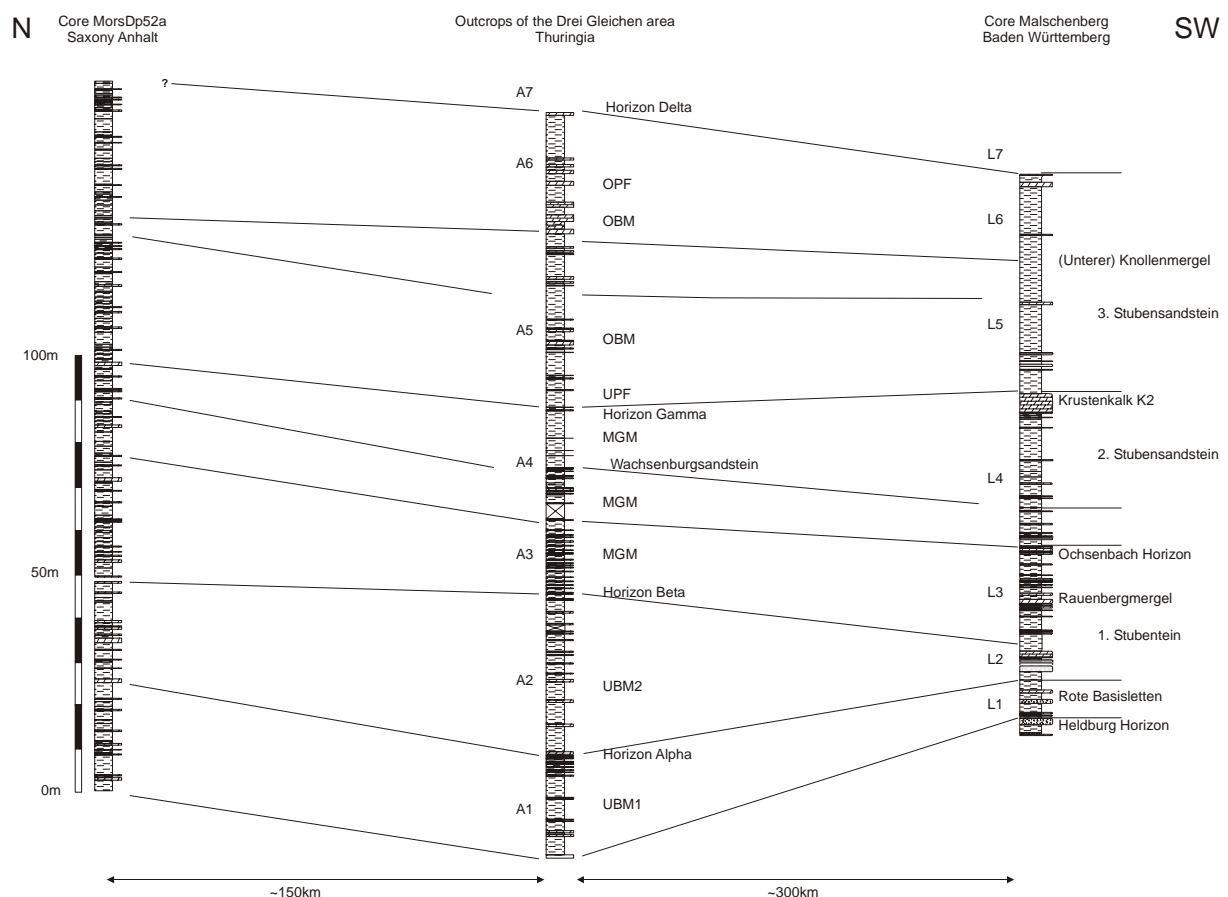


Fig. 8: Stratigraphic correlation of the Steinmergel-Keuper Basin in Germany. After: BRENNER 1973 (S Germany), KELLNER 1997 (Thuringia), AIGNER & HORNING 1999 (S Germany), ETZOLD & SCHWEIZER (2005) NITSCH (2005a) (S and N Germany), LUTZ (2005) BEUTLER 2005 (S and N Germany) and BEUTLER (in press; core MorsDp52a) . A1 to A7 and L1 to L7 “Small Cycles“ after NITSCH 2005. Other abbreviation: see text above.

### 1.4 Paleoclimatology

Several numerical simulations to do with the Pangaeon climate have been performed by some authors (e.g. KUTZBACH AND GALLIMORE, 1989, KUTZBACH, 1994, PARRISH, 1993, a.o.) to get a basic idea of the paleoclimate of the super-continent Pangaea. Even though the geographical conditions are highly idealized the models give an essential insight into Pangaeon climate evolution. The climate of this super continent evolved from a long lasting icehouse during Permian times to an arid and hot climate during Triassic times (CROWLEY, 1994). From the Upper Permian on and during the Triassic the climate changes cyclically from arid to semiarid (see fig. 9).

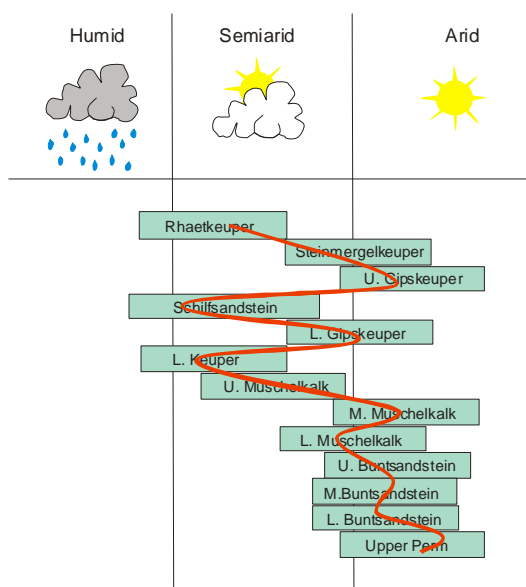


Fig. 9: Climate evolution of central Europe since the Upper Permian and the Trias. From RÖHLING, H.-G., AND HEUNISCH, C.

The Steinmergel Keuper basin was located between 20° N and 30° N. This corresponds after KÖPPEN (1931) to a zone characterized by an arid, steppe climate (see fig. 10).

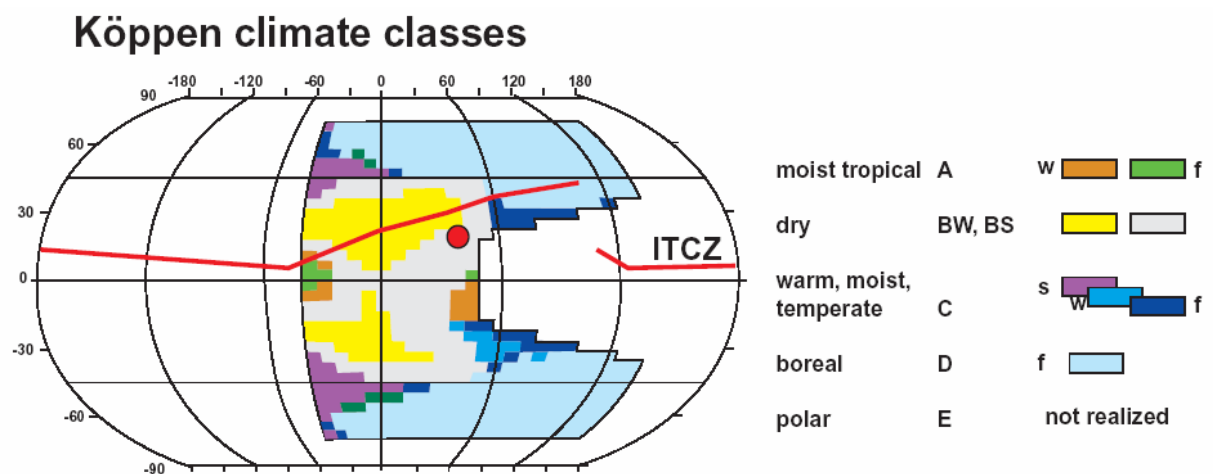


Fig. 10: Köppen climate classes of the Pangaeon super-continent during the Late Triassic. Solely major KÖPPEN climate classes are shown. Abbreviations: moist tropical (A), dry (BW, BS), warm moist temperate (C), boreal (D), and polar (E). The indices (f,w, s) mean: year-round rain (f), summer rain (w), and summer dry (s). The line marks the northward shift of the inner tropical convergence zone (ITCZ). The point marks the approximate position of the Keuper basin. From REINHARDT, 2002.



All climate models are based on the assumption of strong monsoonal activities during Pangaean times. For the Steinmergel Keuper basin REINHARDT (2000a and b, 2002) pointed out the importance of the monsoon for the incoming moisture and sedimentary response within the playa system.

Monsoonal intensity is influenced by orbital parameters such as the precession, obliquity and the eccentricity (e.g. KUTZBACH, 1981, KUTZBACH AND GALLIMORE, 1989, TUENTER, 2003). During Pangaean times the 23kyr precession caused changes in the season of the perihelion (KUTZBACH, 1994). This led to changes in the seasonal insolation which were strong enough to modify the monsoonal activity significantly (see fig. 11).

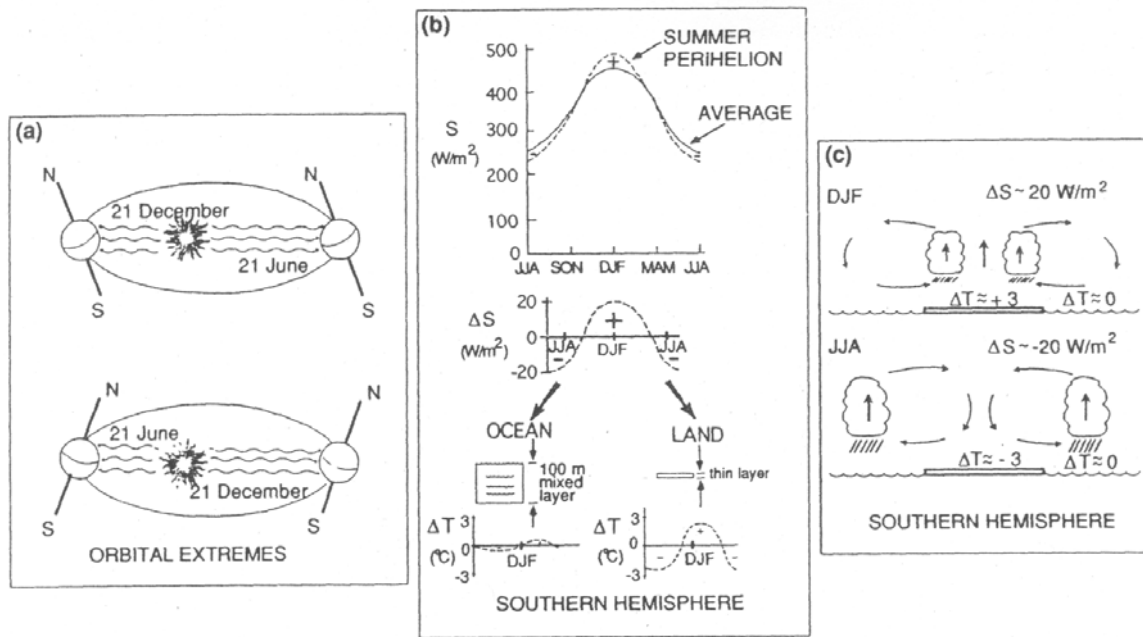


Fig. 11: Orbital influence on climate of Pangaea. a: Top: Perihelion in December (Southern Hemisphere Summer). Bottom: Perihelion in June (Northern Hemisphere Summer). b: Top: Solid curve is the Southern Hemisphere average seasonal cycle of solar radiation (S) for an orbit with zero eccentricity. Dashed curve: the same parameter (S) for an orbit with an eccentricity of 0.25. Middle: the change in solar radiation ( $\Delta S$ ) between the two curves above. Bottom: schematic change in ocean and land temperature ( $\Delta T$ ). c: schematic changes of land-ocean monsoon circulation caused by the different thermal responses of land and ocean to orbital (precessional) forcing. Illustrations are for the Southern Hemisphere with perihelion in southern summer (December-January-February [DJF]). From KUTZBACH (1994).

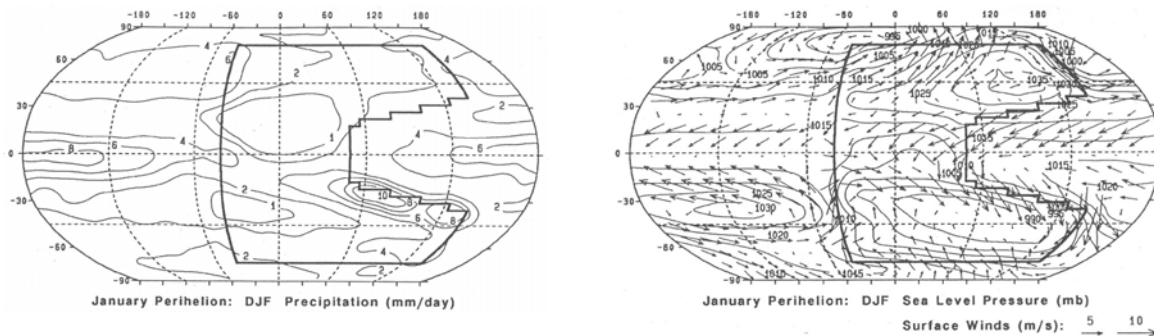


Fig. 12: left: precipitation for December-January-February (DJF) for the southern summer. right: sea level pressure and surface layer winds for DJF for the southern summer. Speed is calibrated for the winds arrows on the bottom right. From KUTZBACH (1994).



With perihelion in southern summer the solar radiation warmed the land while the ocean temperature remained constant. This increased the precipitation and the moisture input from the sea into Pangaea.

Based on this climate model KUTZBACH (1994) simulated the influence of Milankovitch cycles on Pangaeian climate. The enhanced seasonality of the insolation caused by the precession led to cyclic changes in precipitation and runoff of about 25% along tropical coastlines and tropical or subtropical continental interior ( $\sim 40^\circ$  latitude). This means that sedimentation within the Steinmergel Keuper playa system ( $20^\circ$  to  $30^\circ$  N) was controlled by orbital parameters.

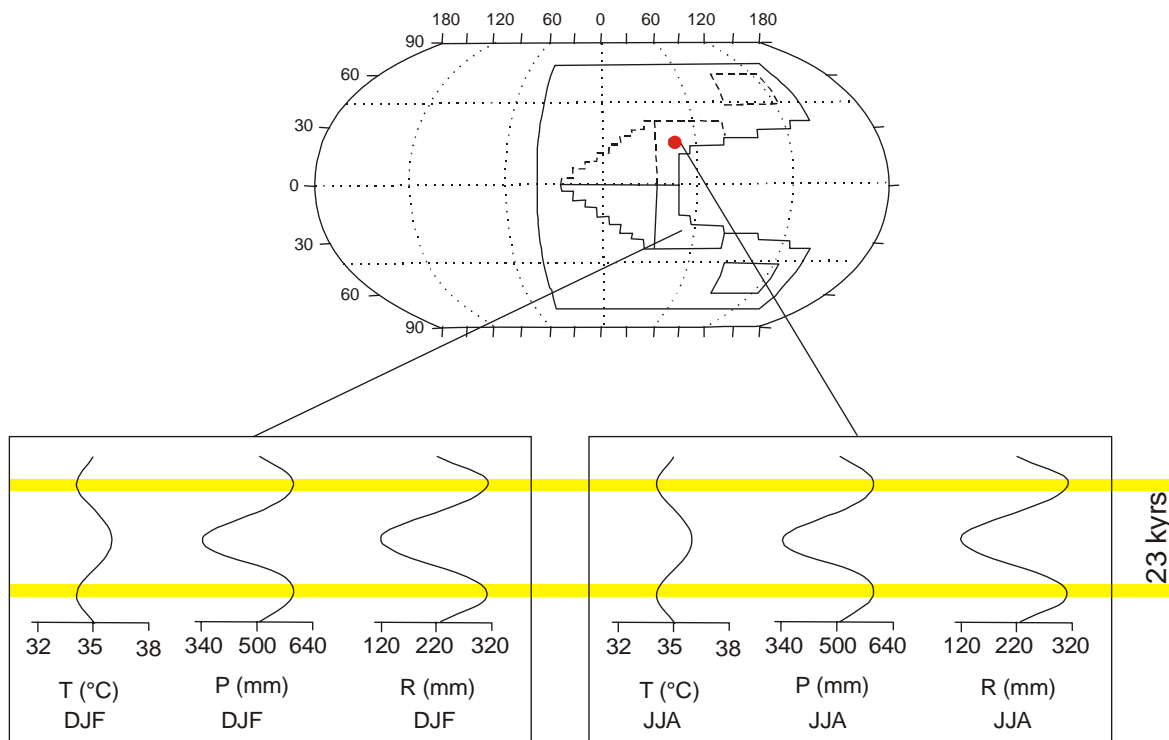


Fig. 13: schematic time series through a precession cycle (23kyrs) of summer (DJF), Temperature T( $^\circ$ C), summer precipitation P(mm), and annual runoff R(mm) for a central region of the southern hemisphere of the idealized Pangaeian super-continent. Because of the symmetric conditions applied in the model the results should be the same for the northern hemisphere during northern summer in June-July-August (JJA). That means there should be a phase shift of  $180^\circ$  with respect to the southern summer. The red point indicates the approximated position of the Steinmergel Keuper basin. After KUTZBACH, 1994.

Evidence of monsoonal variations and orbital control on sedimentation in continental systems during the Upper Triassic has been described for the Newark Basin, Pennsylvania, USA by OLSEN & KENT (1996). Also DUBIEL (1991) found hints of changing monsoonal activity within the Chinle Formation (Upper Triassic, Colorado Plateau). The Jameson Land Basin in East Greenland, which is also an Upper Triassic Playa system, was studied in detail by CLEMMENSEN et al (1998). He clearly showed the monsoonal activities within the Jameson Land Basin.

## 2 Methods

To characterize the cyclicity of the Steinmergel Keuper playa system two cores and several outcrops distributed all over the German basin (see fig. 1 and tab. 1 to tab. 4) were studied in detail and with high resolution to gain the maximum amount possible of stratigraphical, chemical and physical data. To support the present project a diploma thesis on pedogenetic dolocrêtes in the Drei Gleichen area (Thuringia) was carried out by TOUGIANNIDIS, N. (2004). This diploma thesis is based on the same multi-parametric strategy as is used in the present work.

### 2.1 Sampling Strategy

Core MorsDp52a (Morsleben, Allertal, Lower Saxony) was taken as a reference profile for central basin of the Steinmergel Keuper playa system in northern Germany. As core Malschenberg and the outcrops in Baden Württemberg have been widely subject to chemical and physical research (REINHARDT, 2002) only the colors were measured. The resulting data were compared with the existing data (REINHARDT, 2002).

A screen of 33 samples with a mean sampling rate of ~5m was taken from core MorsDp52a for thin sections, cathode luminescence microscopy (CL), XRF and XRD studies. A few samples were taken from precise horizons at outcrop Gleichenburg (Drei Gleichen area, Thuringia). Furthermore, several hundred samples from core MorsDp52a and different outcrops were analyzed with respect to their chemical and physical properties listed below. The sampling rates for the respective methods are given below.

### 2.2 Geochemical and Geophysical Methods

**X-Ray Fluorescence (XRF):** A huge data set of 1422 samples was provided with kind permission from H.-G. RÖHLING (BGR, Hanover) for core MorsDP52a. The resolution is about 10cm average, which allows very detailed studies on cyclicity. More than 200 samples from a profile of the Drei Gleichen area and 46 samples of the Funkenloch section (Hassberge, Bavaria) were analyzed using a PHILLIPS PW 2400 X-ray spectrometer at the Department of Geology and Mineralogy, at the University of Cologne.

**X-Ray Diffractometry (XRD):** The bulk composition of the samples was measured at the Department of Mineralogy at the University of Bonn using a SIEMENS D500 with Cu- $\gamma$  radiation, a W cathode and Ni filter. The filament was heated with 30mA at 40kV. The interpretation software was EVA 7.0. The clay mineral content was analyzed by PETSCHICK, R. at the Senckenberg Institute, at the University of Frankfurt.

**Cathode Luminescence Microscopy (CL):** Thin sections were polished and covered with a thin gold layer to avoid electrical discharge during the measure. Then the sections were analyzed using the CL system HC2-LM from SIMON-NEUSER at the Department of Geology and Mineralogy, at the University of Cologne.

**Carbon and Oxygen Stable Isotopes:** samples from core MorsDp52a were analyzed for their isotopic composition with a FINNIGAN MAT 252 gas spectrometer with an online carbonate precipitation line (CARBO-KIEL 1) at the Department of Geology, at the University of Erlangen. As detailed examinations (RICHTER, 1985) show that the carbonate phase of the dolomite beds of the Steinmergel Keuper playa system is merely stoichiometric the isotope data are given to the V-PDB standard and corrected according to ROSENBAUM AND SHEPPARD (1986).

**Magnetic properties:** Susceptibility and isothermic remnant properties from the samples from core MorsDp52a were measured at the Department of Geomorphology, at the University of Bayreuth.

**Carbon content:** The Total Carbon content TC, the Total Organic Carbon content and sulphur were measured with a LECO 225 at the Institute of Geology and Mineralogy at the University of Cologne. The Total Inorganic Carbon TIC was calculated as follows:

$$\text{TIC} = \text{TC} - \text{TOC}$$

Hence the carbonate content was calculated as follows:

$$\text{Carbonate [\%]} = \text{TIC} * 8.33$$

The results were compared with Mg and Ca contents determined by XRF analysis.

**Color Logging:** The colors of the two cores and several outcrops were measured with a spectrophotometer (CM2002 from Konica Minolta). The spectrophotometer is put on the sample and the flash is released. The light is diffusely dispersed in the Ulbricht chamber and the sample is homogeneously lit. The light that is reflected from the sample under an angle of 8° is captured by the sensor. The flash assures that that no atmospheric light is measured. Hence constant lighting conditions are given. The values are given in L\*a\*b\*- and L\*a\*c\*-coordinates. This method allows in contrast to classic color description (see also BRENNER, 1973 and SCHÜNKE, 1984), allows an objective and quantifiable differentiation of colors. It is also a quite fast method as no special sample preparation is needed. The sampling rate for core Malschenberg was about 3cm on average and for core MorsDp52a the sampling rate was about 1,3cm on average. For the Mönchberg outcrop (Baden Württemberg) and the outcrops in the Drei Gleichen area (Thuringia) the sampling rate is about 1cm average. For the outcrops Ifta (Thuringia) and Funkenloch (Hassberge, Bavaria) the sampling rate is about 5cm on average because of the worse outcrop preservation that did not allow a higher resolution rate.

One problem which one is confronted with when measuring at outcrops is the reproductivity of the measures. The measured color depends strongly on the humidity of the sample that changes the reflectance of the sample. As the weathering conditions changes continuously during the day the humidity may also change, so two measures taken at a different time may differ. But even if the values differ and a given value may not be reproducible the trends of a log do not change and cyclic changes are reproducible. This is true even for different outcrops that are spaced a few kilometers from each other (fig.14). Therefore color cycles can be used for stratigraphic correlation at a local scale. This is not necessarily true at regional scale as the color cycles might not be isochronous within the basin, i.e. a green/red cycle at the margin of the basin may have a dark gray/green equivalent in the central basin. Therefore, a detailed cyclostratigraphy is essential to perform a basin-wide correlation. That the measures must be

considered relatively implies that a given correlation between colors and elements, for example, can not be quantified. But it is possible to conclude some qualitative remarks.

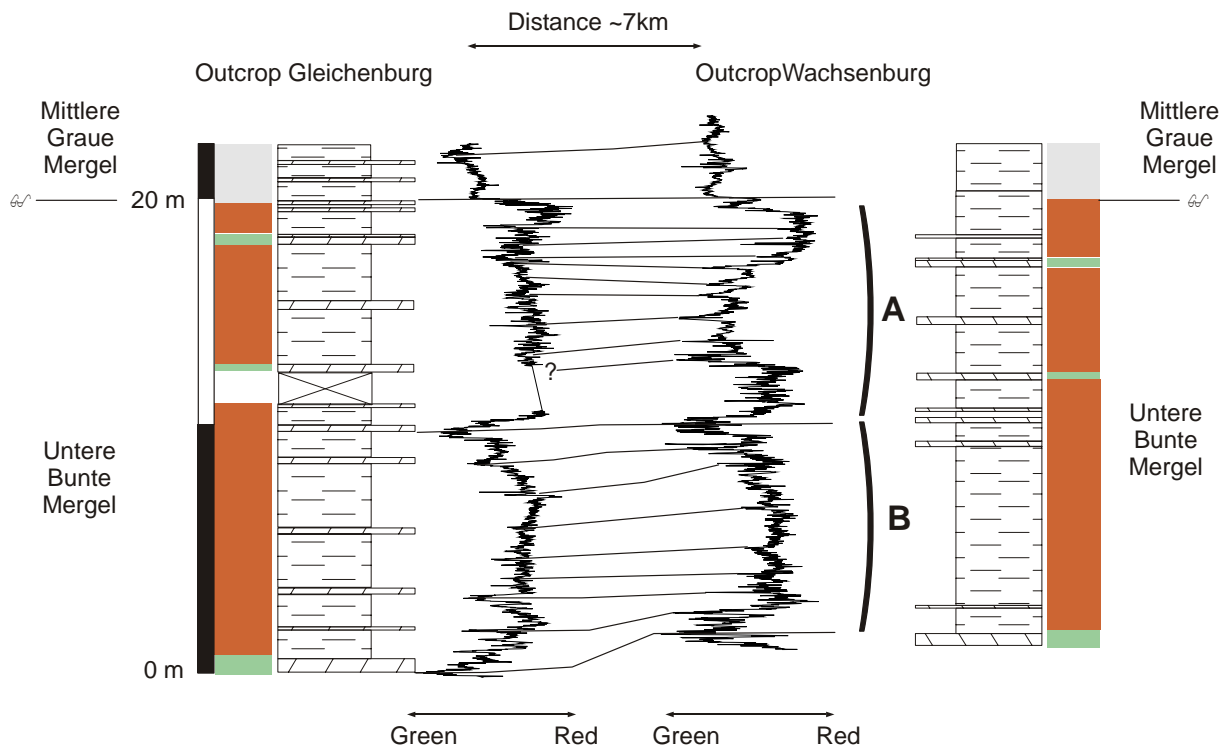


Fig.14: Two color plots from outcrops of the Drei Gleichen area (Thuringia). Even though the outcrops are spaced of  $\sim 7$ km apart the cycles are comparable. Both logs can be correlated and two major cycles (A and B) can be seen. Both cycles are further subdivided and correlated.

### Color Theory:

The biggest problem which occurs when describing colors is the subjectivity of the description itself. A first systematic approach was given by the artist Albert Munsell with his Soil Color Chart. Munsell uses a combination of letters and numbers according to the scheme H V/C. H represents the lightness (hue), V is the value and C defines the chroma. An extensive atlas was put forward by KÜPPER (1978).

Nowadays, numerical color systems are based on a system defined by the CIE (Comission International de l'Eclairage) in 1931. It is a  $Y_{xy}$  from where the norm values X Y Z are derived. The norm values take care of the fact that human beings perceive a mixture of green, red and blue. These values were also standardized by the CIE. This standard is composed of the spectral functions  $x(\lambda)$ ,  $y(\lambda)$  and  $z(\lambda)$  (fig. 15) that describes the spectral perception of a human being's eye.

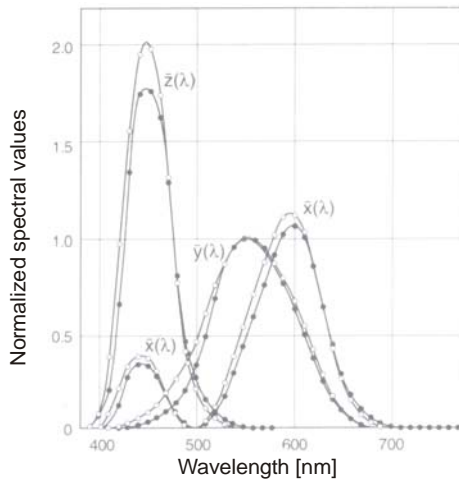


Fig. 15: Normal spectral curves. Black dots: 2° Normal observer. Circles: 10° Normal observer. With kind permission from Konika-Minolta

Based on these a two dimensional system which is independent from lightness was developed by the CIE. The values of the  $Y_{xy}$  are: Lightness reference value Y (= norm value Y) and the norm components x and y. The norm values are calculated as follows and plotted into a triangle:

$$x = X/(X+Y+Z)$$

$$y = Y/(X+Y+Z)$$

$$z = Z/(X+Y+Z) = 1-x-y$$

The resulting triangle (fig. 16) contains all visible colors.

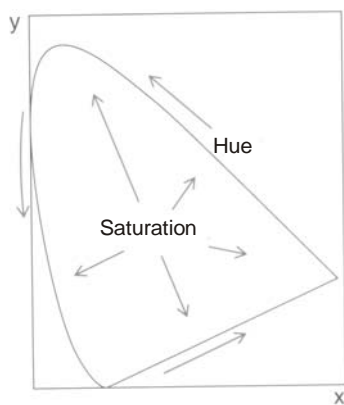
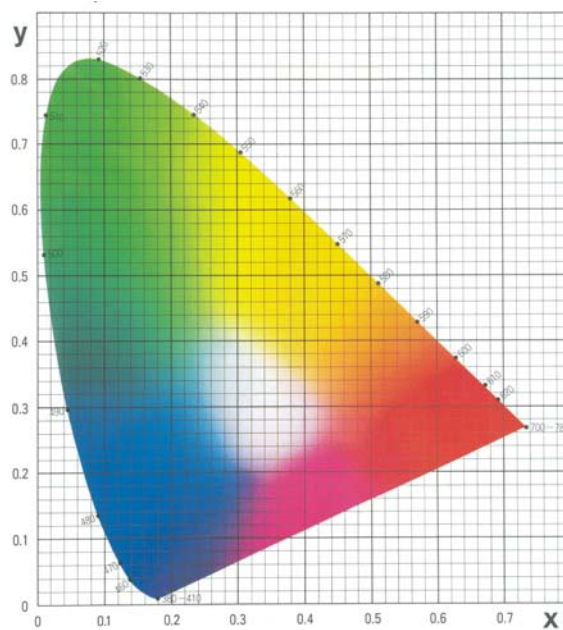


Fig. 16: Normal color table. With kind permission from Konika-Minolta.



The saturation is equal to zero in the center and the value rises towards the border. The cited values refer all to color divisions from small samples which fill a visible field of  $2^\circ$  ( $= 2^\circ$  normal observer). In 1964 an additional norm observatory of  $10^\circ$  was defined by the CIE.

From this color system several different color systems such as the  $L^*a^*b^*$ -, the  $L^*c^*h^*$ - system, the Hunter-Lab-Color-System and  $L^*u^*V^*$  color system are derived. In the following only the  $L^*a^*b^*$  color system is used. But the  $L^*c^*h^*$ - system is also explained as it's derived from the  $L^*a^*b^*$  color system.

**The  $L^*a^*b^*$  color system:** This is a three dimensional spherical space with orthogonal axes. The axes are defined by the lightness  $L^*$  and two color coordinates  $a^*$  and  $b^*$  (fig. 17 and 18). Both  $a^*$  and  $b^*$  define also the chroma of a color.  $-a^*$  corresponds to green and  $+a^*$  corresponds to red. Analogously to this  $-b^*$  is blue and  $+b^*$  is yellow.

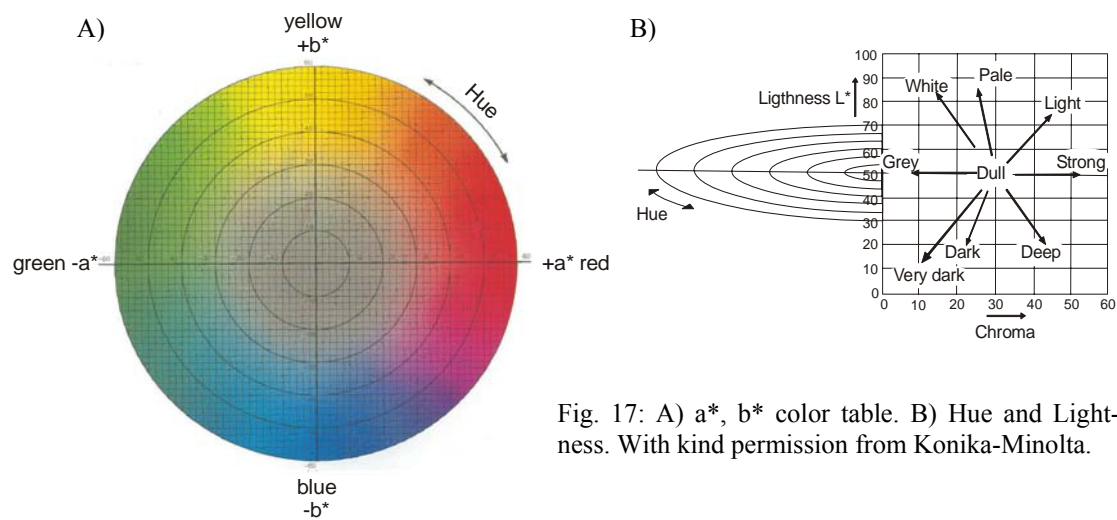


Fig. 17: A)  $a^*$ ,  $b^*$  color table. B) Hue and Lightness. With kind permission from Konika-Minolta.

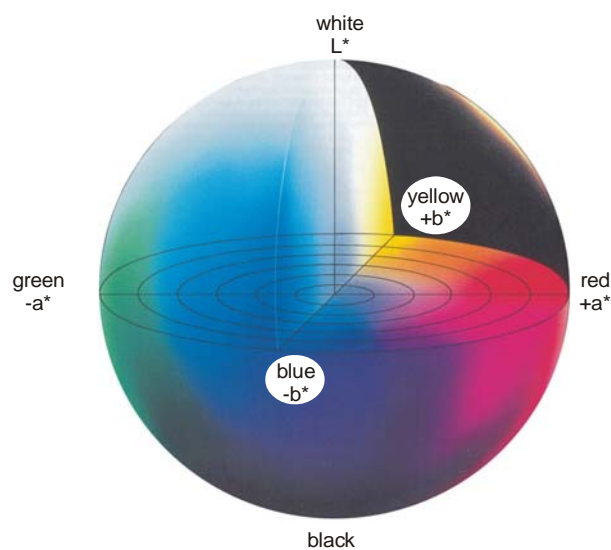


Fig. 18: 3D presentation of the  $L^*a^*b^*$ -color room. With kind permission from Konika-Minolta.

The values are calculated as follows:

$$L^* = 116(Y/Y_n)^{1/3} - 16$$

$$a^* = 500 \{ (X/X_n)^{1/3} - (Y/Y_n)^{1/3} \}$$

$$b^* = 200 \{ (Y/Y_n)^{1/3} - (Z/Z_n)^{1/3} \}$$

With X, Y and Z equal to the norm values of the sample (for 10° norm observer  $X_{10}$  ... respectively).  $X_n$ ,  $Y_n$  and  $Z_n$  are the norm values of of an ideal white reference sample. If the quotient  $X/X_n$ ,  $Y/Y_n$  oder  $Z/Z_n$  is less than 0,008856 then

$$L^* = 116 \{ 7,787(Y/Y_n) + 16/116 \} - 16$$

$$a^* = 500 * 7,787 \{ (X/X_n) - (Y/Y_n) \}$$

$$b^* = 200 * 7,787 \{ (Y/Y_n) - (Z/Z_n) \}$$

The values of the color difference between two samples is given by the formula :

$$\Delta E^*_{ab} = \{ (\Delta L^*)^2 + (\Delta a^*)^2 + (\Delta b^*)^2 \}^{1/2}$$

With  $\Delta L^*$ ,  $\Delta a^*$  and  $\Delta b^*$  equal to the difference of the  $L^*a^*b^*$  values between the sample color and reference sample.

**The  $L^*c^*h^*$ - system:** This is based on the same diagram as described above. Only the polar coordinates are used. The chroma and the angle are calculated as follows.

$$C^* = \{ (a^*)^2 + (b^*)^2 \}^{1/2}$$

$$h = \text{tg}^{-1}(b^*/a^*) [^\circ]$$

With  $a^*$  and  $b^*$  the coordinates are used within the  $L^*a^*b^*$  color system. When measuring the color difference the distance  $\Delta H^*$  is calculated instead of the angle:

$$\Delta H^* = \{ (\Delta a^*)^2 - (\Delta b^*)^2 - (\Delta C^*)^2 \}^{1/2}$$

$\Delta H^*$  is positive if the angle of the sample is bigger than the angle of the reference color, otherwise  $\Delta H^*$  is negative.

## 2.3 Frequency Analysis

A crucial question in earth sciences is the interpretation of changes within the earth's history. These changes may vary significantly through time. Some of the most intriguing changes are climatically induced (Milankovitch Theory). Frequency analysis provides a powerful tool to predict climatic changes within the earth history. This kind of analysis is based on a Fourier transformation (FT). The basic idea using this kind of analysis is that all kind of periodic signal or process can be expressed as a function of harmonic oscillations (compiled from TRAUTH, 2005):

$$x(t) = A_0 \cdot \cos(2ft - \Psi)$$

With  $A_0$  = frequency,  $t$  = time and  $\Psi$  = angle of phase.

A harmonic process is the sum of several oscillations with differing amplitude, frequency and phase:

$$x(t) = A_i \cdot \cos(2f_i t - \Psi_i)$$

If a given continuous signal is transformed into a discrete signal by observing the signal with defined time interval  $\Delta t$  then the sampling frequency is given as

$$f_A = 1 / \Delta t$$

and the maximum resolution of a signal without loss of information is expressed by the Nyquist – frequency that should be twice of the thickness of the analyzed cycle:

$$f_{Nyq} = 1/2 \Delta t$$

i.e. the frequency must have twice the sampling rate of the given time interval. The descriptions are given as a function of time, but the same process can be described as a function of the frequency

$$X(f) = \int_{-\infty}^{\infty} x(t) e^{-2\pi f t} dt = \int_{-\infty}^{\infty} [x(t) \cos(2\pi f t) - i x(t) \sin(2\pi f t)] dt$$

With  $-\infty < f < +\infty$  and  $i$  = imaginary unit.

This calculus has the problem that the data set must be equidistant. But in general paleoclimatic data sets are not equidistant. This problem is solved by the LOMB-SCARGLE algorithm (PRESS et al, 1992). The algorithm is based on the works of LOMB (1976) and SCARGLE (1982, 1989). These methods provides an estimation of the spectrum by fitting the harmonic sinus and co-sinus components to the data set with the method of the lowest square error.

Frequency analyse were performed with the program SPECLAB (with courtesy from GUIDO PORT) which uses the LOMB-SCARGLE algorithm. This program is able to analyze xy-data sets, i.e. time or depth against any variable can be analyzed.



## 2.4 Milankovitch Theory

The research on past climates and cyclic changes within the sedimentary record lead to one of the most remarkable theories in earth sciences: the Milankovitch theory. This theory put forward by MILUTIN MILANKOVITCH (1941) is based on the fact that the yearly earth's insolation varies as a function of the earth's orbital parameters and these variations might be recorded in sediments. The variations of the orbital parameter are caused by the gravitational effect of the sun, the moon and the other planets.

The most important parameters affecting the earth's insolation can be summarized as follows (fig.19):

- A) The eccentricity of the earth's orbit changes the earth-sun distance during one year and has the present periods 100ka and 400ka. Changes within the eccentricity control the amount of insolation during perihelion i.e. when the earth is nearest to the sun and aphelion i.e. when the earth is farthest from the sun. Eccentricity determines also the length of a season.
- B) The obliquity (or tilt) is the inclination of the earth axis of rotation. Its variation from  $21.8^{\circ}$  to  $24.4^{\circ}$  (BRADLEY, 1985) has a mean period of 41ka but extremes of 29 ka and 54ka can also occur. The summer insolation of the north increases with increasing tilt (HAY et al) i.e. the summers get hotter during these times and the winters get colder (BROECKER AND DENTON, 1990). This is an effect which affects mainly high latitudes.
- C) The precession of the elliptical orbit itself is on a 105ka timescale. This precession changes the time when earth is closest to the sun.
- D) The precession of earth's axis of rotation with a period of 27 ka.
- E) The precession of the equinoxes which results from a combination of the effects of the precession of the earth's axis and the precession of the elliptical orbit of the earth with a period of 21.7ka. But extreme periods of 14ka and 28ka can also appear (BERGER AND TRICOT, 1986). The precession of the equinoxes results in a slow shift of the equinoxes (currently March 21 and September 22) and the solstices (currently June 21 and December 21). So the insolation of a given seasons changes through time i.e. a season is strengthened or weakened because of the changing distances to the sun.

A table with the values for the Triassic (BERGER AND LOUTRE, 1989, 1994) is provided within chapter 5, *Controlling Processes of Cyclicality*.

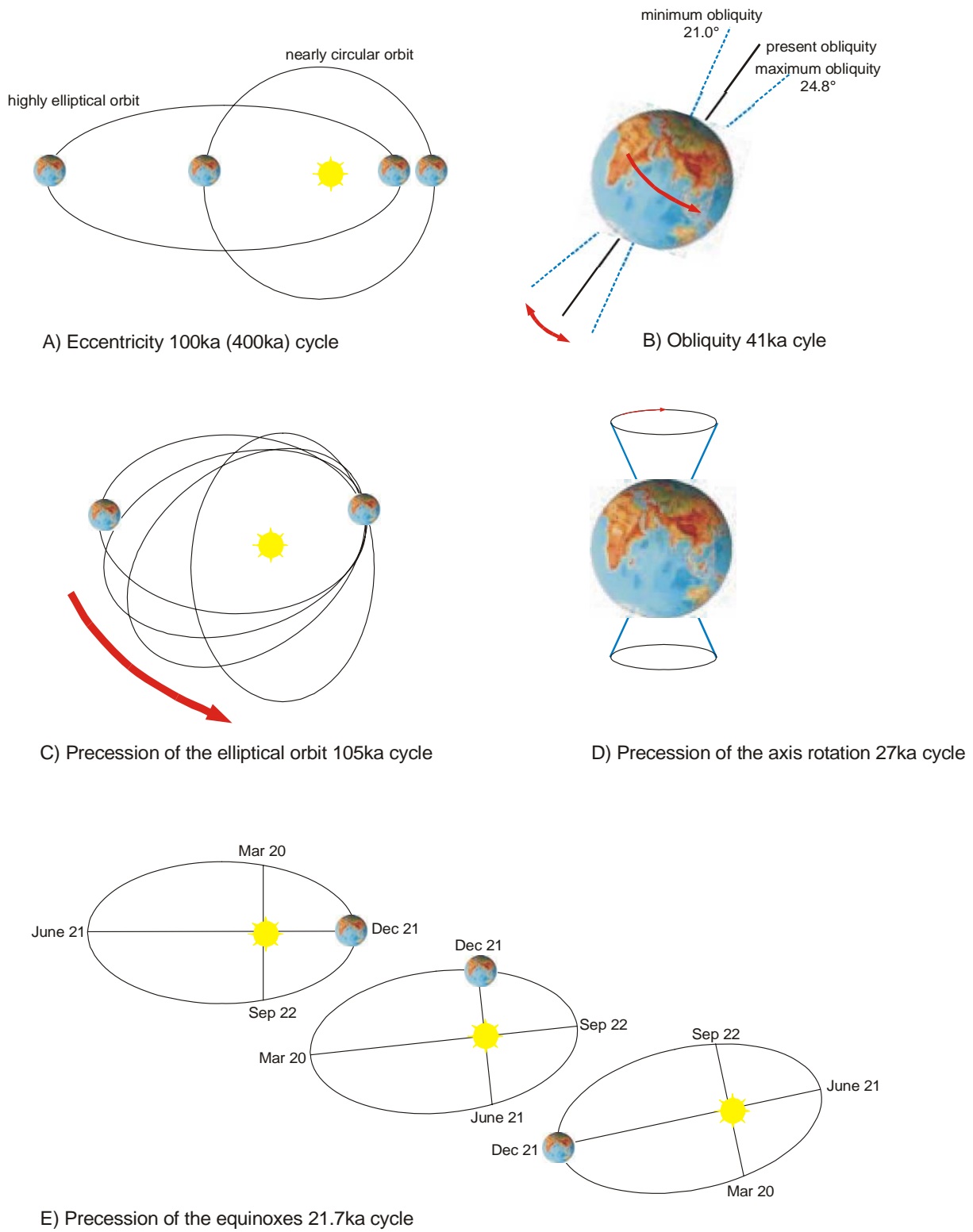


Fig. 19: Milankovitch cycles affecting the earth's insolation.  
 From FLÖGEL 2001, after BERGER, 1992 and HAY et al., 1997.

## 3 Playa Facies

### 3.1 Introduction

#### 3.1.1 Definition and Setting of Playa Systems

The term playa is used strictly in sense ROSEN (1994) who defined a playa with following characteristics:

- 1) *The basin must be intracontinental, i.e. the shallow regional groundwater system is usually closed and does not directly discharge into the ocean.*
- 2) *The water balance of the lake (all sources of precipitation, surface water flow, and groundwater flow minus evaporation and evapotranspiration) must be negative for more than half the year, and the annual water balance should also generally be negative.*
- 3) *The capillary fringe is close enough to the surface of the playa such that evaporation will cause water to discharge to the surface.*

Following the given definition the terms *sabkha* and *salina* are used for marine influenced settings (ROSEN, 1994). This definition of playa with an overall negative water balance, i.e. evaporation always exceeds inflow implies a semi-arid to arid setting of the playas. These climate zones are situated nowadays within two belts approximately 20° to 40° paleolatitude (fig. 20).

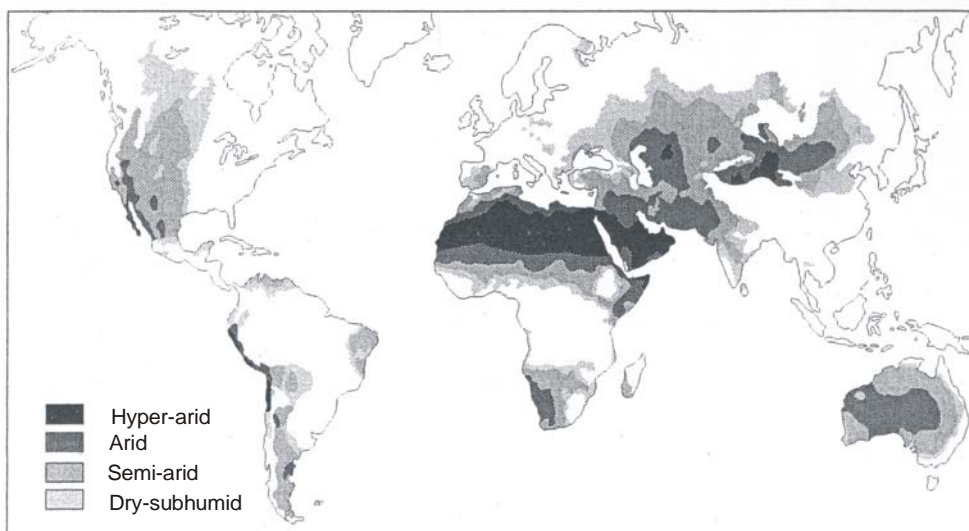


Fig. 20: Global distribution of drylands (after UNEP 1992, from THOMAS, 1997).

### 3.1.2 Classification and Evolution of Playa Systems

Within their position evaporate basins are classified in continental playas (no marine influence), salinas and sabkhas (both influenced by marine waters; fig. 21).

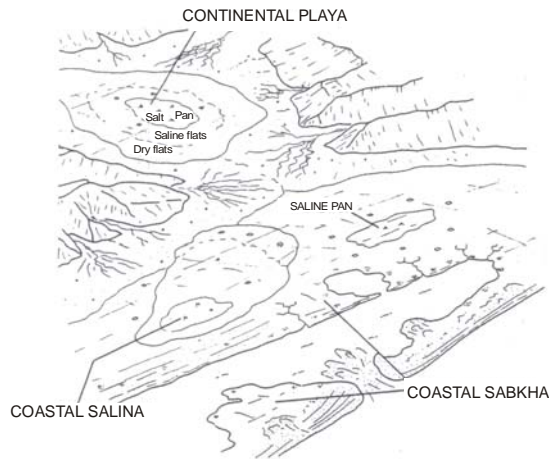


Fig. 21: Modern evaporitic basin environments. After KENDALL (1992).

One of the most important features of evaporitic basins is their hydrological system, which characterizes their evolution depending on the inflow and outflow of the waters concerned. ROSEN (1994) pointed out the importance of the corresponding hydrological system of an evaporitic basin. Depending on whether playas are hydrologically closed or open they are called discharge playas (closed basins) and through flow playas (open basins). In closed playas if the capillary fringe is close enough to the surface the discharge is provoked by evaporation of the water. If the capillary fringe is deep enough a dry playa will develop.

The water input may be originally caused by incoming groundwater, hydrothermal waters, perennial or ephemeral rivers and/or direct precipitation over the playa. Depending on the chemical composition of the inflow five major brine types can develop (EUGSTER AND HARDIE, 1978):

- 1) Ca-Mg-Na- (K)-Cl
- 2) Na-(Ca)-SO<sub>4</sub>-Cl
- 3) Mg-Na-(Ca)-SO<sub>4</sub>-Cl
- 4) Na-CO<sub>3</sub>-Cl
- 5) Na -CO<sub>3</sub>- SO<sub>4</sub>-Cl

Each of these water concentrates leads to a characteristic succession of evaporates and mineral precipitation path (fig. 22). If is enriched in HCO<sub>3</sub> compared to Mg and Ca then the brine will follow path I. If it is depleted in HCO<sub>3</sub> compared to Mg and Ca than path II will be followed. Finally, if HCO<sub>3</sub> is more or less equal to Mg and Ca the path III will develop. The Steinmergel Keuper is mainly characterized by brine type 3 (see also REINHARDT 2002).

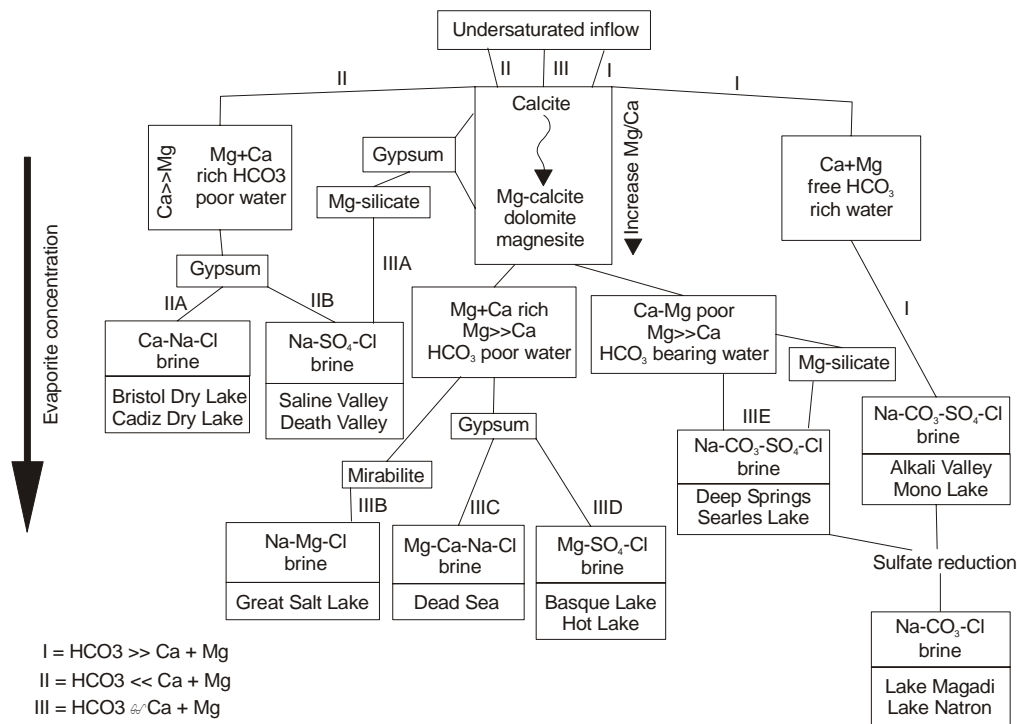


Fig. 22: Hydrologic classification and brine evolution pathways of concentrated non marine waters. From WARREN (1999); after EUGSTER AND HARDIE (1978).

But the initial divisions for brine types as shown above may depend more on the leakage ratio than on the lithology of the surrounding basin (WOOD AND SANFORD (1990), SANFORD AND WOOD (1991) and the scheme above is only valid for entirely closed basins. Furthermore, whether a certain evaporate sequence develops in playas depends not only on the original brine composition but also on the inflow/evaporation rate ratio (fig. 23).

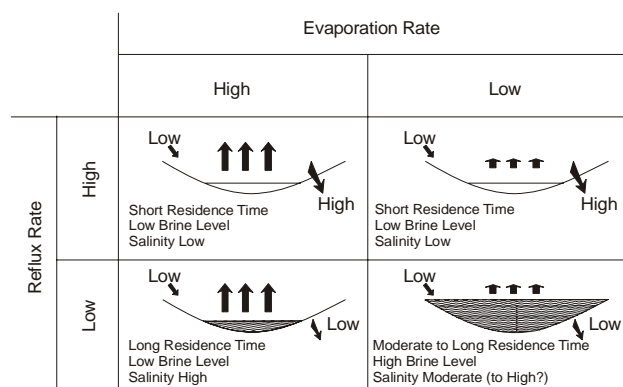


Fig. 23: Models of isolated evaporate basins. Evaporative drawdown occurs in response to low influx rates (relative to evaporation). Deep water evaporates only form in basins with low reflux and evaporation rates. All others dry out. From KENDALL (1984).

If the evaporation rate exceeds the water influx the playa imperatively dries out. Preservation of a perennial lake needs temporary water input and/or lowering of the evaporation rate. In a perennial playa lake sub aqueous evaporates can form (fig. 24a) and during brine evolution evaporates might even form displacively in the existing sediments. When the brine is diluted by input of fresher water crystallisation finishes (fig. 24b). When the playa dries out completely, i.e. no fresh water, the surface of the playa is sub-aerially exposed and in capillary

equilibrium with the water table (fig. 24C) a classic mudflat develops and no higher salts will accumulate. Existing evaporates might be eroded by deflation.

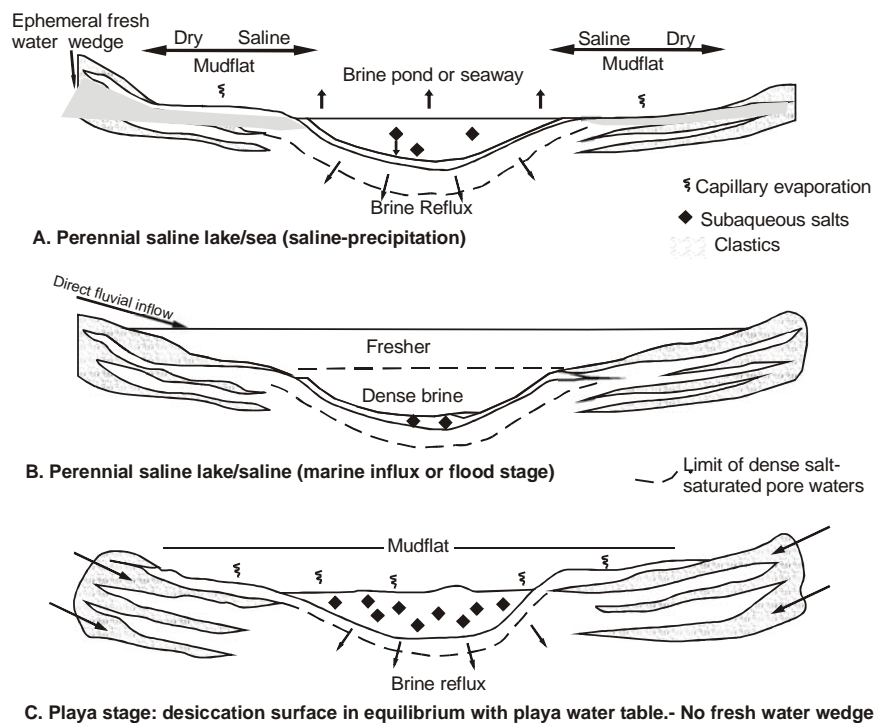


Fig. 24: Cross section hydrological stages in the active phreatic zone in an evaporitic seaway or continental playa system. From WARREN (1999).

Some other important features of playas which influence the brine composition are:

- The reworking of evaporates and efflorescent crust during dilution of the brine when the playa is flooded.
- Early diagenetic reactions as the formation of clay minerals for example may change the ionic composition of the brine significantly as the ions are removed from the pore waters during mineralisation.
- Biological metabolism might form an important contribution to chemical composition during brine evolution. The importance of biological activities in Australian playa lakes has been reported by several authors (HAMMER (1981), BOWLER (1981), HINES et al. (1992)). This primary productivity highly influences the further availability of ions such as phosphorous, silica, sulphur a. o.

### 3.1.3 Depositional Environments

The different environments for playa systems have been widely described by a variety of authors such as WARREN (1989, 1999), MELVIN (1991), KENDALL (1992) etc. Generally a playa shows a typical facies zonation from the playa lake in the central basin over the saline mudflat, the dry mudflat, the sandflat to the alluvial fan at the margin of the basin. After EUGSTER AND HARDIE (1978) three arid zone settings can be differentiated:

- Alluvial/terminal fan – ephemeral saline lakes.
- Ephemeral stream floodplain – dune field – ephemeral saline lakes.
- Perennial stream floodplain – perennial saline lakes.

The alluvial fan – ephemeral saline lakes depositional complex occurs in tectonically active areas. Inflow is predominantly from groundwater, hydrothermal waters and sometimes storm events. This setting contains often extensive dry mudflats (fig. 25). Modern examples are intermountain basins in Tibet and Mongolia etc.

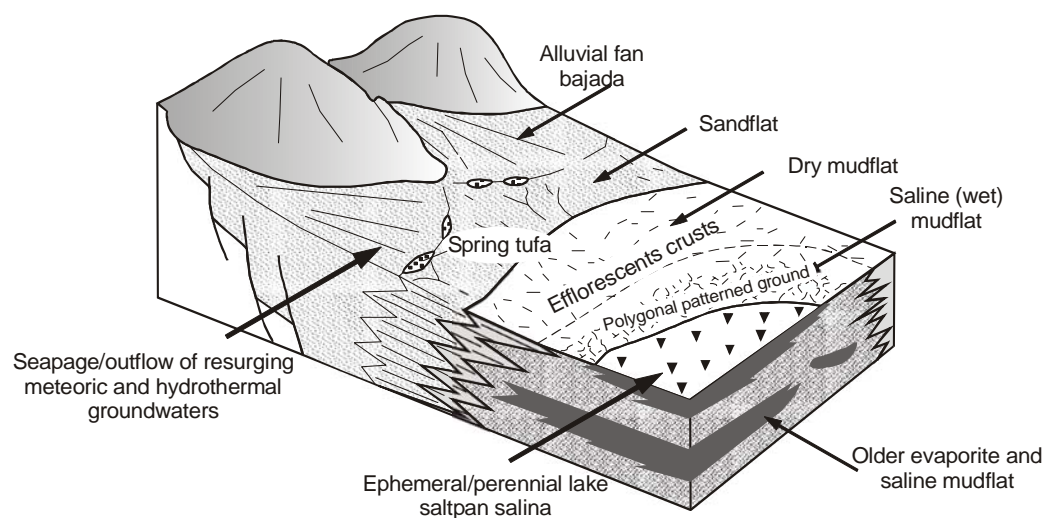


Fig. 25: Continental playa showing the different facies and processes of water supply. From WARREN (1999), in part after KENDALL (1992), EUGSTER AND HARDIE (1978).

The ephemeral stream floodplain – dune field – ephemeral saline lake complex is found in tectonically rather inactive zones associated with arid zone subtropical high pressure belts. The mudflat is less extensive than in the alluvial fan – ephemeral saline lakes complex. Higher salts are often reworked by flooding events and not well preserved. Dune fields occurring are derived by reworked material from floodplain and lake sediments during dry periods. A modern example is Lake Eyre in Australia and a fossil counterpart is the Steinmergel Keuper playa system (fig. 26).

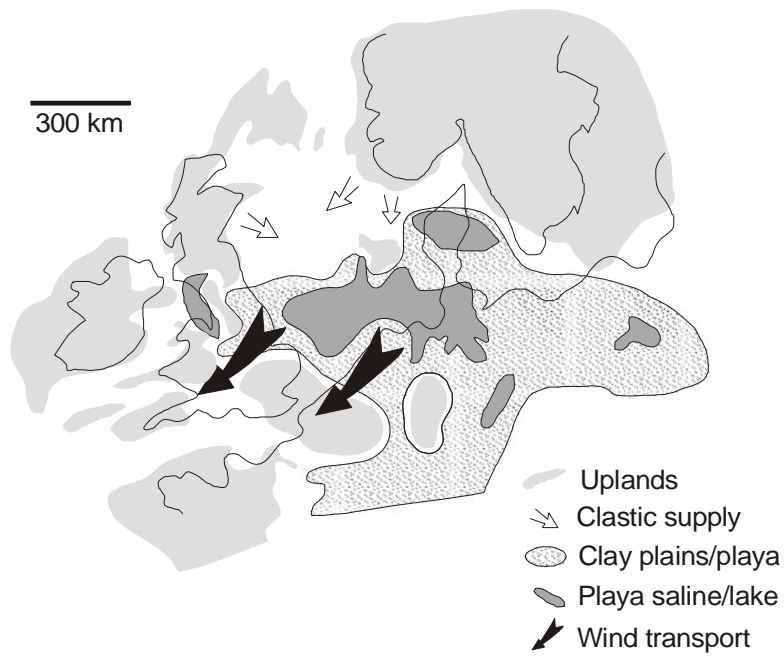


Fig. 26: Example from the Steinmergel Keuper playa system showing how deposition was mainly in a closed basin and wind was blowing dust from mudflats. From WARREN (1999), after TALBOT et al. (1994).

Perennial stream floodplain – perennial saline lakes are presented in various tectonic settings. In general their deposits lack extensive mudflats. The water supply is more permanent than in the two cases mentioned above and steep slopes characterize the perennial lakes. Modern examples are the Dead Sea, Israel and Great Salt Lake, USA.



### 3.2 Clay Mineralogy

#### Description

A screen of 29 samples from core MorsDp52a from Morsleben, Allertal, Saxony Anhalt and 5 samples from dolocrête horizons from Gleichenburg outcrop, Drei Gleichen area, Thuringia were measured for their clay mineral content. The following phases could be distinguished:

- Quartz in small amounts.
- Feldspar (probably albite).
- Small amounts of smectite.
- Mixed layer illite-smectite (regular and irregular).
- Illite (main component) unsorted with raising crystallinity from the top to the bottom of core MorsDp52a.
- Chlorite (with clear portions of vermiculite). Both chlorite and vermiculite are Mg rich. A separation of vermiculite from chlorite was not possible due to the small amounts and the strong overlapping with corrensite.
- Corrensite: chlorite-vermiculite or chlorite-smectite or vermiculite-smectite, a further separation was not possible. The smectite content is probably between 40% and 60%.
- Analcime and Zeolithe (maybe heulandite or clinoptinolithe), but only at the bottom of core MorsDp52a. Both minerals were also not found in the five samples from the dolocrêtes from the Gleichenburg outcrop.
- Neither kaolinite and nor palygorskite were found.

Fig. 27 shows the logs of the clay minerals for core MorsDp52a. It can be seen that illite and the sum of smectite and mixed layer illite-smectite (regular and irregular) show a strong antagonistic pattern. The illite curve raises and diminishes cyclically. Chlorite and corrensite are generally covariant. Their highest peaks coincide with red mudstones, but some chlorite and corrensite are also developed within the green/gray dolomites. Analcime and zeolithes are developed within the first 55m. Smectite is most abundant within green/gray dolomites.

The cyclic pattern of the Na/(Mg +Ca) ratio indicates changing salinities during flooding and evaporation (fig. 27). During times of analcime and zeolithe formation the ratios are also heightened.

The clay mineralogy for the dolocrête horizons at the Drei Gleichen area is more or less the same, with the exception that analcime and zeolithes are not developed (Annexes).

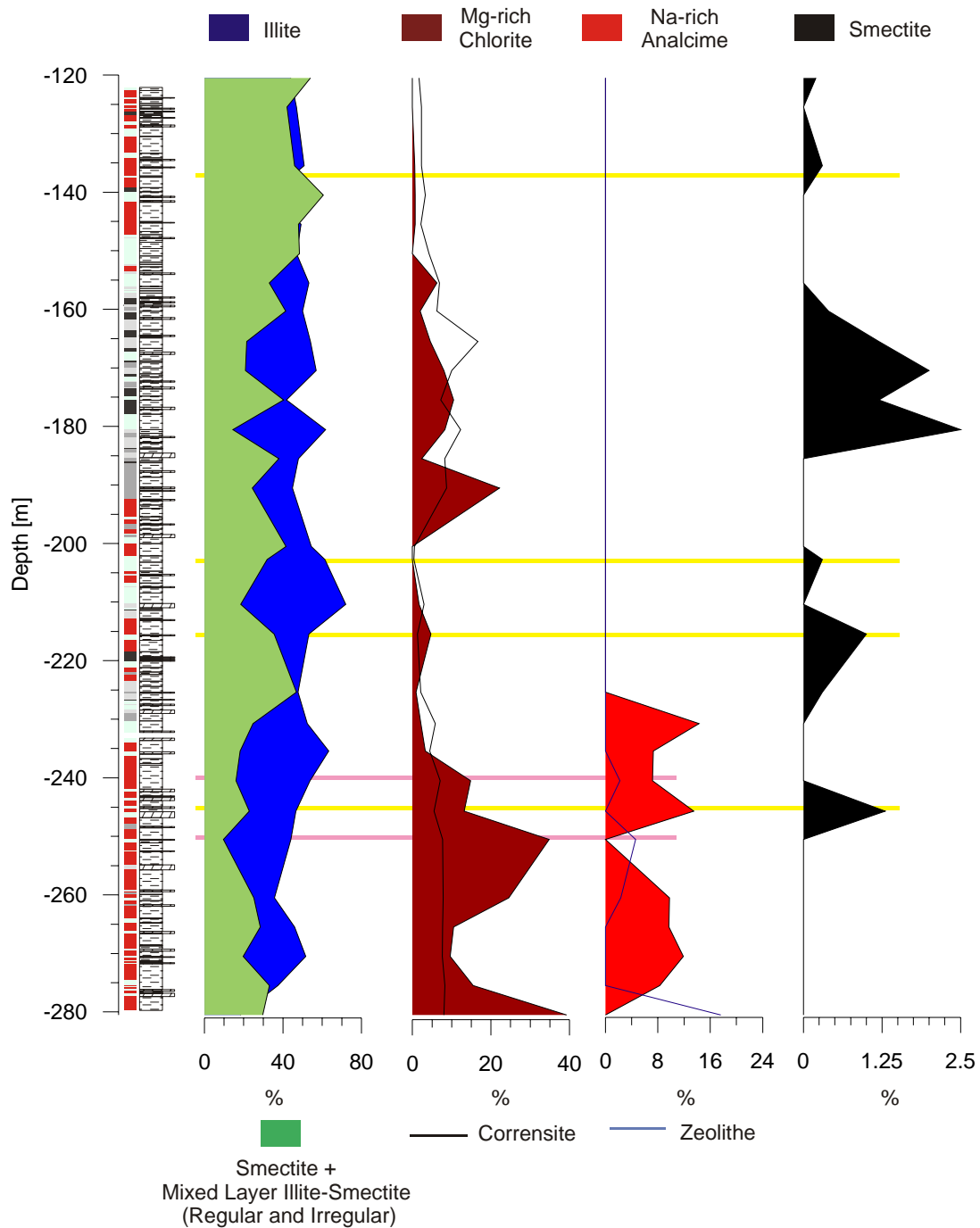


Fig. 27: Clay mineral logs. Note that analcime and zeolites are only developed at the lower part of the playa system and smectite are related to dolomites. For explanations see text. Screen of 29 samples from core MorsDp52a.

An important indicator for cyclic climate changes is the dolomite content. It can be calculated as follows (see also the *Methods* chapter).

$$\text{Dol. [\%]} = \text{TIC} * 8,33 = (\text{TC} - \text{TOC}) * 8.33$$

Where: Dol. = dolomite

TC = Total Carbon

TOC = Total Organic Carbon

TIC = Total Inorganic Carbon

Fig. 28 shows a very good linear correlation between the dolomite content and the sum of MgO and CaO. That means, MgO + CaO reflects mainly the dolomite content and can therefore be used as a proxy for cyclic dolomite precipitation. Some of the Mg is incorporated into clay minerals, but only a minor proportion. The same can be said for Ca that is incorporated in gypsum. Thus the cyclicity reflected is mainly due to variation in the dolomite content.

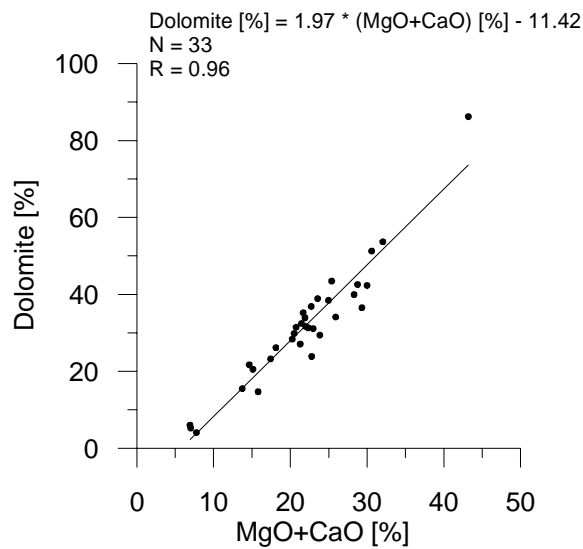


Fig. 28: Correlation between the dolomite content and the sum of Mg- and Ca-oxides from core MorsDp52a (Screening of 33 samples).

The climatic changes can also be described by ternary dolomite-silica-aluminium diagrams (fig. 29) reflecting cyclic changes between dolomites (wet periods) and marls (dry periods). This is a pattern that can be observed at all scales (see below). The type of clay minerals is well characterized by their high variation of the Si/Al- and the K/Al ratio.

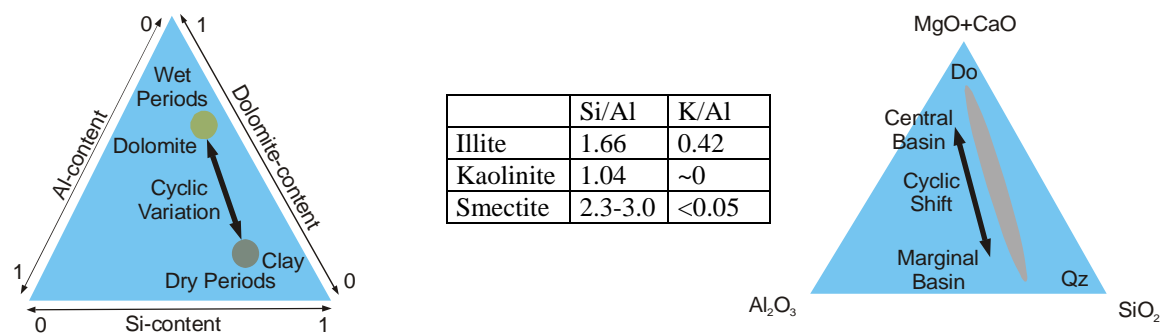


Fig. 29: Left: schematic plot showing the relationship between chosen elements, mineralogy and climatic conditions under which the minerals precipitate. The Element ratios of the clay minerals are calculated after RACHOLD 1994. Right: schematic plot showing the cyclic shift of elements and minerals depending on their position within the playa system.

Comparing the element spectra and clay mineralogy (fig. 30 and fig.31) a clay phase is characterized by the fact that with diminishing dolomite content the silica content and aluminium content rise. This can be attributed to the presence of illite. With raising dolomite content and therefore diminishing silica and aluminium content the clay minerals show a clear shift toward smectite and mixed layer illite-smectite (fig. 30, left). A similar pattern can be observed in the right diagram (fig. 30): the chlorite content rises as the illite content diminishes.

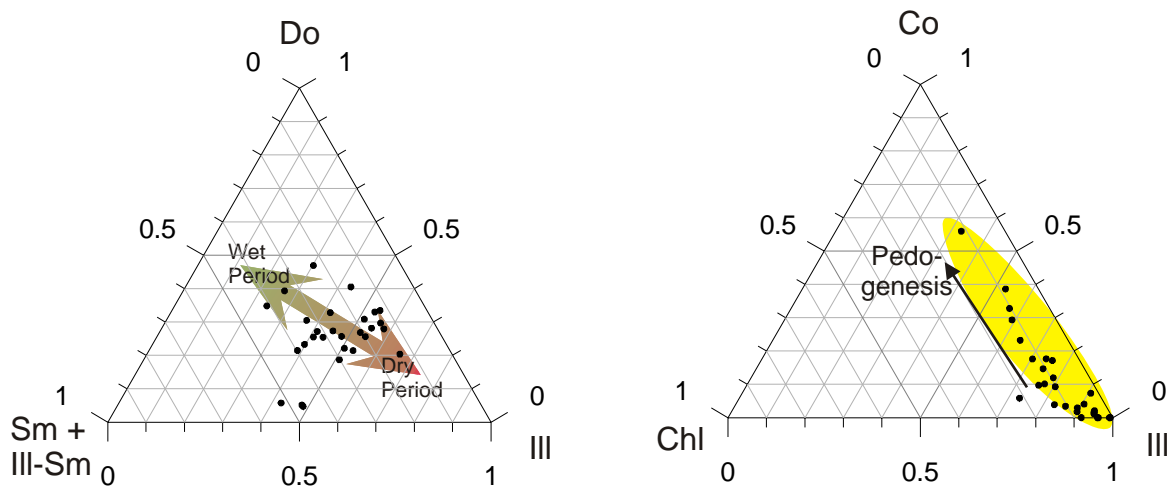


Fig. 30: Ternary Diagrams of clay minerals. Screen of 29 samples from core MorsDp52a. Do: dolomite, Ill: illite, Sm: smectite, Ill-Sm: mixed layer illite-smectite (regular and irregular), Chl: chlorite, Co: corrensite. The dolomite content was calculated as explained in the *Methods* chapter.

The diagrams below show the relation between  $(\text{MgO} + \text{CaO}) - \text{Al}_2\text{O}_3 - \text{SiO}_2$ . The shift between dolomite and quartz is the most evident one, but the shift between illite-(smectite + mixed layer illite-smectite) is also obvious. Both shifts are overlapping and reflect the climatic change from flooding (wet periods) to evaporation (dry periods).

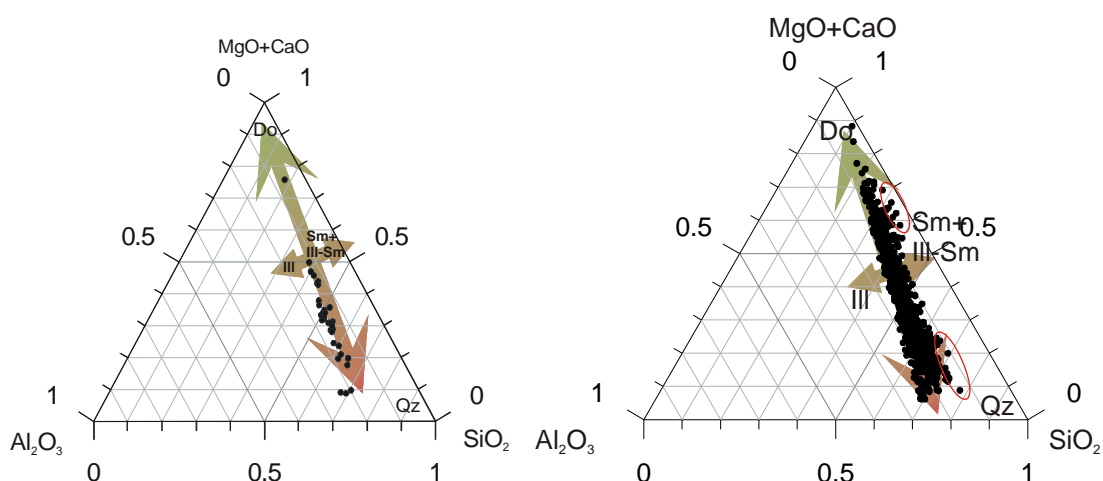


Fig. 31: Ternary diagrams of chosen elements and element ratios from core MorsDp52a. Left: screening of 33 samples, own data. Right: 1422 measures with a resolution of 10cm, data by courtesy of H.-G. RÖHLING, NLFb, Hannover. Do: dolomite, Qz: quartz Ill.: illite, Sm.: smectite, Ill.-Sm.: mixed layer illite-smectite (regular and irregular). The shift between the end members dolomite-quartz and illite-(smectite + mixed layer illite-smectite) is well visible in both diagrams.

## Interpretation

Quartz, feldspar and illite can be interpreted as of clastic origin.

Illite can be degraded to mixed layer illite-smectite during weathering and if weathering is continuous smectite is formed. To weather illite a potassium-depleted environment is necessary (HEIM, 1990) so that the exchange of  $K^+$  from illite and  $Ca^+$  and  $Na^+$  from the surrounding lake waters can take place. During times of increased rainfall, i.e. increased monsoonal activity, the potassium content within the playa lake is lowered and degradation of illite might happen. Conversely, during times of evaporation the playa system became enriched in potassium and the inverse process, i.e. aggradation of illite, may have taken place. Under surficial conditions aggradation of illite in a saline environment can happen if the lake waters are rich enough in potassium (DECONNINCK, 1988). This implies a repeated succession of flooding and evaporation of the lake waters. Illitisation of smectite probably needs only a succession of 40 flooding/evaporation events (SRODON & EBERL, 1984). The formation of smectite from illite under surficial conditions is favored by the presence of high  $Mg^+$  and/or  $Fe^{2+}$  concentrations (HARDER, 1972, 1978).

Under surficial conditions chlorite is generally formed by the decomposition of mafic minerals such as amphiboles and pyroxenes. However, if the pH and the  $Mg^+$  concentration are high enough chlorite can also be formed during early diagenesis.

Vermiculite can be formed with the right conditions during early diagenesis. The neoformation of vermiculite from chlorite during pedogenesis is also possible (DROSTE et al 1962, SCHWERTMANN 1976). This happens in a slightly acid environment. On the other hand a chloritisation of vermiculites happens under elevated pH values.

Corrensite can be formed during weathering from chlorite (BRIGATTI & POPPI, 1984) but it also appears during soil formation (JOHNSON, 1964). Another possibility is the neo formation during early diagenesis under semi arid conditions with elevated  $Mg^+$  concentrations. SCHLENKER (1971) and SCHÜLE (1974, fig. 32 assume an early diagenetic origin for the corrensite and also for the chlorite within the Keuper basin.

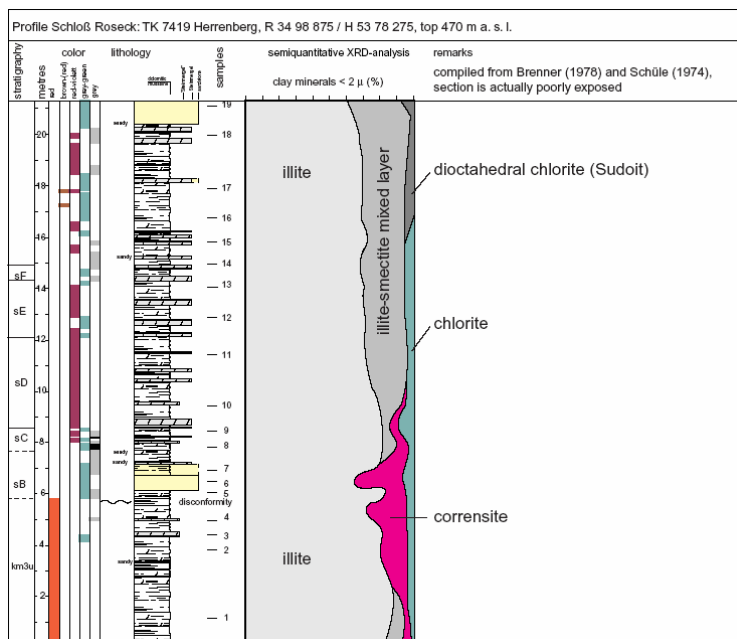


Fig. 32: Example of clay mineral distribution in a profile (Schloß Roseck near Herrenberg). Semi-quantitative clay mineral analyses from SCHÜLE (1974) combined with profile description of BRENNER (1978). At present, the profile is only poorly exposed. Illite is the predominant clay mineral associated with an illite-smectite mixed layer mineral in varying amounts. The mixed layer clay mineral is completely replaced by corrensite during km3su. Additionally, some chlorite is present that is replaced towards km4 by a di-octahedral chlorite (Sudoit). From REINHARDT, 2000.

The fact that the presence of palygorskyte could not be demonstrated is due to the low sampling resolution (29 samples over 162m). The presence of chlorite, corrensite and analcime indicate that a high cation concentration ( $K^+$  and  $Mg^{2+}$ ) and a high pH (analcime and opal {see also chapter *XRF Analysis*) value were present. Hence formation of palygorskyte could have happened. However, the existence of palygorskyte within the playa system was shown by LEWANDOWSKY (1988) in the Osnabrücker Bergland. Other important analyses on clays in the Steinmergel Keuper were performed by CHRISTMANN et al (1990) and ALDINGER (1965).

Summarizing it can be said that the clay minerals within the Steinmergel Keuper playa system might have been formed during early diagenesis strongly influenced by a repeated succession of flooding and evaporation events. This succession of flooding/evaporation led to cyclic changes within the lake water chemistry which is traduced by the cyclicity of the clay minerals (fig. 27). This is also suggested by the ternary diagrams (fig. 30) which shows a clear dependency of smectite + mixed layer illite-smectite (regular and irregular) on the dolomite content. The dolomite represent wet phases. Therefore, smectite + mixed layer illite-smectite (regular and irregular) were formed during wet phases. This happens at all scales as is suggested by XRF data set (fig. 31 and chapter 4.1 *XRF Analysis*) which show a strong cyclic pattern. Pedogenetic processes during evaporation times, in other words during dry periods, can not be totally excluded as suggested by the indirect hint of vermiculite in association with chlorite.

Astonishingly, at the base of the MorsDp52a section analcime and zeolithes are present. Both minerals are indicators of an sodium enriched system. In continental domains analcime and zeolithes are product of weathered volcanic material, i.e. ashes and tuffa (BLATT et al. 1972, VELDE, 1995). But they are also described from continental basins in absence of volcanoclastic detritus. A well documented recent example is the recent Lake Natron, Tanzania (HAY, 1966). It is a shallow lake in an arid climate with highly enriched brine. The pH value measured is 9.7. It sources are alkaline springs, reworked salts, surficial weathering and lavas at the south end of the lake (BLATT et al. 1972). Neither volcanic glass nor nepheline has been found in the lake sediments.

One of the best-known fossil example is the lacustrine Lockatong Formation (Triassic) of New Jersey and Pennsylvania described by VAN HOUTEN (1962). The formation is a huge lens composed a series of cyclic lacustrine deposits of detritical and chemical sequences. After VAN HOUTEN (1962) the chemical sequences were deposited during dry periods with limited rainfall and/or high evaporation rates. This increased the soda content and also the Na/Ca and Na/Mg ratios because of the removal of the ions concerned from the lake water during calcite and dolomite precipitation. Finally salts were deposited on the mudflat and reworked with the next flooding event.

Similar processes are assumed to be responsible for the analcime and zeolithe formation within the Steinmergel Keuper playa system. During times of rainfall, i.e. wet periods, Na was dissolved and during evaporation, i.e. dry periods Na was used to form analcime. The source of the sodium is probably formed by Permian salts that came up because of diapirism caused by tectonic movements. The location of the section studied is nearby the Allertal fracturation zone, which was active in these times. This tectonic phase is known as the *Old Kimberian Phase* (BEUTLER, 1998). WALTER (2002) found that important depressions in the Allertal were caused synsedimentarily by the tectonic movements and the salt diapirism. The sediment thickness ranges from ~50 over the top of salt diapirs to more than 250m within the depressions.

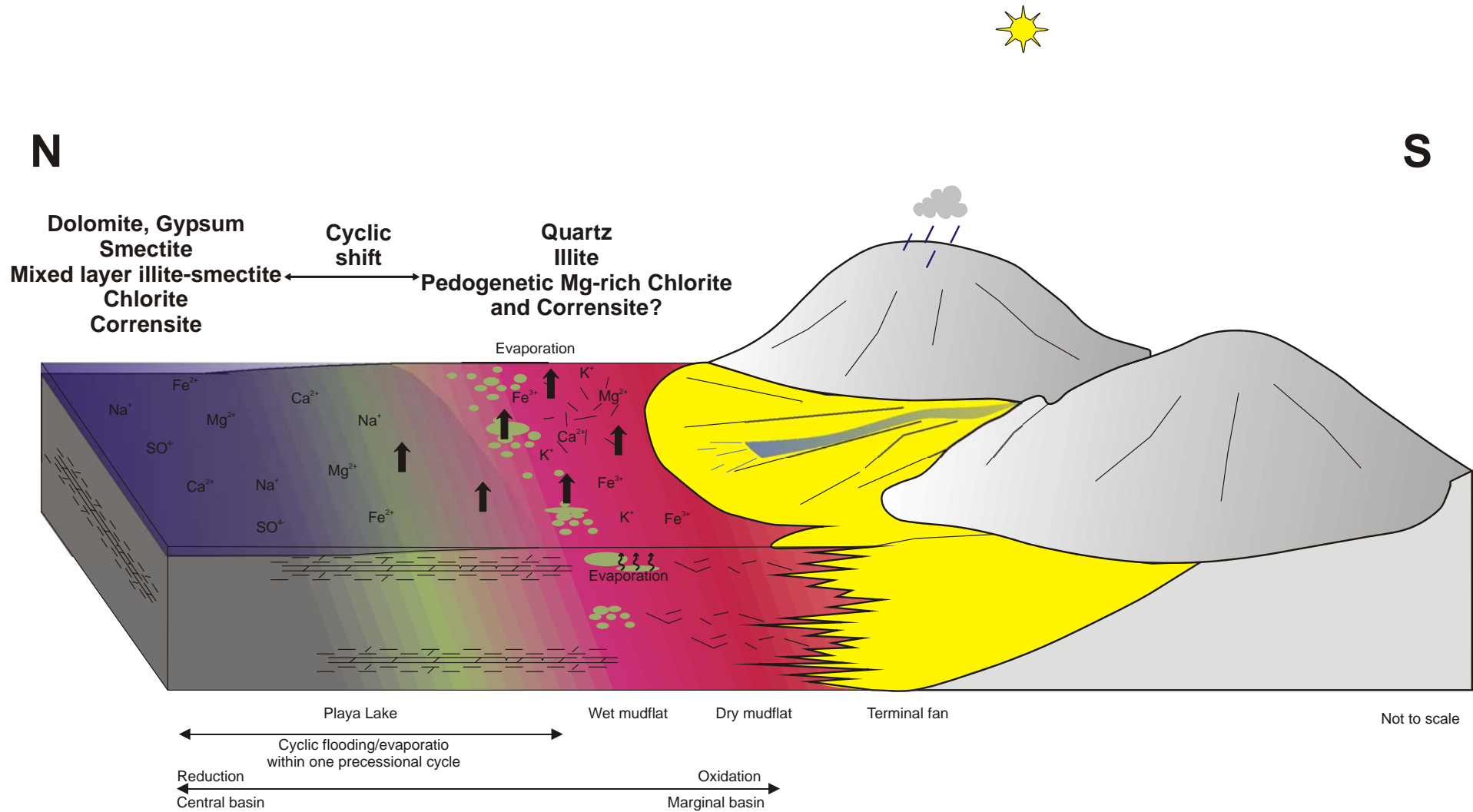


Fig. 33: A simplified scetch illustrating the cyclic formation of clay minerals within the Steinmergel Keuper playa system. During times of increased monsoon activities, i.e. a perennial lake persists and clay minerals are formed during early diagenesis reflecting the chemical composition of the surrounding waters. During times of high evaporation illite is aggraded. It is also possible that chlorite and corrensite have been formed, at least partially, during pedogenesis.

### 3.3 Stratified Lake Facies

#### Description

This Facies is characterized by dark grey, faintly laminated, slightly dolomitic, sometimes silty mudstone (fig. 27). It occurs often in combination with grey, symmetric, non-altered dolomite beds. Very small dolomite beds within the mudstones often have a thickness of less than 1 mm which underlines the faint lamination of the mudstone. There are sometimes very small and thin (less than 1mm thick) sand lenses. Generally, the dark grey mudstones are embedded in green grey mudstones and are accompanied by dolomite beds (fig. 34 and fig. 35). Within this facies fossils like fishes and bivalves (SEEGIS 2005) can be found.

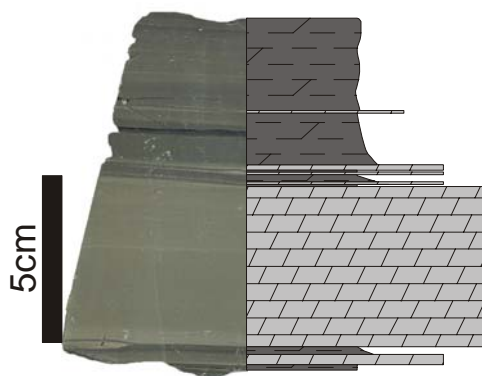


Fig. 34: dark gray well-stratified mudstone contouring a dolomite bed. Note the continuous diminishing thickness of the dolomite beds within the gray sediments.

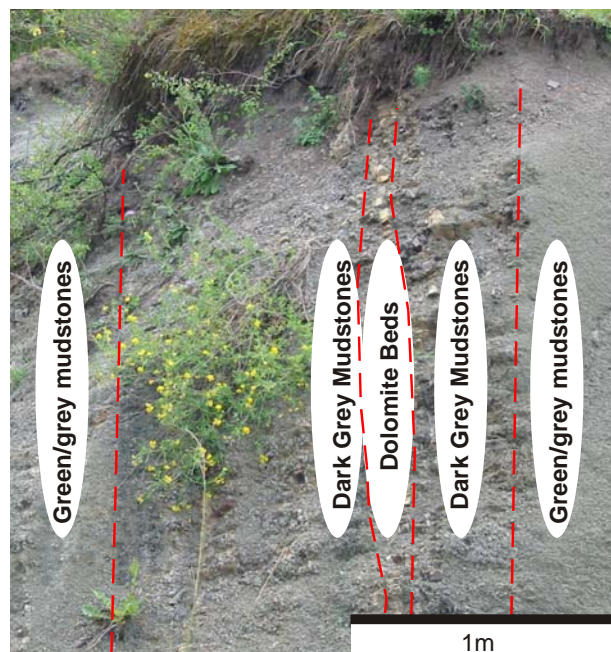


Fig. 35: Dark gray mudstones contouring dolomite beds at an Outcrop nearby Ifta. Stratigraphy: Mittlere Graue Mergel, Arnstadt Formation

The bulk of the stratified facies is composed mainly of quartz, dolomite, and some minor proportions of feldspar, illite and chlorite (fig. 36). Clay mineralogy on the fraction  $<2\mu\text{m}$  shows as well as chlorite and illite also the presence of mixed layer smectite-illite (regular and irregular), smectite and corrensite (fig. 37).



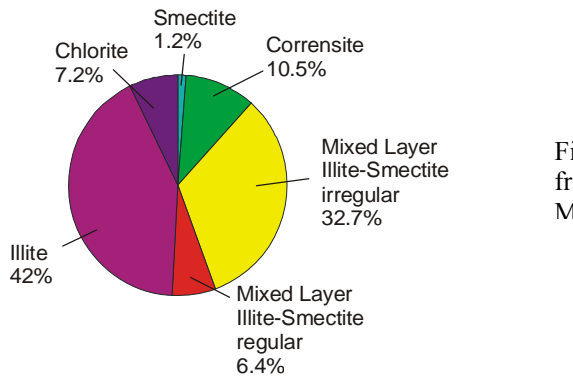


Fig. 37: Clay mineralogy of the fraction  $<2\mu\text{m}$ . Sample from core MorsDn52a

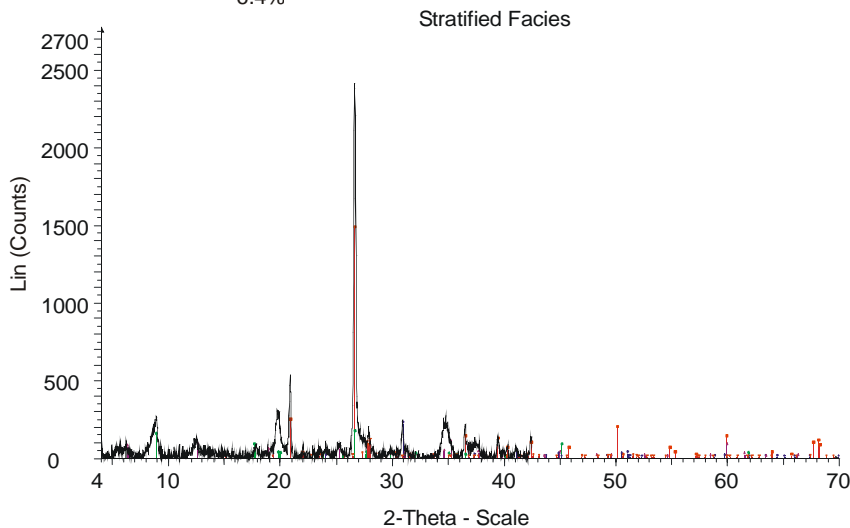


Fig. 36: XRD diagram of a dark grey mudstone. Sample from core MorsDp52a.

### Interpretation:

The high quartz content stands for a rather clastic input of the sediments cemented afterwards by carbonate. As REINHARDT (2002) showed, dolomite cementation within the interstitial was originated by bacterial activity (fig. 38).

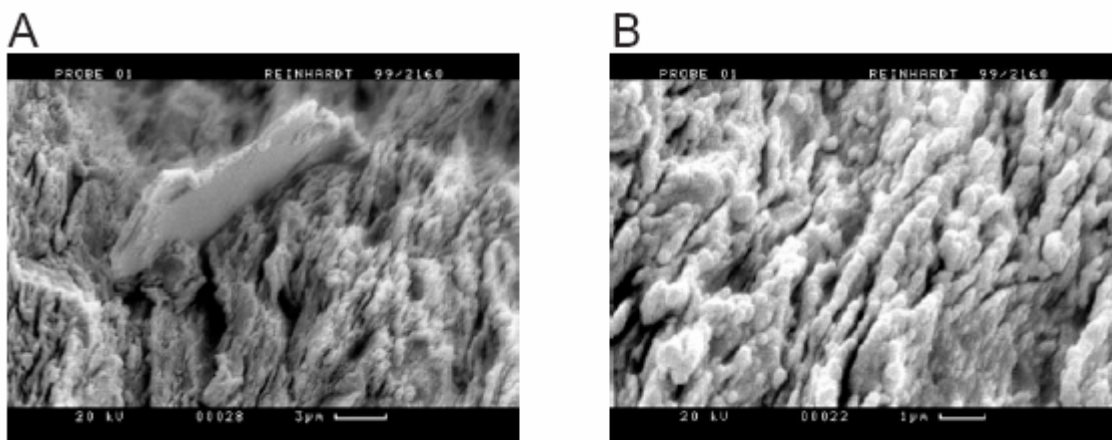


Fig. 38: SEM photographs of a mudstone sample. Outcrop Mönchberg, km3sC, dark grey mudstone containing corrensite. **A:** Aligned clay minerals surrounding small rock fragment. Note pustular surface made up of small bacterial shaped dolomite crystals. **B:** Close-up view (same sample) shows intimate relationship of small dolomite grains covering the clay minerals. From REINHARDT, 2002.

The dark grey colours can not be explained by increased organic matter as the maximum TOC content measured is  $\sim 0.2\%$ . This is far from being enough to be responsible for the dark grey colours. Pyrite or marcasite to black colouring minerals have not been found within the playa system. These facies correspond to the deepest environment of the lake, i.e. the most central part of the basin. This condition was also established when the basin was filled up after rainfall so that the dolomite could not precipitate in bigger amounts because of the water depth. Anyway, as the dolomite is present all of the time the evaporation during the wet period must not have been negligible. The occurrence of the clay mineral paragenesis is due to early diagenetic processes with changing chemistry in the pore waters enhanced by cyclic flooding and evaporation events. During diagenesis illite was degraded to smectite but also the inverse process, i.e. the aggradation of illite may have happened (see also chapter 3.2 *Clay Mineralogy*).

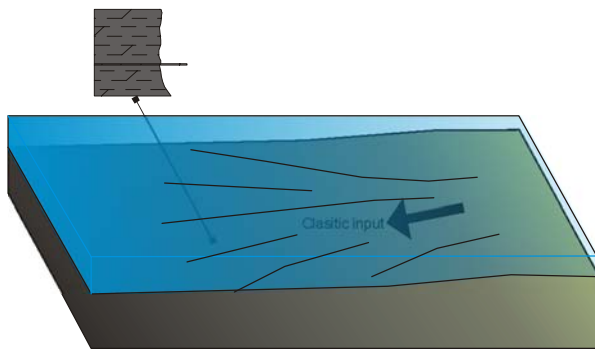


Fig. 39: Interpretative scheme of the depositional environment of the facies type described. The sediments were deposited in the deepest part of the lake. Dolomite beds within these sediments indicate a shallowing up of the water column.

### 3.4 Dolomite Beds

The dolomite beds occurring in the playa were described extensively by Reinhardt (2002) for the more marginal part of the Steinmergel Keuper basin in Southern Germany. They range from a symmetrical and non altered dolomite type to a partially eroded dolomite at the basin's margin where the playa system dried out and subaerial exposure happened. The northern part of the basin (Thuringia and Saxony Anhalt) the dolomite beds evolved similarly as a function of the water depth.

#### Description

The thickness of the dolomite beds varies from about 1mm to a few dm. At the transition to the dark grey stratified facies, i.e. towards the more central part of the perennial playa lake, the dolomite beds fade out. The maximum thickness is reached at the intermediate position (perennial lake) between the central basin and the marginal basin (episodic dry out). The colours vary from light grey to green/grey as a function of the dolomite and clay content. Depending on the carbonate content and on their thickness dolomites are normally more resistant to weathering processes than mudstones and form a positive relief in outcrops.

The carbonate fraction itself consists of micritic solely stoichiometric dolomite. Sometimes a very faint lamination is visible within the dolomite (fig. 40). This lamination is often visible at the top of the dolomite beds. The dolomite shows under the cathode luminescence microscope (CL) a bright red/orange luminescence typical for dolomites (fig. 40) with some small non-luminescent black dots which might be reprecipitated opal.

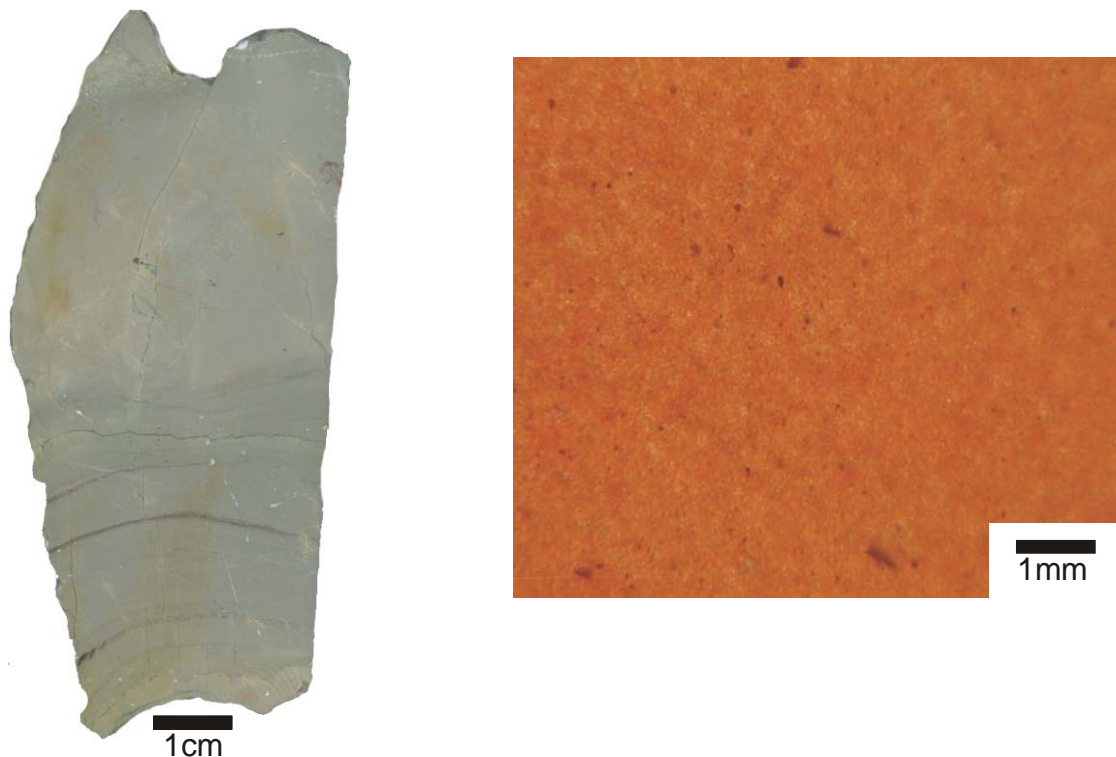


Fig. 40: Polished section of a faintly laminated and incrusting dolomite with a typical bright red/orange CL image from core MorsDp52a. The small black dots may be reprecipitated opal.

The non carbonate fraction is mainly composed of quartz, illite chlorite and feldspars (fig. 41). Clay mineralogy on the fraction  $<2\mu\text{m}$  show that this facies is composed of illite, mixed layer illite-smectite (regular and irregular), chlorite and corrensite (fig. 41).

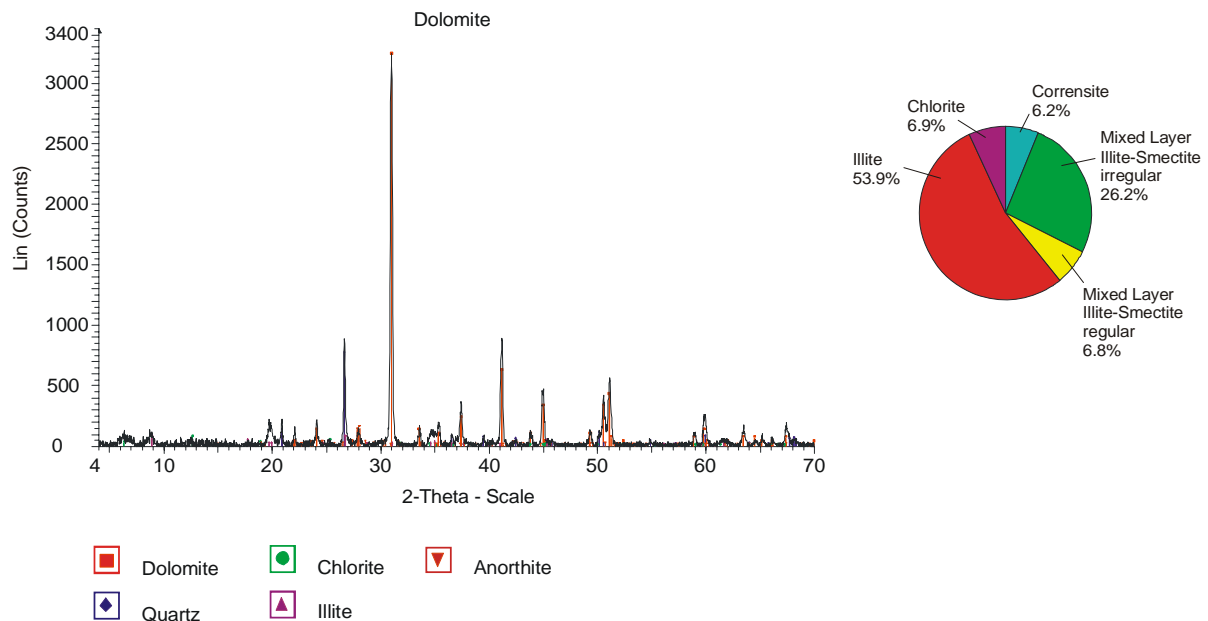


Fig. 41: XRD on the dolomite. Left: diffractogram on a bulk composition. Right: clay mineralogy on the fraction  $<2\mu\text{m}$ . Sample from core MorsDp52a.

Despite the poor sedimentary features of the dolomite beds they show an alteration pattern at their top depending on the position within the playa system. These characteristic features lead REINHARDT (2002) to his five fold differentiation of the dolomite beds (in the S German Basin) into cycle type starting from a non altered, symmetric dolomite bed (symmetric cycle type 1) in the more central part of the basin. At the marginal basin where sub-aerial exposure occurred the dolomite beds are intensively cracked and even partially eroded (asymmetric cycle type 5, REINHARDT, 2002). In the northern basin these cycle types were also found with the exception of the cycle type 4 (intensive cracking with tepee-like structures, REINHARDT, 2002) which has not been found.

The symmetric dolomite beds (fig. 34 and 42) show no alteration on their top. They are embedded in green/grey and dark grey, laminated sediments (fig. 42). The thickness of the dolomite beds diminish continuously when sedimentation changes from dolomite to dark grey sediments.

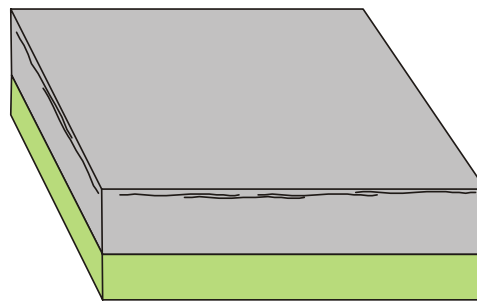


Fig. 42: symmetric dolomite bed in the central basin with interpretation from an outcrop nearby Ifta, Thuringia.

Often the dolomite beds are intensively cracked (fig. 43) at their top. The desiccation cracks are often filled up with somewhat coarser material.

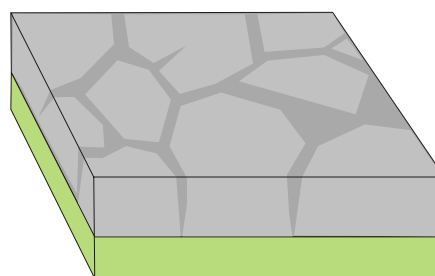


Fig. 43: Top of an asymmetric dolomite bed in the central basin with interpretation from core MorsDp52a.

## Interpretation

The formation of dolomite beds within the Steinmergel Keuper has been widely subject to discussion. First indications of the primary origin of the dolomite beds in modern settings were given by FISCHER (1925). His results were confirmed more recently by RICHTER (1985a and b) who also established the modern playa lake interpretation for the Steinmergel Keuper playa system. He distinguished between an evaporitic playa setting and dolocrête playa setting. RICHTER (1985a and b) also mentioned sulphate reducing bacteria as responsible for light carbon values. His studies reveal also a solely stoichiometric composition and good ordering of the dolomites. Another indicator for primary production of dolomite is given by covariant trends between stable carbon and oxygen isotopes in closed continental basins (TALBOT, 1990, see also chapter 4.2 *Stable Carbon and Oxygen Isotopes*). After LAST (1990) reported that most of the recent dolomite precipitation in the continental domain is related to salt lakes or in saline phases of a basin. He also noted that dolomite deposition happens in playa settings and the pore waters are Na-Cl type and have high alkalinities and high Mg/Ca ratios. Most of the recent dolomites are of primary origin: deposited directly from the lake water or from interstitial pore water.

Furthermore, WRIGHT (1999) demonstrated well that evaporation alone is not enough for dolomite precipitation. The most important arguments are of chemical nature: even that the Mg/Ca ratios might be high in evaporate basins the  $\text{CO}_3^{2-}$  content is lowered during evaporation. Then the disposability of  $\text{CO}_3^{2-}$  is even more reduced when  $\text{Mg}^{2+}$  complexes are formed with  $\text{CO}_3^{2-}$ . WRIGHT (1999) also stressed the importance of sulphate reducing bacteria and other microbes, especially cyanobacteria, in overcoming the inhibition of dolomite precipitation with the example of the Coorong Lake in Australia. During their activity the bacterial communities remove the kinetic inhibitor sulphate, and Mg is released into the highly alkaline, strongly electrolytic, sulphate-depleted brine. The bacterial communities build up faintly laminated stromatolitic structures.

Comparing the dolomites from the Steinmergel Keuper with the recent dolomites from the Coorong Lake described above a similar origin of the dolomites can be assumed:

- The faint lamination of dolomite beds in the Steinmergel Keuper playa (fig 40) is of stromatolitic nature and is quite similar to stromatolitic outlook of the recent Coorong lake, Australia.
- The stoichiometric composition and well-orderedness of the dolomites in the Steinmergel Keuper playa is also characteristic of recent primary dolomites
- Covariance of stable carbon and oxygen isotopes (TALBOT, 1990) and also light carbon values (RICHTER, 1985) might be the results of bacterial activity during evaporation of the lake (see also chapter 4.2 *Stable Oxygen and Carbon Isotopes*).
- Another hint to microbial activity is the fact that the dolomite beds fade out towards the central basin and are replaced by dark grey dolomitic mudstones (see chapter above). Microbial metabolism is often relied on incoming light and when the lake is too deep there might not be enough light to enhance biological activity depending on photosynthesis.



- SEM photographs from the Coorong Lake, Australia (WRIGHT, 1999) show strikingly similar features to those of the Steinmergel Keuper published by REINHARDT (2000); (fig 44).

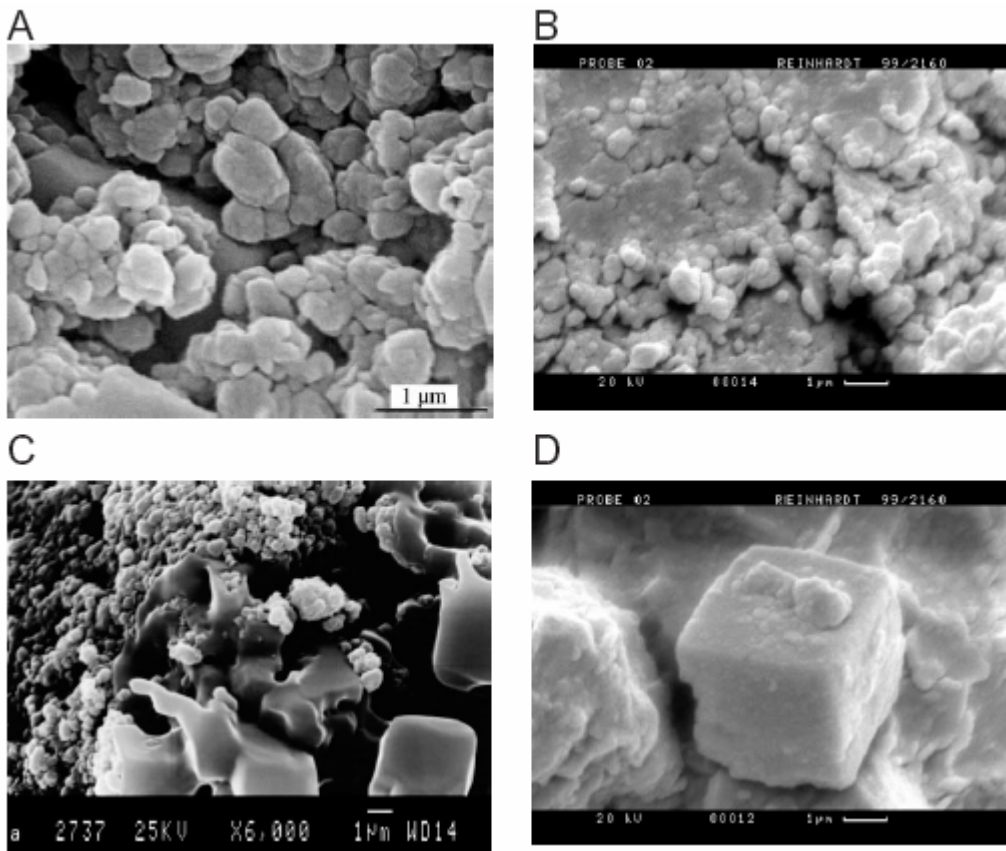


Fig. 44: **A:** SEM photo of dolomite sediment from Dolomite Lake (Coorong). Grains are sub-micron-sized. The sub-spherical/elliptical form of single grains resembles shapes of bacteria and is interpreted to result from mineral encapsulation of bacterial cells (WRIGHT 1999). **C:** ditto of dolomite sediment from Lake McFaiden. Small bacteria-shaped grains overly structured grains with developing crystal faces. Beginning diagenetic self-organisation of mineral grains (from WRIGHT 1999). **B:** SEM photo of dolomite bed, Mönchberg outcrop, km3sC. Pustular, bacteria-shaped dolomite grains cover already-developed crystal faces. **D:** SEM photo of dolomite bed, outcrop Mönchberg, km3sC. Bacteria-shaped, pustular dolomite located on a single rhombohedral dolomite crystal. All pictures and text from REINHARDT, 2000.

### Clay Mineralogy

The presence of clay minerals as mixed layer illite-smectite (regular and irregular) and illite shows clearly the changing conditions between flooding and evaporation of the playa. Illite as the detrital component is degraded by a succession of several flooding/evaporation events. The products of this degradation are the mixed layer illite-smectite minerals. As the alteration process is completely reversible some aggradation of illite may have taken place. This would explain the disordered appearance of the illite (see also Chapter 3.2 Clay Mineralogy). The presence of chlorite and corrensite within the playa lake may indicate rather very early diagenetic processes than pedogenesis.

## Depositional Environment

As the dolomite beds fade out towards the central basin they represent a somewhat more marginal position. But the characteristic features of alteration of the top of the dolomite indicate an evolution depending on the position within the playa lake. Towards the more central part of the lake symmetric non altered dolomite beds are developed. The more the dolomite beds are situated by the marginal basin, the more the top of the dolomite beds are altered. This happens starting from simple cracks within the dolomite via intensive cracking and refilling of these cracks with red mud, transforming them into tepee like structures. In where sub-aerial exposure happened the dolomites might be partially eroded. This pattern has been widely described by REINHARDT (2000) for S-Germany (fig. 45) with the differentiation into five cycle types.

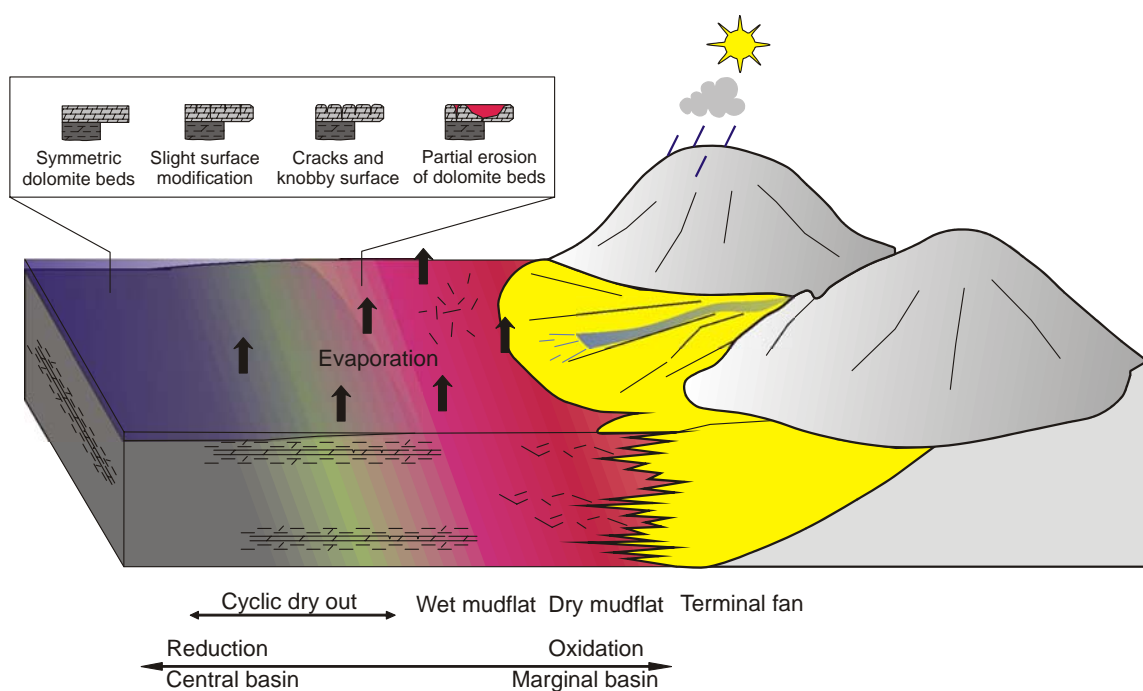


Fig. 45: Schematic representation of the Steinmergel-Keuper playa system in North Germany. General subdivision distinguishes between playa lake, playa margin, and alluvial fan. Inset shows the different dolomite cycle types and their respective positions relative to the former playa margin. Inset after REINHARDT, 2000.



### 3.5 Gypsum Facies

#### Description

This facies is characterized by displacive growth of mm sized gypsum spherules within grey dolomites (fig. 46 left). As the growth of the spherules goes on they coalesce to form nodules of several cm of diameter. The nodules themselves grow together and form irregular horizons up to some dm in thickness (fig. 46).



Fig. 46: Left: gypsum nodules in a grey dolomite bed. Right: often the gypsum nodules grow together and form irregular horizons destroying the sedimentary features. Both pictures from core MorsDp52a, right picture with interpretative litholog.

Generally the colour of gypsum is white, but it happens because of finely dispersed hematite within the gypsum that the gypsum has a reddish aspect (fig. 47).

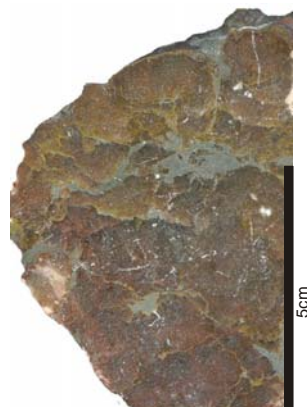


Fig. 47: polished section of gypsum concretion with finely dispersed hematite in the Gypsum (red colour). From core MorsDp52a.

The mineralogical composition also shows alongside gypsum and dolomite, the presence of quartz, illite, chlorite and feldspar (fig. 48, left ). Clay mineralogy on the fraction  $<2\mu\text{m}$  dem-

onstrates the presence of illite, mixed layer illite-smectite (regular and irregular), chlorite and corrensite (fig. 48, right).

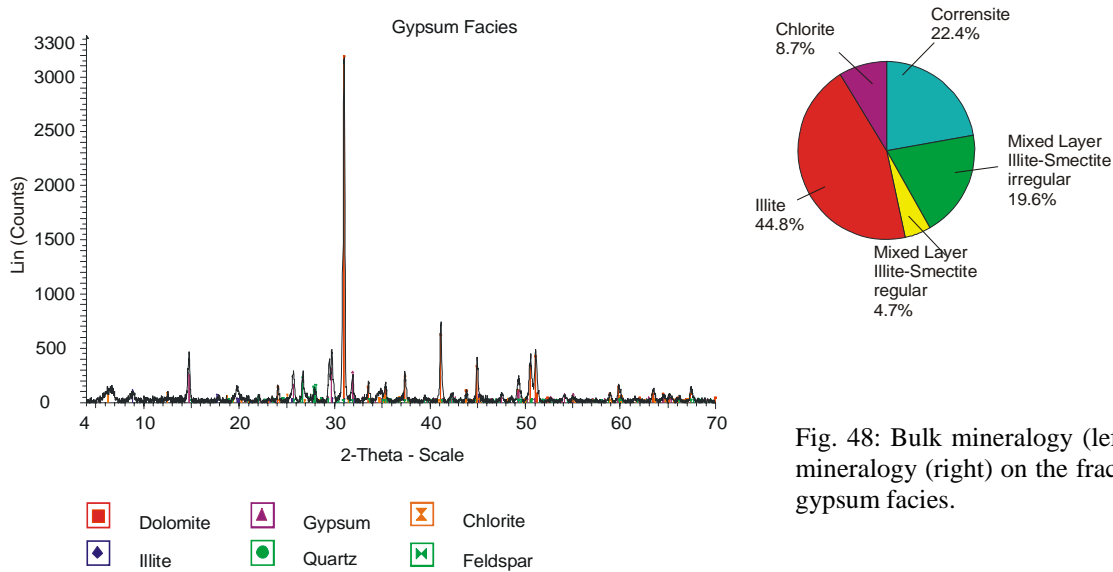


Fig. 48: Bulk mineralogy (left) and clay mineralogy (right) on the fraction of the gypsum facies.

## Interpretation

After dolomite precipitation, when evaporation went further and there was still enough water present to evolve, gypsum was able to precipitate within the dolomite, destroying former sedimentary features. The brine evolved just until the gypsum phase and Ca and S ions were enriched in the water. With further evaporation the lake dried out and a wet mudflat developed. As the mudflat was subaerially exposed hematite was formed within the gypsum. Some higher salts may have precipitated but if so they were dissolved with the next flooding event, marked by the dark grey mudstones. With a new flooding event a new cycle started with deposition of dark grey mudstones followed by dolomite followed by gypsum precipitation.

The clay minerals within this facies are also interpreted as of early diagenetic origin (see chapter 3.2 *Clay Mineralogy*) controlled by cyclic variations in lake water chemistry enhanced by cyclic flooding and evaporation events.

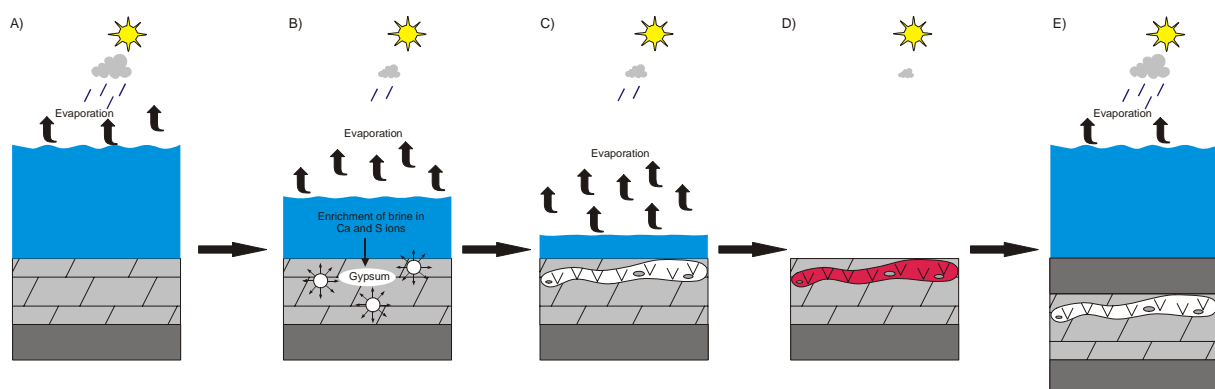


Fig. 49: Sketch illustrating the evolution of gypsum cycles within the playa system. From left to right: A) After flooding of the playa and deposition of the dark grey sediments the evaporation rate raised and dolomite was precipitated. B) As evaporation continued small spherules of gypsum grew displacively in the dolomite. C) The gypsum nodules grew together and formed irregular horizons D) With further evaporation a wet mudflat established and hematite was formed. E) With the next flooding event a new cycle started.

### 3.6 Red Mudstone Facies

#### Description

Volumetrically the red mudstone facies clearly dominates the whole Steinmergel Keuper playa system. Its thickness ranges from a few mm when intercalating the green/grey dolomite facies up to several m between two successive dolomite horizons. There is no significant variation in thickness within one single mudstone horizon in S Germany. However, in the Drei Gleichen area, Thuringia the thickness of red mudstones may vary considerably from one outcrop to the next outcrop (fig. 14, chapter 2 *Methods*) perhaps due to non negligible differences in the subsidence pattern (KELLNER, 1997).

The colour variation shows all shades from green/grey to intensive red. The colour description used in the present work is summarized below.

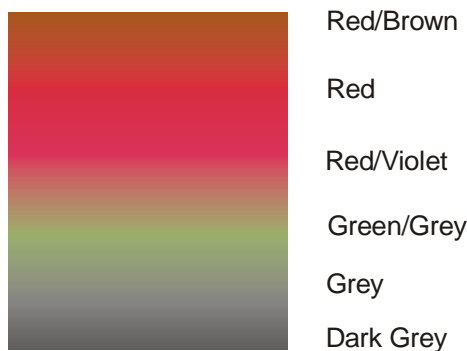


Fig. 50: Colour description used in the present work.

The transition from green/grey to red can be continuous without any recognizable boundary between the different colours (fig. 51 left). The passage from green/grey is often characterized by a sharp boundary between the colours (fig 51 right).

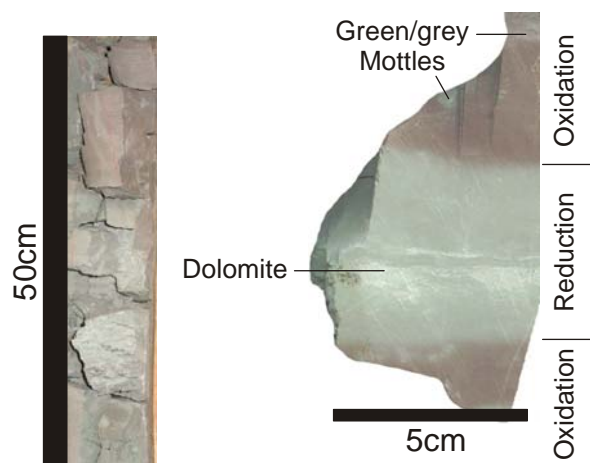


Fig. 51: Left: continuous colour changes within the red mudstone. Right: the sharp boundary when the colour changes is characteristic for this facies. Both samples from core MorsDp52a.

Mottling of the red mudstones occurs frequently with varying sizes of the dots. The size of the green/grey dots varies from few mm up to several cm. Very often they grow together and form green/grey horizons (fig. 52). The transition from red to green/grey is often characterized by intercalated violet to red/violet horizons. Red mottling in green/grey sediments can also happen but is less common than the inverse.



Fig. 52: Mottling of red mudstones. Note that the mottles coalesce and form small horizons within the mudstone. Sample from core MorsDp52a.

The intensity of the red colour depends strongly on the hematite content which is finely dispersed within the mudstone (fig. 53) As iron is a luminescence quencher (ADAMS & MCKENZIE, 2001) it appears non luminescent under CL microscope filling up the space between dolomite grains.

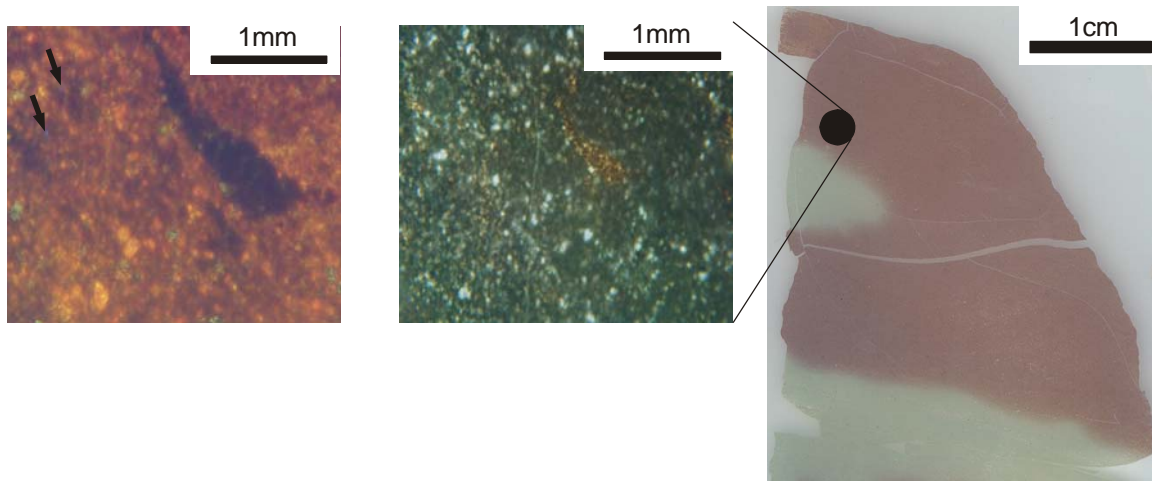


Fig. 53: Thin section of a red mudstone with microphotograph and CL picture. Arrows indicates the clear blue dots which may represent reprecipitated opal. Note the finely dispersed hematite (non-luminescent under CL and opaque under normal microscopes) within the dolomite (typically bright orange under CL).

The weathering behaviour of the mudstones depends strongly on their dolomite content. Small dolomite amounts have intensive weathering as a consequence and the resulting size of the sharp wedged clasts is about a few mm. With higher dolomite content the mudstone is more resistant to weathering and the clasts reach sizes of several cm.

Brecciation of the mudstones is common (fig. 54). The unsorted angular, sharp wedged clasts are often graduated and are embedded in red mud. Their size can reach some cm in diameter. Another common phenomenon is desiccation cracks which may reach to a depth of several cm deep into the sediment.



Fig. 54: Red/violet pedomorphic structures in a red/violet mudstone. Sample from core MorsDb52a.

The mineralogy of the red mudstone facies is characterized by high quartz contents, in contrast to the green/grey dolomite horizons which are characterized by higher dolomite contents (fig. 55). The red mudstone contains furthermore dolomite, feldspars (anorthite?) illite, chlorite and hematite. The hematite is not present within the green/grey dolomite facies.

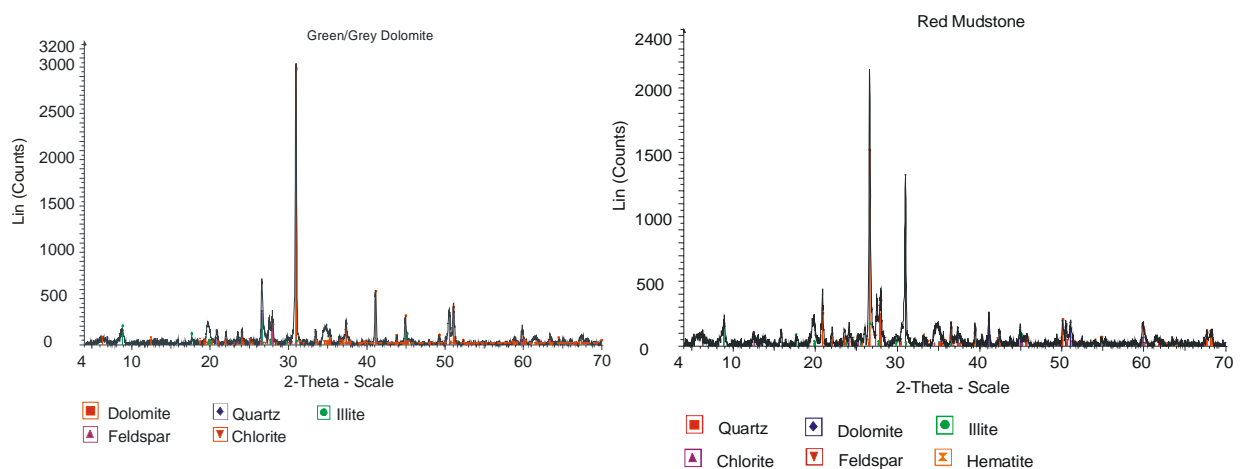


Fig. 55: XR diffractograms from the green/grey dolomite facies (left) and the red mudstone facies (right) showing well the mineralogical differences between both facies, mainly by the presence of hematite within the red mudstones. Both samples from core MorsDp52a.

The clays (fraction <2 $\mu$ m) are composed of illite, mixed layer illite-smectite (regular and irregular), corrensite and chlorite (fig. 56).

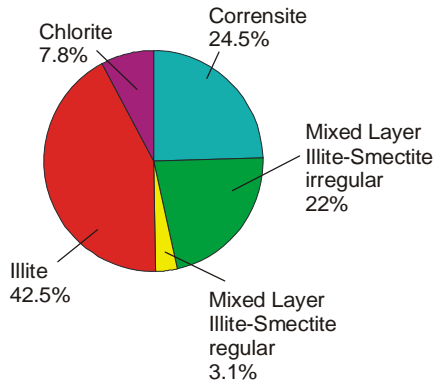


Fig. 56: Clay mineralogy of the red mudstone facies. Sample from core MorsDp52a

Tetrapodes fishes and bivalves (also within the central basin) were described by SEEGIS (2005). Minor proportion of ostracodes is reported by BEUTLER AND OPPERMANN (2005). BEUTLER (2005) mentioned also the presence of mega spores within the playa system.

## Interpretation

### Origin of Colors

One of the most obvious features of the Steinmergel Keuper sediments is the striking cyclic colour change from intensive red to green/grey. The most important colouring pigment which is responsible for the intensive reddish shades is the finely dispersed hematite. After SCHÜNKE (1984) hematite is formed during early diagenesis by the alteration of Fe bearing mineral. He stressed the importance of changing Eh and pH conditions within the playa system due to changing between lacustrine and fluvial influences. The general interpretation of the origin of colours within the Steinmergel Keuper playa system follows the discussion by SCHÜNKE (1984) :

The red colours are evidently produced by hematite as shown above (fig. 55). Just small amounts up to 2 % (SCHÜNKE, 1984) are enough to produce the intensive colouring of rocks.

The origin of violet shades still remains unclear. But their relative position in between the intensive red, red/brown and green/grey coloured sediments (fig. 57) suggests early diagenesis with slightly reducing conditions. Fe ions were mobilized and reprecipitated immediately afterwards preventing the loss of ions. Formerly chemical and mineralogical investigations (SENGERLING, 1979 and SCHINLE, 1979) gave no hints of either a dependency of the violet shades on the  $Fe^{3+}/Fe^{2+}$  ratio or an incorporation of ions as  $Al^{3+}$ ,  $Ti^{3+}$  or  $Mn^{2+}$ .





Fig. 57: Photograph from an outcrop near Ifta, Thuringia (Untere Bunte Mergel, Arnstadt Formation). Note the evolution from green/grey dolomitic mudstones via red violet mudstones to intensive red mudstones and vice versa.

Grey, dark grey and green/grey colours are often discussed to have their origins in organic material, finely dispersed pyrite or marcasite. The organic carbon content within the Steinmergel Keuper playa system at seems  $\sim 0.2\%$  too low to have an effect on the colours of the sediments. Neither pyrite nor marcasite were found, so these minerals can also be excluded as grey colouring pigments. Grey colours are also produced by the presence of carbonates which are present everywhere within the playa system. Greenish shades are thought to have their origins in the presence of clay minerals as illite and chlorite. Both minerals are present in the playa system. Dolomite beds are often embedded in green/grey mudstones, indicating longer lasting reducing conditions due to a long-lasting water body or better percolation of reducing pore waters.

The mottling of red mudstones could be explained by the former presence of organic material which inhibited the oxidation of  $\text{Fe}^{2+}$  to  $\text{Fe}^{3+}$ . SCHÜNKE (1984) remarked that within the red mudstones not only is hematite is formed but also 50% of  $\text{Fe}^{2+}$  in the clay minerals is oxidized to  $\text{Fe}^{3+}$ . In the mottles the whole iron is found only within the clay minerals. The organic matter could be some detritus of plants but also some living plants which may have produced locally reducing conditions so that iron was not oxidized. Living plants imply pedogenesis, which is also suggested at least partially by the clay mineralogy (see chapter 3.2 *Clay Mineralogy*). The presence of chlorite (with clear portions of vermiculite) and corrensites might in this case be indicators for pedogenesis.

### Flooding and evaporation:

Despite the poorly preserved sedimentary structures the dry-out of the playa lake is indicated by structures such as desiccation cracks (fig. 58) and dissolution breccias. The cracks of different sizes lead to polygonal structures. With the next flooding event the sediments have been removed but often they are filled again with fine grained material with the next flooding event. Stagnant waters produce a reducing environment so that in filled the material within the cracks stays green/grey and is not oxidized. These cracks also indicate that the capillary fringe did not reach the surface anymore, destroying the sedimentary structures in the mudstones.

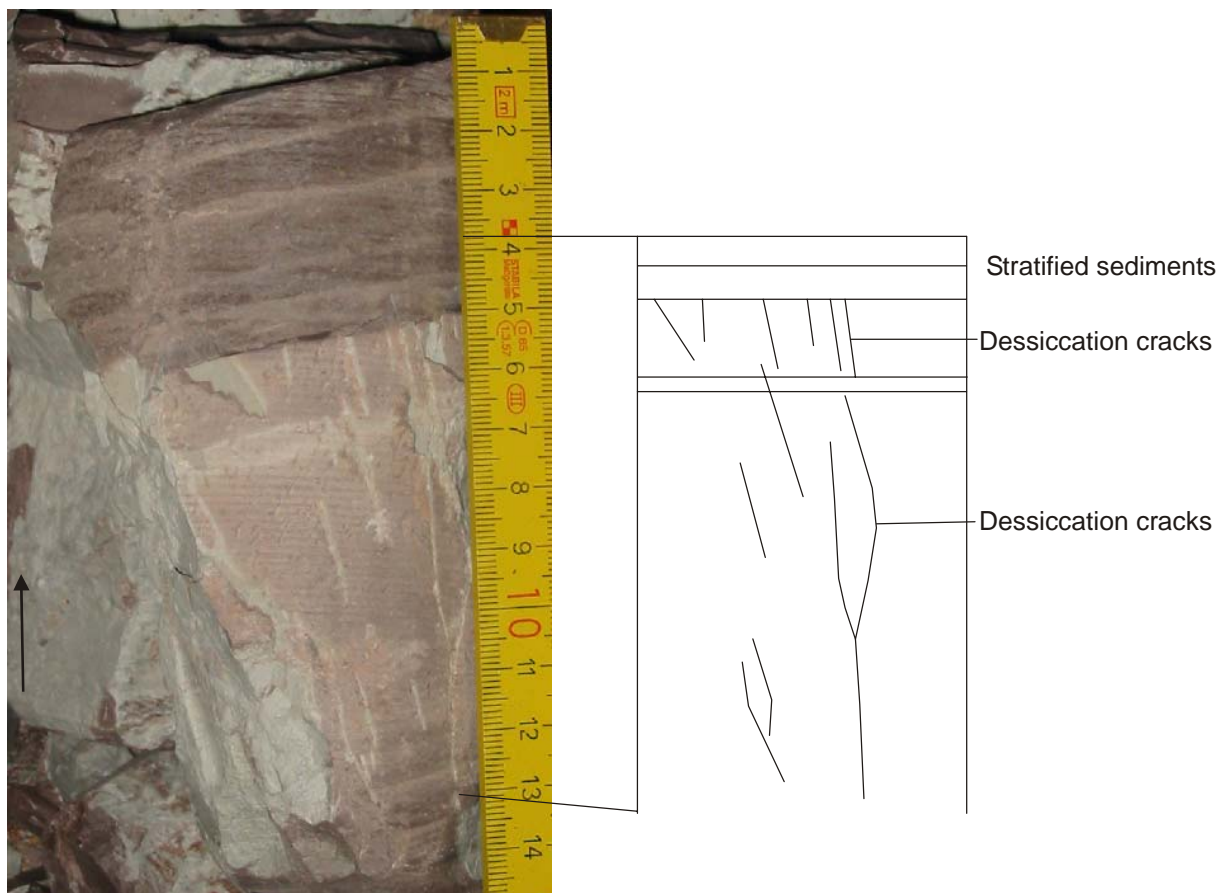


Fig. 58: Desiccation cracks in red mudstone. The cracks reach from 1cm up to several cm into the sediment. Note that colour of the in filling material is green/grey, and not red like the surrounding material.

Dissolution breccias are formed during the last stage of an evaporation cycle. Higher salts formed efflorescent crust within the top of the formerly deposited sediments and destroyed the sedimentary structures in the sediments. With the next flooding event these salts were reworked and transported toward the central part of the playa system. Sometimes this breccia has been reworked and transported during flooding as is indicated by the gradation of these breccia. But the clasts were not transported far from their origin, as they preserved their angular, sharp wedged shape.



**Depositional environment:**

The complete dry-out of the playa suggested by the brecciation of the mudstones, desiccation structures, the red colours formed during early diagenesis under oxidizing conditions and the assumed pedogenetic overprint indicated by the clay mineralogy show that the deposition took place within the wet and dry mudflat (fig. 59):

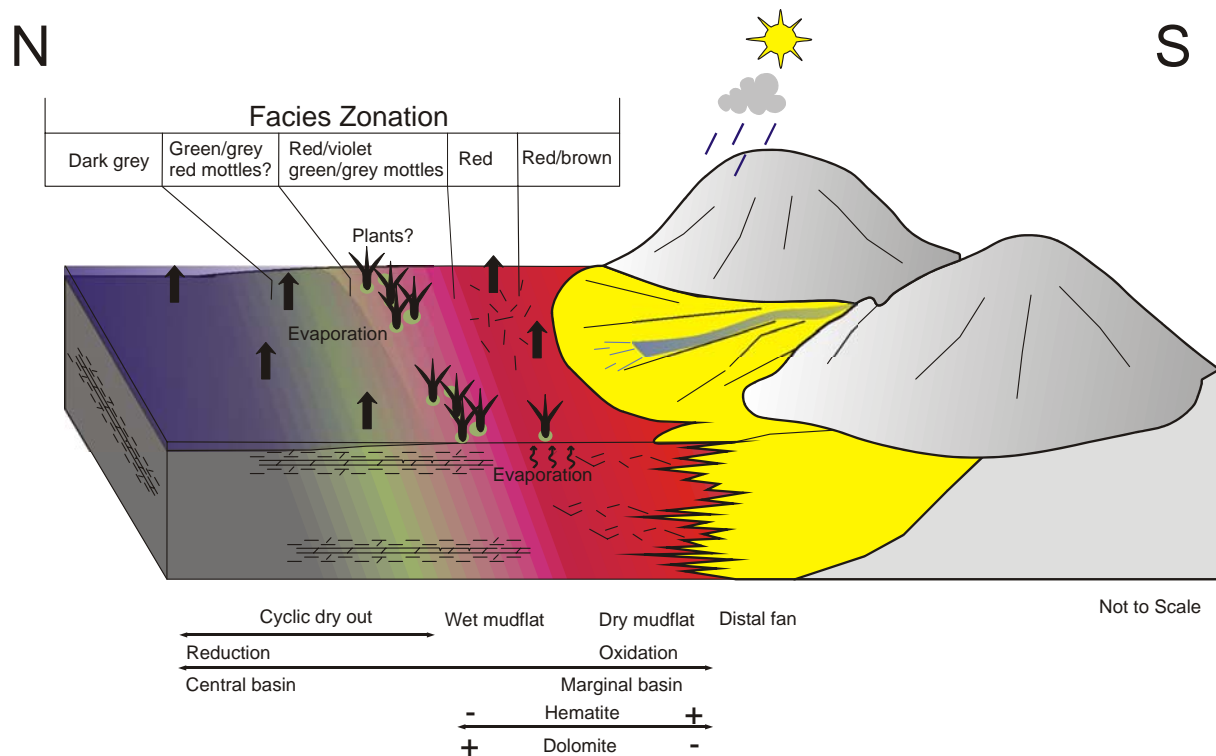


Fig. 59: Simplified depositional environment model for the red mudstones. The possible presence of plants requires a minimum of water, i.e. the green/grey mottles may indicate the presence of the lake nearby. It could be that some plants may exist within the dry mudflat, but only where the capillary fringe reached high enough. The hematite content increases in the dry mudflat, in contrast to the dolomite content which increases towards the central basin. Inset shows colour facies zonation of the playa.

### 3.7 Dolocrête Facies

#### Description

Important and characteristic sedimentary features within the Steinmergel Keuper playa system are dolocrête horizons. A single horizon can reach a thickness up to 50 cm and form duricrust (fig. 60).



Fig. 60: Dolocrête horizon forming a duricrust within Obere Bunte Folge. Note the lateral varying aspect of the dolocrête horizon due to the fact that single nodules coalesce together and the dolomite content can change significantly at the boundary between two nodules. The transition from the red mudstone to the dolocrête at the base of this horizon is continuous. By Contrast the boundary at the top is well defined and sharp. Mühlenburg outcrop, Drei Gleichen area, Thuringia.

The dolocrêtes are organized in cycles (fig. 61) which reach a total thickness of about 16m at the outcrops Gleichenburg and Mühlenburg, Drei Gleichen area, Thuringia. Red mudstones are developed between two successive dolocrête horizons. The transition from the mudstone to the dolocrête is generally continuous, whereas the transition from the dolocrête horizon to the mudstone is rather sharp than continuous. The dolomite content also evolves asymmetrically from bottom to top (TOUGIANNIDIS, 2004). First the dolomite content rises constantly, and at the top of a dolocrête horizon it diminishes abruptly. The same pattern can be observed with the colours. The colour changes gradationally from red within the mudstone to grey in the dolocrête horizons. At the top of a dolocrête horizon the change from grey to red again is sharp. One exception is given at Mühlenburg outcrop; there is one horizon which evolved symmetrically and shows no significant colour change.



Fig. 61: Dolocrête horizons within the Obere Bunte Folge. Note the nodular, lenticular aspects of the dolocrête horizons (black circles) and also the rather symmetric red horizon between the two inferior horizons. Mühlenburg outcrop, Drei Gleichen area, Thuringia.

The morphology is strongly influenced by the presence of the dolocrêtes as they are more resistant to weathering than the mudstone because of the increased dolomite content within the dolocrêtes.

The most abundant mineral in the dolocrêtes is dolomite. Furthermore, they contain quartz, illite, chlorite and feldspars. The clay minerals (fraction <math><2\mu\text{m}</math>) are composed of illite, mixed layer illite-smectite (regular and irregular) corrensite, smectite and chlorite (fig 62). In one sample of Morsleben calcite was found. This is due to the fact that late cracks (not belonging to playa system) were filled with calcite (fig. 63).

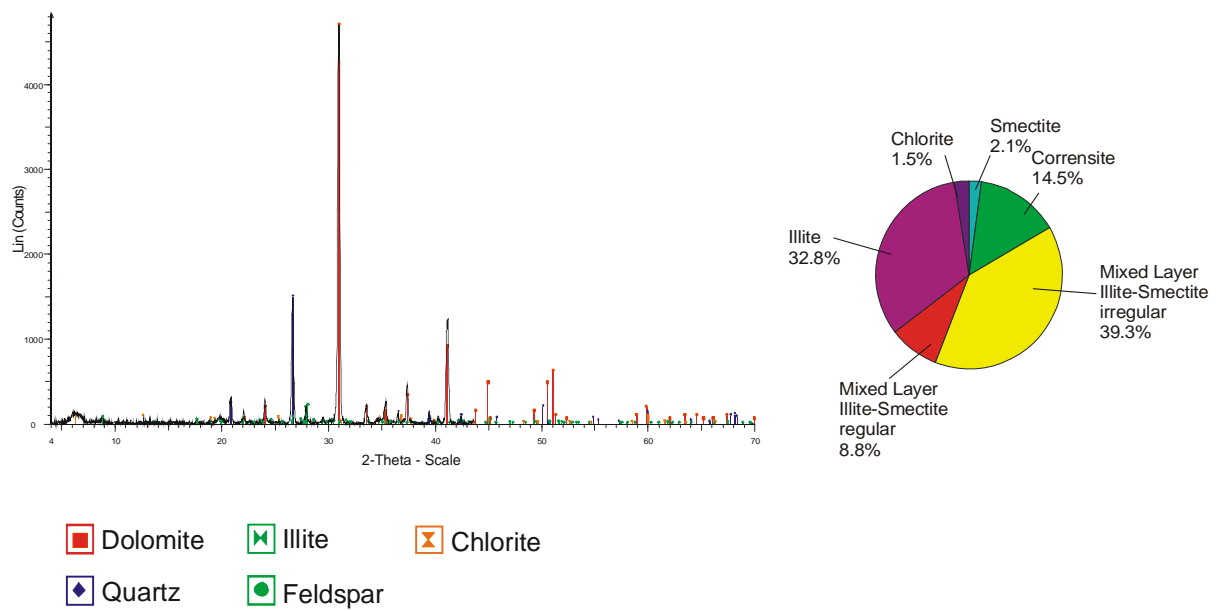


Fig. 62: XR diffractometry of a dolocrête horizon. Sample from outcrop Gleichenburg, Drei Gleichen area, Thuringia.

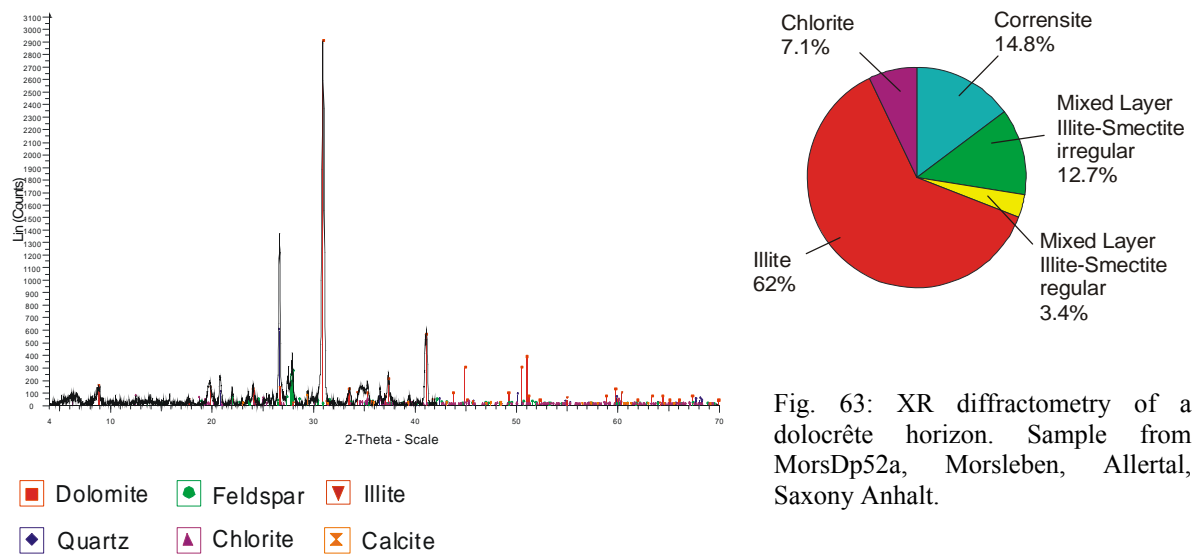


Fig. 63: XR diffractometry of a dolocrête horizon. Sample from MorsDp52a, Morsleben, Allertal, Saxony Anhalt.

## Interpretation

Interpretations of calcrête and dolocrête as terrestrial in origin were already given by FISCHER (1925) and MÜLLER (1955). Dolocrêtes and calcrêtes are seen as the product of groundwater evolution during evaporation within the playa system.

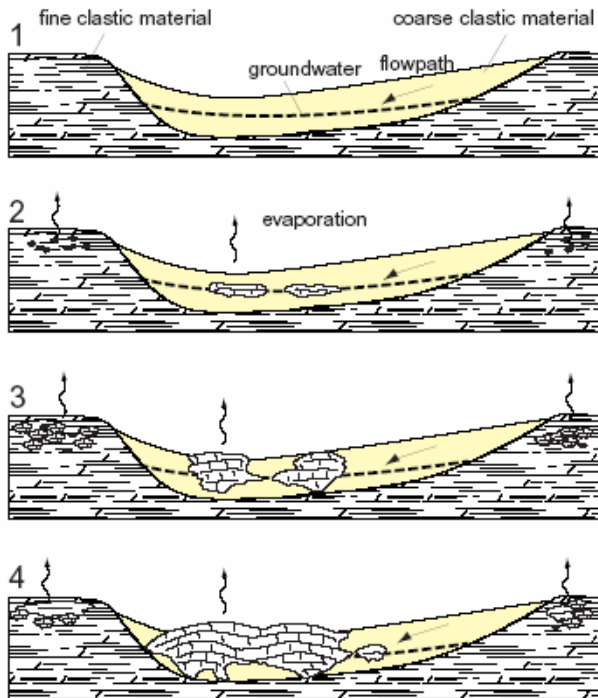


Fig. 64: Different stages of development of both a groundwater and a pedogenic calcrete/dolcrete. Stage 1: a shallow groundwater system (hatched line, arrow) in a drainage channel filled with coarse clastic material. The channel is cut into fine clastic floodplain deposits characterized by reduced poroperm values (schematized). Stage 2: initial precipitation of carbonate; as small nodules during beginning pedogenesis of the floodplain and as more massive precipitation from the flow of evolved groundwater in the coarse material. Stage 3: nodules on the floodplain begin to coalesce, whereas groundwater calcrete/dolcrete begins to form domes and pods. Stage 4: Maturation of the profiles; both pedogenic and groundwater forms are reworked on the surface. From REINHARDT 2002, adapted from NASH (1997)

PIMENTEL et al (1996) provided useful criteria to differentiate calcrête/dolocrête with regard to pedogenetic or groundwater origin.

Origin of calcrete/dolcrete	
Pedogenic	Groundwater
Generally thin, 1–2 m. Thicker forms exhibit complex brecciated, pisolitic and peloidal fabrics	May reach thicknesses of 10 m or more, typically massive throughout
Typically display profile with orderly set of horizons; sharp topped, gradational base	Uniformly massive; gradational top and base
Macrostructures include nodular, massive, laminar, pisolitic	Rarely display laminar horizons; never pisolitic or prismatic unless at the top of unit
Rhizocretions may be common	Less abundant rhizocretions, associated with phreatophytic plants
Microfabric may exhibit beta-fabrics (biogenic microbial/root-related carbonates such as alveolar septal structure, needle-fibre calcite <i>Microcodium</i> )	Typically alpha-fabrics (densely crystalline)
Vadose fabrics such as meniscus and pendant cements	If present, likely to occur only near top of carbonate body
Typically finely crystalline	May show wider range of crystal sizes, including spheroidal dolomite
Porosities are low	Porosities locally high (> 25%), typically horizontally elongate
Rarely display lateral changes such as calcrete to dolcrete to gypsumcrete	May show regular mineralogical changes reflecting salinity gradients
Typically associated with more stable surfaces on floodplains	Associated with drainage channels, playas and lake deposits
Mottling, if present is minor, reflecting lack of Fe-translocation in generally oxidised setting	Associated with extensive mottling and Fe-translocation in reducing groundwaters
Most commonly found in finer units in alluvial cyclothem	More common in more permeable coarser units in alluvial cyclothem

Tab. 5: Criteria for the differentiation between calcretes/dolcretes of pedogenic or groundwater origin. From REINHARDT 2002, From PIMENTEL et al. (1996).

---

According to the criteria given by PIMENTEL (1996) it can be said that in general the dolocrête horizons in N Germany are of pedogenetic origin. The obvious change in the colour is due to a dilution effect of the increased carbonate precipitation. Within one horizon the coalescing nodules are still discernible. One exception may be present at outcrop Mühlenburg: the symmetric horizon indicates a groundwater dolocrête rather than a pedogenetic dolocrête. This depends on the fact whether the capillary fringe reach the surface or not. In any case, it has to be kept in mind that all transitions between groundwater and pedogenetic dolocrête do exist. Hence it could be also a transitional dolocrête horizon. In S Germany REINHARDT (2002) discussed the problem of the origin of the dolocrête horizons. He found that the dolocrêtes in S Germany are generally of pedogenetic origin but he also found hints of groundwater dolocrêtes or at least those from a transitional origin. An exhaustive discussion of the pedogenetic origin of dolocrêtes with examples from the Steinmergel Keuper is given by NITSCH (2005b)

Interestingly, the clay minerals give no hint of pedogenesis, as the chlorite and corrensite contents, at least in the Drei Gleichen area, are not high enough to be interpreted as of pedogenetic origin. The chlorite content in Morsleben is somewhat higher. The other minerals can interpreted in the same way as the other examples before, i.e. they are of early diagenetic origin. This seems to be the same for the chlorite and corrensite.



### 3.8 Erosional Channels and Sandstones

#### Erosional Channels

The present work is restricted to the playa system itself and sandstones do not belong to the playa (they only interfinger with the playa system), therefore they are described but not interpreted in detail. Furthermore, in the central playa system of the North German basin they are restricted to the outcrops of the Drei Gleichen area, Thuringia. Exhaustive descriptions and interpretations on the sandstones of the Steinmergel Keuper in the South German basin are given by REINHARDT 1994, KOSTREWA 1995, KERN & AIGNER 1997, KONSTANTY 1997, JUNGHANS 1997, HORNING 1998, Aigner, T. et al. (1998, 1999), Hornung, J. & Aigner, T. (1999).

Erosional channels occur mainly in the marginal basin. They incise the red mudstones (fig.65) a few cm to some dm and can be up to some decametres wide. They are filled with green/grey sediments at the base: the colours change through red/violet to red from bottom to top. At the top of these channels are dolomite beds a few cm thick. The passage from mudstone to dolomite is continuous at the base of the dolomite bed. The passage from dolomite to mudstone at the top of the dolomite beds is sharp.

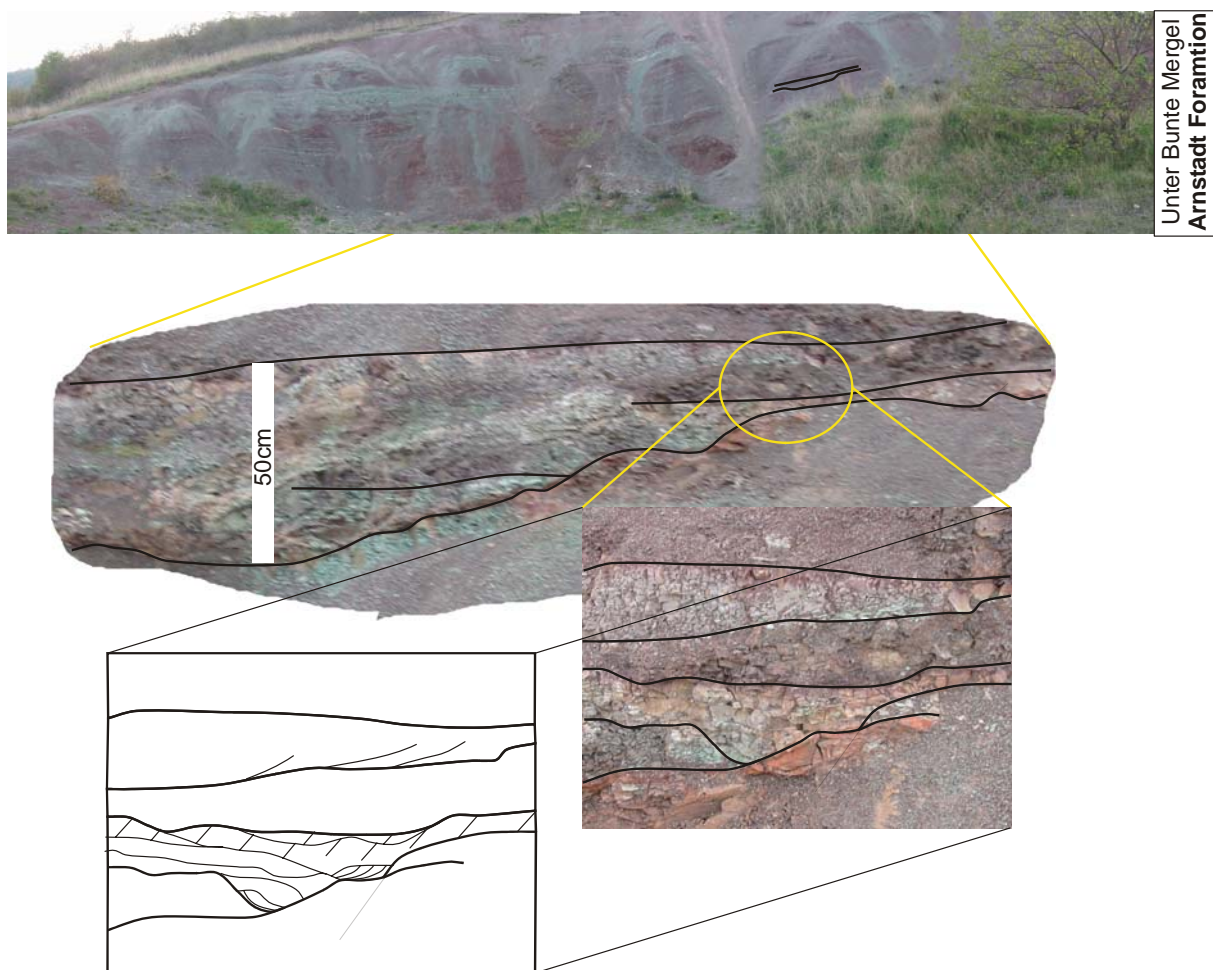


Fig. 65: erosional channels with interpretative sketch within red mudstone at Seebergen outcrop (Drei Gleichen, area, Thuringia).

## Sandstones

In contrast with to the South German basin, sandstones in the central basin of the North German basin are localized at the outcrop Wachsenburg, Drei Gleichen area, Thuringia. The first one referred to as the equivalent of the Semionotus Sandstone is developed within the Untere Bunte Mergel (fig. 66). It is a fine grained, yellow sandstone that passes laterally into green/grey clayey material. The second sandstone at top of the Wachsenburg section within the Mittlere Graue Mergel is about 1m thick (fig. 67). It is a yellow sandstone with fish scales, remnants of plant and ichno fossils (KELLNER, 1997). Internal cross bedding and fining upward indicate a transition of the fluvial system into a meandering river system (KELLNER 1977, HAUSCHKE 1991).



Fig. 66: The equivalent of the Semionotus Sandstone within the Untere Bunte Mergel, Arnstadt Formation. Top: overview. Bottom: detail.





Fig. 67: The Wachsenburg Sandstone at the top of outcrop Wachsenburg within the Mittlere Graue Mergel, Arnstadt Formation.



### 3.9 The Steinmergel Keuper facies model

The different playa facies described in chapter 3 can mainly be grouped into three distinct types of basic cycles with varying depositional mechanisms. The appearance of a certain cyclic pattern depends on its position within the playa system and also on the climatic conditions under which it has been developed (fig. 69). So, the gypsum cycle evolved during long lasting wet periods with a periodic succession of flooding and shallowing through enhanced evaporation of the water table. Then during long lasting dry periods the wet/dry cycles were built up by a cyclic dry-out of the playa system after flooding events. However, the importance of flooding/evaporation events depends strongly on the earth's position respective to the sun (fig. 68) and flooding may have been shifted with the cyclicity. The playa system was not flooded entirely every time. Thus, during times when only a part of the playa was flooded dry mudflats developed. Within these dry mudflats where the playa system was not flooded dolocrite cycles developed.

From these cycles two major cycle hierarchies can be deduced: one at a seasonal scale reflecting changes within the monsoonal activity over a year and the other one at an orbital scale modulating the frequency of increased or decreased monsoonal activity over longer periods. Yearly events are generally not preserved because of secondary overprinting but orbital parameters are of the fundamental cycles described above. Changes in monsoonal activity are directly translated to changes in precipitation. For the Upper Triassic the highest rainfalls occurred in December, January, February (DJF) when summer happened during aphelion in the southern hemisphere (KUTZBACH, 1994). This assumption was made because it is not possible to calculate the cycles in such old sediments (>200 Myr). The symmetric conditions applied in KUTZBACH'S model imply that highest rainfall in the Steinmergel Keuper playa system (20° N) occurred during cooler summers (aphelion) than normal in the northern hemisphere (fig. 68) and therefore reduced evaporation. In turn, water could accumulate in the playa system and a persisting lake was formed. But when summer happened to coincide with perihelion (JJA) evaporation was maximized as the summers were hotter than normal and the lake dried out completely. As a result wet periods are related when summer coincided with aphelion (DJF) and dry periods when summer happened to be at perihelion (JJA) within one precessional cycle (23kyr, fig. 68).

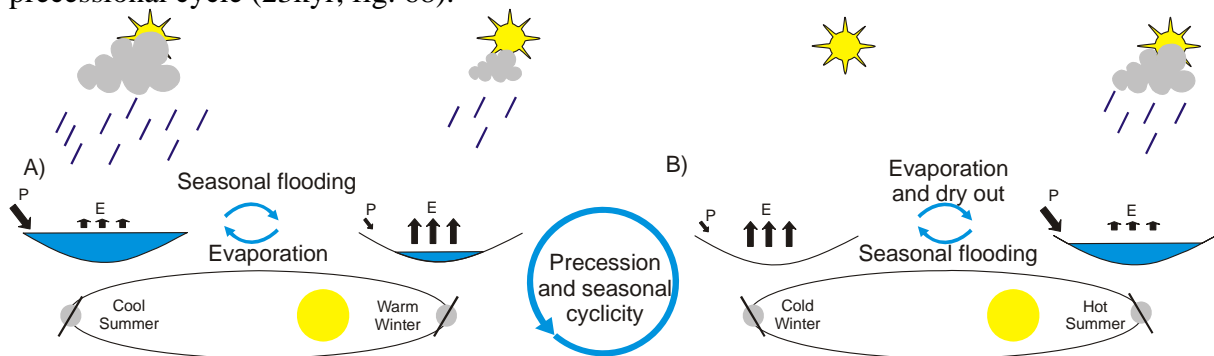


Fig. 68: Cyclic lake level changes of the Steinmergel Keuper playa system depending on orbital control A) summer occurred in perihelion (JJA) in the northern hemisphere and B) summer occurred at aphelion (DJF).

The basic assumption about wet and dry periods is that the climatic setting in Upper Triassic times was generally an arid, steppe climate and wet or dry periods refer to the fact whether there was a persisting lake or not in the basin.

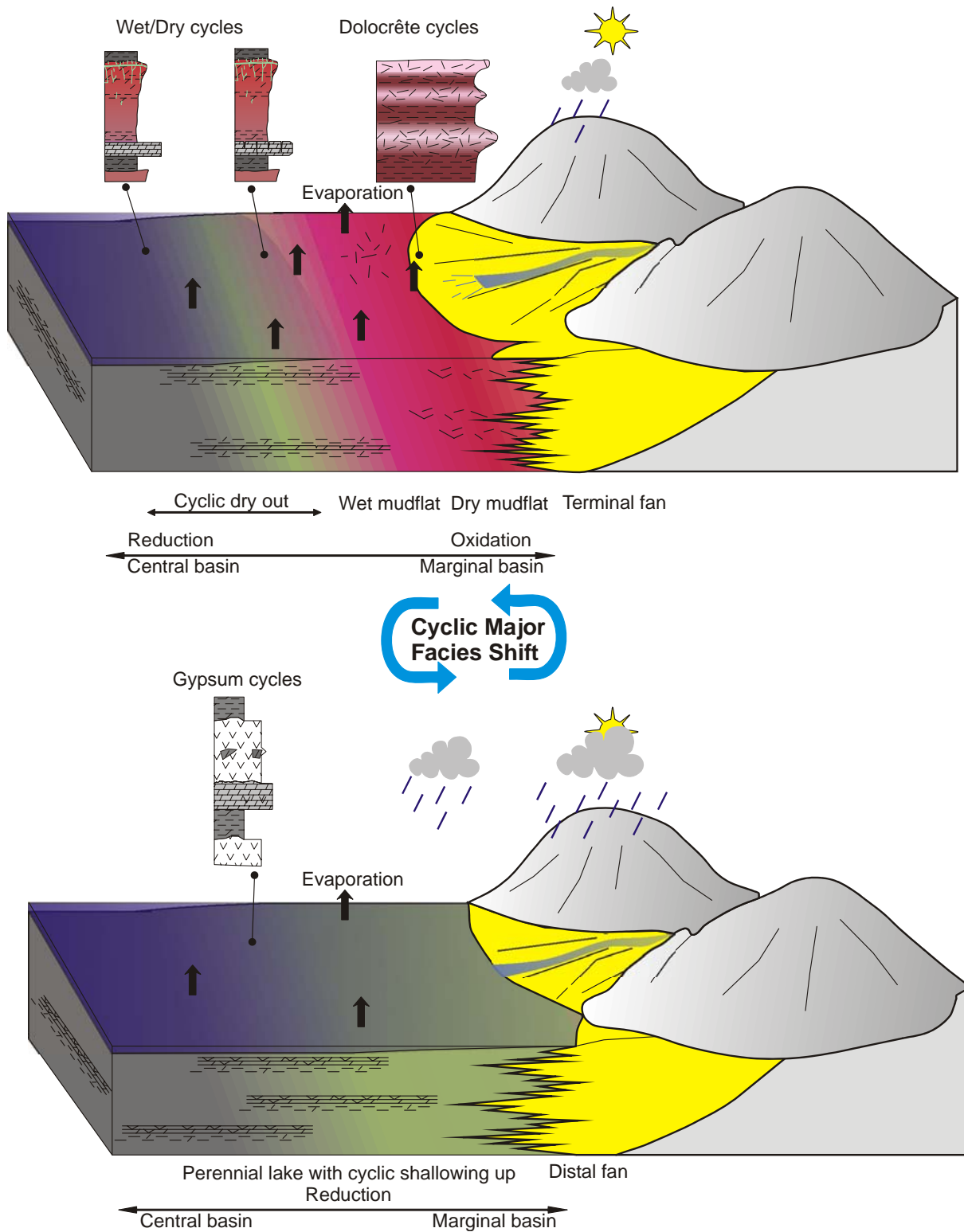


Fig. 69: Schematic diagram of the Steinmergel Keuper playa system with the different basic cycle types. Top: Cyclic wet/dry variations within a major dry cycle. When the playa was not flooded entirely dolocrête cycles developed in the dry mudflat. Bottom: During periods with long lasting water bodies cyclic shallowing through enhanced evaporation of the water table led to periodic gypsum precipitation within dolomites.

## Cycles during long-lasting dry periods

### Wet/dry cycles

Even during long dry periods the playa system might have been flooded episodically with increased monsoonal activity and a wet-lake-dominated period was established for a certain time. It was within these periods when dolomite precipitated. The most striking feature of this cycle type is his asymmetric evolution from the bottom to the top. At the bottom dark gray, well stratified sediments are deposited (fig. 70). During this period monsoonal activity may have been strong enough to establish a lake deep enough to enable sedimentation of the described strata. However, seasonal evaporation was significant enough to allow cementation by dolomite. With ongoing evaporation of the playa, green/gray dolomites were precipitated. Further evaporation of the water may have lead to precipitation of minor quantities of higher salts as gypsum and/or halite within the pore space of the sediments. With the onset of the next monsoonal season these salts were dissolved. After the complete dry-out of the playa system the sediments were sub-aerially exposed and became oxidized during evaporation of the ground waters within the capillary fringe. The surface of the red clays is often characterized by desiccation cracks. Some efflorescent crust which precipitated at the surface might have been deflated by aeolian activity over the dry mudflat or reworked with the following flooding event.

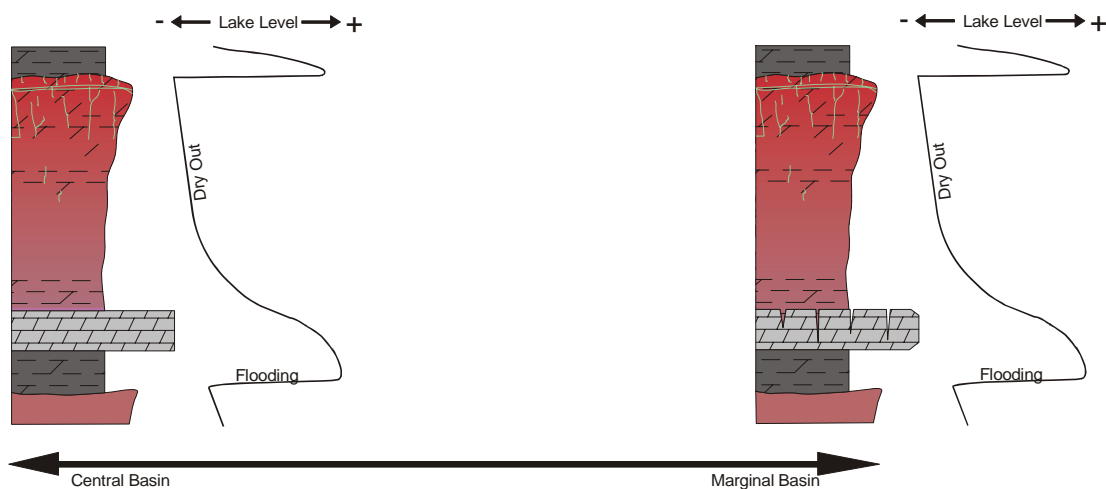


Fig. 70: Idealized wet/dry cycles. Left: a cycle with a symmetrically developed dolomite bed corresponding to sedimentation in the more central position of the basin. Right: a cycle with a cracked dolomite bed corresponding to marginal position.

The symmetrical or asymmetrical aspect of a dolomite bed depends strongly on its position within the basin. Symmetric beds are an indicator of a more central position whereas asymmetric dolomite beds with visible alterations on their tops correspond to a more marginal position. Here only two dolomitic cycle types (*sensu* REINHARDT, 2000) are shown, but all cycle types are developed.

The cycles described above are somewhat idealized. It occurs that the dark gray stratified sediments are not developed at all and a cycle may start immediately with green gray dolomite beds. It is also possible that the dolomite might be eroded totally by incoming waters when exposed to the atmosphere.

Note that this cycle can be divided into two sub-cycles. As the basic cycle is thought to be originally caused by the precession the sub-cycles are supposed to reflect the hemi-precession.

The hemi-precession can be originated in two different ways (RUTHERFORD AND D'HONDT, 2000):

- The alignment of the perihelion with each equinox during one precession cycle produces a hemi-precessional cycle, analogous to semiannual cycle produced by the passage of the sun over the equator twice a year. This will lead to an increased insolation on the equator during these periods, which can be recorded in the sedimentary record.
- Because the Northern and Southern hemisphere are 180° out of phase, the export of a Southern hemisphere precession signal to the Northern hemisphere will produce a hemi-precessional cycle in the Northern hemisphere.

During Pangaean times in the northern hemisphere a lake could be established during relatively cool summers with earth at aphelion (DJF, fig. 71). Rainfall over the hinterlands flooded the playa system and the dark gray sediments were deposited. The orbital shift of the seasons during one basic cycle led to a successive dry-out of the playa system. During the first transition of the equinoxes through perihelion evaporation was strong enough to form dolomite. After the seasonal flooding during northern summer in perihelion (DJF) the basin dried out completely during, exposing the sediment to oxidation. Monsoonal intensity was reduced. Rainfall during these times might not even have reached into the basin, and only occasionally an input of some ephemeral rivers occurred. With the following transition of the equinoxes through perihelion pedogenesis took place and dolocrête was formed and the dry mudflat was deflated.

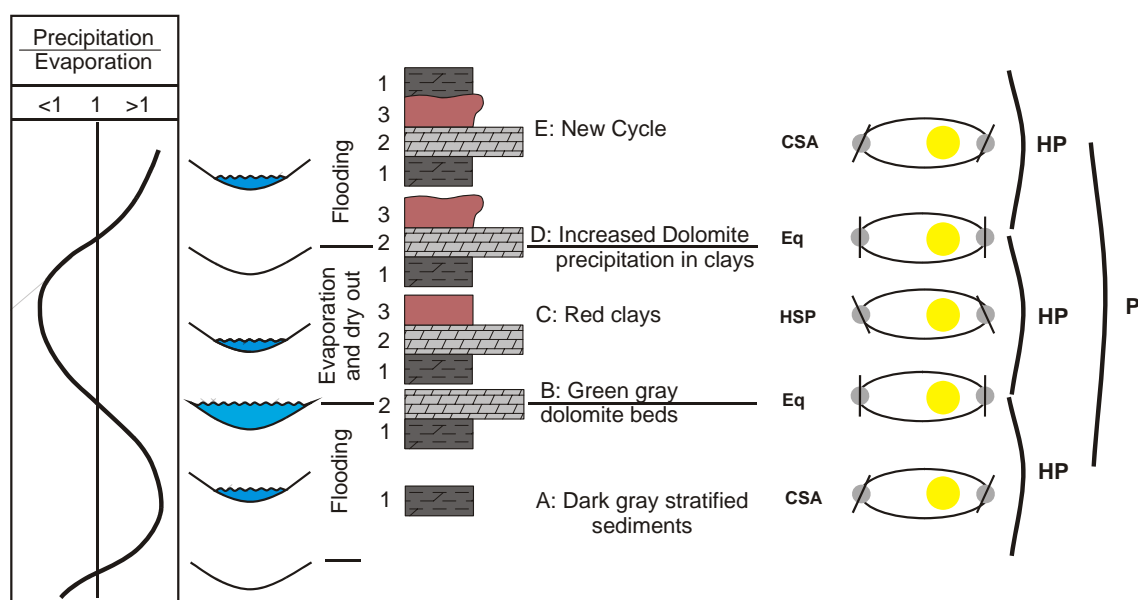


Fig. 71: Evolution of a wet/dry cycle within a precessional cycle. A: Because of the rainfall within cool summer at aphelion (CSA) the playa was flooded, a perennial lake formed and the dark grey sediments were deposited. B: As evaporation during equinoxes (Eq) at perihelion and aphelion got more important, dolomite beds were formed. C: The evaporation rate exceeded the precipitation rate when hot summers happened at perihelion (HSP). D: During next equinox (Eq) pedogenetic dolocrête is precipitated in the red clays and the surface is also deflated. E: Within the next cool summer at aphelion (CSA) a new cycle started. HP: Hemi-precession, P: Precession. Precipitation curve and basin levels after HORNUNG et al., 2002a and b.

**Pedogenetic dolocrête cycles**

It happened that rainfall was not enough to fill up the basin entirely. Thus, towards the margin the playa system was not flooded and only the groundwater system remained active and pedogenetic dolocrêtes evolved (fig. 72). Because of the lack of distinctive sedimentary features the deposition of red clays and the following dolomite precipitation can be roughly assigned only to summer coinciding with perihelion or aphelion. Any division considering the equinoxes during perihelion and aphelion is too uncertain within the dolocrête facies, as there are no further sedimentary and geochemical hints. First, the playa was flooded and the sediments were deposited during northern summer in perihelion (JJA). After seasonal flooding the playa dried out completely, exposing the formerly deposited sediments to oxidation. During northern summer at aphelion (DJF) precipitation was reduced but also the evaporation during winter times and displacive dolocrête growth took place within the capillary fringe of the groundwater system (fig. 73).

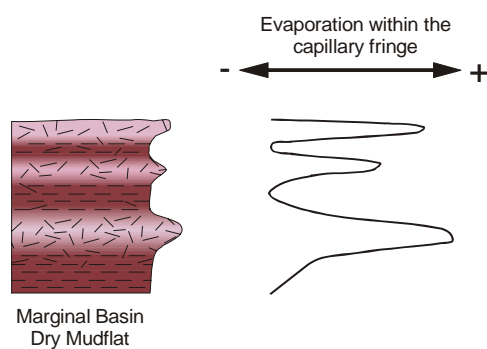


Fig. 72: Pedogenetic dolocrête cycle in a dry mudflat.

The hemi-precessional signal can not be proved and a further subdivision is too uncertain.

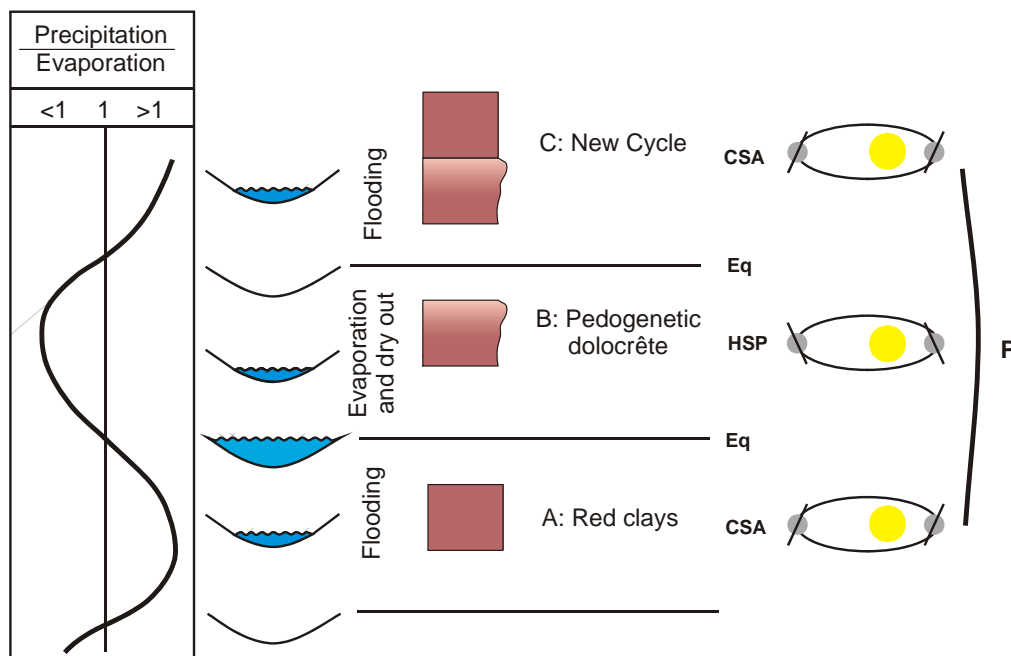


Fig. 73: Evolution of a pedogenetic dolocrête cycle within a precessional cycle. A: During CSA (DJF) the sediments were deposited. Seasonal evaporation exposed the clays to oxidizing conditions. B: During HSP the evaporation within the capillary fringe was more important and dolomite precipitated. C: A new cycle started. Abbreviations see fig. 71. Precipitation curve and basin levels after HORNUNG et al., 2002a and b.

**Gypsum cycles**

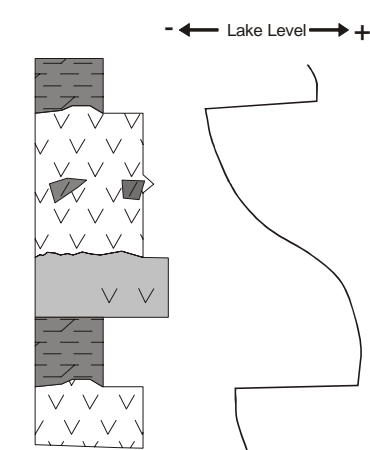


Fig. 74: Gypsum cycle within a long lasting wet period. A perennial lake was established even in times of increased evaporation.

A major facies shift occurred when the climate changed from the long dry periods to the long-lasting wet period. During these times the playa system was flooded with the onset of a long-lasting increased monsoonal activity and a wet-lake-dominated period could be established. The Gypsum cycle is an asymmetrically developed cycle beginning with dark gray, well-stratified sediments (fig. 74) deposited during cool summers (JJA, fig. 75). With successive evaporation and shallowing of the playa, green-gray dolomites were precipitated when earth's equinoxes passed through perihelion and aphelion. Further evaporation of the water led to an evolution of the brine during times of warm summers and displacive precipitation of major quantities of higher salts such as gypsum and/or minor quantities of halite within the pore space of the sediments took place sometimes destroying the structures of the surrounding sediments. As the playa did not dry out, gypsum could accumulate over longer periods of time and successive seasonal flooding events did not dissolve the entire gypsum. Here the hemi-precessional signal is recorded again, indicated by the presence of displacive gypsum in dolomite and the finely dispersed hematite in gypsum (fig. 75).

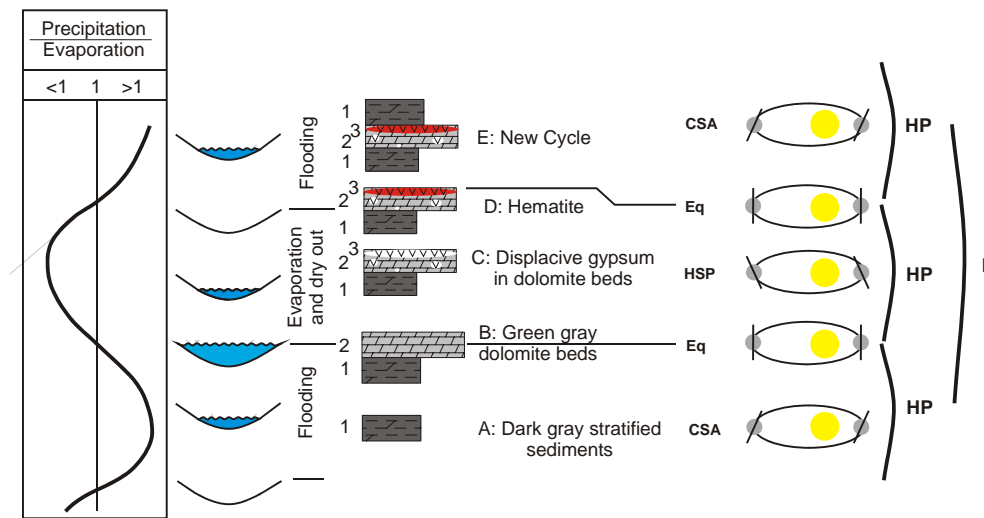


Fig. 75: Evolution of a gypsum cycle within a precessional cycle. A: Because of the rainfall within CSA the playa was flooded, a perennial lake formed and the dark gray sediments were deposited. B: As evaporation during Eq got more important dolomite beds were formed. C: The evaporation got more important and the brine evolved (i.e. the salinity of the lake raised) during HSP. Displacive growth of gypsum took place. D: After the next passage of the Eq with formation of finely dispersed hematite in Gypsum (red colour) a new cycle started. Abbreviations see fig. 71. Precipitation curve and basin levels after HORNUNG et al 2002a and b.



## Stacking pattern and hierarchy of the cycles

The three basic cycle types are the smallest recognizable units. From the facies analysis a climate model based on orbital parameters explaining the striking could be deduced. Moreover, these cycles show a well visible hierarchic pattern.

### Bundles of cycles

The basic cycles are organized in bundles of 5 to 7 cycles. The bundling is well visible in outcrops in southern and northern Germany. The example given below shows one of the bundles of cycles at Seebergen outcrop in the Drei Gleichen area.



Fig. 76: View on Seebergen outcrop (Drei Gleichen area, Thuringia) showing the bundling pattern of the basic cycles. Stratigraphically the outcrop is situated at the base of the Arnstadt Formation. S: stratigraphy.

The larger scale cycles can be seen at the outcrops Gleichenburg, Mühlentburg and Wachsenburg (Drei Gleichen area, Thuringia), but also in drill cores (fig. 77). These large-scale cycles are composed of bundles representing the shift from long lasting dry to long-lasting wet periods and vice versa.

The overall trend of the playa system shows that the Steinmergel Keuper is the continental part of a second-order cycle starting from a marginal marine sabkha environment (Weser Formation) passing through a continental playa milieu and finally transforming into an open marine environment.

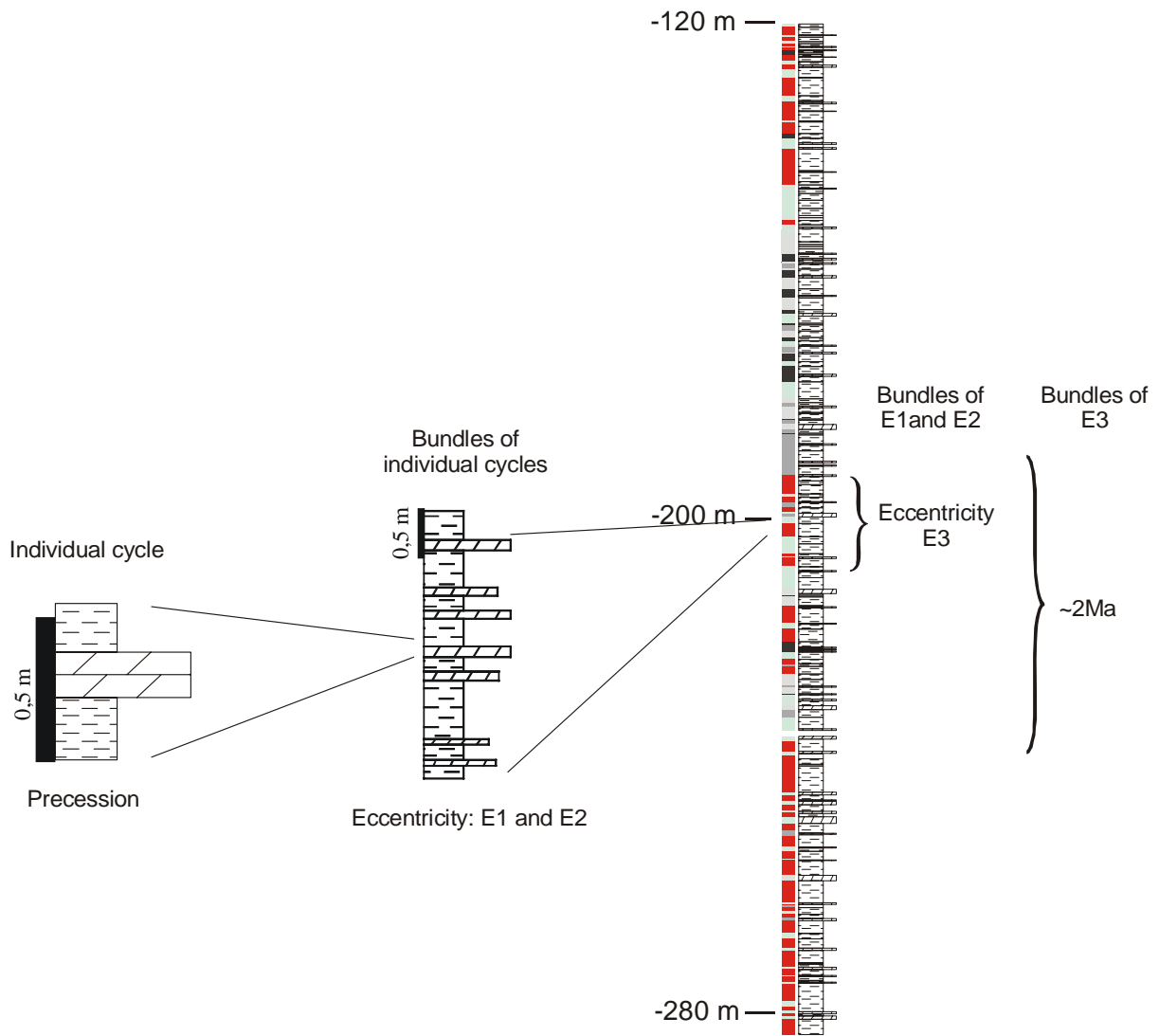


Fig. 77: Hierarchical stacking pattern of cycles within the Steinmergel Keuper playa system, thought to be of orbital origin. Core MorsDp52a.



## 4 Geochemistry and Geophysics

### 4.1 XRF Analysis

High resolution analysis of the geochemical bulk composition of rocks furnishes detailed information about major and minor element distribution within the different facies. Furthermore it gives an idea about the chemical and cyclic evolution of the playa system through time.

For reason of comparison the elements were Al-normalized. As Al is considered to be entirely of clastic origin, the element/Al ratios indicate changes during evaporation and therefore precipitation of minerals within the playa system. All these changes that happen in a playa system have their ultimate origin in climatic changes:

- 1) Climate has a strong influence on the weathering pattern of the hinterland. During times of increased monsoonal activity the weathering type of the hinterland shifts to towards more chemical weathering. This is traduced by lowered K/Al ratios in the playa system. On the other hand during dry periods, i.e. when the monsoonal activity decreases, a physical weathering of the hinterland is established and within the playa system the K/Al ratio raises.
- 2) However, the evaporation rate and brine evolution are directly influenced by climatic changes. Evolution of the brine during a succession of flooding and evaporation has cyclic variations within the salinity as a consequence. High evaporation rates lead to a dry out of the playa system with less brine evolution. This means that only smaller amounts of higher salt precipitate as efflorescent crust over the dry mudflat. This crust may either be removed by aeolian activity or be washed out by the next flooding event. By contrast, when evaporation rates are low the chemical composition of the lake waters evolves and salinity rises during evaporation. Then higher salts may precipitate after dolomite formation.
- 3) During early diagenetic processes the chemical composition of the pore room varies considerably. This variation depends highly on the influx (e.g. rainfall, fluviatile input, groundwater system) into the playa and the reflux (e.g. groundwater system) of the playa. However, the diagenetic processes are also influenced by the evaporation.
- 4) Microbial processes during carbonate precipitation play an important role in the evolution of a playa system as it is shown by the well known example from the Coorong lake, where primary dolomites have been precipitating in recent times (WRIGHT, 1999).
- 5) A climatically independent factor is the source area which can change in the central part of the playa system. In the present case there might be an influence not only from the Vindelicean High but also from the Fenno-Scandian-High, especially during times of higher aeolian input (see above).

The element/Al ratios are compared with the average chemical composition of shale (see Annexes) put forward by WEDEPOHL (1971, 1991). They characterize the increase or decrease of individual ratios.

### 4.1.1 The Basic Cycles

The three different cycle types (i.e. the Wet Dry Cycle, the gypsum Cycle and the pedogenetic Dolocrête Cycle) discussed above represent the evolution of the Steinmergel Keuper playa system at different climatic conditions, so they may serve as good examples to illustrate how the chemical and mineralogical composition varies through time and lithology.

#### Wet Dry Cycle

##### Description

A typical well-developed wet-dry cycle from the Obere Bunte Mergel has been chosen as an example (fig. 78). At the bottom of this cycle dark gray faintly laminated sediments are deposited. Then follows a symmetric dolomite bed, which shows no alteration at the bottom. At the top red clays appear. As the red clays are cemented by dolomite they have a rigid appearance and they also useful for stable oxygen and carbon isotopes analysis.

The Al-normalized plots (fig. 78) clearly show two different groups:

- Peaks at dolomite beds: Si/Al, Mn/Al, (Mg/Al+Ca/Al), Na/Al, Ni/Al, P/Al, Cl/Al, Co/Al, and V/Al.
- Peaks at mudstones: Fe/Al and K/Al.
- Ti/Al, Cr/Al Ba/Al, and Sr/Al show an ambivalent behavior.

Comparing with the average shale of WEDEPOHL (1971, 1991) following groups can be distinguished:

- Higher values for: Si/Al, Mn/Al, (Mg/Al+Ca/Al), K/Al and P/Al
- Lower values for: Ti/Al, Na/Al, Ni/Al, Sr/Al and V/Al
- Similar values for: Ba/Al, Co/Al and Cr/Al

The behavior for the oxides plots (fig. 79) is a quite different one than for the Al-normalized elements.

- Peaks at dolomite beds: Mn, (Mg + Ca), Co, Ni and Sr.
- Peaks at mudstones: Si, Ti, Fe, Na, K, P, Cr and V.

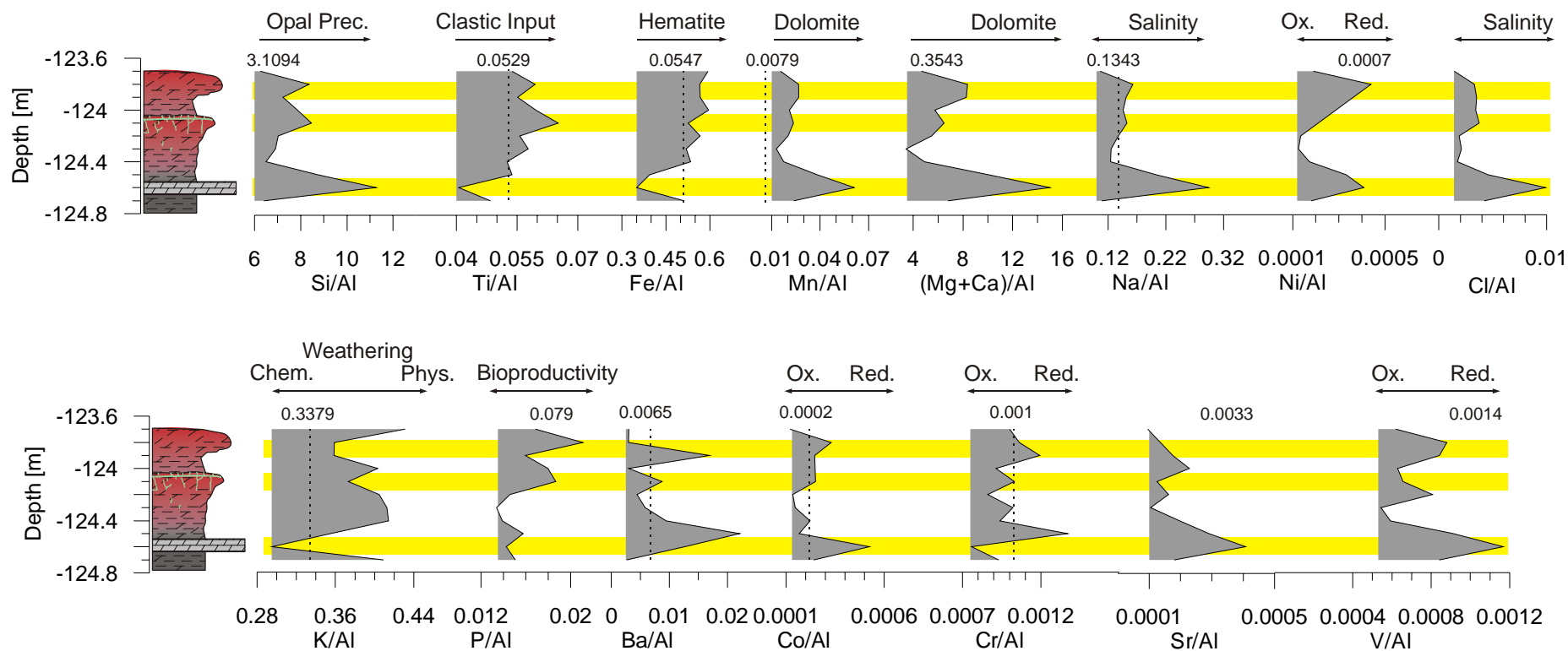


Fig. 78: Element/Al pattern within a basic wet-dry cycle. The dashed lines with values at the top indicates the average after WEDEPOHL (1971, 1991). Some of the plots do not show the average shale because the line plots largely out of the graph itself (see also text). Sample from core MorsDp52a. XRF data by courtesy of RÖHLING, H.-G., NLFb Hannover.

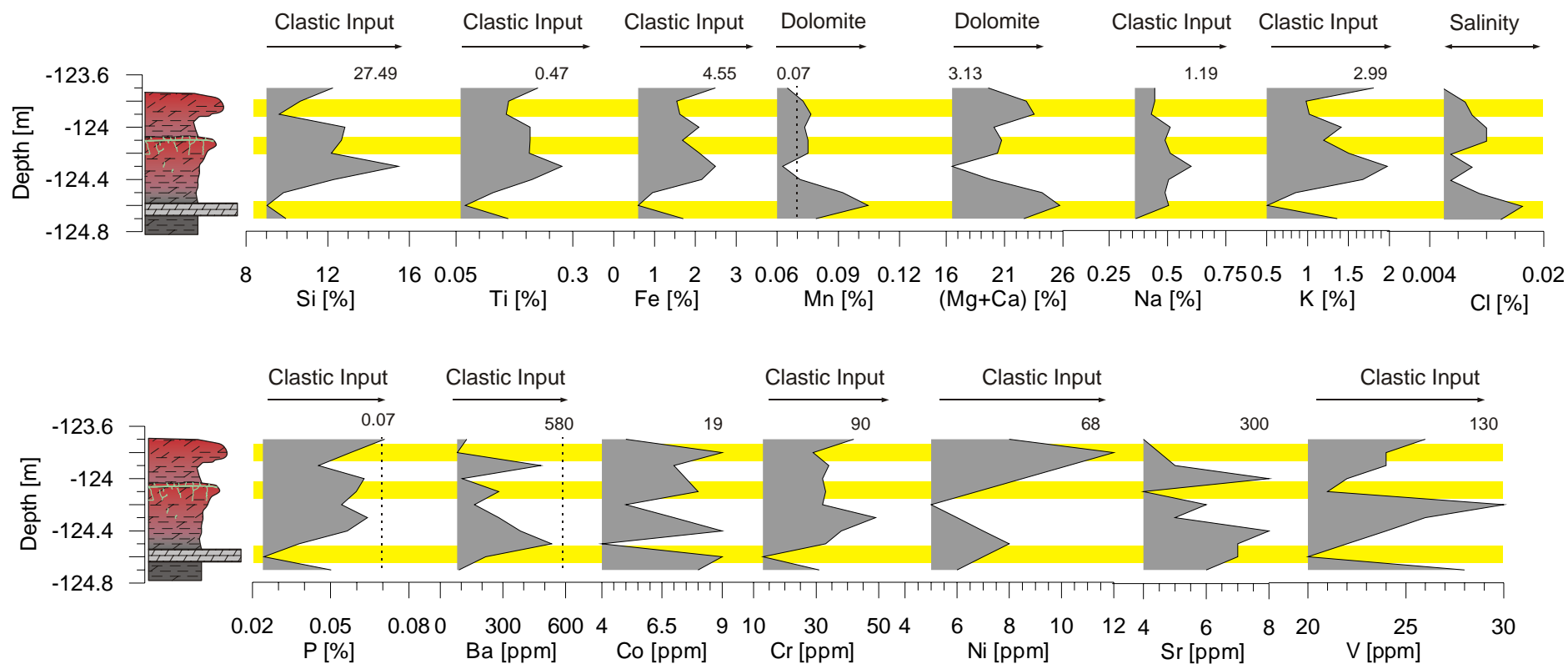


Fig. 79: Element distribution within a wet-dry cycle. The dashed lines with values at the top indicate the average after WEDEPOHL (1971, 1991). Some of the plots do not show the average shale because the line plots largely out of the graph itself (see also text). Sample from core MorsDp52a. XRF data by courtesy of RÖHLING, H.-G., NLfB Hannover.

The ternary plot  $\text{SiO}_2 - (\text{MgO} + \text{CaO}) - \text{Al}_2\text{O}_3$  (fig.80) shows two overlapping shifts:

- One between the dolomitic and quartzitic end members
- One between  $\text{SiO}_2$  and  $\text{Al}_2\text{O}_3$ .

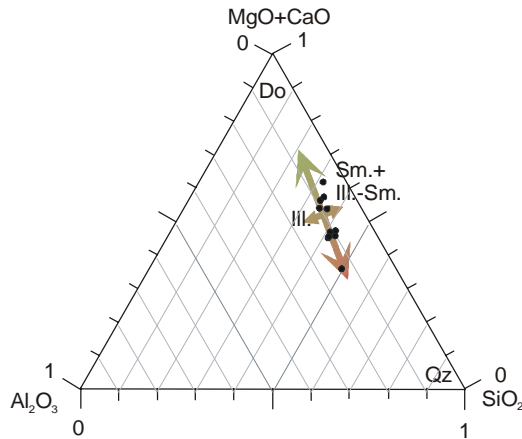


Fig. 80: Ternary diagram of chosen elements and element/Al ratios of the basic wet dry cycle. Do: dolomite, Qz: quartz Ill.: illite, Sm.: smectite, Ill.-Sm.: mixed layer illite-smectite (regular and irregular), red.: reducing conditions, ox.: oxidizing conditions. XRF data by courtesy of RÖHLING, H.-G., NLFb, Hannover.

## Interpretation

The  $(\text{Mg}/\text{Al} + \text{Ca}/\text{Al})$  ratio clearly represents the dolomite phase that precipitated during wet periods when the monsoonal intensity increased. The  $\text{Mn}/\text{Al}$  plot shows a similar pattern to the  $(\text{Mg}/\text{Al} + \text{Ca}/\text{Al})$  curve. Mn can be incorporated into the dolomite during precipitation by replacing the Mg. As Mn is an activator element under the CL – microscope (ADAMS AND MACKENZIE, 2001) the dolomite shows a bright red luminescence (see above). Normally, the coincidence of the Ba/Al and Sr/Al peaks with the dolomite show their close relation to the dolomite lattice. In any case, Ba/Al and Sr/Al peaks do not fit together every time with  $(\text{Mg}/\text{Al} + \text{Ca}/\text{Al})$  peaks, suggesting that may be a threshold value, which must be overcome so that Ba and Sr can be incorporated into the dolomite lattice.

Peaks of Cr/Al, Co/Al, Ni/Al and V/Al indicate the presence of reducing conditions during early diagenesis and carbonate precipitation.

The presence of phosphorous shown by the P/Al peak indicates higher primary bio production during dolomite precipitation.

The high Si/Al ratio reflects the dissolution of quartz and its precipitation as opal. The pH value of the lake water can vary significantly during the flooding and evaporation of a playa lake as PETERSON AND VAN DE BORCH (1965) showed. Silica is dissolved at  $\text{pH} > 9$ . When pH lowers amorphous silica precipitates.

The Na/Al and Cl/Al ratios suggest variations within the salinity of the evolving brine within the playa lake and the groundwater system of the mudflat. This is strengthened by the fact that their respective curves parallel the  $(\text{Mg}/\text{Al} + \text{Ca}/\text{Al})$  plot. But the general low values of the Cl/Al ratios also suggest that salinity does not play such an important role as one would expect in such extreme environments as the Steinmergel Keuper represents.

All three of the Ti/Al -, Fe/Al – and K/Al ratios indicate the overall detrital input into the playa system. The K/Al ratios rise during dry periods reflecting the increased physical weathering pattern of the hinterlands. During wet periods the weathering pattern of the hinterlands shifts toward more chemical weathering, which is traduced specially by lowered K/Al within the playa lake. This indicates the reducing conditions during dolomite precipitation and sedimentation of dark gray sediments in the playa system.

Increased Fe/Al ratios coincide with red clays indicating the dry-out of the playa margin. As hematite is the red coloring pigment (see above) the relative variation of the iron content is at the origin of the different shades of red that may appear. Despite the similar trends of the Ti/Al- and the Fe/Al ratios their peaks do not correlate.

The similar behavior of the Si, Ti, Fe, Na, K, P, Cr and V plots show obviously the overall clastic input into the playa. This seems contradictory to the fact that the Si/Al, Na/Al and P/AL suggest increased bioproductivity and salinity (Na/Al). But this means that only minor components of the clastic silica, phosphorous and sodium were dissolved and precipitated afterwards, so that the elements still show their detrital origin.

The Mn, (Mg + Ca), Cl, Co, Ni and Sr plots show the enrichment of these elements in the playa lake during wet periods and within the groundwater system of the mudflat.

Co has an ambivalent behavior. At the beginning it seems that it derives from a clastic input but then the pattern of the plot changes indicating a dissolved input.

The ternary plots  $\text{SiO}_2 - (\text{MgO} + \text{CaO}) - \text{Al}_2\text{O}_3$  shows clearly a cyclic trend from a more dolomitic end member to a clastic end member. Overlapping this trend a cyclic shift from illite to smectite and mixed layer illite-smectite (regular and irregular) can be deduced (see also chapter 3.2, *Clay Mineralogy*). This reflects the cyclic shift of the playa system from reducing (playa lake, wet periods) to oxidizing (mudflat, dry periods) conditions. It runs parallel with the cyclic evolution of the salinity. The salinity is highest during dolomite precipitation in the playa lake. After flooding and within the dark gray sediments the salinity has its lowest values. Intermediate values are observed during dolomite precipitation within the capillary fringe of the mudflat. A succession of wetting and drying leads to cyclic variation within the salinity.

---

## Gypsum Cycle

### Description

The typical gypsum cycle is characterized by cyclic change of dark gray faintly laminated sediment at the bottom and a dolomite bed with displacive gypsum growth within the dolomite bed at its top. The example described core MorsDp52a, belongs stratigraphically to the Mittlere Graue Mergel of the Arnstadt Formation.

The elements and their respective –Al ratios behave differently from the cycle described before, reflecting the more complex chemical pattern due to the evolution of the lake waters. Two main groups can be differentiated (fig. 81):

- Peaks at dolomite beds: Fe/Al, Mn/Al, (Mg/Al + Ca/Al), Na/Al, P/Al, S/Al, Ba/Al, Sr/Al and V/Al
- Peaks at mudstones: Si/Al, Ti/Al, K/Al, Co/Al, Cr/Al, and Ni/Al

Comparing with the average shale of WEDEPOHL (1971, 1991) following groups can be distinguished:

- Higher values for: Si/Al, Fe/Al, (Mg/Al+Ca/Al), K/Al P/Al, S/Al, Ba/Al at dolomite beds and Sr/Al
- Lower values for: Ti/Al, Na/Al, Ba/Al at mudstones, Co/Al, Cr/Al, Ni//Al and V/Al with somewhat higher values at dolomite beds

The behaviour for the oxides plots (fig. 82) is quite a different one than for the Al-normalized:

- Peaks at dolomite beds: Mn, (Mg + Ca), S, Ba and Sr.
- Peaks at mudstones: Si, Ti, Fe, Na, K, P, Co, Cr, Ni and V.

The ternary plot  $\text{SiO}_2 - (\text{MgO} + \text{CaO}) - \text{Al}_2\text{O}_3$  (fig. 83) shows two overlapping shifts:

- One between the dolomitic and quartzitic end members
- One between  $\text{SiO}_2$  and  $\text{Al}_2\text{O}_3$ .

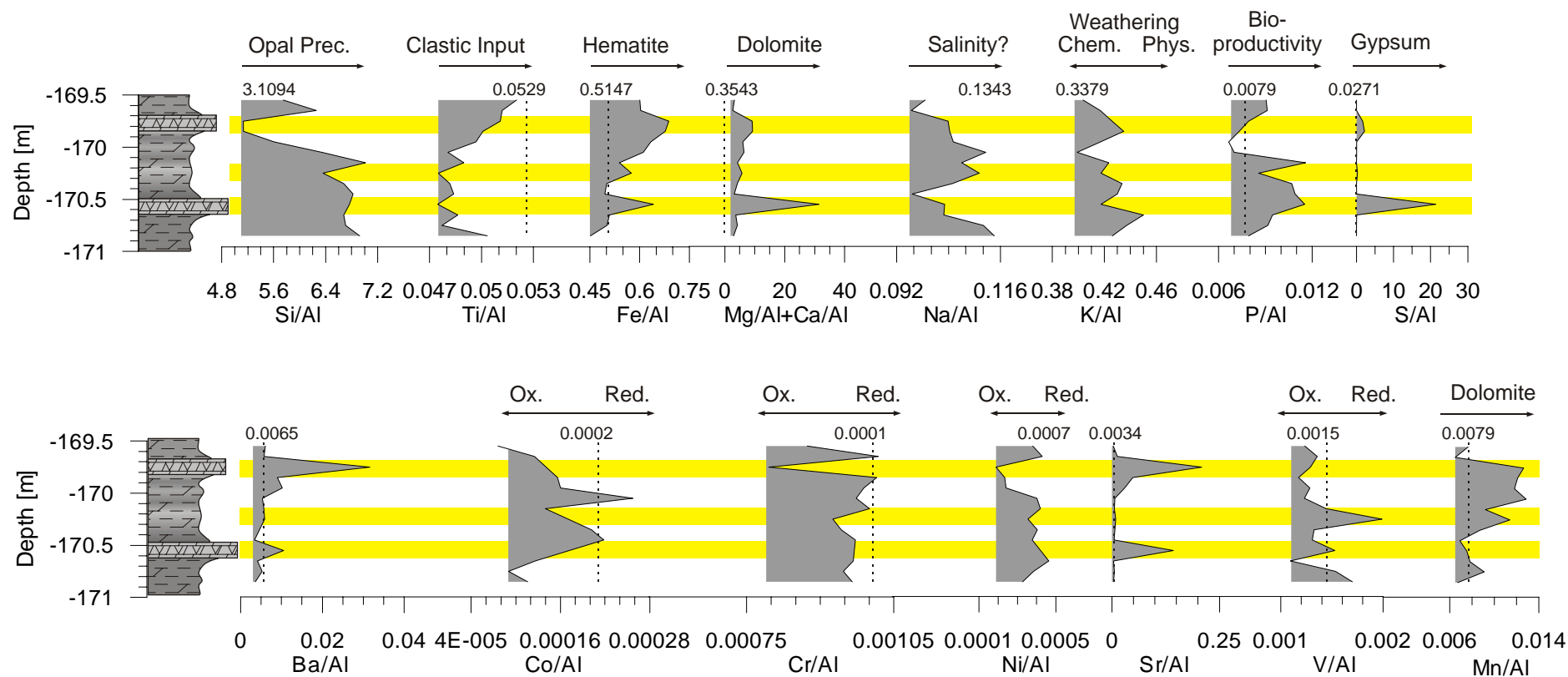


Fig. 81: Element/Al pattern within a basic gypsum cycle. The dashed lines with values at the top indicate the average after WEDEPOHL (1971, 1991). Some of the plots do not show the average shale because the line plots largely out of the graph itself (see also text). Sample from core MorsDp52a. XRF data by courtesy of RÖHLING, H.-G., NLFb Hannover.



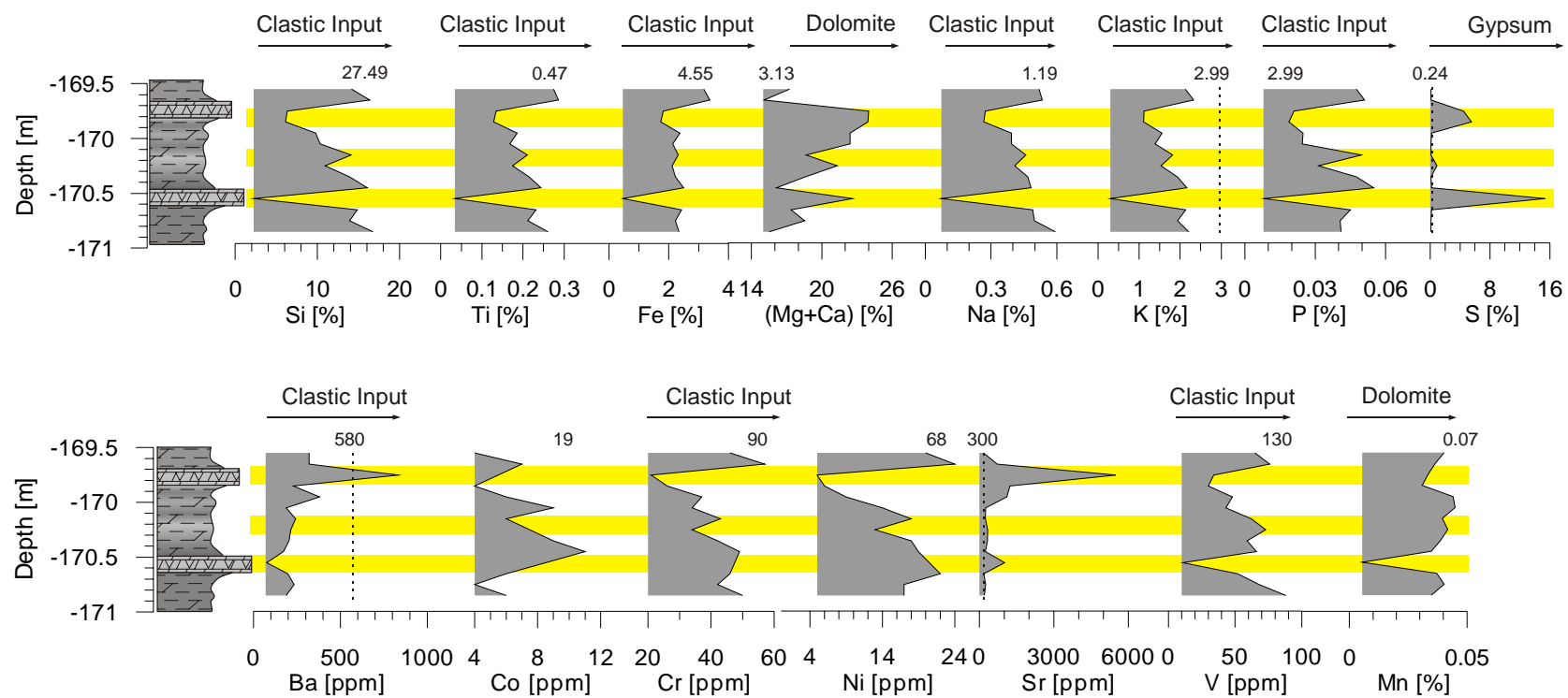


Fig. 82: Element distribution within a basic gypsum cycle. The dashed lines with values at the top indicate the average after WEDEPOHL (1971, 1991). Some of the plots do not show the average shale because the line plots largely out of the graph itself (see also text). Sample from core MorsDp52a. XRF data by courtesy of RÖHLING, H.-G., NLfB Hannover.

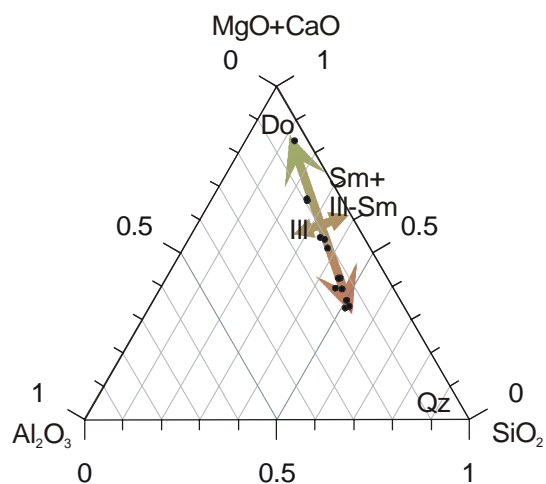


Fig. 83: Ternary diagrams of chosen elements and element/Al ratios of a basic gypsum cycle from core MorsDp52a showing the shift between illite (Ill.) and smectite+mixed layer illite-smectite regular and irregular (Ill.-Sm.). The overall quartz (Qz) and dolomite (Do) content provokes a general shift of the trend towards the quartz and dolomite end members. The arrows indicate the cyclic variations between the end members. RFA data by courtesy of RÖHLING, H.-G., NLFb Hannover.

## Interpretation

The (Mg/Al + Ca/Al) ratio clearly represents the dolomite phase. The Mn/Al plot indicates the incorporation of Mn in dolomite phase. Astonishingly the Mn/Al peaks do not exactly fit together with the (Mg/Al + Ca/Al) peak, even though the trends of the plots are similar. This is due to the fact that within the dolomite displacive growth of gypsum took place. So considerable amounts of Ca are bound in the gypsum. But the plot still reflects the dolomite precipitation. The coincidence of the Ba/Al and Sr/Al peaks with the dolomite show their close relation to the dolomite lattice.

Astonishingly the Fe/Al ratio coincides well with the dolomite and gypsum beds. This is surely due to secondary dissolution of iron oxides and its precipitation as finely dispersed hematite within the gypsum (see chapter 3.5, *Gypsum Facies*) during early diagenesis. That means that during the latest phase of brine evolution the conditions within the playa system changed from reducing to oxidizing conditions. This explains well the fact that the gypsum is partially red.

Another surprising fact is that sometimes high K/Al ratios fit together with the dolomite and gypsum phase. This reflects rather the weathering conditions of the hinterlands during gypsum (and not dolomite!) precipitation. The gypsum grew later than the dolomite but it displaced the dolomite (see above). So it may be a mixed signal composed of the input during dolomite precipitation, i.e. increased monsoonal activity and chemical weathering of the hinterlands, and during gypsum precipitation, i.e. somewhat decreased monsoonal activity and chemical weathering of the hinterlands relative to times of dolomite formation.

The Na/Al ratios again suggest variations of salinity during brine evolution. After a flooding event with deposition of dark gray sediments the ratios are low and then with on going evaporation the ratios raise. The values are lowered again with the onset of the next cycle.

Peaks of Cr/Al, Co/Al, Ni/Al and V/Al indicate the presence of reducing conditions during early diagenesis.

The phosphorous peak indicates higher primary bio production.

High Si/Al ratio reflects the dissolution of quartz and its precipitation as opal.

Again the similar behaviour of the Si, Ti, Fe, Na, K, P, Co, Cr, Ni and V plots show obviously the overall clastic input into the playa. On the other hand, the (Mg+ Ca), S, Ba and Sr are derived from the dissolved input into the playa. Due to the fact of gypsum formation the Mn plot is not parallel to the (Mg+ Ca) plot.

The ternary plot  $\text{SiO}_2 - (\text{MgO} + \text{CaO}) - \text{Al}_2\text{O}_3$  indicates the trend from a more dolomitic component to a clastic component, reflecting cyclic flooding/evaporation events. After flooding the detritus is deposited and with ongoing evaporation the brine evolves (i.e. the salinity rises) and first dolomite is formed and then gypsum within the dolomite. The other superimposed trend reflects the cyclic shift between illite and smectite, mixed layer illite-smectite.

## **Pedogenetic Dolocrête Cycle**

### **Description**

The typical dolocrête cycle consists of a cyclic change from red clays with relatively low dolomite content to slightly red shaded gray dolocrête horizons. The example below from core MorsDp52a belongs to the Untere Bunte Mergel of the Arnstadt Formation.

The Al-normalized plots (fig. 84) show three different groups:

- Peaks at dolomite beds: Si/Al, Mn/Al, (Mg/Al + Ca/Al), Na/Al, P/Al, and Ni/Al
- Peaks at mudstones: K/Al
- The following ratios show an ambivalent behaviour: Ti/Al, Fe/Al, Ba/Al, Co/Al, Cr/Al, and V/Al and Sr/Al

Comparing with the average shale of WEDEPOHL (1971, 1991) following groups can be distinguished:

- Higher values for: Si/Al, Fe/Al, Na/Al, K/Al, Sr/Al and P/Al
- Lower values for: Ni/Al and V/Al
- Similar values for: Co/Al, Ba/Al

The behaviour for the oxides plots (fig. 85) the following groups:

- Peaks at dolomite beds: Mn and (Mg + Ca)
- Peaks at mudstones: Si, Ti, Fe, Na, K, Cr, Ni and V.
- Ambivalent behaviour: P, Co, Ba Sr

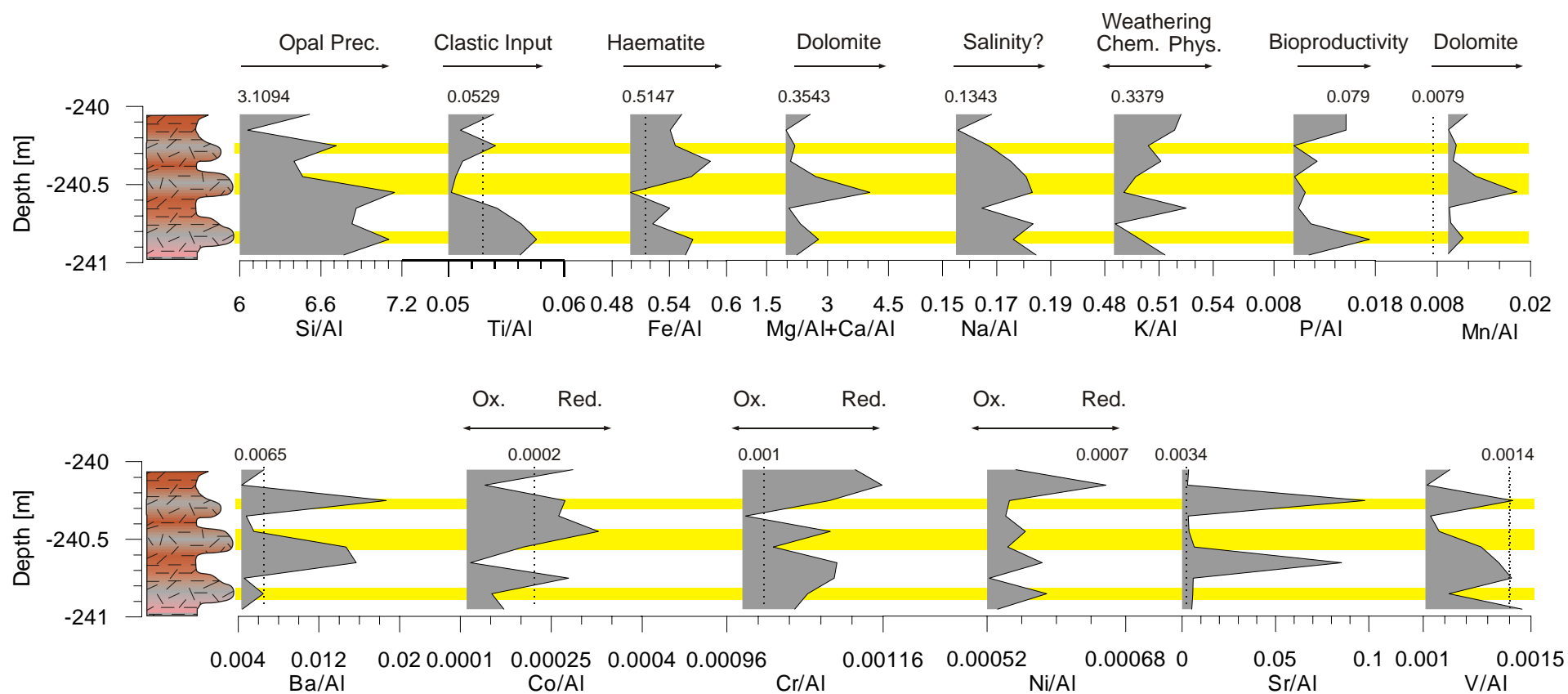


Fig. 84: Element/Al pattern within a pedogenetic dolocrête cycle from core MorsDp52a. The dashed lines with values at the top indicate the average after WEDEPOHL (1971, 1991). Some of the plots do not show the average shale because the line plots largely out of the graph itself (see also text). Sample from core MorsDp52a. XRF data by courtesy of RÖHLING, H.-G., NLFb Hannover.

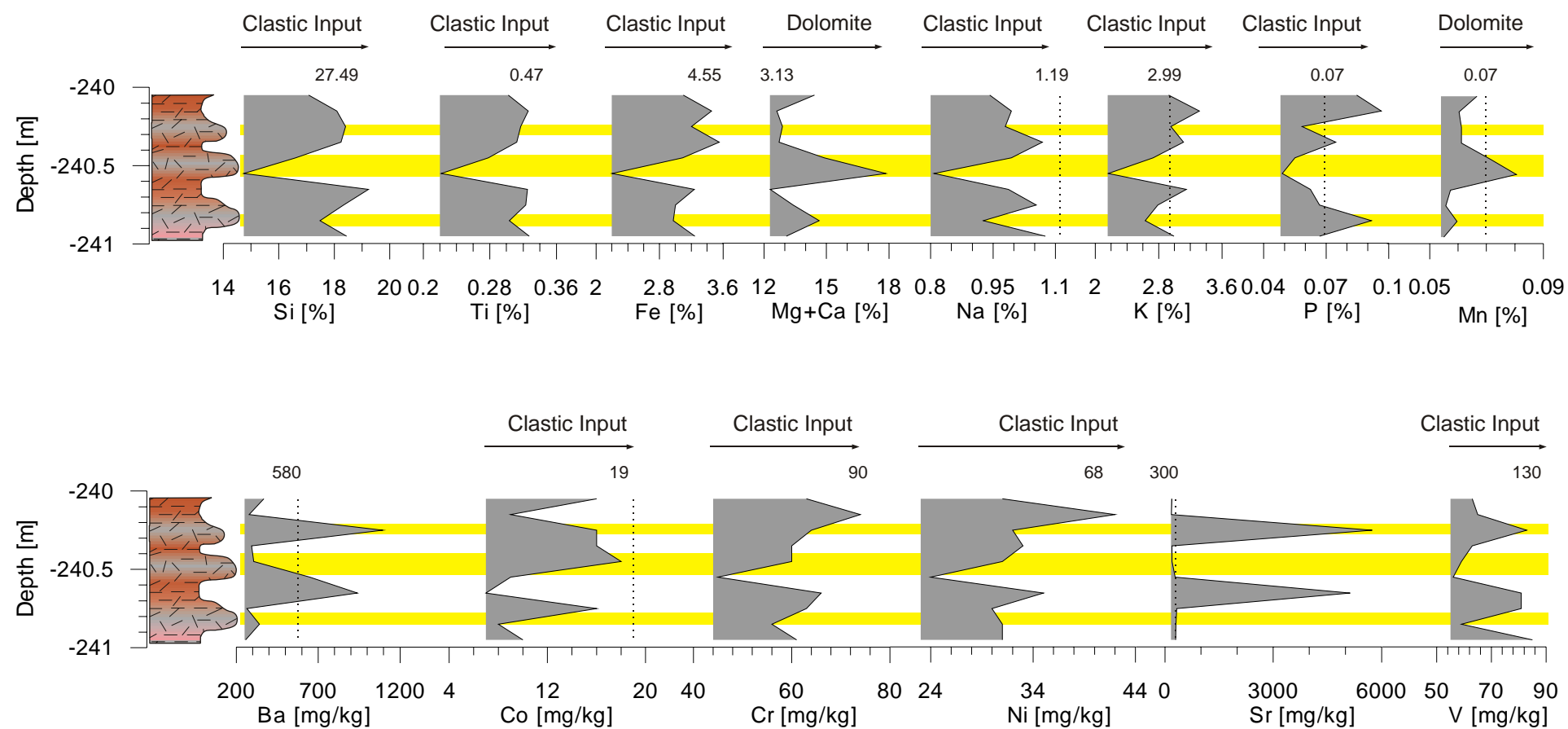


Fig. 85: Element distribution within a basic dolocrête cycle. The dashed lines with values at the top indicate the average after WEDEPOHL (1971, 1991). Some of the plots do not show the average shale because the line plots largely out of the graph itself (see also text). Sample from core MorsDp52a. XRF data by courtesy of RÖHLING, H.-G., NLfB Hannover.

The ternary plot  $\text{SiO}_2 - (\text{MgO} + \text{CaO}) - \text{Al}_2\text{O}_3$  (fig.86) shows two overlapping shifts:

- One between the dolomitic and quartzitic end members
- One between  $\text{SiO}_2$  and  $\text{Al}_2\text{O}_3$ .

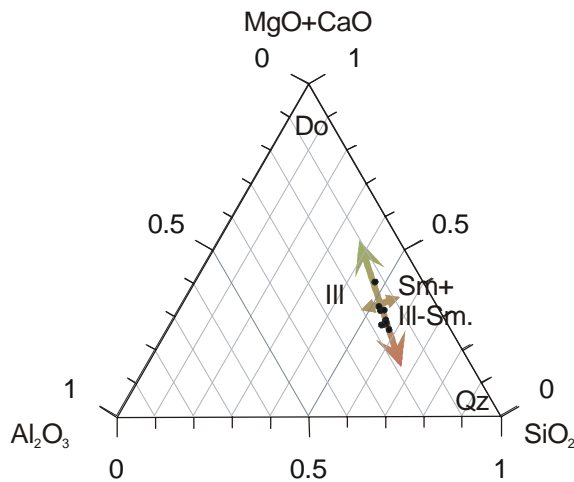


Fig. 86: Ternary diagram of chosen elements of a basic pedogenetic dolocrête cycle from core MorsDp52a showing the shift between illite (Ill.) and smectite+mixed layer illite-smectite regular and irregular (Ill.-Sm.). The overall quartz (Qz) and dolomite (Do) content provokes a general shift of the trend towards the quartz and dolomite end members. The arrows just indicate the cyclic variations between the end members. RFA data by courtesy of RÖHLING, H.-G., NLFb Hannover.

## Interpretation

The  $(\text{Mg}/\text{Al} + \text{Ca}/\text{Al})$  ratio clearly represents the dolomite phase. The  $\text{Mn}/\text{Al}$  plot indicates the incorporation of Mn in the dolomite lattice. The coincidence of the  $\text{Ba}/\text{Al}$  and  $\text{Sr}/\text{Al}$  peaks with the dolomite shows their close relation to the dolomite. Interestingly, their peaks do not coincide every time with the dolomite phase.

The  $\text{Fe}/\text{Al}$  ratio shows an ambivalent behaviour, suggesting a change to more oxidizing conditions after dolomite formation. Surprisingly, the  $\text{Ti}/\text{Al}$  also behaves ambivalently. It seems that Ti was partially incorporated in the hematite lattice.

The  $\text{K}/\text{Al}$  ratio shows the weathering pattern of the hinterlands. During dolomite formation the chemical weathering of the source area rose and conversely during formation of red clays physical weathering predominated in the source area.

Peaks of  $\text{Cr}/\text{Al}$ ,  $\text{Co}/\text{Al}$ ,  $\text{Ni}/\text{Al}$  and  $\text{V}/\text{Al}$  indicate the presence of reducing conditions during early diagenesis.

$\text{Na}/\text{Al}$  may reflect to some degree the evolution of the salinity within the groundwater system. But it is more probable that Na is used to build up the Analcime and Zeolithe minerals which were formed within the dolocrête horizons.

The phosphorous peak indicates higher primary bio production.

The high  $\text{Si}/\text{Al}$  ratio reflects the dissolution of quartz and its precipitation as opal.

The similar behaviour of the Si, Ti, Fe, Na, K, P, Co, Cr, Ni and V plots show clearly the overall clastic input into the playa, whereas the (Mg + Ca), Mn, Ba and Sr are derived from the dissolved input into the playa.

The ternary plot  $\text{SiO}_2 - (\text{MgO} + \text{CaO}) - \text{Al}_2\text{O}_3$  indicates the trend from a more dolomitic component to a clastic component reflecting cyclic flooding/evaporation events. After flooding the detritus was deposited but a playa lake was not formed, and only the groundwater table was raised. With on going evaporation the groundwaters evolved (i.e. the salinity raised) and first dolocrête was formed and afterwards the hematite (sometimes within the dolocrête). The other superimposed trend reflects the cyclic shift between illite and smectite, mixed layer illite-smectite.

### 4.1.2 Bundles of Cycles

#### Wet Dry Cycle

The conspicuous bundling pattern of the XRF data for this cycle type is also reflected by the striking lithologic cyclicity. The example described from the top of the core MorsDp52a has a thickness of about 6m and belongs stratigraphically to the Obere Bunte Folge of the Arnstadt Formation.

#### Description

The Al-normalized plots (fig. 87) also show clearly two different groups:

- Peaks at dolomite beds: Si/Al, Mn/Al, (Mg/Al + Ca/Al), Na/Al, P/Al, Ba/Al, Ni/Al, and Sr/Al. Specially Si/Al, Mn/Al and (Mg/Al + Ca/Al) show a striking symmetric bundling pattern running parallel to the dolomite beds. The values rise systematically from a minimum to maximum and diminish systematically to a minimum.
- Peaks at mudstones: Ti/Al, Fe/Al, K/Al, Co/Al, and Cr/Al

Comparing with the average shale of WEDEPOHL (1971, 1991) the following groups can be distinguished:

- Higher values for: Si/Al, (Mg/Al + Ca/Al), Na/Al, K/Al, P/Al and Ba/Al at dolomite beds.
- Lower values for: Ba/Al at mudstones, Ni/Al, Sr/Al and V/Al.
- Values close to the average: Fe/Al, Ti/Al, Co/Al and Cr/Al.



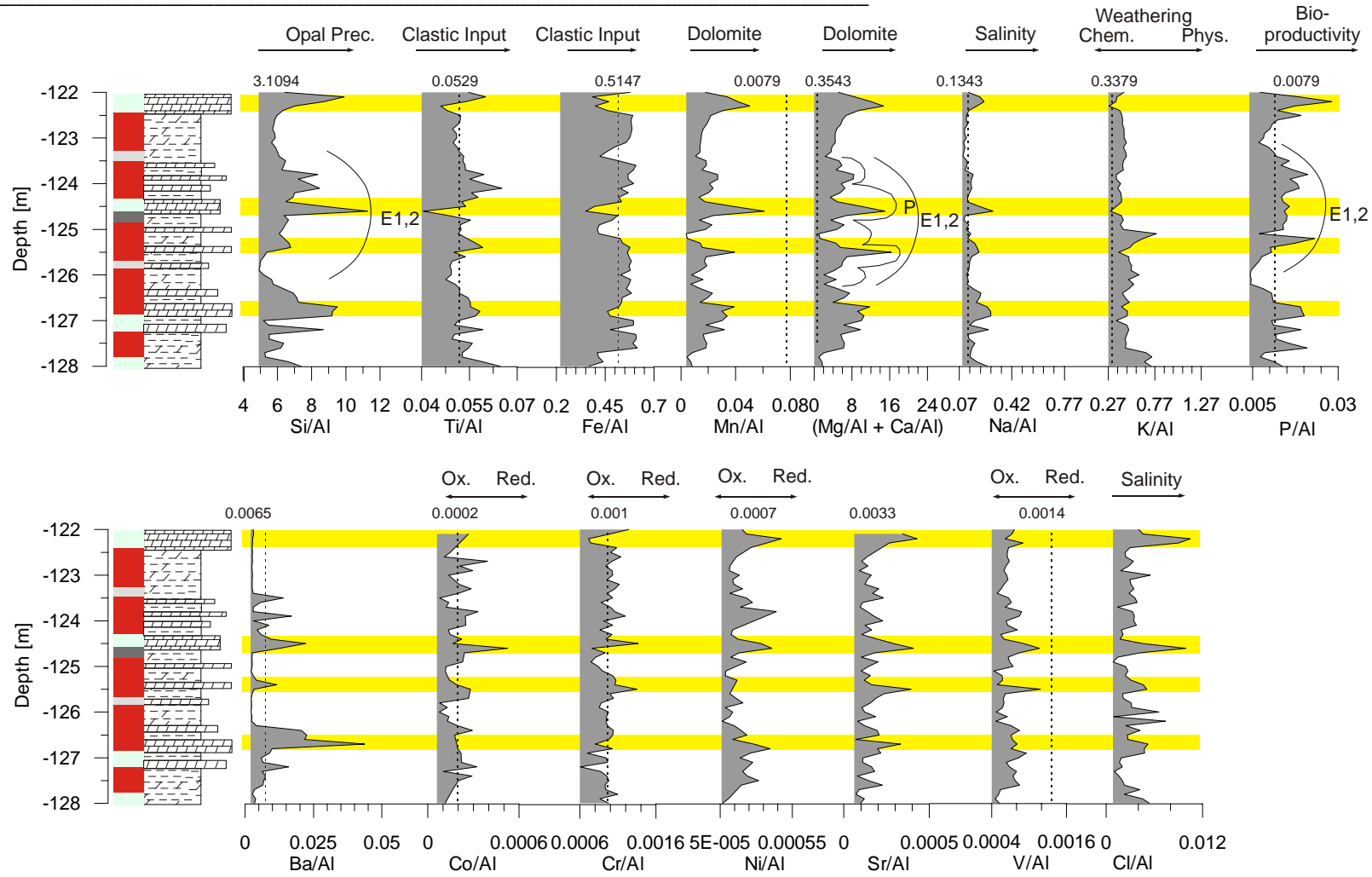


Fig. 87: Element/Al ratios from the bundled Wet-Dry Cycle. From the top of core MorsDp52a. Note that the development of basic cycles is not ideal every time. P: precession, E1,2: eccentricity of. RFA data by courtesy of RÖHLING, H.-G., NLFb Hannover.

---

## Interpretation

The striking bundling pattern of dolomite succession shows well the cyclic evolution from a somewhat deeper lake to the mudflat. The overall trend within this period is generally dry with some smaller intercalated wetter phases. The bundling pattern of the basic cycles reflects strong changing monsoonal activity traduced by increased/decreased precipitation over the hinterlands and the playa system.

The Mg/Al + Ca/Al ratio reflects clearly the dolomite phase. The highest peaks were reached during wet periods when a lake was established. Higher dolomite content in the red mudstones reflects the dolomite formation during groundwater evolution when waters evaporated within the capillary fringe of the mudflat. As the Mn/Al plot parallels exactly the dolomite evolution again the close relationship with the dolomite lattice is demonstrated. The coincidence of Ba/Al and Sr/Al bundles with Mg/Al + Ca/Al bundles supports the assumption of Ba and Sr incorporation. The similarity of Si/Al bundles and P/Al bundles strengthens the interpretation of biological activity in the playa system. The systematic raising and diminishing of their peaks within the bundles suggest a systematic amelioration/deterioration of climatic conditions which prevailed in the playa system.

Salinity cycles indicated by the Na/Al and Cl/Al ratios are less conspicuous than the dolomite cycles, but the coincidence of their peaks with the dolomite peaks strongly suggests a parallel variation of the salinity of the lake and groundwater during wetting and drying.

High Fe/Al ratios occurred in red mudstones, highlighting the fact that Fe<sup>3+</sup> was used to form hematite when oxidizing conditions prevailed. Variations in the Fe/Al ratios reflect clearly changing red/ox conditions.

Ti/Al, K/Al and also Fe/Al indicate the overall clastic input into the playa. This is especially neatly shown by the antagonistic behavior of the K/Al and the Fe/Al ratios respective to the dolomite.

The red/ox sensitive parameters V/Al and Ni/Al parallel well the Mg/Al + Ca/Al plot, indicating the reducing conditions during dolomite formations. Co/Al and Cr/Al appear to be enriched sometimes within the red mudstones, maybe reflecting a threshold value that has to be overcome to enrich these elements.

## Crossplots

### Description and Interpretation

The good correlations between Ca-Mg and Mn-Mg (fig. 88) clearly represent the dolomite phase in the playa.

Sr-(Mg + Ca) shows a poor inverse correlation and P-(Mg + Ca) has a moderate correlation. Both curves suggest a detritical origin of strontium and phosphorous. Sr seems not be enriched within the dolomite as also observed within the basic wet dry cycle.

The positive correlation between K-Ti and Si-Ti shows clearly the clastic origin of these elements. As silica was used to form opal and the clastic origin is still visible the same as for phosphorous must be deduced: only minor amounts of silica were used for opal formation.

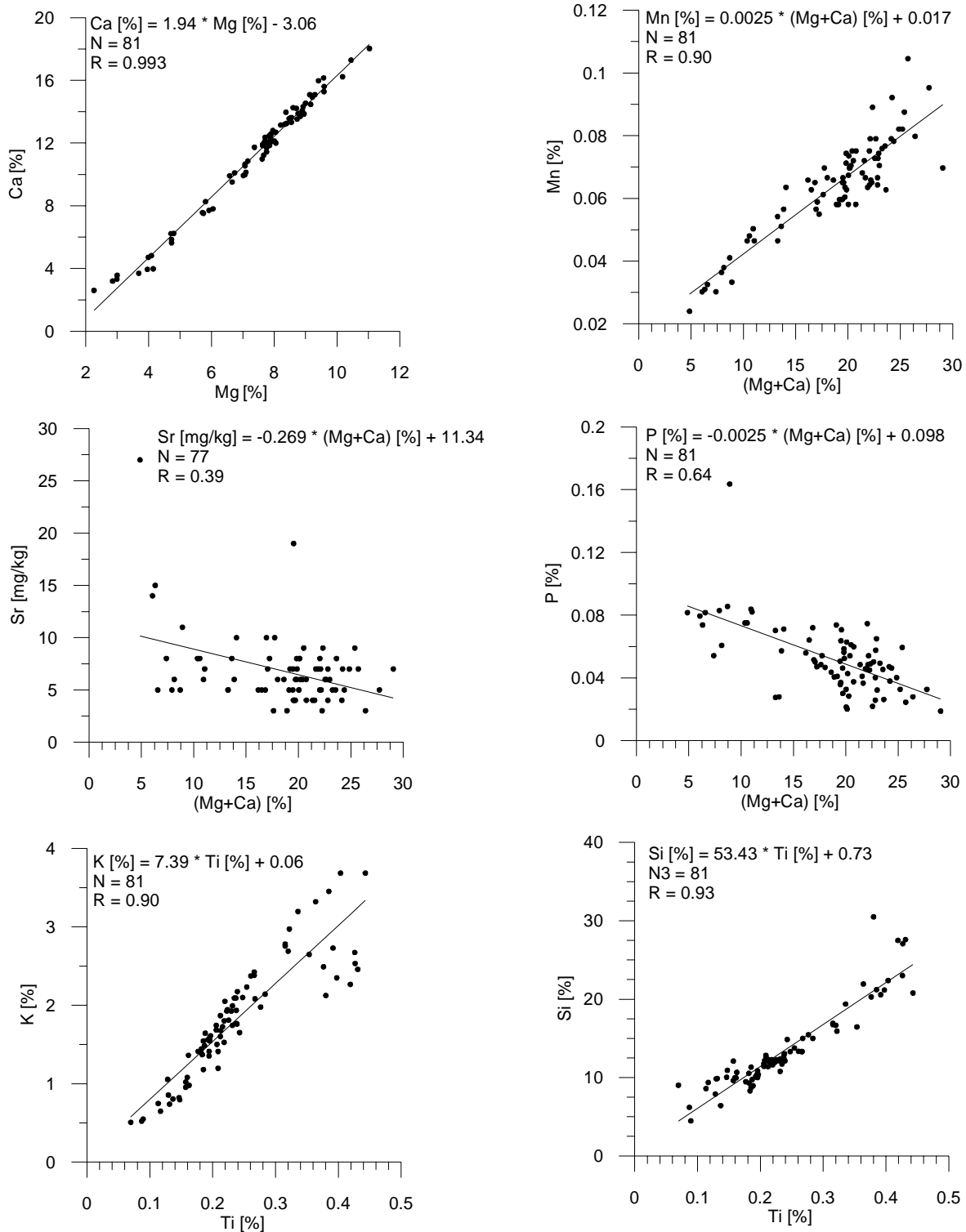


Fig. 88: Cross plots of chosen elements within the bundled wet dry cycle. Note the inverse relationships between Sr and (Mg+Ca) and P and (Mg+Ca). From the top of core MorsDp52a. RFA data by courtesy of RÖHLING, H.-G., NLFb Hannover.

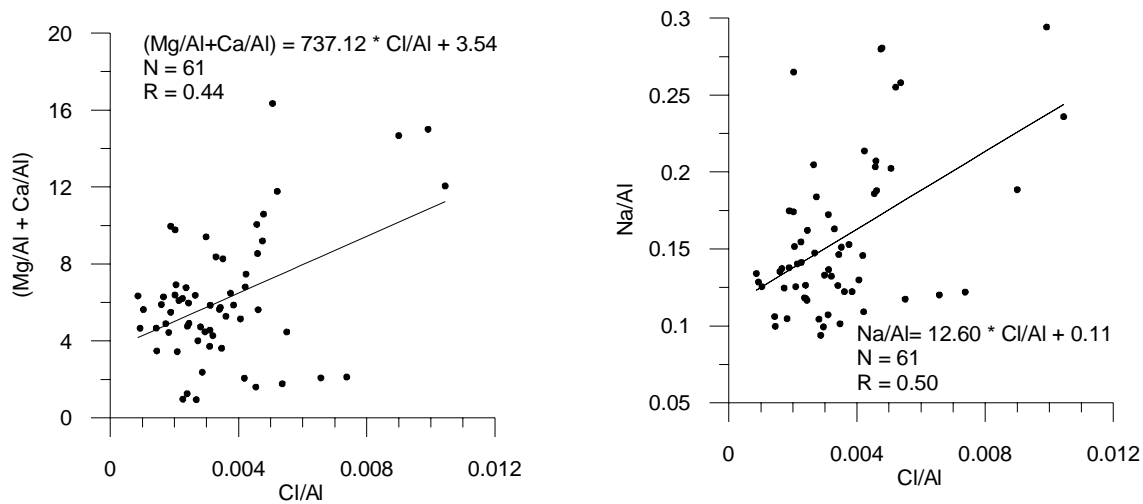


Fig. 89: Cross plots of (Mg/Al + Ca/Al) - Cl/Al ratios and Na/Al-Cl/Al ratios of the bundled wet dry cycles. From the top of core MorsDp52a. RFA data by courtesy of RÖHLING, H.-G., NLFb Hannover.

The cross plots of the (Mg/Al + Ca/Al) - Cl/Al ratio show a rather poor correlation (fig. 89). The positive relation between Na/Al and Cl/Al is moderate. Therefore salinity, indicated by the Cl/Al ratios, rises with the dolomite content, i.e. wet-dry cyclicity is also traduced by cyclic changes of the salinity. However, as Cl contents are very low the importance of variations within the salinity is questioned again. The positive correlation between Na/Al and Cl/Al suggest that Na/Al might be an indicator for salinity.

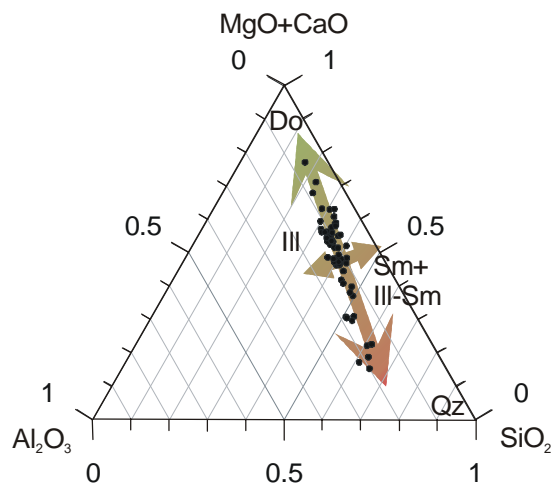


Fig. 90: Ternary diagrams of chosen element/Al ratios of a bundled wet dry cycle from core MorsDp52a showing the shift between illite (Ill.) and smectite+mixed layer illite-smectite regular and irregular (Ill.-Sm.). The overall quartz (Qz) and dolomite (Do) content provokes a general shift of the trend towards the quartz and dolomite end members. The arrows just indicates the cyclic variations between the end members. RFA data by courtesy of RÖHLING, H.-G., NLFb Hannover.

The ternary plot (fig. 90) is interpreted in the same way as in the basic cycles: the shift from the dolomitic end member to the quartzitic end member represents the shift from dry periods (quartz) to wet periods (dolomite); this shift is overlapped by a second shift from illite (dry) to smectite and mixed layer illite-smectite (wet).

---

## Gypsum Cycle

An intriguing bundling pattern of basic gypsum cycles is nicely shown by cyclic variation of dolomite beds and gypsum horizons. The example taken from core MorsDp52a has a thickness of about 10m. Stratigraphically it belongs to Mittlere Graue Folge, Arnstadt Formation.

### Description

Following groups can be differentiated (fig. 91):

- Peaks at dolomite beds: Mn/Al, (Mg/Al + Ca/Al), Na/Al, S/Al, Ba/Al and Sr/Al
- Peaks at mudstones: Ti/Al and K/Al
- No clear affiliation: Si/Al, P/Al, Fe/Al, Co/Al, Cr/Al, Ni/Al, and V/Al

Comparing with the average shale of WEDEPOHL (1971, 1991) following groups can be distinguished:

- Ratios higher than the average shale: Si/Al, (Mg/Al + Ca/Al), K/Al, S/Al and Sr/Al
- Ratios lower than the average shale: Ti/Al, Na/Al, Cr/Al and Ni/Al
- Ratios close to the average shale: Fe/Al, Mn/Al, P/Al, Ba/Al (with higher values at dolomite beds), Co/Al and V/Al

### Interpretation

(Mg/Al + Ca/Al) ratios again reflect the dolomite phase and Mn, Ba and Sr are incorporated into the dolomite lattice as suggested by the coincidence of their respective peaks with the (Mg/Al + Ca/Al) peaks. The cyclic pattern of the Mn/Al ratios exactly parallels the cyclic pattern of the (Mg/Al + Ca/Al) ratios.

The high Si/Al ratios indicate opal precipitation. Interestingly, the highest peaks do not fit together with the dolomite beds and the cyclicity of Si/Al is rather antagonistic to the cyclicity of the (Mg/Al + Ca/Al) ratios.

Low P/Al values close to WEDEPOHL's average do not suggest an important bioproductivity over long times. An exception is formed by the strong peak at -172m (fig. 91) and some smaller peaks.

Gypsum is clearly represented by the S/Al ratios. The bundling pattern of the cycles is well shown by the systematic raising/diminishing of the ratios.

Fe/Al cycles parallels the (Mg/Al + Ca/Al) cycles, even though not all Fe/Al peaks fit together with dolomite beds. This is due to hematite formation within the Gypsum. The cyclic pattern of the Fe/Al ratios implies a cyclic change from reducing to oxidizing conditions. It is possible that evaporation was strong enough so that most of the water evaporated and a wet mudflat could establish.

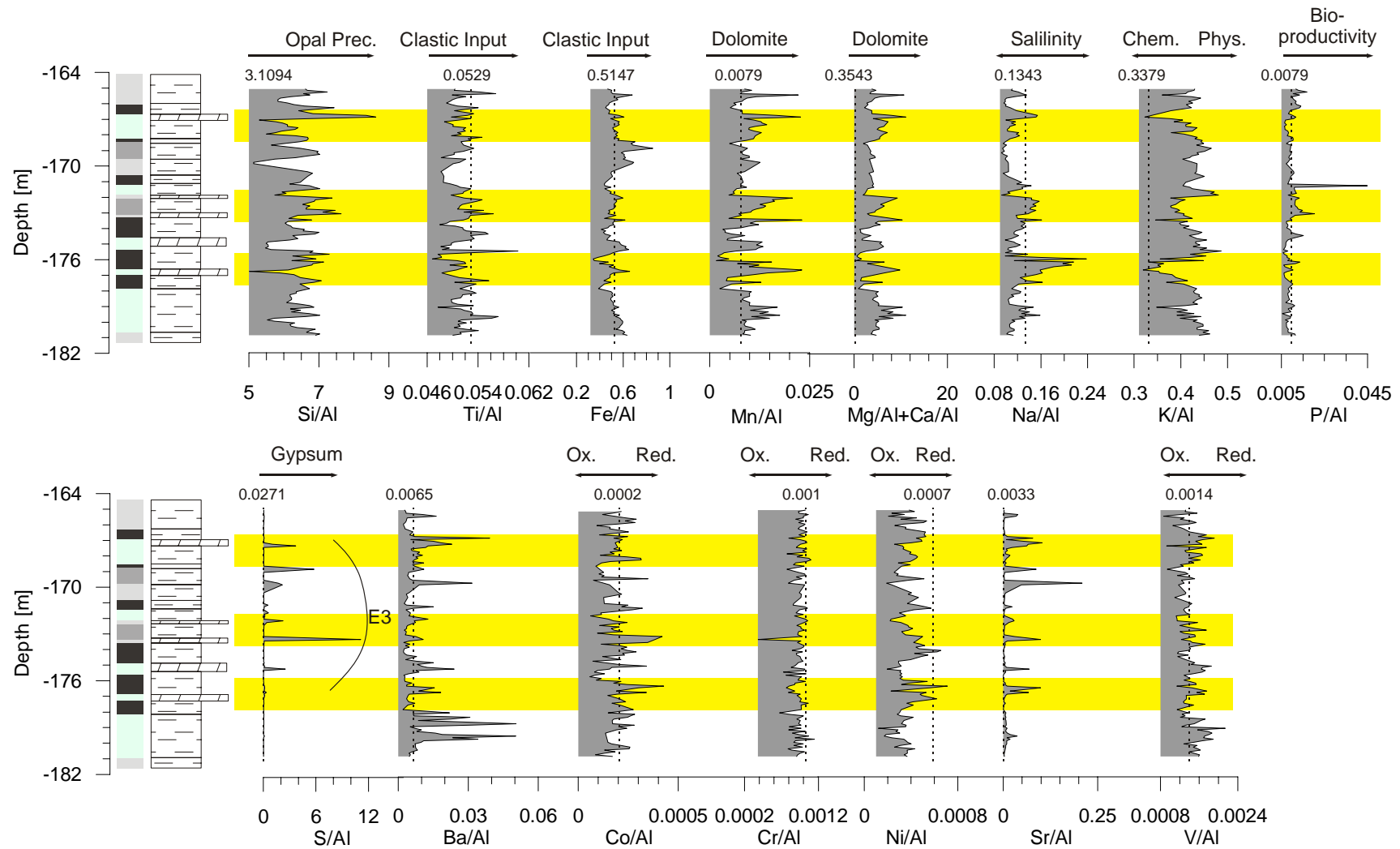


Fig. 91: Element/Al ratios from the bundled Gypsum Cycle. From core MorsDp52a, Mittlere Graue Folge. E3: eccentricity of 413kyr. RFA data by courtesy of RÖHLING, H.-G., NLFb Hannover.

Cyclic changes in the salinity are implied by cyclic variations of the Na/Al ratios, which parallel the dolomite cyclicity. The variations of the salinity reflect well the cyclic chemical evolution of the lake waters during evaporation and formation of minerals.

Ti/Al and K/Al behave antagonistically to (Mg/Al + Ca/Al) showing the overall clastic input into the playa lake. Even though some K/Al ratios are elevated during dolomite formation (fig. 91, -177m to -173m) the different weathering patterns of the hinterlands as explained before can be deduced. A possible explanation of the increased values during dolomite formation, taking into account gypsum precipitation and hematite formation was given in the interpretation of the basic gypsum cycle.

Co/Al Cr/Al, Ni/Al and V/Al ratios reflects the cyclically changing redox conditions during early diagenesis. In general the cyclicity is less conspicuous but it is still visible for example via the Co/Al ratio.

The different patterns of the element/Al ratios of the gypsum cycles (compared with the wet-dry cycles) show a more complex chemical evolution of the brine. This is suggested by the presence of gypsum and the strong cyclic changes of salinity. But also the redox sensitive parameters, especially Fe/Al, implies a different chemical evolution. Another problem is that during these times the lake did not dry out completely, so it might be better to focus the attention on salinity cycles rather than on wet-dry cycles.

## Crossplots

### Description and Interpretation

The positive correlation between Ca and Mg show clearly the dolomite content. Mg+Ca and Sr are poorly correlated indicating again the poor enrichment of Sr into the dolomite. This is somewhat in contradiction of the fact that Sr/Al peaks generally fit with (Mg/Al+Ca/Al) peaks (fig. 91 and fig. 92). Phosphorous is inversely correlated to (Mg/Al + Ca/Al). This suggests a detrital origin of phosphorous. The positive correlations between K – Ti and Si – Ti also implies a clastic origin of these elements. Mn and Ni are inversely correlated. That means Ni is also of clastic origin. Therefore, Cr must also reflect the detrital input as it is suggested by the normal correlation between Co and Cr. The positive relationship between Ca and S obviously represent the gypsum phase.

The presence of Cl within the gypsum phase could not be demonstrated. Hence, neither Cl nor Na provide trustworthy indicators for variations of salinity.



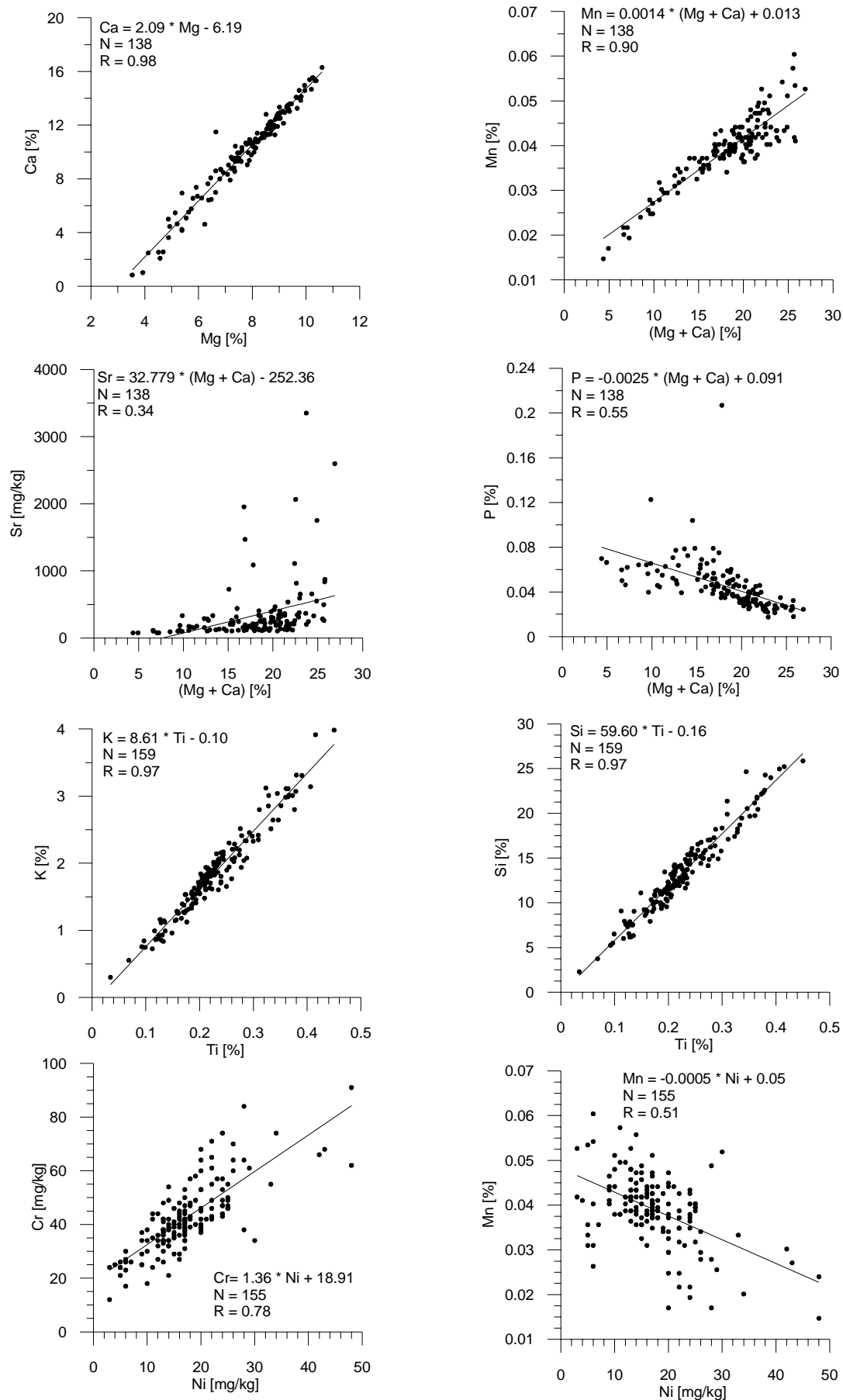


Fig. 92: Cross plots of chosen elements within the bundled gypsum cycle. From core MorsDp52a, Mittlere Graue Folge. RFA data by courtesy of RÖHLING, H.-G., NLfB Hannover.

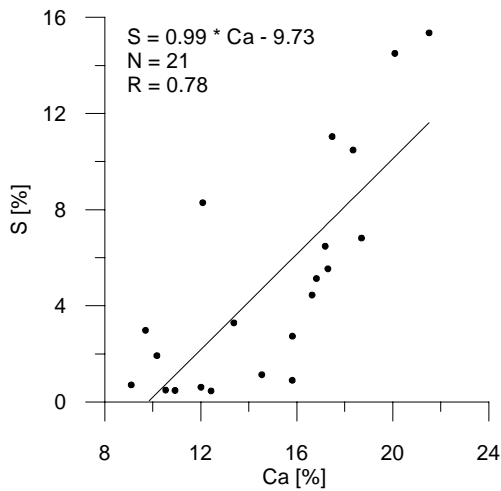


Fig. 92 (continued): Cross plots of chosen elements within the bundled gypsum cycle. From core MorsDp52a, Mittlere Graue Folge. RFA data by courtesy of RÖHLING, H.-G., NLFb Hannover.

The ternary plot (fig. 93) is interpreted in the same way as in the basic cycles: the shift from the dolomitic end member to the quartzitic end member represents the shift from evaporation (increasing salinity) to flooding (dolomite); this shift is overlapped by a second shift from illite (evaporation) to smectite and mixed layer illite-smectite (flooding).

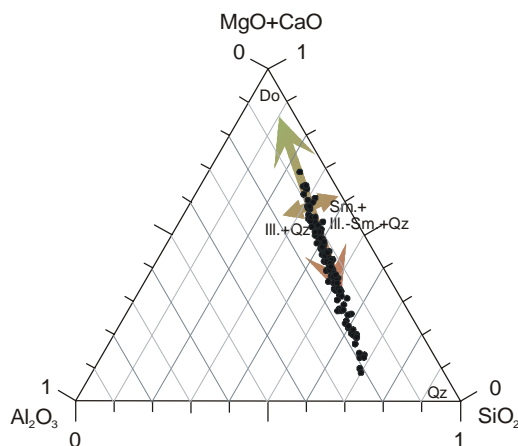


Fig. 93: Ternary diagrams of chosen element/Al ratios of a bundled wet-dry cycle from core MorsDp52a showing the shift between illite (Ill.) and smectite+mixed layer illite-smectite regular and irregular (Ill.-Sm.). The overall quartz (Qz) and dolomite (Do) content provokes a general shift of the trend towards the quartz and dolomite end members. The arrows just indicates the cyclic variations between the end members. RFA data by courtesy of RÖHLING, H.-G., NLFb Hannover.

## Dolocrête Cycle

Following the example of Gleichenburg outcrop, Drei Gleichen area shows a striking stacking pattern of pedogenetic dolocrête cycles. The thickness of the succession is about 16m. The dolocrêtes are developed within the Obere Bunte Folge, Arnstadt Formation.

## Description

The Al-normalized plots (fig. 94) also show clearly two different groups:

- Peaks at dolomite beds: Si/Al, Mn/Al, (Mg/Al + Ca/Al), Na/Al, Ba/Al, Ni/Al, and Sr/Al. Especially Mn/Al and (Mg/Al + Ca/Al) show a striking staking pattern of cycles. The values rise systematically from a minimum to maximum and diminish mostly abruptly to a minimum.
- Peaks at mudstones: Ti/Al, K/Al (with an offset of the low values respective to the (Mg/Al + Ca/Al) maxima).
- Ambivalent behavior: Fe/Al, P/Al, Co/Al, Cr/Al and V/Al.

Comparing with the average shale of WEDEPOHL (1971, 1991) following groups can be distinguished:

- Higher values for: (Mg/Al + Ca/Al), K/Al, Ba/Al at dolomite beds and Cr/Al.
- Lower values for: Na/Al, P/Al, Ni/Al, Sr/Al and V/Al.
- Values close to the average: Si/Al, Fe/Al, Ti/Al, Ba/Al at mudstones, Co/Al, Cr/Al and V/Al.

## Interpretation

(Mg/Al + Ca/Al) ratios again reflect the dolomite phase and Mn, Ba and Sr are incorporated into the dolomite lattice as suggested by the coincidence of their respective peaks with the (Mg/Al + Ca/Al) peaks. The cyclic pattern of the Mn/Al ratios parallels exactly the cyclic pattern of the (Mg/Al + Ca/Al) ratios.

The high Si/Al ratios indicate opal precipitation. The ratios are close and even lower than the average shale of WEDEPOHL, which suggests a less important opal precipitation. The same can be deduced from the low P/Al ratios: they do not indicate an important bioproductivity over long periods.

The Fe/Al cycles parallel the (Mg/Al + Ca/Al) cycles even though not all Fe/Al peaks fit together with dolomite beds. The cyclic pattern of the Fe/Al ratios shows well the cyclic formation of hematite, and implies a cyclic change from reducing to oxidizing conditions.

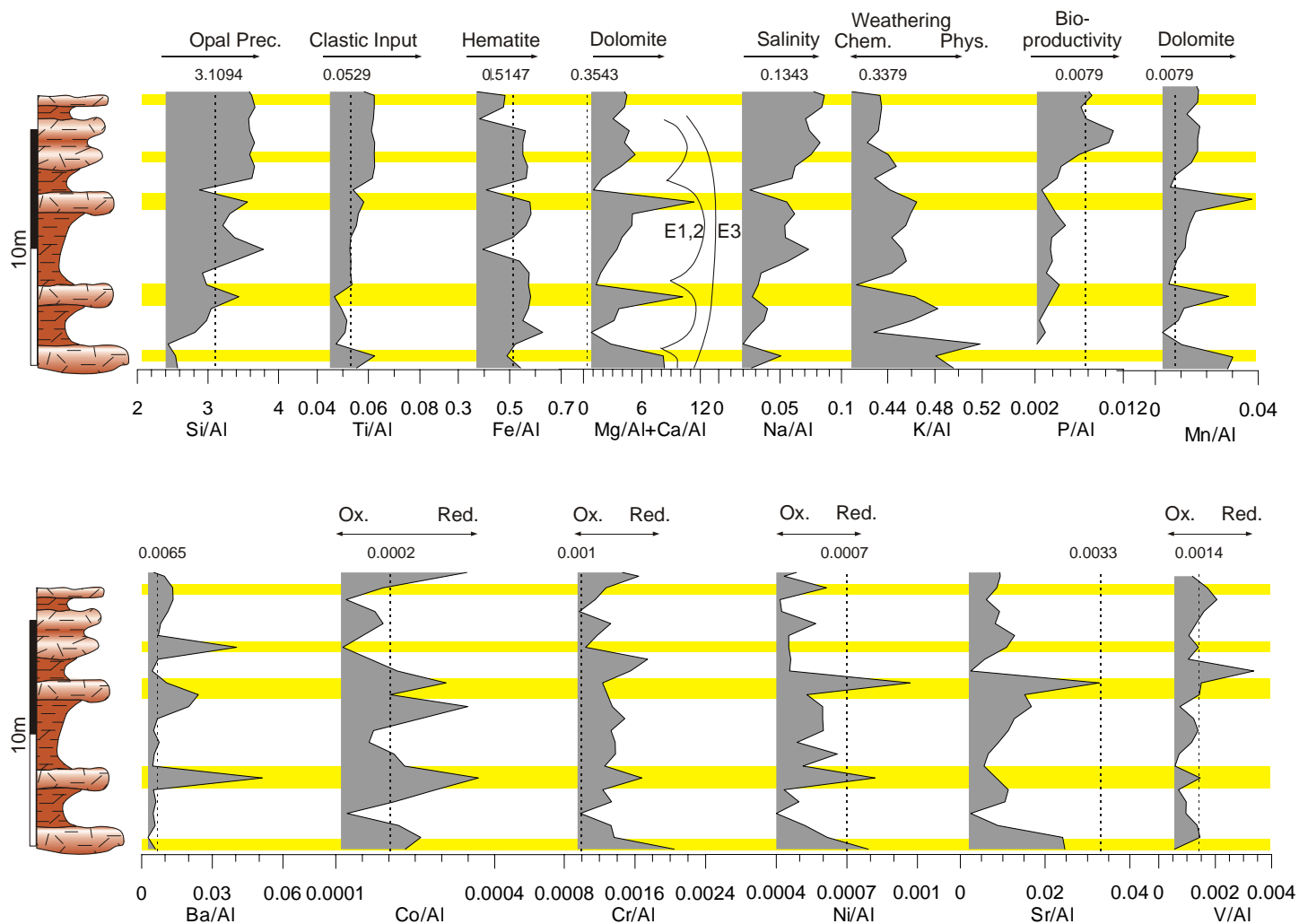


Fig. 94: Element/Al ratios from the bundled dolocrite cycle from outcrop Gleichenburg, Drei Gleichen area, Thuringia, Obere Bunte Folge. RFA data from TOUGIANNIDIS, N. unpub. Master Thesis.

Ti/Al and K/Al reflect the cyclic detrital input into the playa. Astonishingly, the minima of the K/Al ratios do not fit together with the dolocrite horizons. The minima of the K/Al ratios are systematically arranged just above the dolocrite horizons. This might be due to an offset between precipitation and evaporation within the capillary fringe (fig. 95). Before precipitation the weathering pattern of the hinterlands is dominated by physical weathering. With rainfall sediments are deposited over the mudflat and the groundwater system is filled up. That means the weathering pattern of the hinterlands tends towards more chemical weathering. During evaporation dolomite is formed within the capillary fringe which may reach up to the surface. Therefore the (Mg/Al + Ca/Al) peaks are systematically somewhat deeper than the K/Al peaks.

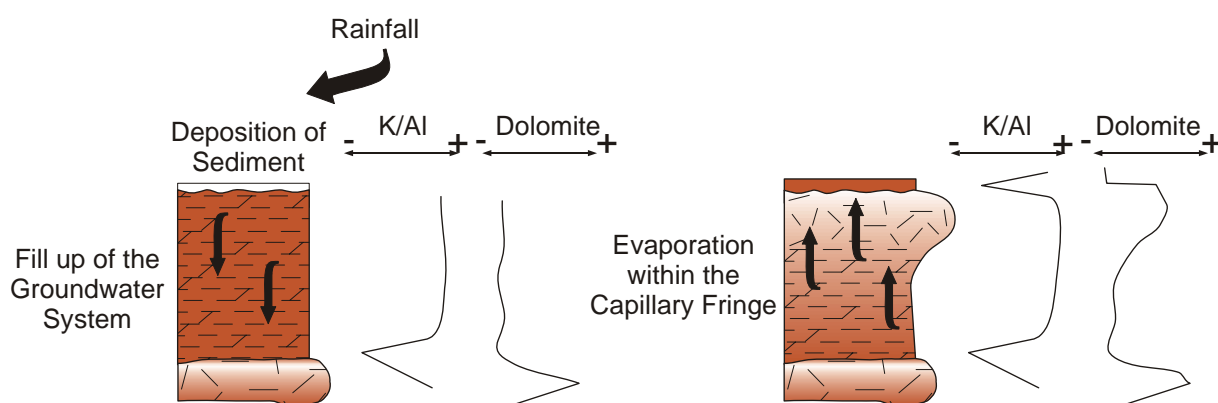


Fig. 95: Sketch illustrating the offset of the K/Al and (Mg/Al + Ca/Al) ratios. Left: with rainfall sediments are deposited on the dry mudflat and groundwater system is filled up. Right: the uppermost part of the sediments reflects the lowered K/Al ratios, whereas the dolocrite is formed within the capillary fringe, which may reach up to the sub aerially exposed surface. Therefore, the (Mg/Al + Ca/Al) peaks are systematically below the K/Al peaks.

Cyclic changes of the salinity cannot be shown directly as Cl was not detected and variations within the Na/Al ratio may also reflect variations of Analcime and Zeolithes.

Co/Al Cr/Al, Ni/Al and V/Al ratios reflects the cyclic changing redox conditions during early diagenesis. In general the cyclicity is less conspicuous but it is still visible, for example via the Co/Al ratio.

As in this case a perennial lake is not formed it is better to focus the attention on groundwater evolution than on wet and dry phases. A real wet period did not occur during these times even though the monsoonal activity increased cyclically. However, it was just enough to recharge episodically the groundwater system of the playa margin.

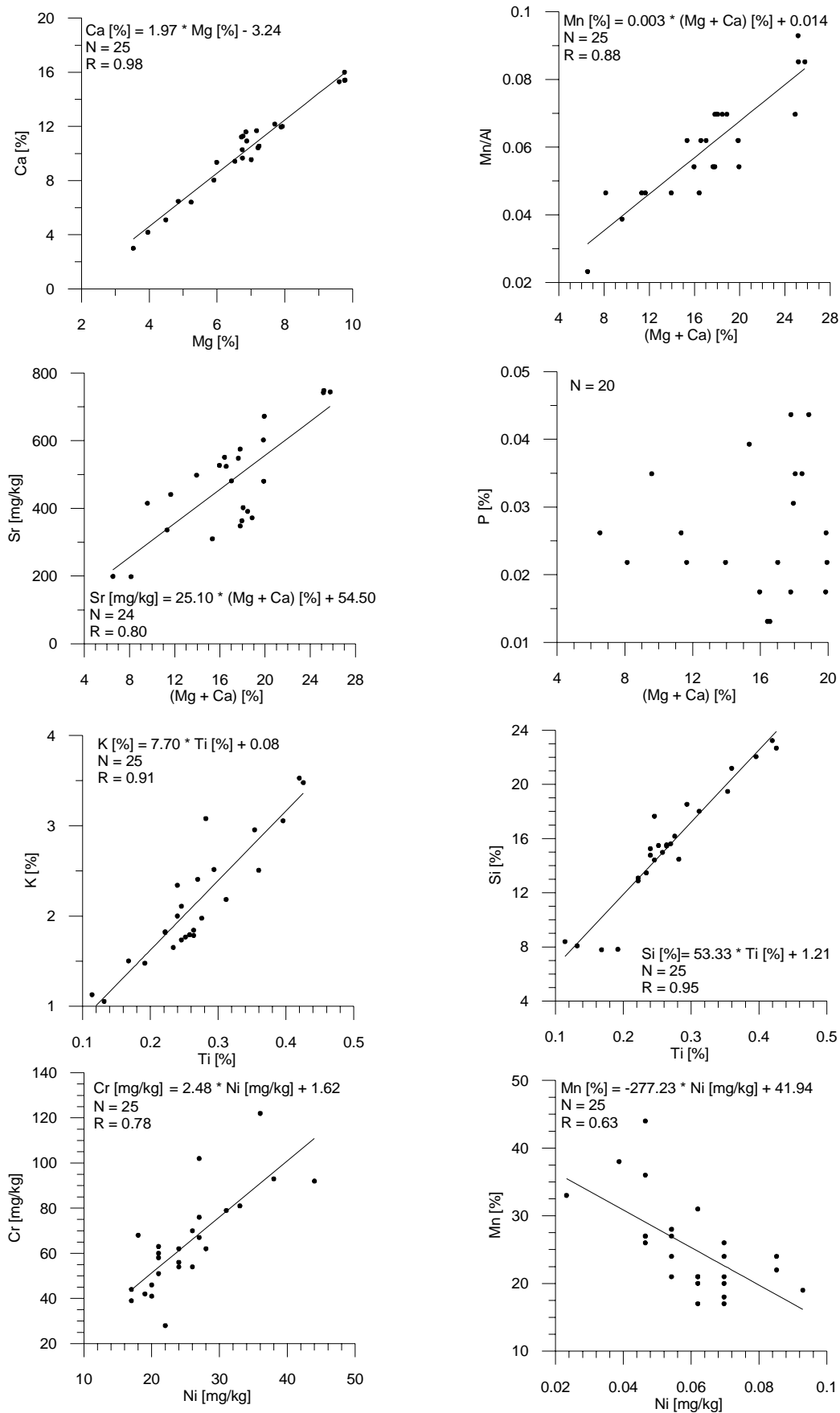


Fig. 96: Cross plots of chosen elements within the bundled dolocrête cycle from Gleichenburg outcrop, Drei Gleichen area, Thuringia, Obere Bunte Folge. RFA data from TOUGIANNIDIS, N. unpub. Master Thesis.

The positive correlation between Ca and Mg clearly show the dolomite content (fig. 96). Mn and Sr are positively correlated with, reflecting their incorporation in the dolomite. Phosphorous show no correlation to  $(Mg/Al + Ca/Al)$ . This suggests a detrital origin of phosphorous. The positive correlations between K – Ti and Si – Ti also implies a clastic origin of these elements. Mn and Ni are inversely correlated. That means Ni is also of clastic origin. Therefore, Cr must also reflect the detrital input as it is suggested by the normal correlation between Co and Cr.

The ternary plot (fig. 97) is interpreted in the same way as in the basic cycles: the shift from the dolomitic end member to the quartzitic end member represents the shift from evaporation to flooding. This shift is overlapped by a second shift from illite (evaporation) to smectite and mixed layer illite-smectite (flooding).

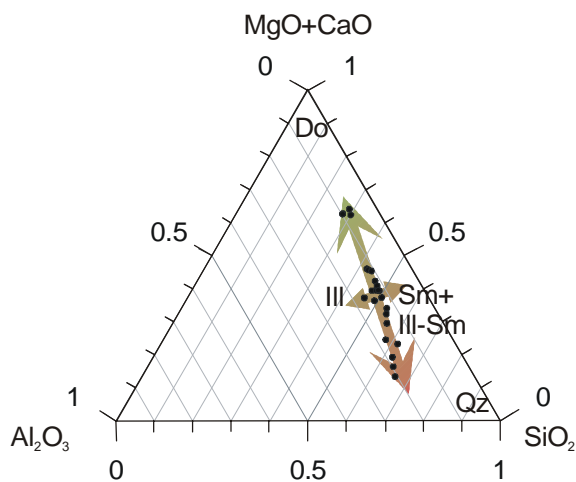


Fig. 97: Ternary diagrams of chosen element/Al ratios of a bundled dolocrête cycle from Gleichenburg outcrop, Drei Gleichen area, Thuringia showing the shift between illite (Ill.) and smectite+mixed layer illite-smectite regular and irregular (Ill.-Sm.). The overall quartz (Qz) and dolomite (Do) content provokes a general shift of the trend towards the quartz and dolomite end members. The arrows just indicate the cyclic variations between the end members. RFA data from TOUGIANNIDIS, N. unpub. Master Thesis.



### 4.1.3 Long Term Trends: example core MorsDp52a

Long term trends of element distribution were examined using data from core MorsDp52a from Morsleben, Allertal, Saxony Anhalt. The section represented by the core is the most complete in N Germany and represents the central playa of the Steinmergel Keuper playa system. The core is subdivided into three subunits: Unter Bunte Mergel, Mittlere Graue Mergel, Obere Bunte Mergel. These subunits form the Arnstadt Formation. The core has the advantage that all three basic cycle types described above are present. So the evolution from the marginal basin to central basin can be shown. The Untere Bunte Mergel and the Obere Bunte Mergel represent the marginal basin, i.e. the wet and dry mudflat with all its features, whereas the Mittlere Graue Mergel represents the central part, i.e. the playa lake of the system. The sampling rate is 10cm and 1422 samples were analysed.

#### Description

The carbonate proxy ( $Mg/Al + Ca/Al$ ) show a general increasing trend from bottom to top the same as the  $Mn/Al$  plot, which parallels well the ( $Mg/Al + Ca/Al$ ) plot (fig. see Annexes 2, inlet of the book, sheet: Long Term Trends of XRF Data of Core MorsDp52a).  $Ba/Al$  and  $Sr/Al$  peaks fit together with the carbonate phase. Despite this they show no trend. (Fig.129: see Appendix: p 156 -159).

$Si/Al$  has a general diminishing trend from bottom to top, despite some important peaks from  $-230m$  to  $190m$  and  $-130m$  to  $-120m$  which fit together with carbonate peaks. From  $-190m$  to  $-140m$  no important peaks can be seen.

The  $P/Al$  ratio plot has a minimum around  $-200m$ . High peaks plot together with the carbonate phase. Its highest peak is at  $-200m$ .

$S/Al$  ratios are seen only from  $-181m$  to  $-164$  (Mittlere Graue Mergel).

Some of the peaks of  $Na/Al$  and  $Cl/Al$  fit together with peaks of the carbonate proxies. In any case, the general trend of the  $Na/Al$  ratios is the opposite of the ( $Mg/Al + Ca/Al$ ) ratios and the  $Mn/Al$  ratios. The  $Cl/Al$  ratios have the highest values from  $-230m$  to  $-215m$  (Mittlere Graue Mergel). At the top the values are generally lower. It is not possible to point out clearly a diminishing trend parallel to the  $Na/Al$  curve as too much data is missing because of the lower amounts of  $Cl$ .

$Ti/Al$ ,  $Fe/Al$  and  $K/Al$  behave similarly despite some minor differences.  $K/Al$  values reach a maximum within the red clays from  $-200m$  to  $-192m$  than the values diminish and reach a minimum within the dark grey sediments (around  $-160m$  ). At the top they raise slightly again.

$Co/Al$  and  $Cr/Al$  show no clear trend but some of their peaks coincide with carbonate peaks.  $Ni/Al$  and  $V/Al$  show a clear diminishing trend from bottom to top. High  $Ni/Al$  and  $V/Al$  ratios overlap with the carbonate phase.

#### Interpretation

Variation of the monsoonal activity is shown at all scale: the basic cycles reflect the changing monsoonal intensity on a yearly scale, whereas bundles of cycles suggest climatic changes

over longer time intervals. The large scale cycles are composed of bundles of cycles between long-lasting wet and dry conditions.

Dolomite precipitation augments cyclically from the bottom to the top as the (Mg/Al + Ca/Al). Highest dolomite precipitation is reached within wet periods. A maximum value of dolomite formation happened in the Mittler Graue Mergel when a long time persisting lake was present. Interestingly, dolomite precipitation is generally high at the uppermost top of the section studied (Obere Bunte Mergel). This is a hint that pedogenesis and, related to pedogenesis, dolocrête formation play an important role in the Obere Bunte Mergel. This is also suggested by the pedogenetic dolocrête horizons within the Obere Bunte Mergel of the Drei Gleichen area, Thuringia (outcrops Gleichenburg and Mühlenburg).

The Si/Al peaks indicate that most of the opal precipitated within during times of longer lasting dry periods. During long periods of a persisting lake the opal precipitation seems to be less. Bioproductivity suggested by the P/Al ratio is minimized from -235m to -200m.

Important amounts of gypsum were formed only within a long lasting perennial lake (Mittlere Graue Mergel) as the S/Al ratios indicate.

Variations in salinity seem to be less important during the whole Steinmergel Keuper, as suggested by the Na/Al and Cl/Al ratios and also by the Cl log. Just at the uppermost part of the section studied variations of the salinity can be observed (see Basic Wet-Dry Cycle). The strongest variations in Cl/Al ratios can be seen at the base of the Mittlere Graue Mergel. High Na/Al ratios in the Untere Bunte Mergel and at the base of the Mittlere Graue Mergel reflect the presence of Na-rich clay minerals as analcime and zeolithes (see chapter 3.2 *Clay Mineralogy*). Therefore, soda lakes persisting for a short-time existed during these times. The origin of Na and Cl was discussed in chapter 3.2 *Clay Mineralogy*.

Ti/Al, Fe/Al and K/Al reflect the overall detritical input into the playa system. The generally lowered K/Al ratios during the Mittlere Graue Mergel indicate long times of increased monsoonal activity within the hinterlands and the playa system.

Co/Al, Cr/Al, Ni/Al and V/Al apparently reflect the changing redox conditions during early diagenesis.

## **Cross plots**

### **Description and Interpretation**

The positive correlation between Mg and Ca (fig. 98) unambiguously represent the dolomite phase. The normal correlations between K-Al, K-Fe, K-Ti and Si-Ti reflect clearly the detritical input into the playa. The inverse correlation between (Mg + Ca) and Ni suggests a clastic origin of the Ni. Therefore, the positive relationship between Ni and Cr indicate a clastic origin of Cr, too.

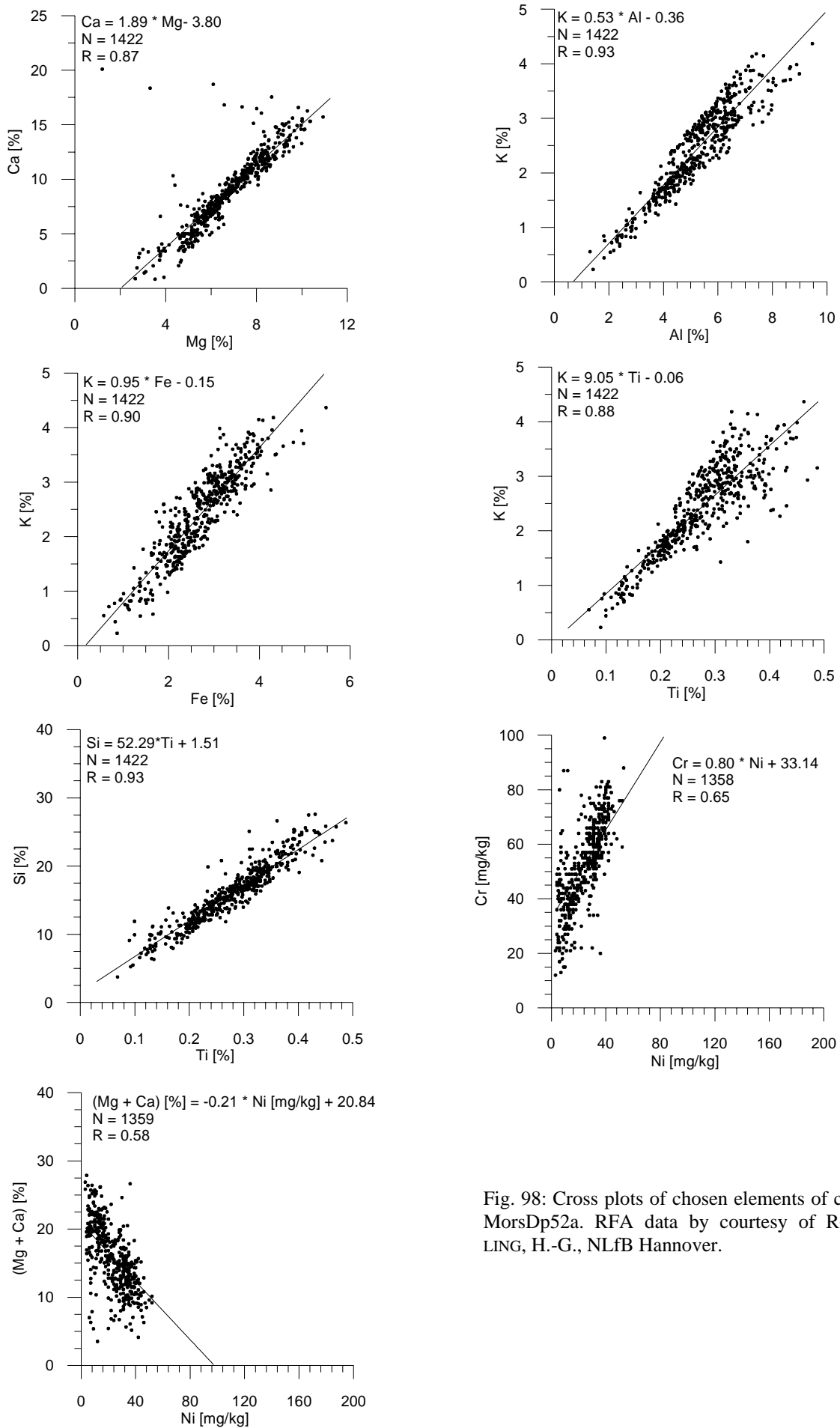


Fig. 98: Cross plots of chosen elements of core MorsDp52a. RFA data by courtesy of RÖHLING, H.-G., NLFb Hannover.

The bad covariances between (Mg/Al + Ca/Al) and Na/Al and Na/Al and Cl/AL (fig. 99) do not suggest important influences of salinity in the long term. Variations of salinity seem to be somewhat more important in smaller scale cycles at the top of the core MorsDp52a (see above).

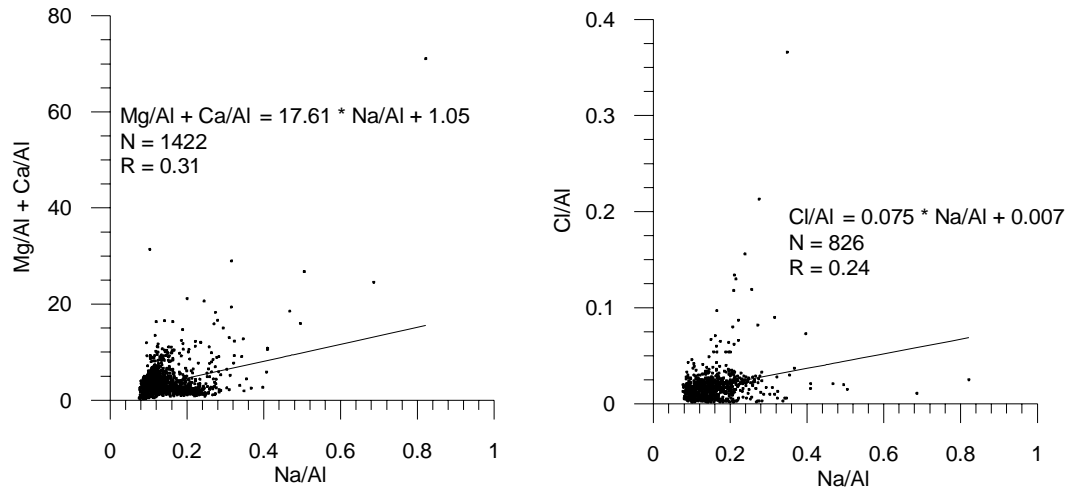


Fig. 99: Cross plots of (Mg/Al + Ca/Al)- Na/Al ratios and Na/AL-Cl/Al ratios core MorsDp52a. RFA data by courtesy of RÖHLING, H.-G., NLfB Hannover.

The ternary plot (fig. 100) can be interpreted in the same way as before: the shift from the dolomitic end member to the quartzitic end member represents the shift from dry periods (quartz) to wet periods (dolomite); this shift is overlapped by a second shift from illite (dry) to smectite and mixed layer illite-smectite (wet). A few exceptional values (red circles in fig.100) indicating some enrichment in the quartzitic component may be due to some particular flooding events or an increased aeolian input.

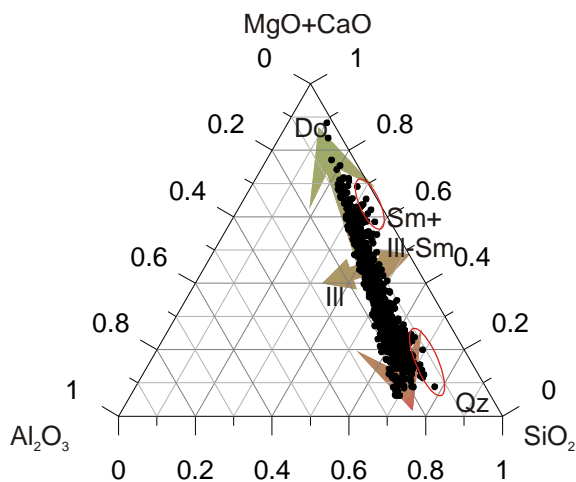


Fig. 100: Ternary diagram of chosen elements of core MorsDp52a showing the shift between illite (Ill.) and smectite+mixed layer illite-smectite regular and irregular (Ill.-Sm.). The overall quartz (Qz) and dolomite (Do) content provokes a general shift of the trend towards the quartz and dolomite end members. The arrows just indicate the cyclic variations between the end members. RFA data by courtesy of RÖHLING, H.-G., NLfB Hannover.

## 4.2 Stable Oxygen and Carbon Isotopes

Two of the most-used and most-interesting parameters in paleoclimatology are the stable oxygen and carbon isotopes. As the oxygen shows a strong fractionation which depends on the temperatures it is assured that the carbonates are of primary origin. For the Steinmergel Keuper playa system the dolomites are primary, as REINHARDT (2002) showed (see also above). Even if the dolomite is produced in the pore room of the sediments the isotopes serve as a paleohydrological parameter, as the groundwater system of the playa remained in contact with the lake waters during precipitation. Thus the isotopic composition of the dolomites reflects the isotopic composition of the surrounding brine. As the evolution of the brine is a function of changing climatic conditions the stable isotopes reflect the paleoclimatic conditions of that time.

Several factors influence the fractionation of the isotopes during carbonate precipitation (fig. 101 and 102) in closed continental playa systems, as in the present study case. The amount of evaporating seawaters (fig. 102), i.e. the monsoonal activity, led to a depletion of heavier oxygen isotopes. The waters became more and more depleted as it rained over the Vindelicean High and the Steinmergel Keuper playa system. Furthermore, the continentality and the latitude effect, when the clouds drifted far into the continent and towards higher latitude, led to a depletion of  $\delta^{18}\text{O}$ . This is true for the southern part of the Steinmergel Keuper playa system. But for the northern basin it has to be taken into account that there might be some influences from source areas from the North (i.e. the Fenno – Scandian – High, fig. 101). This means that there may be a mixing of isotope components and the  $\delta^{18}\text{O}$  might be enriched.

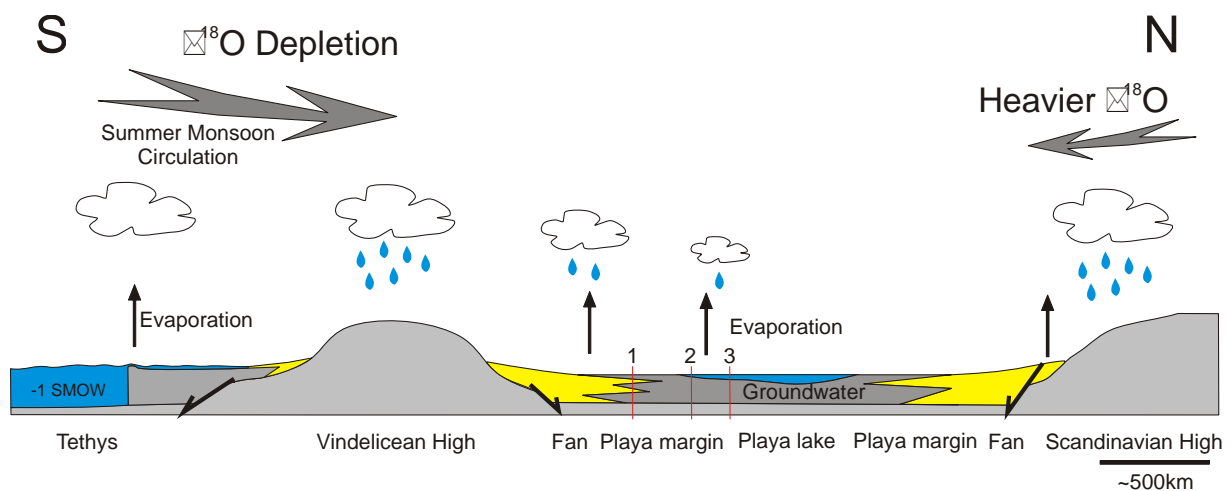


Fig. 101: Simplified sketch illustrating the factors of the paleoclimatic system. Isotope value for the Tethys from VEIZER et al (1997). Red lines indicate sites studied: 1: core Malschenberg, Baden Württemberg, 2: Outcrops of the Drei Gleichen area, Thuringia, 3: core MorsDp52a. After REINHARDT (2002).

After TALBOT (1990) the isotopic evolution of a playa lake depends also from the evaporation rate of the lake. This leads to an enrichment of  $\delta^{18}\text{O}$ . Furthermore, the residence time of both oxygen and carbon isotopes in the playa lake results in an enrichment of both isotopes. Therefore, there is a visible correlation between  $\delta^{18}\text{O}$  and  $\delta^{13}\text{C}$  in closed continental playa

systems. The gradient of the correlation line gives an idea of the relationship between the covered area and the depth of the water column. If the gradient is high then the ratio area/depth is low, i.e. there is only a small area covered by the water and/or the lake is deep. If the gradient is low then the ratio area/depth is high, i.e. huge areas are covered by water and/or there is only a shallow lake. The origin of the regression line gives the value of the less evolved water, i.e. the lowest value corresponds to a relative maximum of the playa lake.

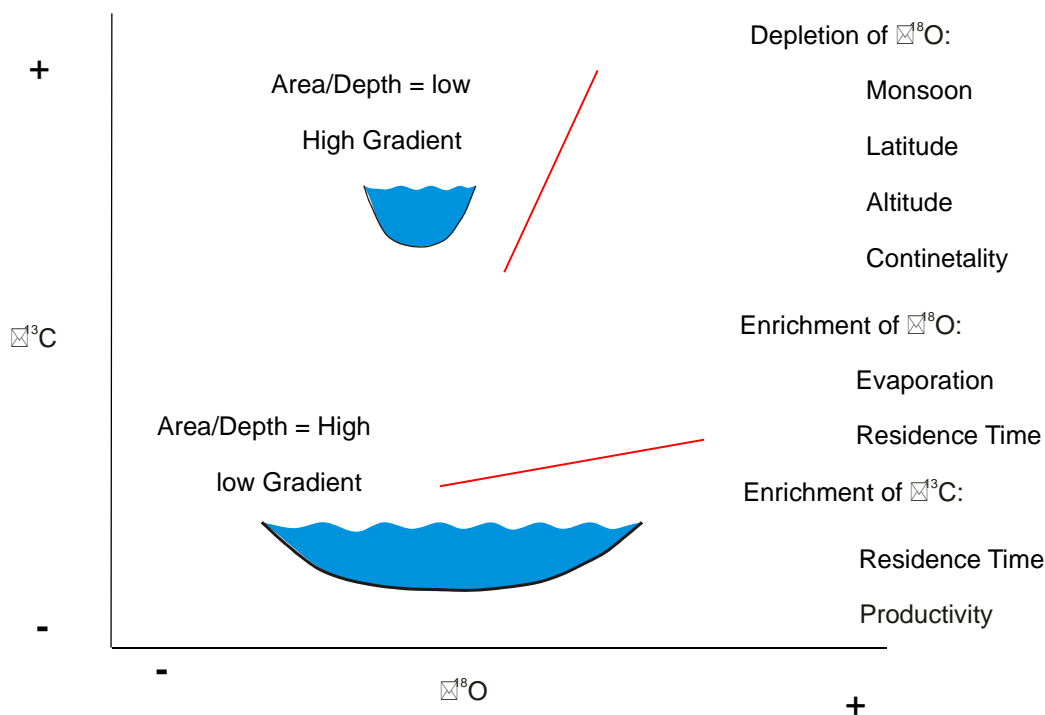


Fig. 102: Interpretative scheme for stable oxygen and carbon isotopes in closed continental basins. After TALBOT 1990.

A detailed study on the covariance between  $\delta^{18}\text{O}$  and  $\delta^{13}\text{C}$  in closed-basin lakes by LI AND KU (1997) revealed a dependence of the trend on hydrological changes, vapor exchange, lake productivity and the total  $\text{CO}_2$  concentration. This trend might not be present in hyper-alkaline lakes because of the insensitivity of  $\delta^{13}\text{C}$  to lake volume changes.

#### 4.2.1 The Basic Cycles

Due to the overall dolomite content it was possible to measure the isotopic composition at all scales

##### Description

The wet dry cycle show a variation from  $-0.46\text{‰}$  to  $0.043\text{‰}$  for the  $\delta^{13}\text{C}$  (V-PDB) values and a variation from  $-2.59\text{‰}$  to  $-1.53\text{‰}$  for the  $\delta^{18}\text{O}$  (V-PDB) values (fig. 103). The lightest  $\delta^{18}\text{O}$  value is reached within a dark gray mudstone, the same as for  $\delta^{13}\text{C}$ . The heaviest values are

found within the red mudstones. The values within the dolomite bed are intermediate. Within the gypsum cycle the isotopic composition ranges from  $-0.97\text{‰}$  to  $2.78\text{‰}$  for  $\delta^{13}\text{C}$  (V-PDB) and from  $-2.75\text{‰}$  to  $-1.85\text{‰}$  for  $\delta^{18}\text{O}$  (V-PDB). The lightest  $\delta^{18}\text{O}$  values are within the dark gray mudstones and the values for the dolomite again take an intermediate position. The dolocrête cycle shows a range from  $2.52\text{‰}$  to  $2.78\text{‰}$  for  $\delta^{13}\text{C}$  (V-PDB) and from  $-2.46\text{‰}$  to  $-0.25\text{‰}$  for  $\delta^{18}\text{O}$  (V-PDB). A direct relationship between  $(\text{Mg}/\text{Al} + \text{Ca}/\text{Al})$ ,  $\text{K}/\text{Al}$  can not be seen.

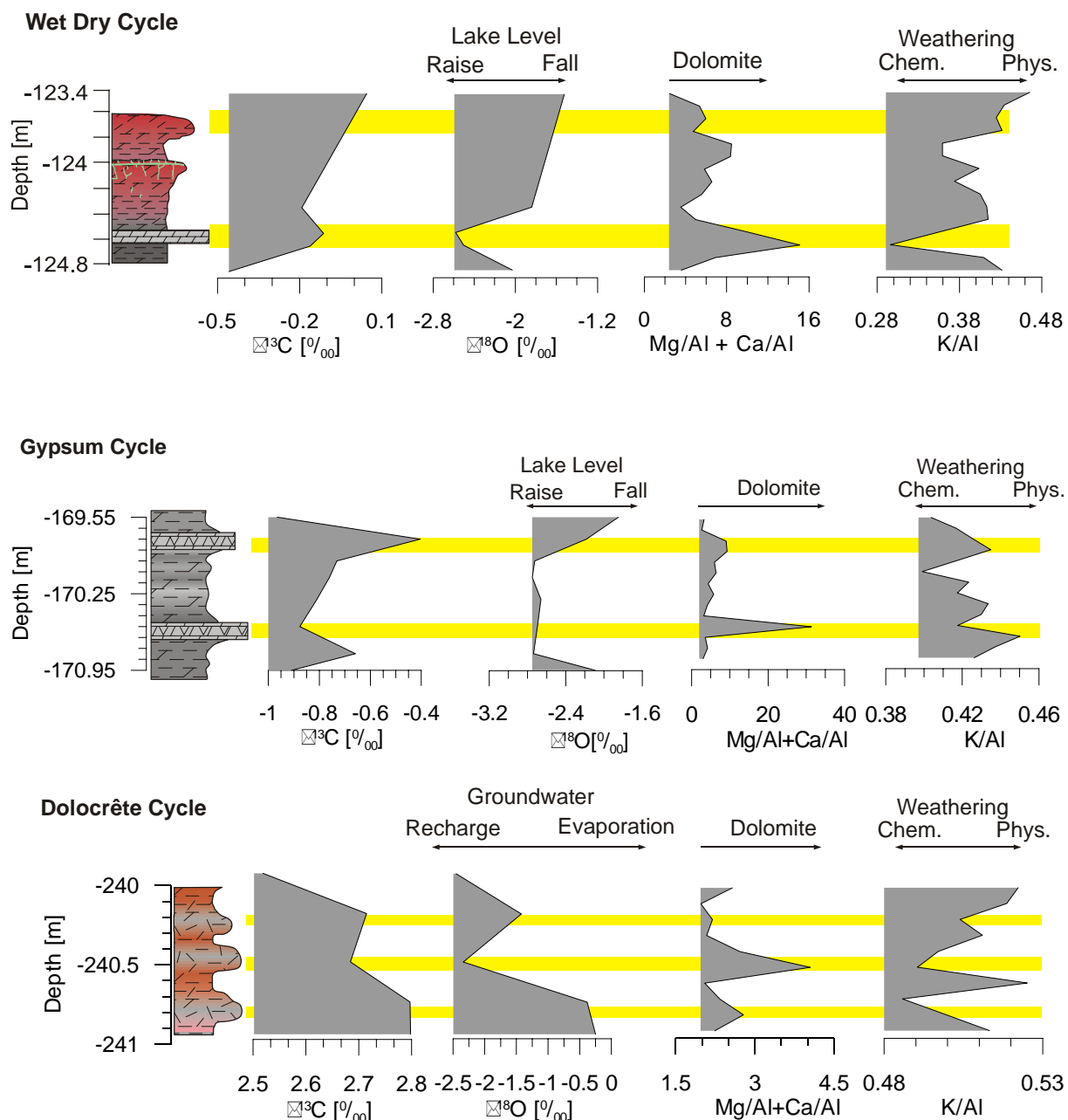


Fig. 103: Stable oxygen and carbon isotopes for the three basic cycle types. Carbonate and weathering proxy are provided for comparison. All three examples from core MorsDp52a. XRF data by courtesy of RÖHLING, H.-G., NLfB Hannover.



## Interpretation

The general facies model suggests that the isotope values should be lighter within the dark gray mudstones and somewhat heavier within the dolomite beds, and heaviest within the red mudstones. This is roughly the case for the wet-dry cycle, and the gypsum cycle even if the data set is not very large. In the dolocrête cycle the lightest values are found, as expected within the dolocrête. This reflects the evolution of the groundwater system after a recharge event. The fractionation is due to the fact that the playa system is subject to long periods of evaporation, hence the values get heavier. It seems that evaporation controls not only isotopic composition within the playa lake but also within the groundwater system of the mudflats. The fact that evaporation controls isotopic composition within the groundwater systems of shallow waters was demonstrated by HERCZEG et al (1992) for Lake Tyrell.

A discussion assuming a non-diagenetic origin of the isotope values is given by REINHARDT (2002). He emphasized the carbonate precipitation process itself: primary dolomite is precipitated during repeated flooding/evaporation events within the playa system. Isotopic composition changed toward heavier values during repeated evaporation.

### 4.2.2 Bundles of Cycles

#### Description

The values of the wet dry cycle range from  $-0.85\text{‰}$  to  $0.48\text{‰}$  for  $\delta^{13}\text{C}$  (V-PDB) and from  $-3.03\text{‰}$  to  $-0.85\text{‰}$  for  $\delta^{18}\text{O}$  (V-PDB) (fig. 104). The correlation between  $\delta^{13}\text{C}$  and  $\delta^{18}\text{O}$  is good. The gypsum shows values from  $-3.83\text{‰}$  to  $0.12$  for  $\delta^{13}\text{C}$  (V-PDB) and from  $-3.70\text{‰}$  to  $-1.71\text{‰}$  for  $\delta^{18}\text{O}$  (V-PDB). The correlation between  $\delta^{13}\text{C}$  and  $\delta^{18}\text{O}$  is rather poor. Within the dolocrête cycle the isotopic composition has a variation from  $-3.64\text{‰}$  to  $-1.26\text{‰}$  for  $\delta^{13}\text{C}$  (V-PDB) and from  $-3.53\text{‰}$  to  $-0.19\text{‰}$  for  $\delta^{18}\text{O}$  (V-PDB). The correlation between  $\delta^{13}\text{C}$  and  $\delta^{18}\text{O}$  is good.

#### Interpretation

Contrary to the basic cycles it can be seen easily that dark gray sediments have the less evolved isotopic compositions (Gypsum Cycle). The isotopic compositions are generally higher within the red mudstone (Wet-Dry Cycle and Dolocrête Cycle). Within the Dolocrête Cycle lowest isotopic compositions fit together with the dolocrête horizons, strengthening the assumption of evolving groundwater. The general K/Al trend follows well the general isotope trends of the Dolocrête cycles. The correlations between  $\delta^{13}\text{C}$  and  $\delta^{18}\text{O}$  in all three cases are moderate to good. This indicates a closed basin, even though within the Gypsum Cycle the correlation is somewhat weaker. The weaker correlation within the Gypsum cycles may be due to some increased leakage of the basin, i.e. during these times the groundwater system was not completely closed and an exchange of isotopes may have happened.

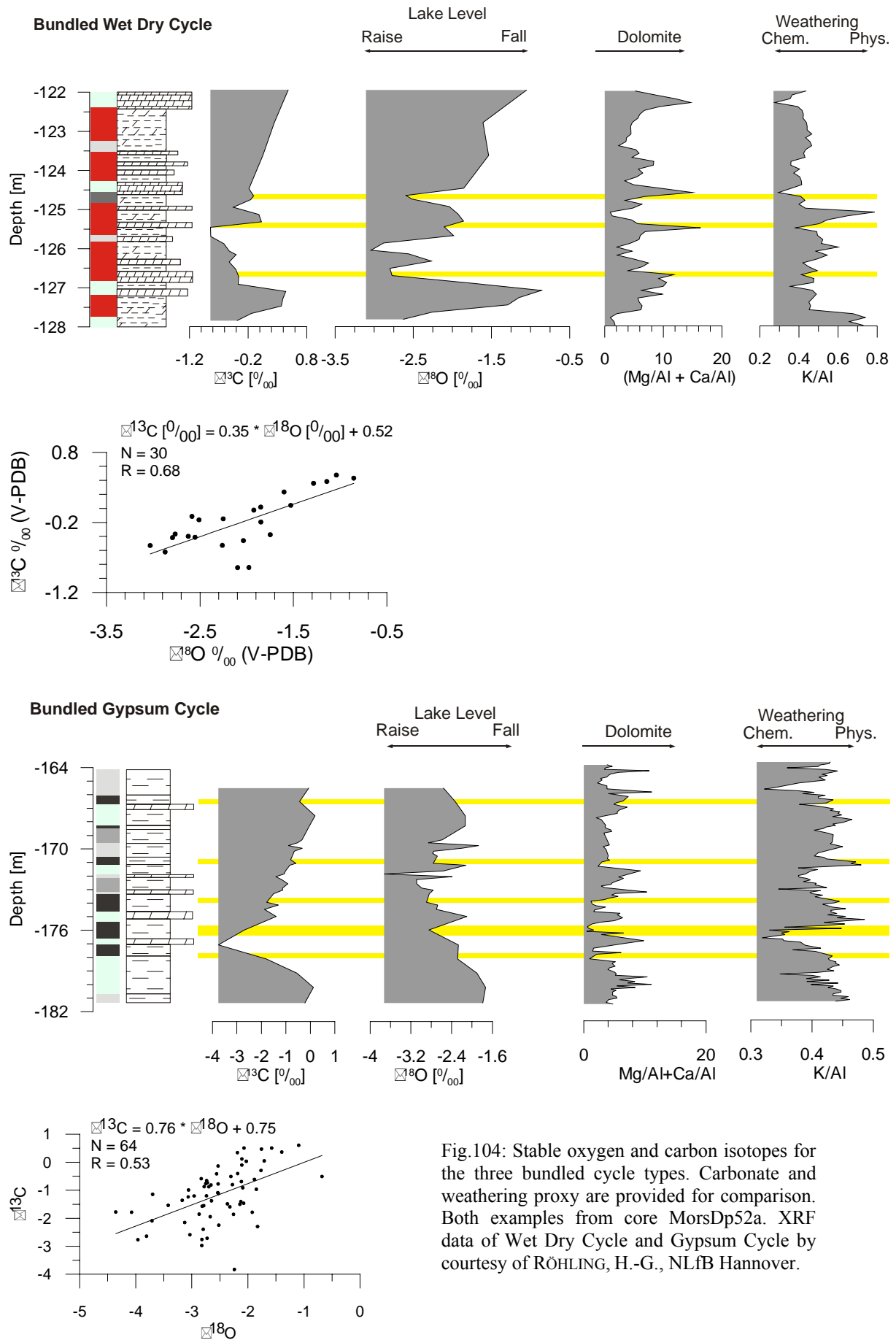


Fig.104: Stable oxygen and carbon isotopes for the three bundled cycle types. Carbonate and weathering proxy are provided for comparison. Both examples from core MorsDp52a. XRF data of Wet Dry Cycle and Gypsum Cycle by courtesy of RÖHLING, H.-G., NLFb Hannover.

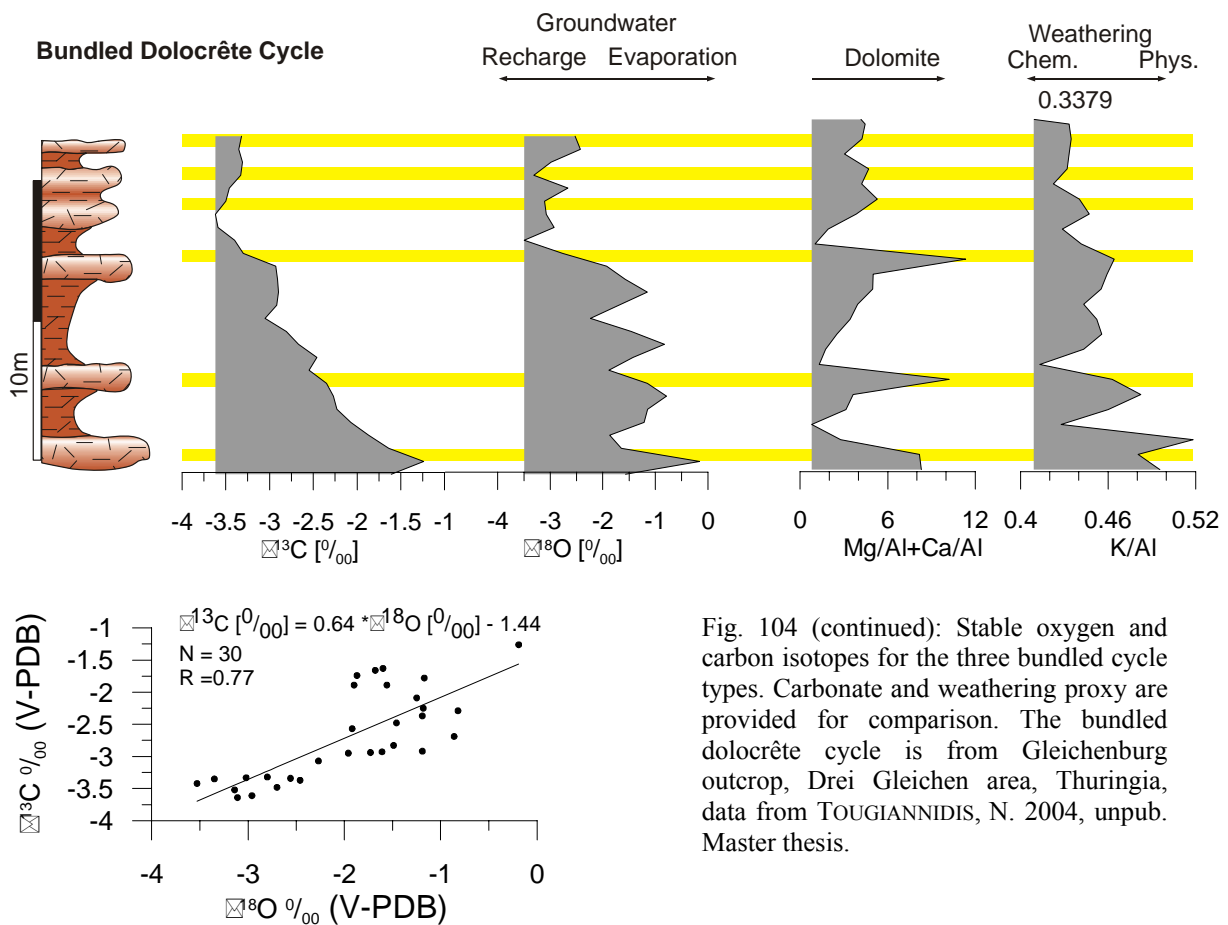


Fig. 104 (continued): Stable oxygen and carbon isotopes for the three bundled cycle types. Carbonate and weathering proxy are provided for comparison. The bundled dolocrête cycle is from Gleichenburg outcrop, Drei Gleichen area, Thuringia, data from TOUGIANNIDIS, N. 2004, unpub. Master thesis.

### 4.2.3 Long Term Trends

The long-term isotopic composition of the core MorsDp52a was measured with a sampling rate of about 1m average.

#### Description

The isotopic composition ranges from  $-3.83$  to  $3.19$  for  $\delta^{13}\text{C}$  (V-PDB) and from  $-4.62$  to  $1.23$  for  $\delta^{18}\text{O}$  (V-PDB). There is striking covariance within the isotopes (fig. 105). A subdivision into six periods was done using different sedimentological criteria (such as pedogenetic horizons, occurrence of gypsum).

#### Interpretation

Using the criteria from TALBOT (1990) and LI AND KU (1997) ( see above) an evolution of the playa system can be traced from the bottom to the top:

- Period I shows no covariance. This implies a marine influence at the beginning of the Steinmergel Keuper (Arnstadt Formation). This is possible as the underlying formation (Weser Formation) is a marine-influenced sabkha facies. But that means that the transition from the Weser Formation to the Arnstadt Formation is continuous

---

and therefore the basin-wide discordance D3 (BEUTLER, 1998) is not developed at Morsleben.

- Period II has a moderate covariance reflecting the hydrological closure of the basin. This is a period of increased pedogenesis reflected by dolocrête horizons. The strong variations of the  $\delta^{18}\text{O}$  values reflect repeated recharges/evaporations of the groundwater system of the dry mudflat.
- Period III show a moderate to good covariance reflecting the variation of the lake water volume during evaporation.
- In period IV the correlation is poor but still visible. A general shift towards lighter values reflects the passage from the marginal basin with episodic dry-out to a long persisting lake.
- Period V is characterized by the lightest values within the whole section reflecting the existence of a perennial lake over long times. The correlation is moderate.
- Period VI shows the best correlation of all periods. The values are generally somewhat higher than during period 5.

The long-term trends of the K/Al suggest a transition from a physical-dominated weathering (high K/Al ratios) with short-term shifts to chemical weathering (low K/Al peaks) to a general chemical weathering pattern reflected by the presence of a long-persisting lake as suggested by the evolution of the isotopic composition.

Low frequency isotope cycles are associated with K/Al cycles. Low K/Al ratios reflect trends toward chemical weathering of the hinterlands. This is reflected by a lowered isotopic composition, i.e. the lake level rises. Three main hierarchies of stacking pattern can be differentiated: from period 1 to 4: stacking pattern of clastic-dominated cycles. Period 5 is mainly dominated by chemical weathering of the hinterlands and period 6 again is dominated by physical weathering of the hinterlands. Thus the isotopic composition provides a proxy parameter for flooding and evaporation processes, and therefore climatic processes are also documented by the isotopes.

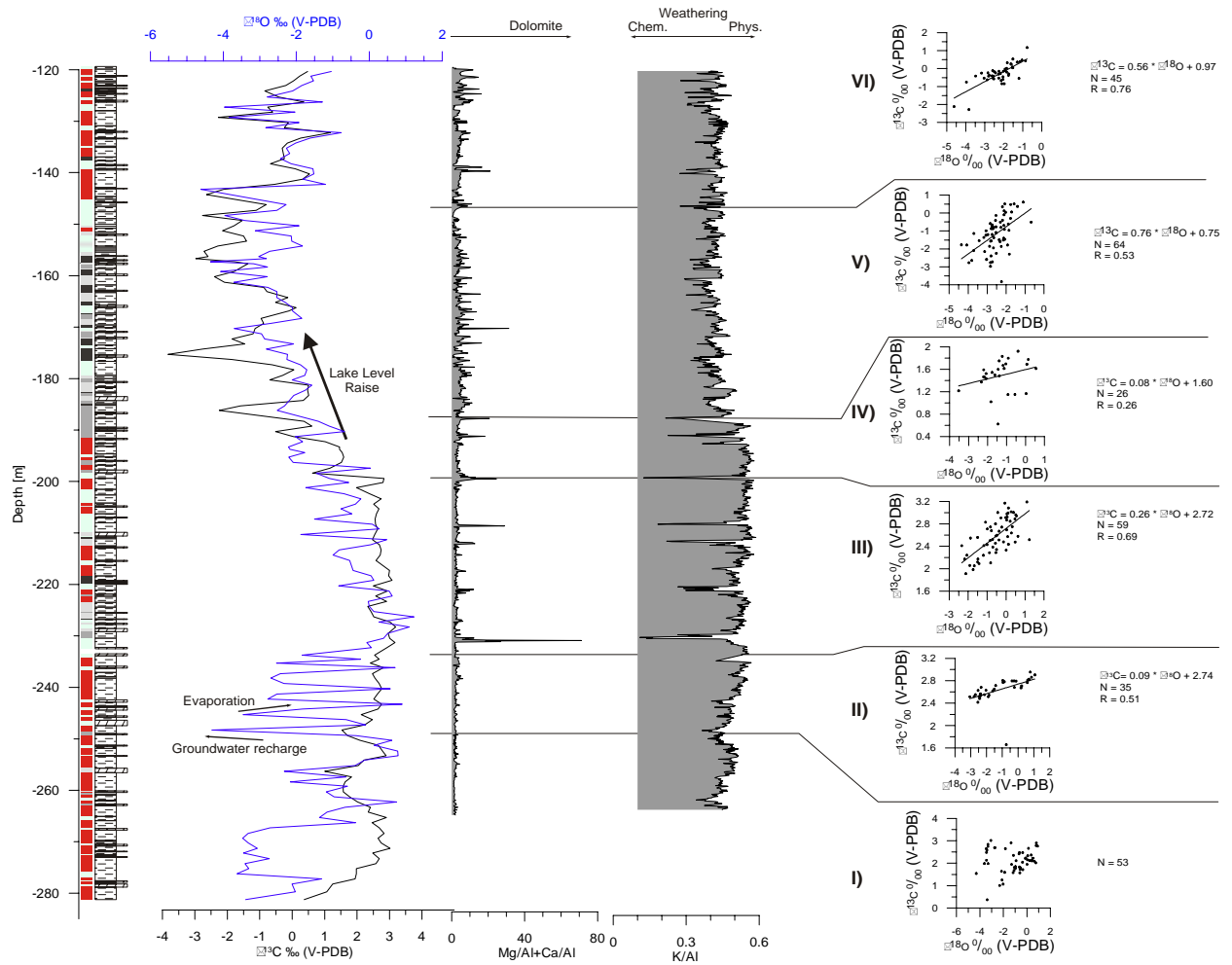


Fig. 105: Long-term trends of stable oxygen and carbon isotopes from core MorsDp52a. Carbonate and weathering proxy are provided for comparison. XRF data by courtesy of RÖHLING, H.-G., NLF Hannover.

### 4.3 Magnetic Susceptibility

Core MorsDp52a were sampled with a resolution of 1m . The samples were measured for their susceptibility and Isotherm Remnant Magnetic (IRM) properties.

There exist a broad range of applications using magnetic properties in environmental studies such as climatic changes, pedogenesis, erosion and sediment source etc. In the present case the focus is centred on climatic changes. The climatic impact on magnetic properties of sediments has been proven by several authors, e.g. BLOEMENDAL (1993), FORSTER AND HELLER (1997) etc. The IRM/ $\chi$  ratio is used as a parameter to differentiate the most important magnetism-bearing minerals such as magnetite, maghaemite, greigite, hematite and goethite (OLDFIELD, 1999). Ferrimagnets such as magnetite and maghaemite for example are generally characterized by low IRM/ $\chi$  ratios (OLDFIELD, 1999). This contrasts with antiferromagnetic minerals such as hematite and goethite which are characterized by high IRM/ $\chi$ . In the present study neither greigite nor goethite has been demonstrated to be present within the mineral assembly.

#### Description

The magnetic susceptibility shows a striking high-frequency stacking pattern throughout the whole section (fig. 106). The IRM at 2T were normalized to the magnetic susceptibility. The plot shows a three fold low-frequency bundling pattern. High IRM/ $\chi$  ratios correlate well with red mudstones and low ratios generally fit together with green/grey sediments. Exceptional high values within the green/grey sediments occur at the transition from red mudstones to green/grey sediments and vice versa. Another high peak within green/grey sediments can be observed from -170m to -168m.

#### Interpretation

The high IRM/ $\chi$  ratios reflect clearly the hematite content within the red mudstones. This is also implied by the high Fe/Al occurring together with red mudstones, as the Fe/Al ratio is a proxy for hematite formation. Simultaneously high K/Al ratios are observed, i.e. within dry periods and when there is more physical weathering of the hinterlands.

Lowering of IRM/ $\chi$  ratios happened parallel to the lowering of Fe/Al ratios and K/Al ratios. Low IRM/ $\chi$  ratios suggest a more magnetite component. The low K/Al ratios imply a chemical weathering of the hinterland, i.e. increased monsoonal activity. The whole system shifts towards more reducing conditions, reflected by the presence of a persisting lake.

The high IRM/ $\chi$  ratios from -170m to -168m are due to hematite formation within the gypsum. That means that after gypsum precipitation oxidizing conditions prevailed within the playa system.

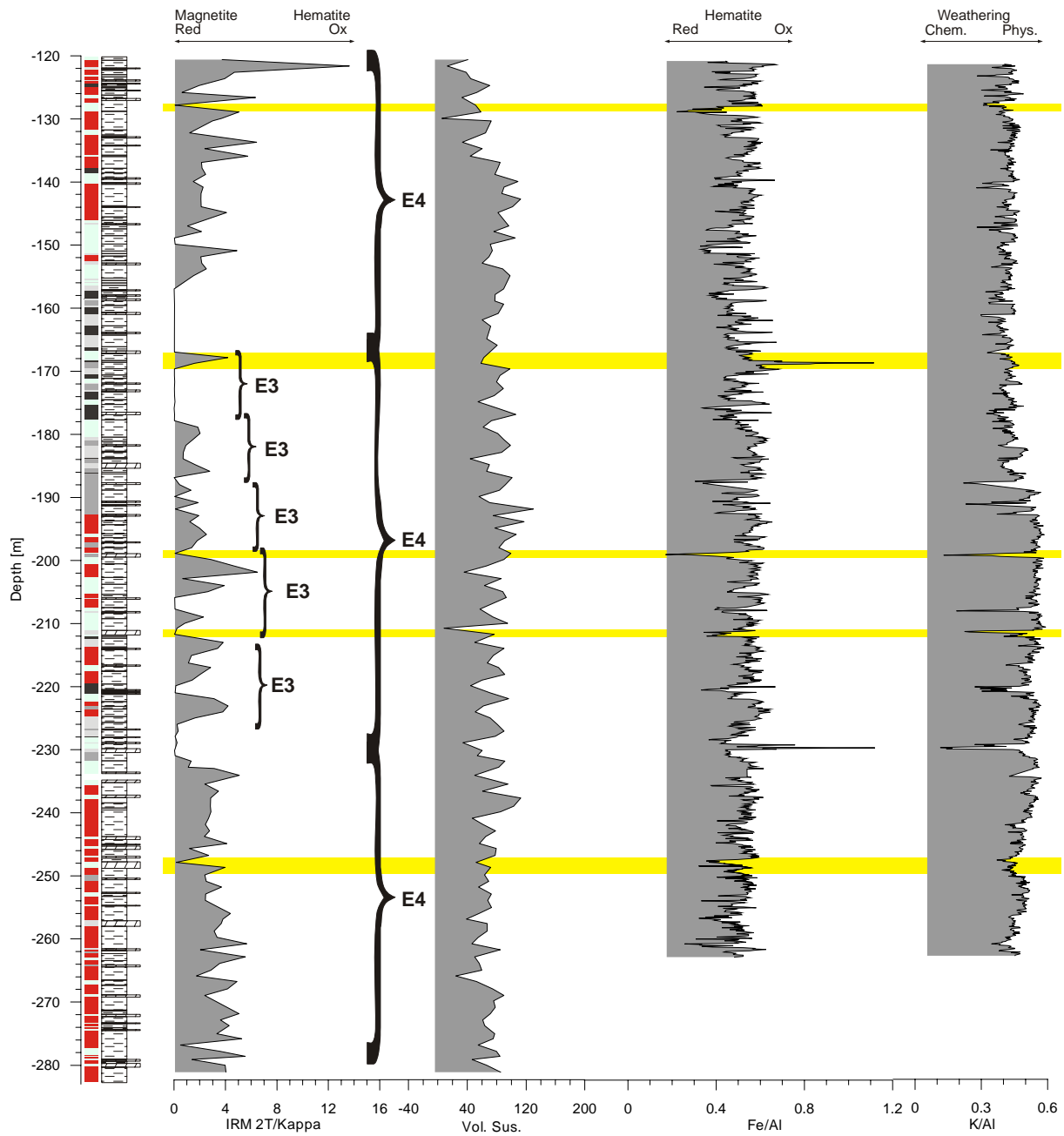


Fig. 106: Susceptibility logs and chosen element/Al ratios from core MorsDp52a. XRF data by courtesy of RÖHLING, H.-G. NLfB Hannover.

## 4.4 Colour Logging

The colours of the two cores MorsDp52a, Saxony Anhalt (sampling rate 1cm) and Malschenberg (sampling rate 3cm), Baden Württemberg were measured and analysed to work out the high cyclic variations within their colours. Furthermore, the colours of several outcrops such as the outcrops of the Drei Gleichen area (sampling rate 1cm) in Thuringia, an outcrop nearby Ifta (sampling rate 2cm) also in Thuringia, Mönchberg outcrop (sampling rate 1cm) in Baden Württemberg, Funkenloch outcrop, Anadenkmal outcrop and B19 outcrop (sampling rate 5cm) in the Hassberge region, Bavaria were measured and analyzed.

The striking cyclic variations of the colours within the Steinmergel Keuper are shown with the cycle types described above. The long term trends of core MorsDp52a are compared with those of the Drei Gleichen area and core Malschenberg. Next an attempt to explain the origin of the colours of the Steinmergel Keuper is given.

### 4.4.1 The Basic Cycles

#### Description

The basic wet dry cycle is characterized by changes from dark grey colours to intensive red from bottom to top (fig. 107 top). The general trend of variation from blue to yellow is similar to the trend from grey to red. The lightness diminishes from bottom to top. DE\*Lab rises from bottom to top. Green/grey values fit together with dark grey mudstones and dolomite beds. High red values correspond to red mudstones. The maximum of lightness coincides well with the dolomite bed.

The green-red values of the gypsum cycle are generally negative (green/grey) with exceptional high peaks (red) at gypsum horizons (fig. 107 middle). Blue-yellow and lightness behave similar to the green-red plot. DE\*Lab shows a rather antagonistic pattern.

Within the dolocrête cycle (fig. 107 bottom) the green-red and the blue-yellow curves show a striking cyclicity with generally lowered values at dolocrête horizons. The pattern of the lightness is antagonistic to the other plots. DE\*Lab behaves similarly to the green-red plot.

#### Interpretation

The colour changes within the wet dry cycle from grey to red are due to the hematite within the red mudstone. Increasing red values are parallel to increasing Fe/Al ratios. The sediments tend toward greyish colours when dolomite precipitation increases (fig. 107 top). Comparing the colours with the K/Al ratios it can be seen that K/Al ratios are somewhat lowered within the dark grey mudstones and lowest in dolomite beds, i.e. the monsoonal activity of the hinterlands is highest during dolomite precipitation even though lake level high stand is reached during deposition of the dark grey mudstones. High K/Al ratios correspond well to the red colours and high Fe/Al ratios reflecting the physical weathering of the hinterland.

The gypsum cycle behaves somewhat differently: the exceptional high red values within the gypsum horizons are due to finely dispersed hematite formation after gypsum precipitation (fig. 107 middle). High lightness, i.e. white colours, is originated by the gypsum itself. K/Al



ratios again reflect the changing climatic conditions. As expected they are generally lowest within the dolomite beds. However, due to gypsum precipitation within the dolomite the K/Al ratios might be somewhat increased, reflecting the decreased monsoonal activity of the hinterlands during evaporation and therefore gypsum formation.

The colour changes within the dolocrête cycles mostly reflect changes within the hematite and dolomite precipitation. Hematite again is accompanied by increased green/red values, lowered lightness and high Fe/Al ratios. The climate was mainly dominated by physical weathering as also shown by high K/Al ratios. High lightness reflects dolocrête formation. Dolocrête was formed during increased chemical weathering traduced by lowered K/Al within the playa system. Hence, the increased lightness also reflects the increased monsoonal activity over the playa.

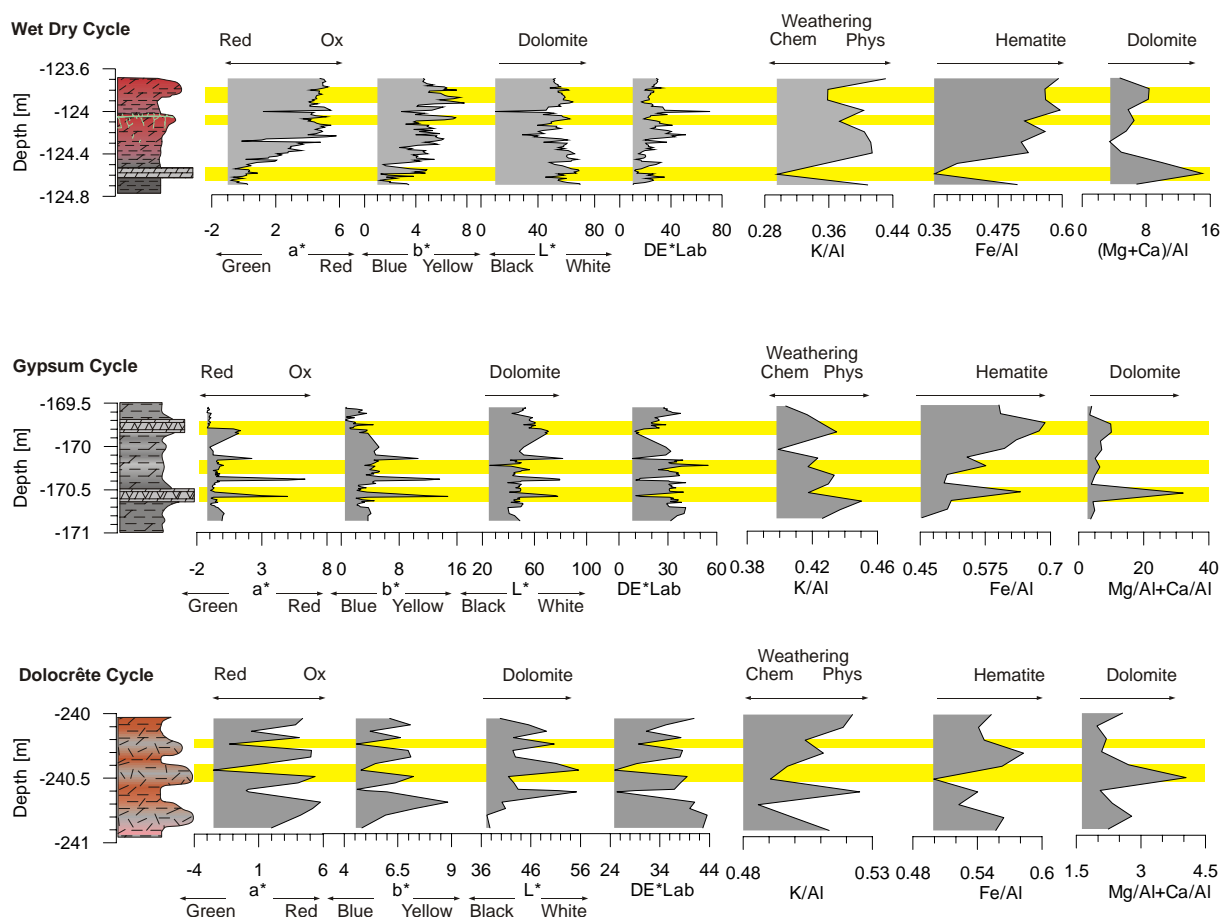


Fig. 107: Colour logs for the basic cycle types with chosen element/Al ratios. XRF data by courtesy of RÖHLING, H.-G. NLfB Hannover.

#### 4.4.2 Hierarchical Bundling of Colour Cycles and Long Term Trends Example Core MorsDp52a

The most intriguing cyclicity is shown by the colour changes from green/gray to red (fig. 108). Five basic cycles (precession) are organized in lower frequency (eccentricity 1 and 2) cycles which are themselves organized in cycles of eccentricity 3. These cycles again are bundled and form eccentricity 4 cycles. The same pattern can be observed within the gypsum cycle. Fig. 109 shows the long-term evolution of the colours within core MorsDp52a. The green-red values show a three-fold pattern starting with a cyclic decrease within the Untere Bunte Mergel. This trend is continued within the Mittlere Graue Mergel until  $-193.93\text{m}$ . From this depth up to  $-152.45\text{m}$  the trend is rather constant. Then within the Obere Bunte Mergel the values rises cyclically. The trend of the yellow/blue curve is similar within the Untere and Obere Bunte Mergel. But within the Mittlere Graue Mergel similarities are only visible at red mudstones. The lightness shows an antagonistic cyclicity to the green-red plot. Peaks within the lightness correlate with peaks of the dolomite proxy ( $\text{Mg/Al} + \text{Ca/Al}$ ). Hence increased lightness reflects increased dolomite content within the sediments. This fact has been shown by several authors within marine sediments (e.g. SCHAAF 1995). SCHÜNKE, 1984 and NITSCH, 1996 discussed this problem exhaustively for the Steinmergel Keuper. The general lightness trend rises from the bottom to the top. This behaviour is parallel to the ( $\text{Mg/Al} + \text{Ca/Al}$ ) ratio indicating a dependency of lightness on dolomite content on a long-term scale. DE\*Lab shows a striking cyclicity through the whole section.

The red colouring pigment is hematite which is shown by the proxy parameters  $\text{Fe/Al}$  and susceptibility (fig. 109). This corresponds well to high green/red value. The  $\text{IRM/k}$  ratio in particular parallels well the green-red plot. As hematite is formed under oxidizing conditions cyclic variations of green/red values reflect cyclic variations of reducing/oxidizing conditions. When the playa system shifted from oxidizing to reducing conditions hematite was replaced by a more magnetic component as shown by lowered  $\text{IRM/k}$  ratios within the green/gray sediments. This is concordant with a colour change from red to green/gray. Green/gray sediments fit together with low  $\text{d}18\text{O}$  values, which indicates lake level rise. On the other hand, the red mudstones correlate with high  $\text{d}18\text{O}$  values suggesting evaporation and successive dry-out of the playa lake (see also chapter 4.2 *Stable Carbon and Oxygen Isotopes*). This is strengthened by the  $\text{K/Al}$  ratio pattern: low  $\text{K/Al}$  ratios fit together with green/gray sediments reflecting the increased monsoonal activity and reducing conditions within the playa system (see also chapter 4.1 *XRF Analysis*). High  $\text{K/Al}$  ratios within the red mudstones reflect the increased physical weathering pattern, i.e. the decreased monsoonal activity of the hinterlands. Summarizing it can be said that the green/red values are a good parameter reflecting changing reducing/oxidizing conditions within the playa system.

The three fold pattern of the green/gray colours demonstrates clearly the cyclic shift from long lasting dry periods with short-term flooding events to a long-lasting wet period with establishment of a perennial lake. During these times lake waters evaporated but they did not dry-out completely. The farthest evolution of the lake reached just up to the wet mudflat. Then hematite was formed within the gypsum indicating that the conditions got somewhat oxidizing (see also *The Basic Cycles* above). With the next flooding event dark gray sediments were deposited in the playa lake. This is also shown by lowered lightness values (fig.109). After this long wet period the climate changed again and the playa dried out completely.

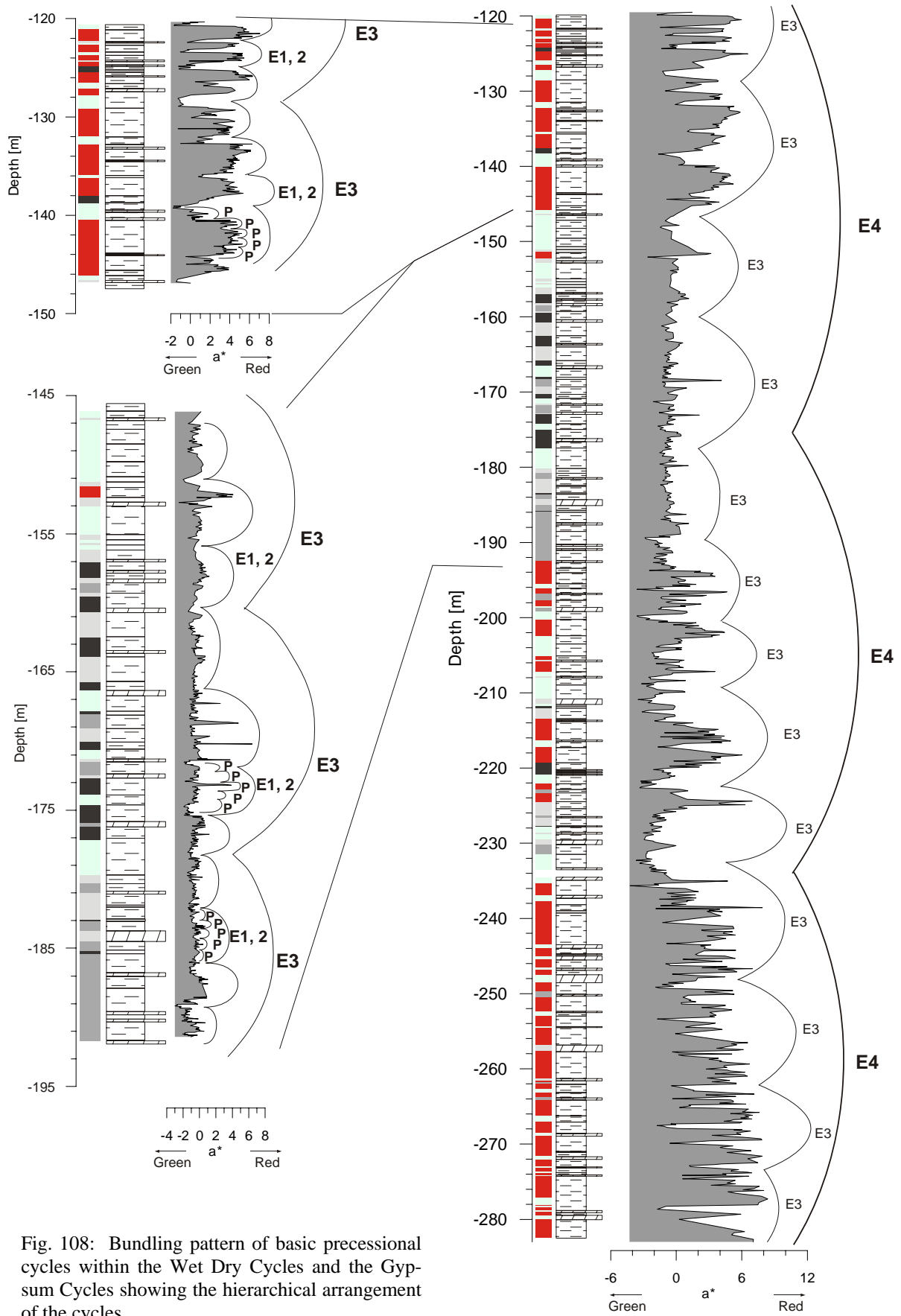


Fig. 108: Bundling pattern of basic precessional cycles within the Wet Dry Cycles and the Gypsum Cycles showing the hierarchical arrangement of the cycles.

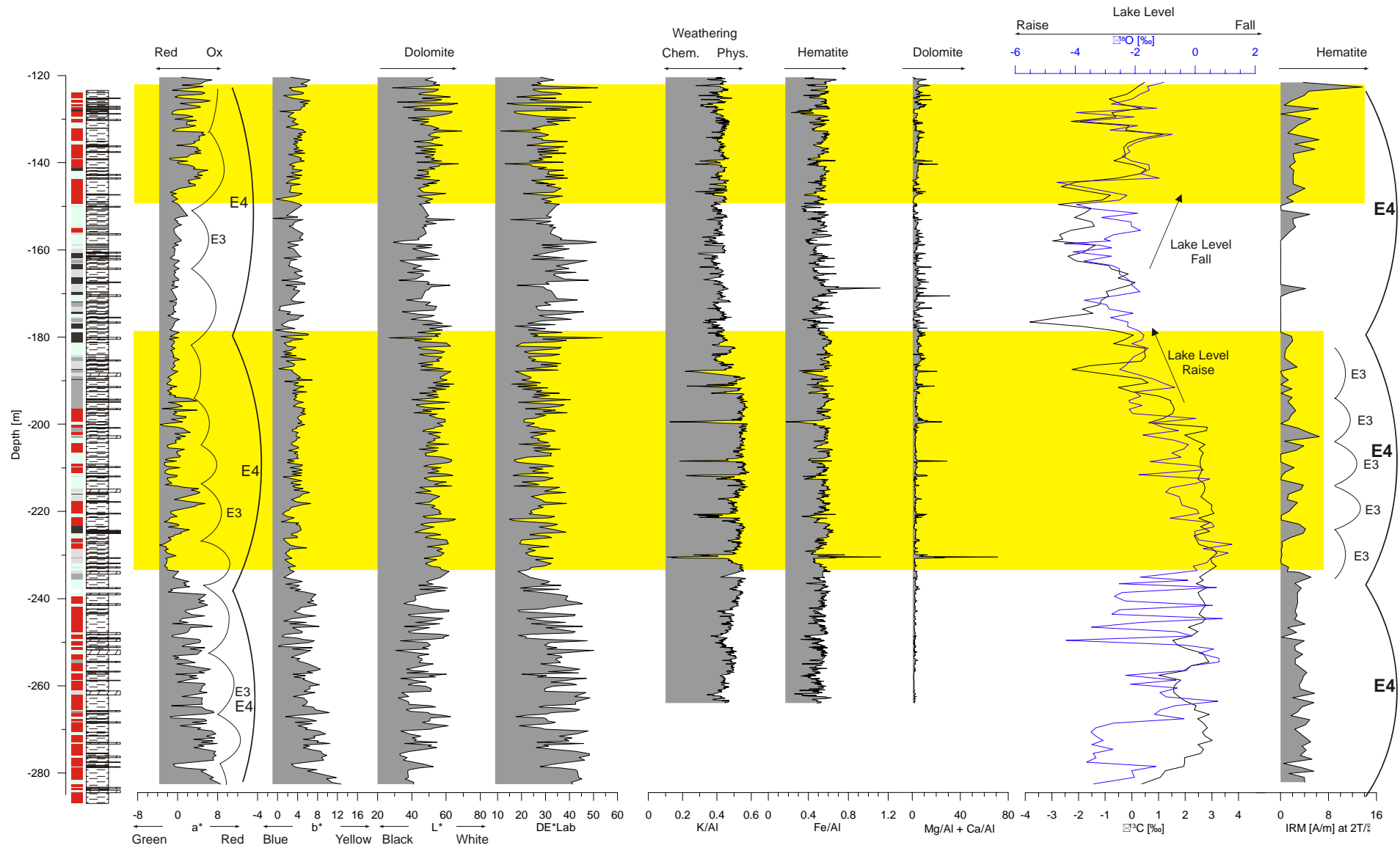


Fig. 109: Long term trends within the Steinmergel Keuper in N Germany. Core MorsDP52a. E3: eccentricity of 413 kyr, E4: eccentricity of ~2Myr. For comparison chosen element/al ratios (XRF data by courtesy of Röhling, H.-G. NLFb Hannover) stable isotope data and magnetic susceptibility are provided.

---

Lakes having existed for a short time are suggested by green/gray colours working out the bundling pattern of the red mudstones.

## Comparison with other section

### **Drei Gleichen area, Thuringia (composed section of outcrops Gleichenburg and Wachsenburg)**

Within this section only the first 80m are described because of the lack of ~20m at the top of section presented. Then follow the ~10m bundled dolocrête cycles described in former chapters (e.g. chapter 4.1 *XRF Analysis*). In any case, the interpretation of the colour changes from red to green/gray does not change.

The long-term trends are also visible within the outcrops: the green/red plot (fig. 110) show at the bottom (UBM) a bundling pattern of red mudstones intercalated with green/gray sediments. Comparison with the K/Al plot suggest that lowered green/gray values are connected to a lake phase, i.e. increased chemical weathering of the hinterlands (low K/Al ratios), whereas during dry periods, i.e. increased physical weathering of the hinterlands (higher K/Al) green/red values are higher, reflecting the hematite within the red mudstones. This is also shown by increased Fe/Al ratios. In contrast with the section MorsDp52a the transition from long-lasting dry periods to long lasting wet periods (MGM) in the Drei Gleichen area is rather abrupt. Somewhat higher green/red values are observed from 0m to ~55m. The assumption of the existence of a perennial lake is strengthened by lowering of d18O ratios (see also chapter 4.2 *Stable Carbon and Oxygen Isotopes*). During this phase dolomite precipitation increased as suggested by increased (Mg/Al + Ca/Al) ratios. Generally lowered K/Al ratios indicate a long period of increased chemical weathering of the hinterland, i.e. increased monsoonal activity (see also chapter 4.1 *XRF Analysis*). In OBM the climatic conditions changed to higher aridity, as clearly shown by increased green/red values.

The blue/yellow plot is somewhat similar as the green/red plot during dry periods, but it is not as clear as in the MorsDp52a section. The lightness rises from the UBM to the MGM and diminishes again in OBM. The high lightness within the MGM fit with increased dolomite precipitation.

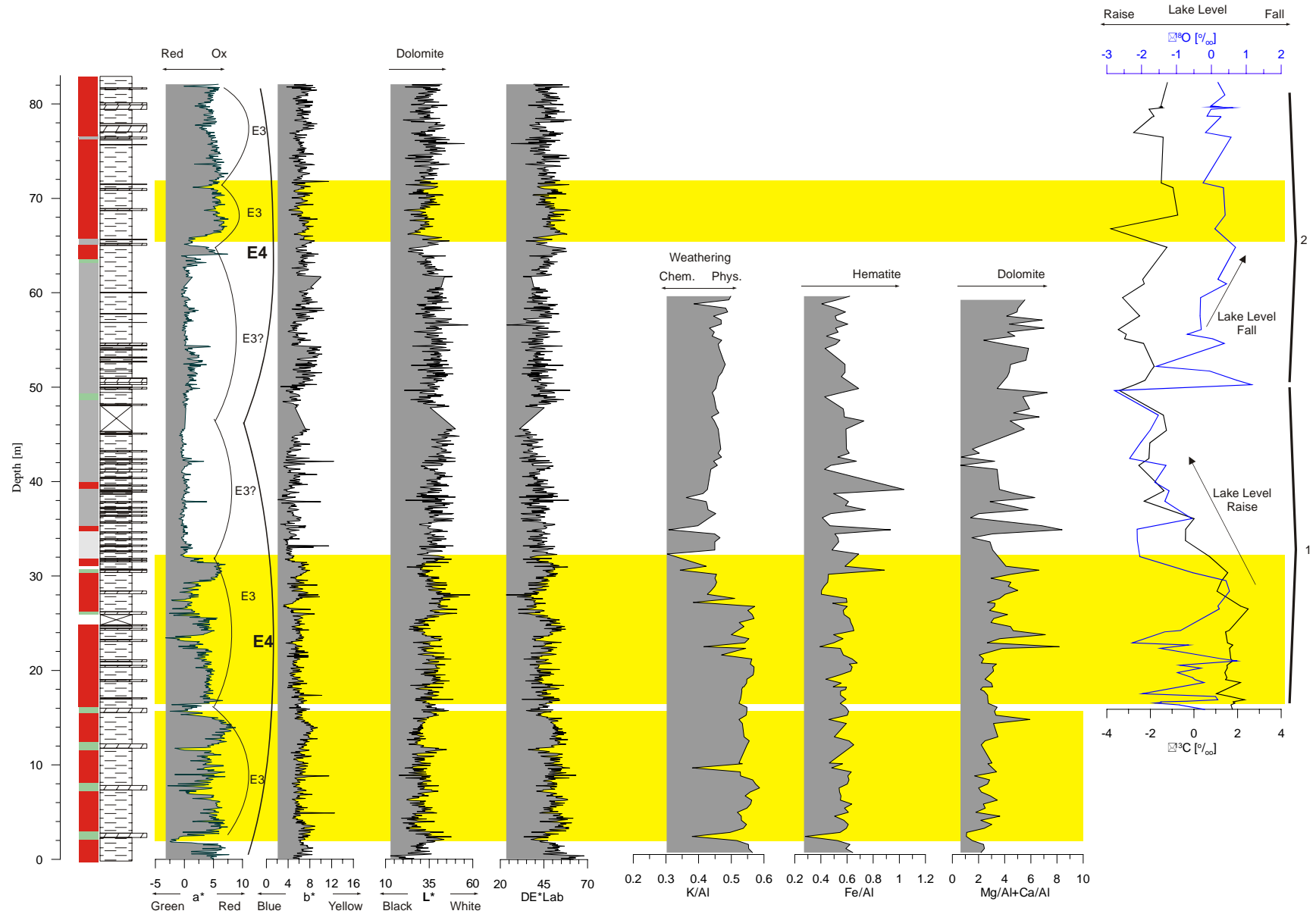


Fig. 110: Long term trends of colours within the Steinmergel Keuper in the Drei Gleichen area, Thuringia (composit of outcrops Wachsenburg and Gleichenburg). For comparison XRF data and stable isotope data are provided (1: isotope data from Reinhardt, 2002; 2: own data), E3: eccentricity of 413kyr, E4: eccentricity of ~2Myr.

---

**Section Malschenberg (Baden Württemberg)**

There is a clear cyclic pattern within the colour plots (fig. 111). The red-green plot shows a three fold bundling cyclicity which parallels well the three fold cyclicity of the K/Al ratio. That means green values reflect lake level rise and reducing conditions and red colours represent dry periods and oxidizing conditions as in N Germany. The Fe/Al ratios are not as clear as within core MorsDp52a. This might be due to the reduced data set available for core Malschenberg. Exceptional high Fe/Al ratios are observed at the Ochsenbach horizon. This is a horizon interpreted as influenced by a marine ingression as stable isotope data suggest (REINHARDT, 2002, see also chapter 4.2 *Stable Carbon and Oxygen Isotopes*), hence the high Fe/Al ratios might not be representative. Even less information is provided by the (Mg/Al + Ca/Al) plot. The highest ratios fit with the Ochsenbach horizon. The proxy for lake level trends in stable carbon and oxygen isotopes indicates that green colours represent lake-level rise and red colours suggest lake-level fall and dry periods. The yellow-blue plot shows a similar pattern to the green-red plot during dry periods. Exceptionally high values are observed again at the Ochsenbach horizon, strengthening the interpretation of a marine ingression into the playa. The cyclic evolution of the lightness represents cyclic variations within the dolomite content. The results for S Germany are not as clear as for N Germany due to the reduced data set in S Germany. However, the data suggests a similar climatic evolution in S Germany and in N Germany. A major difference between both sections is the dolomite distribution within the sediments. In S Germany the dolomite seems to be concentrated in well traceable horizons throughout Baden Württemberg beds, suggesting a shallow water body. This is strengthened by the assumption of a microbial origin of the dolomite beds. In N Germany much fewer dolomite beds are developed but the dolomite content within the whole sediment is increased relative to S Germany, indicating deeper water bodies in N Germany. This is also supported by the higher occurrence of dark gray mudstones in N Germany. Interestingly the three-fold division of the green-red plots is present in both sections. Despite the fact that the section Malschenberg is considered to be more marginal than core MorsDp52a. This suggests that the playa might have dried out completely during dry periods.

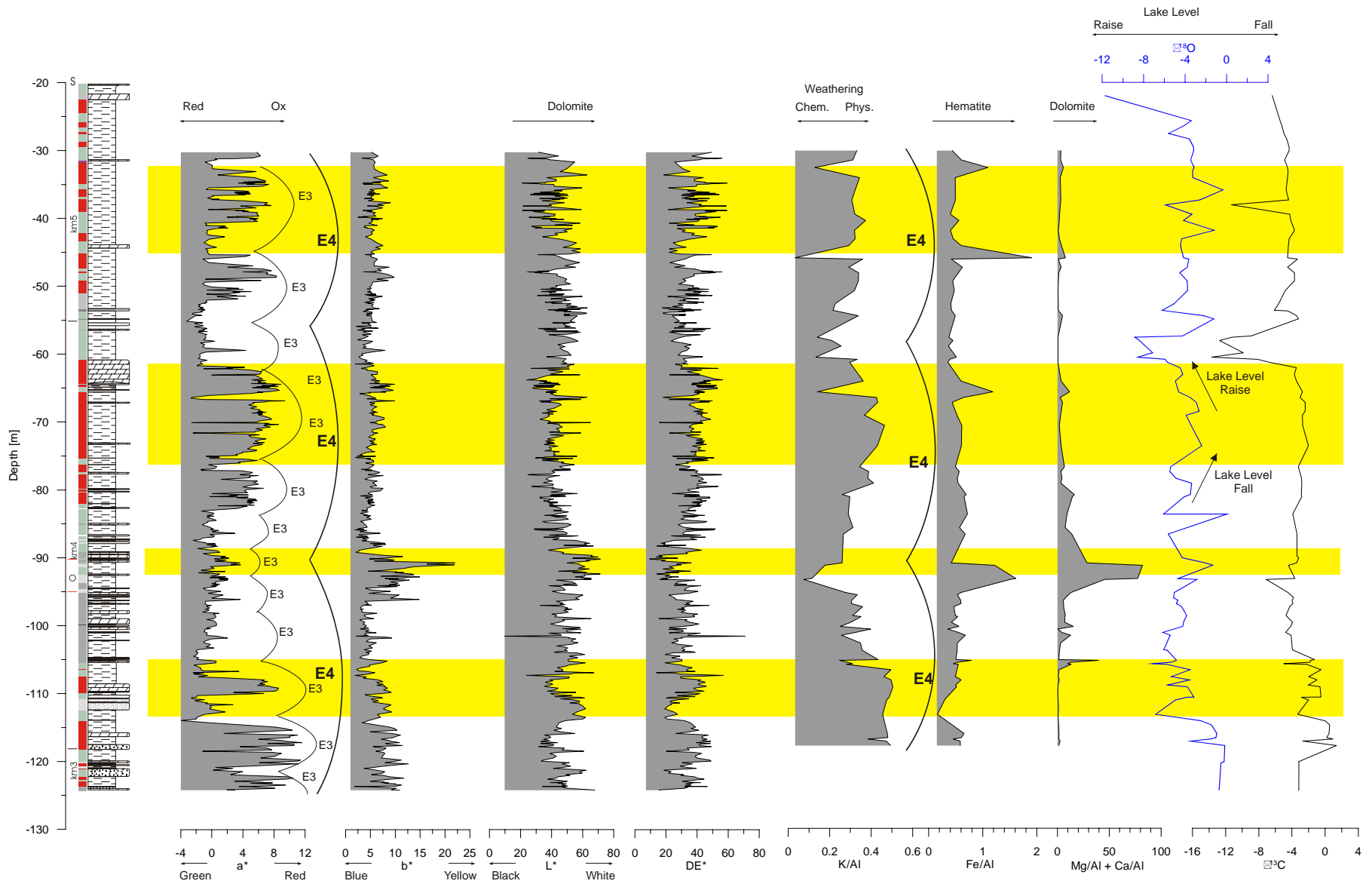


Fig. 111: Long term trends within the Steinmergel Keuper in S Germany. Core Malschenberg. For comparison chosen element/Al ratios and stable isotope data (XRF and isotope data from REINHARDT 2002) are provided. E 1,2: eccentricity of 100kyr, E3: eccentricity of 413kyr, E4: eccentricity of ~2Myr.



### 4.4.3 Origin of the Colours of the Steinmergel Keuper Playa system

Some deductions about the origin of the colours of the playa system can be made. However, it is not possible to explain all colours with the present data, and it is not the issue of this work to give a detailed interpretation of the colours. Exhaustive discussion on this topic can be found in SCHÜNKE (1984) and NITSCH (1996).

The colour cross plots of all three sections show more or less the same behaviour (fig. 112):

- Blue/yellow ( $b^*$ ) against green/red ( $a^*$ ): the values plot into two well distinguishable fields that can be attributed to humid and dry periods (fig. 112 A, D and G). There is no correlation between  $b^*$  and  $a^*$  during wet periods, i.e. playa lake dominated system. But there is a visible correlation between  $b^*$  and  $a^*$  during dry periods, i.e. a mudflat dominated playa reflecting continuous colour changes during dry periods.
- Lightness ( $L^*$ ) against  $a^*$ : the data plot again into two fields reflecting humid and dry periods. A general diminishing of  $L^*$  in function of  $a^*$  can be observed (fig. 112 B, E and H). The correlation coefficient in the sections MorsDp52a and Malschenberg are moderate whereas at the outcrop the coefficient seems too bad to be reliable.
- $L^*$  against  $b^*$ : here neither does a correlation exist nor can a separation into two fields be observed as before. The data of dry and humid periods overlap.

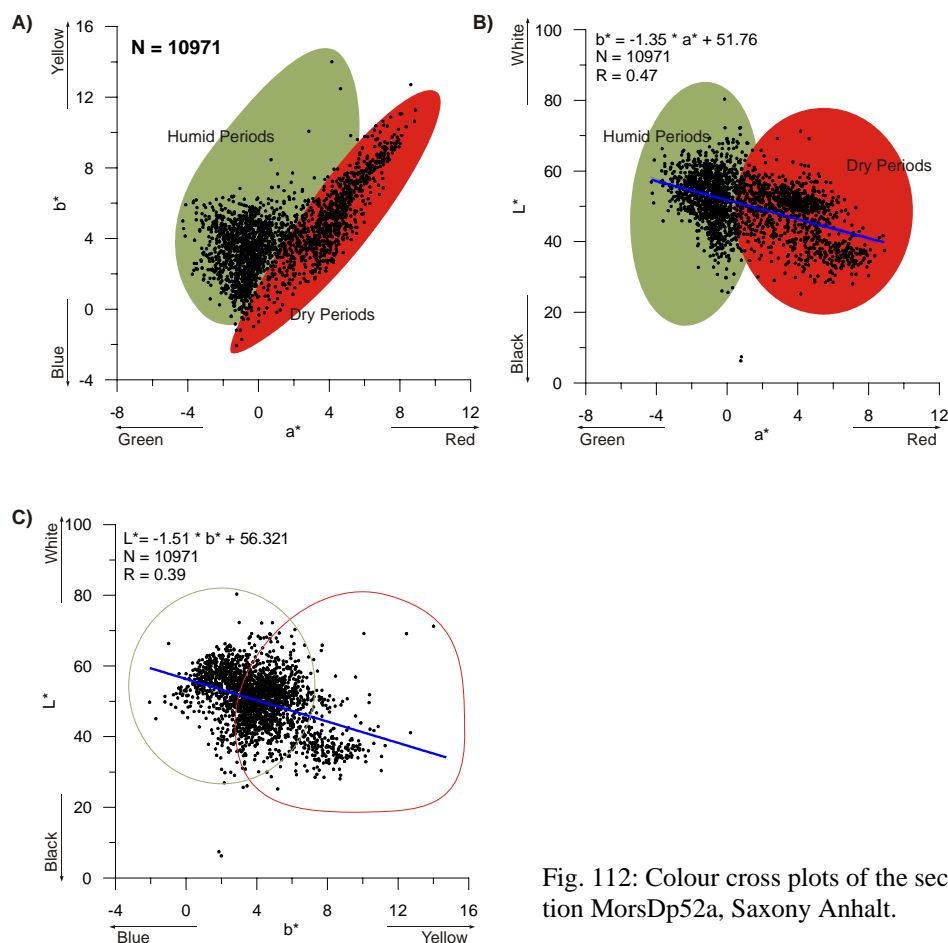


Fig. 112: Colour cross plots of the section MorsDp52a, Saxony Anhalt.

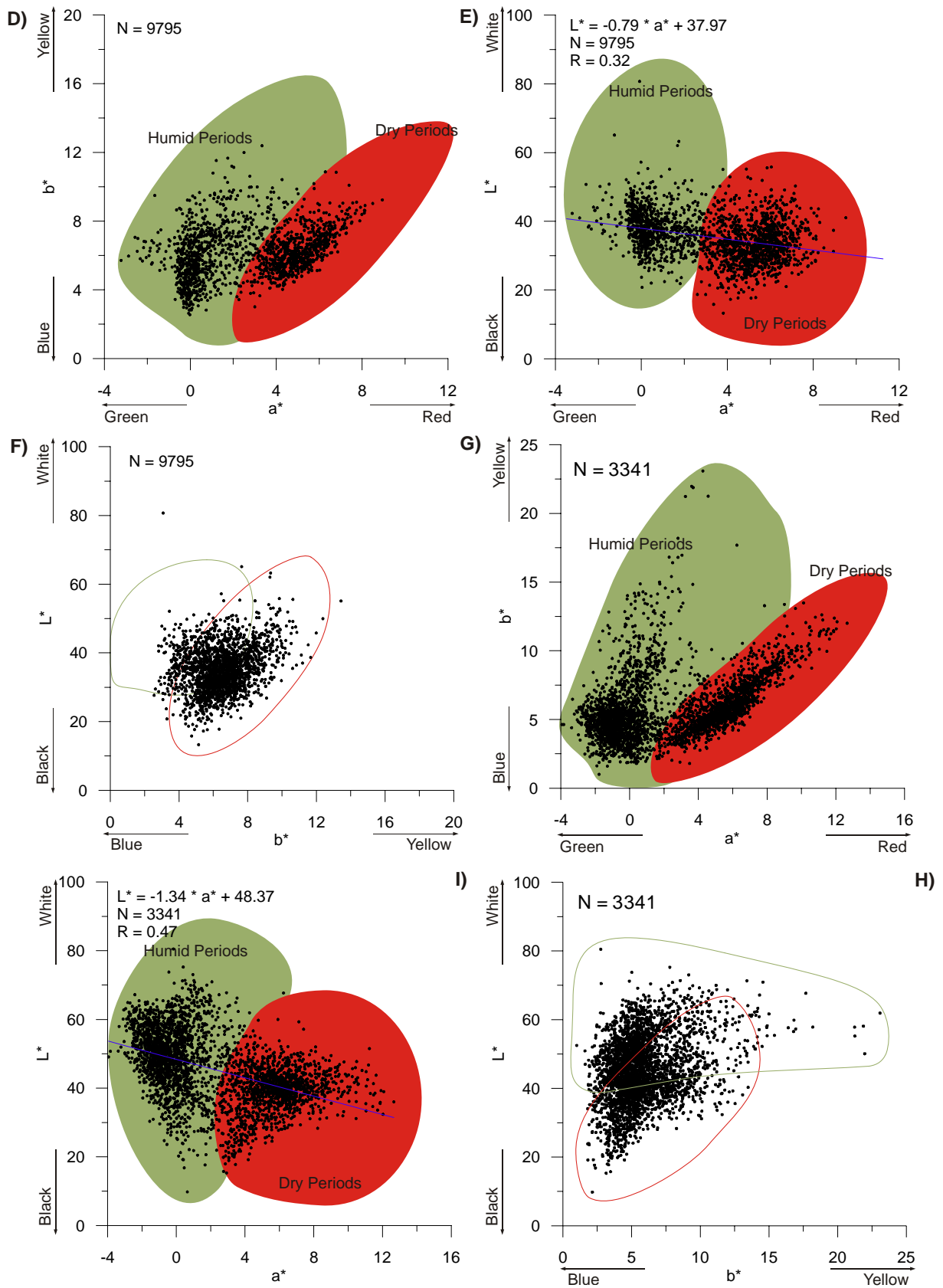


Fig. 112 (continued): Colour cross plots from the sections: Drei Gleichen area, Thirungia (D, E and F) and core Malschenberg, Baden Württemberg (G,H and I).

Fig. 113 (left) shows the relationship between Fe and  $a^*$ . The data plot into two fields, which can be attributed to humid and dry periods. There is no correlation between Fe and  $a^*$  during humid periods, i.e. playa lake dominated systems. A moderate positive correlation exists between both during dry periods, i.e. mudflat dominated playas. This means that during dry periods the mudstones get red with increased iron content. This affirms the fact that within the red mudstones the hematite content increases. Fig. 113 (right) shows an inverse correlation between Fe and (Mg + Ca). This suggests a dilution of iron with increased dolomite precipitation. As the iron content diminishes with increasing dolomite precipitation, hence the colours changes continuously from red to more gray during dry periods.

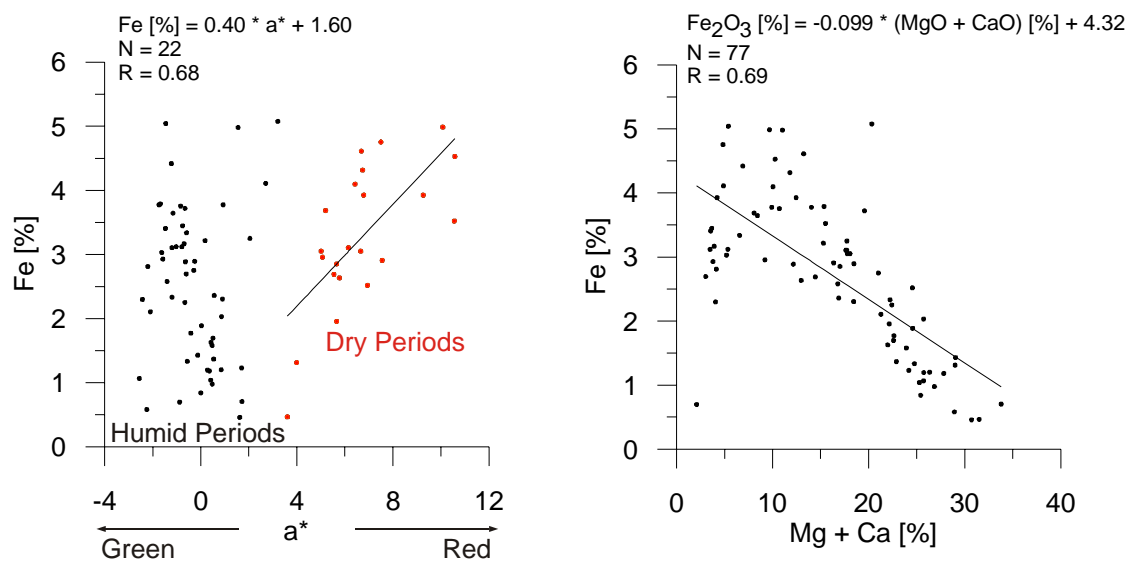


Fig. 113: Fe- $a^*$  (left) and Fe-(Mg +Ca) (right) cross plots of core Malschenberg, Baden Württemberg. XRF data from REINHARDT 2002.

The switching of the data between humid and dry periods may be due to the presence of  $Fe^{2+}$ .

A dependency of dark gray colours within the sediments on organic material (TOC content of 33 samples from section MorsDp52a were measured) could not be demonstrated. In any case, a screen of 33 samples is nothing approaching enough to demonstrate this dependency; hence more research is necessary to clear this question. Neither pyrite nor marcasite were found, thus it is less probable that dark gray colours have their origins in by these minerals.

The question of the origin of violet colours can neither be answered here, as XRF analysis provides only the total of elements and does also not make a distinction between the cations of a given element.

## 5 Controlling Processes of the Cyclicality

### 5.1 Frequency Analysis

To test the hypothesis of orbitally-controlled sedimentation within the playa system the geochemical and the geophysical data set were further investigated by applying frequency analysis. For these purposes the program SPECLAB (with courtesy from G. PORT) was used. This program has the advantage that it does not need a time equidistant sampling, as it is based on a LOMB-SCARGLE algorithm (see also chapter 2 *Methods*).

In S Germany only the colours were analysed and then compared with results from REINHARDT, 2002 and HAMBACH et al, 1999. DE\*Lab is the result composed of all three colour variables and therefore show the cyclicality of the components. Therefore spectral analysis was carried out on DE\*Lab but also on susceptibility data. Strong and sudden variations within the K/Al ratios of core MorsDp52a do not give interpretative results. Thus these ratios were not used for spectral analysis.

#### 5.1.1 Example 1: Core MorsDp52a, Saxony Anhalt, N Germany

Sedimentation within the playa system is strongly influenced by changing monsoonal activity over the playa. This is shown by a repeated alternating succession of green/gray dolomites (reflecting relative humid periods) and red mudstones (relative dry periods). As monsoonal activity depends on the insolation an orbital control on sedimentation within the playa system is suggested.

The power spectrum of the bundled Wet Dry Cycle was performed on the De\*Lab data set. The very high sampling resolution (1 cm) revealed not only the existence of all Milankovitch cycles but also the presence of hemi precessional cycles.

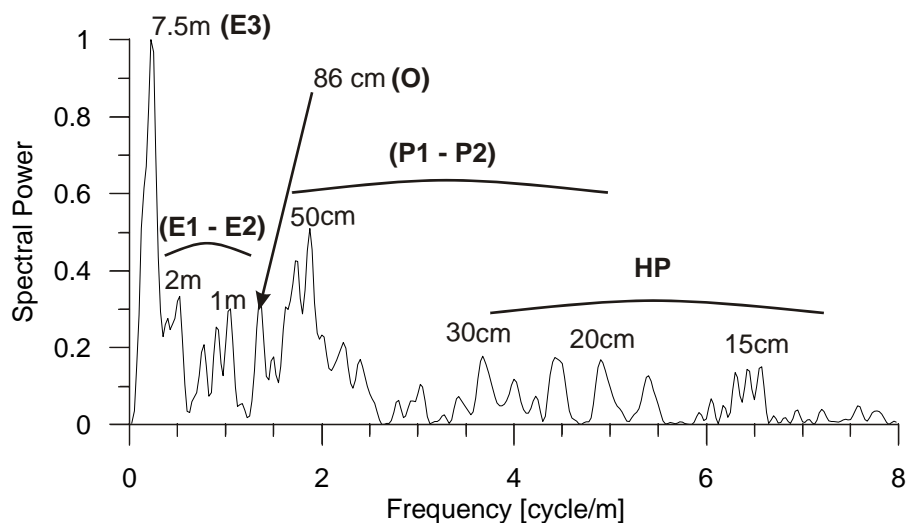


Fig. 114: Power Spectrum of colour data of the bundled Wet Dry Cycle (from core MorsDp52a) showing the Milankovitch cycles and the hemi precessional cycles. HP: hemiprecession, other index names in brackets see fig. 117.

The power spectrum (fig. 114) shows discrete peaks from 15 cm up to 7.5 m. The 50 cm represent the basic wet dry cycle. The thickness of such a cycle changes from 20 cm to 50 cm. As the lowest thickness of a basic cycle is 20 cm the 13 cm peak represents a sub-cycle. The peaks of the sub-cycles overlap with those of the precessional cycle. The lower frequent cycles of 2m and 1m show the bundled arrangement of the precessional cycles. These lower frequent cycles themselves are bundled into a dominant cycle of 7.5 m.

The periodicities for the Triassic were calculated as follows: two precessional periods with a mean of 19.8 kyr (P1+P2), with P1=18ky and P2=21.5ky. The eccentricity cycles are calculated as 95ky for E1, 123ky for E2 (with a mean of 108ky {E1+E2}) and 413ky for E3 (see BERGER AND LOUTRE 1989, 1994). A comparison for the ratios of Milankovitch cycles for the Triassic and the spectral analysis is provided in tab.6. The ratios show a reasonable fit for all cycles from P to E3. The ratio for E4 is higher than the ratio given by BERGER AND LOUTRE (1989, 1994). Therefore the basic Wet-Dry Cycle is interpreted to be originated by the precession. This means that the sub-cycles found in the spectral analysis are hemi precession cycles. The somewhat weaker 1 m and 2 m cycles are interpreted as eccentricity cycles E1+E2 and the strong signal of 7.5 m therefore has its origin in the 413Ky (E3) cycle.

	Precession	Obliquity	Eccentricity		
Late Triassic Periods (kyr)	19.8 (P1+P2) P1=18, P2=21.5	36 (O)	109 (E1+E2) E1=95, E2=123	413 (E3)	~2000 (E4)
Ratios	1	1.8	5.5	20.9	101
Periods (m) (power spectra)	0.2 to 0.81	0.86	0.98 to 4.1	4.1 to 19	66.3
Mean ratio	1	1.72	5.5	21.8	131

Tab.6: Orbital periods for the Triassic (after BERGER AND LOUTRE, 1989, 1994) compared with periods derived from the power spectra of core MorsDp52a.

The evolutionary spectral analysis (fig. 115) gives evidence of the evolution of the precessional and hemi-precessional cycles. The evolution of the precessional shows a striking cyclic shift of the power spectra, suggesting a cyclic variation of the sedimentation rate, which is also shown by the hemi-precessional cycle. Sedimentation rates are lowered during wet periods.

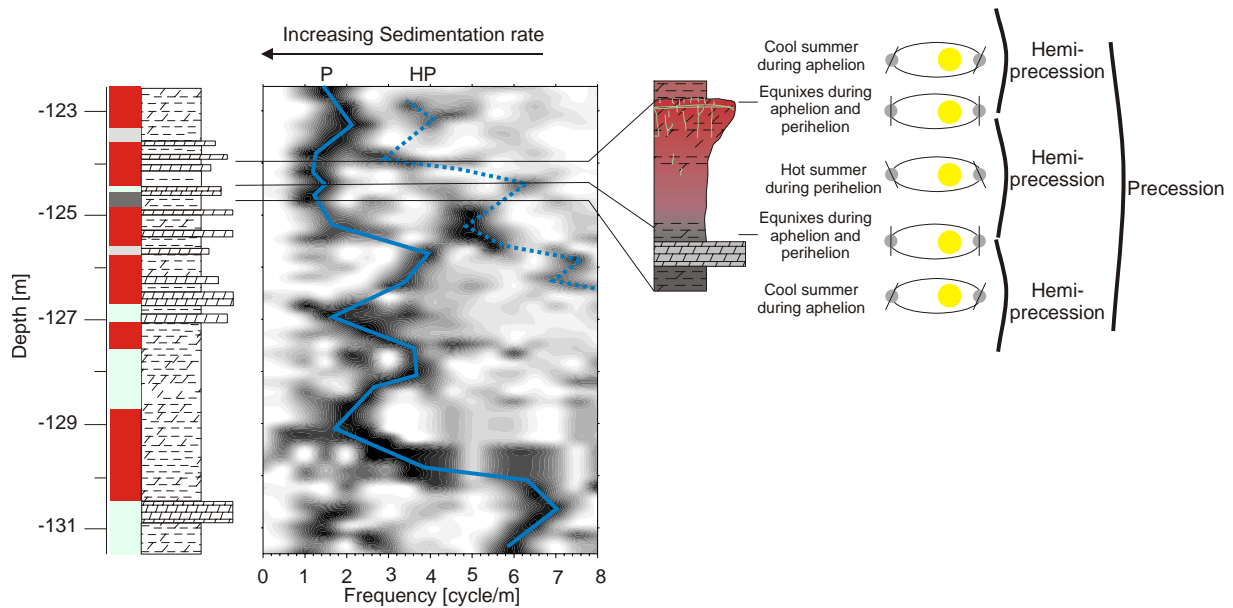


Fig. 115: ESA of colour data of a bundled Wet Dry Cycle (from core MorsDp52a) showing a simplified model for the evolution of cycles related to the precession (blue line) and hemi-precession (blue dashed line). Power legend see fig. 122.

The spectral analysis for the whole core (fig. 116) is quite a bit more complex. Variation of the sedimentation rates can be seen easily at all scales. The power spectrum shows discrete peaks in the ranges of 0.36 m to 0.81 m, 0.86 m, 0.98 m to 4.3 m, 4.3 m to 7.5 m and 129 m. The high frequency cycles from 0.36 to 0.8 m can be attributed to the precession. A weak obliquity signal is shown by the period of 0.86 m. the eccentricity (E1-E2) ranges from 0.98 m to 4.3 m and overlaps with the E3 peaks that range from 4.3 m to 7.5 m. Interestingly there is a very low-frequency signal with a wavelength of 129m, which suppress the E4 and some E3 signals. This low-frequency signal may be due to a response to tectonic movements. In any case, to work out all the E3 and the E4 signals the low-frequency signal was filtered out by analysing the upper 100m of the core.

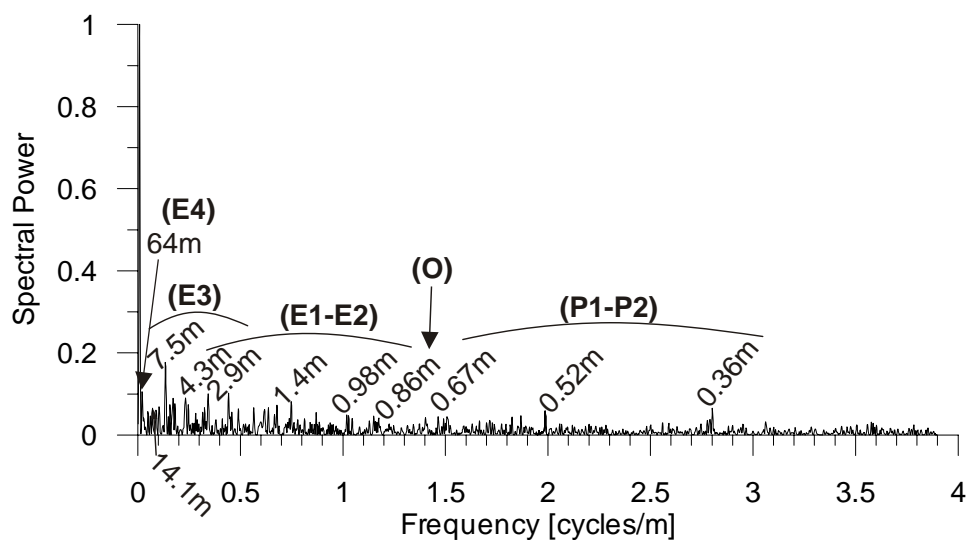


Fig. 116: Power Spectrum of colour data of core MorsDp52a showing the Milankovitch cycles with their respective sedimentation rates. Index names in brackets: see fig. 117.

The power spectrum of the upper 100m of the core is shown in fig. 117. Beside the above mentioned periods, further discrete peaks with following periods are present within the core: 19 m (E3) and 66.3 m (E4). The dominant peaks are the 66.3 m peak, interpreted as a climate cycle of ~2 Myr, the eccentricity cycles of E3 cycle (413 kyr) and (E1-E2, 95 kyr-123 kyr). The dominance of these cycles is typical for low latitudes, as expected for monsoonally influenced playa systems as in the present case. Thus, it seems surprising that an obliquity signal is detected, as obliquity signals are indicator of influences from higher latitudes, and not expected at low latitudes (e.g. IMBRIE et al. 1992, DE BOER & SMITH 1994). TALBOT (1994) showed that the winds within the playa system came from NE, i.e. from the Scandinavian High, and brought aeolian dust into the playa. Hence, the weak obliquity signal could have its origin in these sediments.

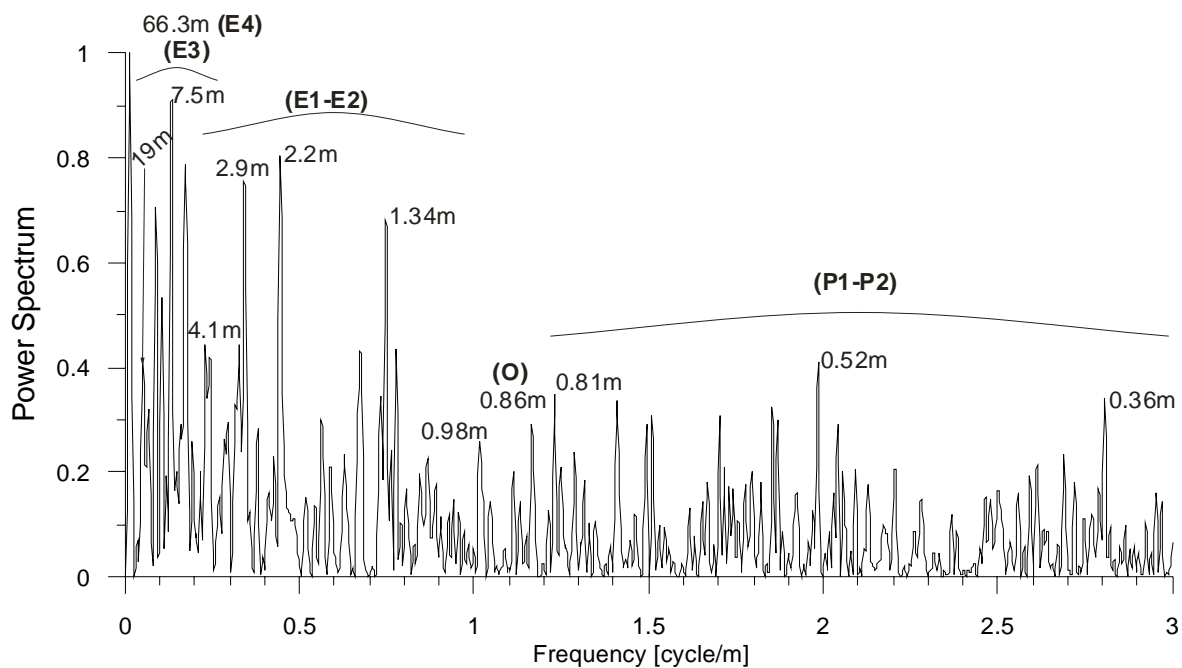


Fig. 117: Power Spectrum of colour data (DE\*Lab) of the upper 100m of core MorsDp52a showing the Milankovitch cycles with their respective sedimentation rates. E4: eccentricity of ~2Myr, E3: eccentricity of 413kyr, E1-E2: eccentricity of 100kyr, O: obliquity, P: precession.

The ESA (fig. 118) of DE\*Lab and susceptibility for E3 (413kyr) data show significant cyclic shift of the spectral power. This suggests (as discussed above) a cyclic variation of the sedimentation rates. Interestingly, highest sedimentation rates are related to red mudstones, i.e. the marginal basin and lowered sedimentation fit together with green/gray sediments, i.e. the central basin. HORNUNG (1998) and also REINHARDT (2002) described this behaviour of sedimentation in the playa system. According to HORNUNG (1998) this is due to the extreme conditions that prevailed in the playa system. During dry periods because of evaporation and infiltration there was not sufficiently water available to transport the sediments further and the sediments were deposited over the mudflat even though the mudflat was sub-aerially exposed.

The smaller differences between the ESA plots for DE\*Lab and susceptibility are due to the different resolution of the data (1m average for susceptibility and 1cm average for colour data).

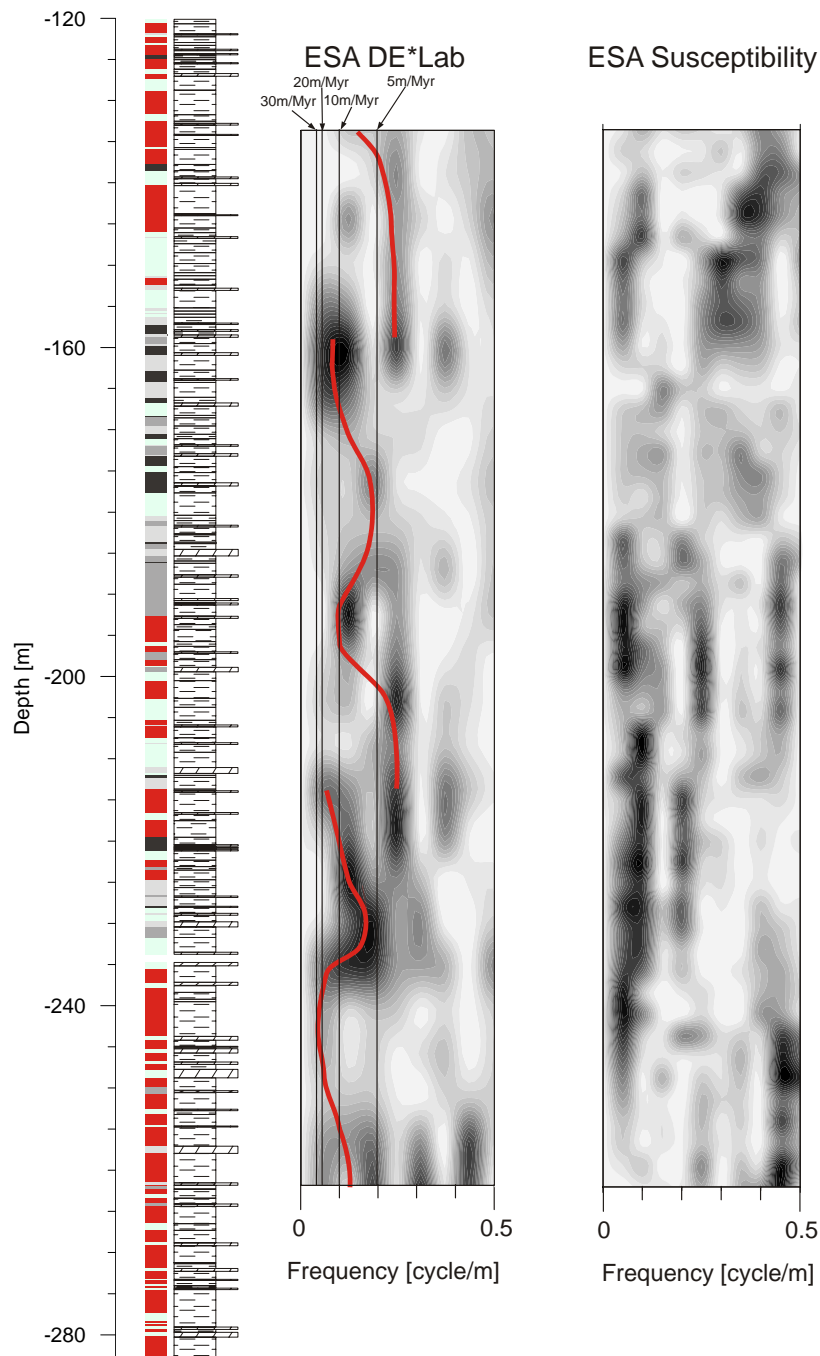


Fig. 118: Left: ESA of colour data (DE\*Lab) of core MorsDp52a showing a simplified model for the evolution of cycles related to the eccentricity of 413ky (red line). Right: ESA of susceptibility data for comparison. Black lines with numbers: sedimentation rate. Power legend see fig. 122.

An independent time frame for the Arnstadt Formation represented within the studied section can be calculated by the mean sedimentation rates. The time span covered within the section is  $\sim 5.3$ Myr, which is in good agreement with the one given above.



### 5.1.2 Example 2: Core Malschenberg, Baden Württemberg, S Germany

The power spectrum (fig. 119) has discrete peaks in the ranges of 0.4 m to 0.6 m, 0.7 m 0.8 m to 3.4 m, 3.4 m to 11.4 m and 37.7 m. The low-frequency peak with the period of 37.7m is interpreted as 2Myr (E4) climate signal. The E3 is represented by range 3.4m to 11.4m overlapping with the E1-E2 cycles. The range from 0.8m and 3.4m is attributed to the E1-E2 eccentricities. Again a weak obliquity signal (0.7m) seems to be present. The precession is reflected by the range from 0.4m to 0.6m.

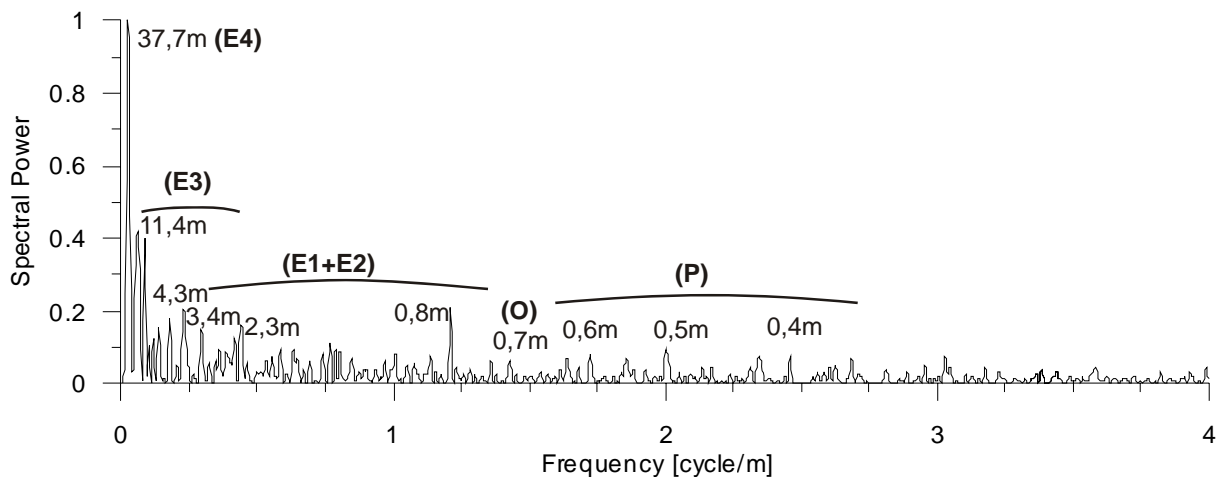


Fig. 119: Power Spectrum of colour data (DE\*Lab) of the core Malschenberg showing the Milankovitch cycles with their respective sedimentation rates. Index names in brackets: see fig. 117.

The ESA (fig.120) of the E3 (413kyr) cycles again shows a cyclic variation of the sedimentation rate depending on the position within the playa system: at the marginal basin the sedimentation rate is high, whereas in a more central position the sedimentation rate is lowered. The sedimentation rate is generally lowered relative to the North German basin because of lowered subsidence of the basin in the South German basin. The calculated time span for the section is also about 5.3Myr, which is in good agreement with the time span of 5Myr calculated by REINHARDT (2002).

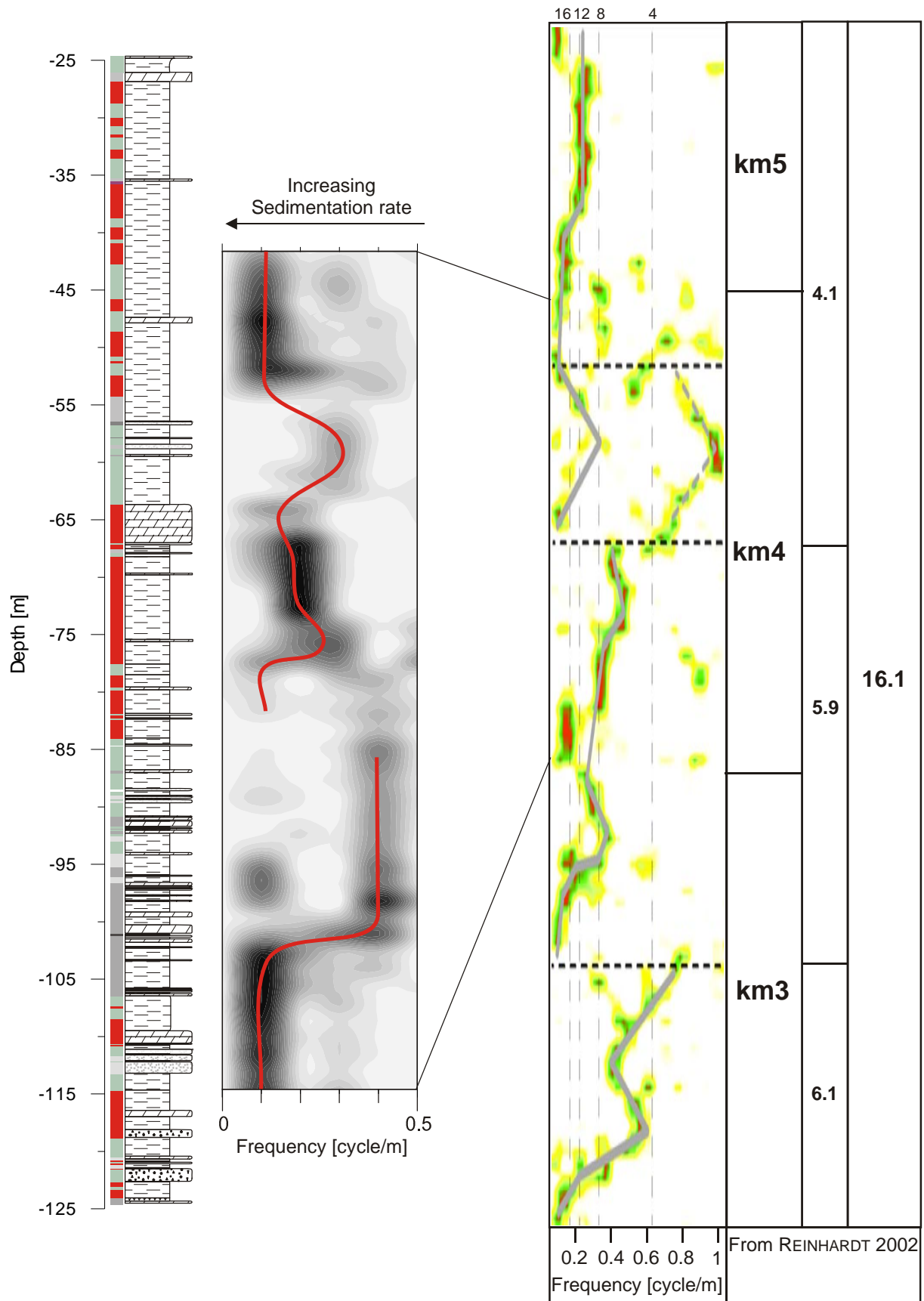


Fig. 120: Left: ESA of colour data (DE\*Lab) of core Malschenberg showing a simplified model for the evolution of cycles related to the eccentricity of 413ky (red line). Right: ESA K/Al data for comparison (from REINHARDT 2002). Power legend see fig. 122.

### 5.1.3 Example 3: Outcrop Mönchberg, Baden Württemberg, S Germany

The power spectrum (fig. 121) of the colour data (DE\*Lab) also shows different ranges of peaks: the lowest frequency has a period of 4 m and is interpreted as representing the E3 eccentricity. The eccentricities E1-E2 are given by the range 1.1 m to 1.5 m. The obliquity signal has a period of 0.67 m. The presence of the precessional signal is shown by the range 0.20 m to 0.50 m. Then overlapping with the precession the hemi-precessional signals can be identified: 0.13 m to 0.20 m.

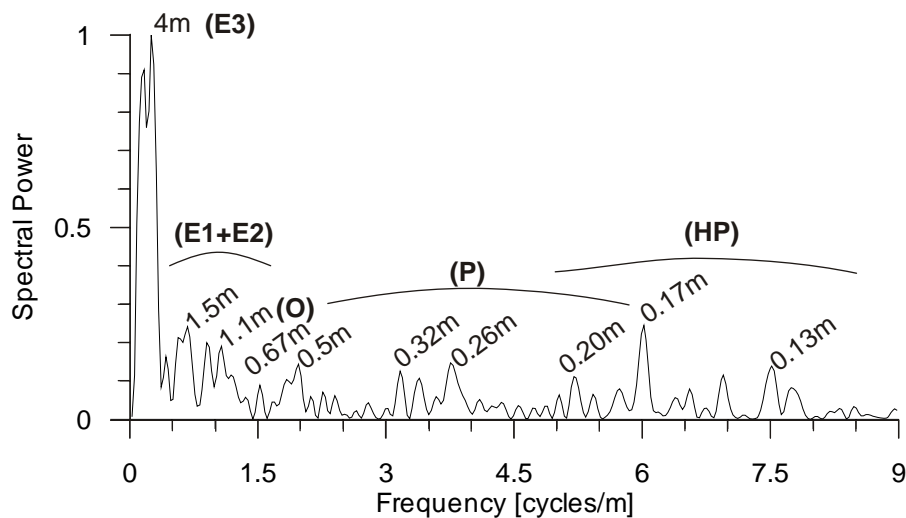


Fig. 121: Power Spectrum of colour data (DE\*Lab) of the outcrop Mönchberg showing the Milankovitch cycles with their respective sedimentation rates. HP: hemiprecession, other index names in brackets: see fig. 117.

The ESA (fig. 122) show that the sedimentation rates for the E1-E2 eccentricities rises continuously from the bottom to the top. The plot also reveals clearly the precessional and the hemiprecessional cycles.

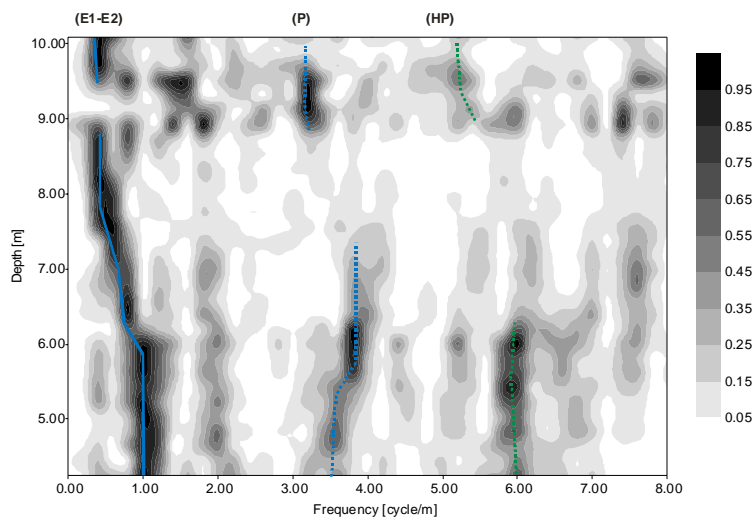


Fig. 122: ESA of colour data (DE\*Lab) from Mönchberg outcrop showing a simplified model for the evolution of cycles related to the eccentricity (E1-E2) (blue line), the precession (P1-P2, blue dashed line) and the hemi-precession (HP, green dashed line).

#### 5.1.4 Example 4: Composit of the outcrops Gleichenburg and Wachsenburg from the Drei Gleichen area, Thuringia

The power spectrum (fig. 123) of the DE\*Lab data from the outcrops of the Drei Gleichen area reveals as before different ranges with discrete peaks: a peak with a period of 65.7 m that is attributed to E4 eccentricity, then a range with peaks from 4.2 m to 19.3 m, which represent the eccentricity E3. The eccentricities E1-E2 are present with the range from 2.1 m to 4.2 m. A weak signal with a period of 0.86 m is interpreted to have its origin with the precession. Interestingly, the obliquity signal cannot be identified. The sedimentation rates are comparable to those of core MorsDp52a.

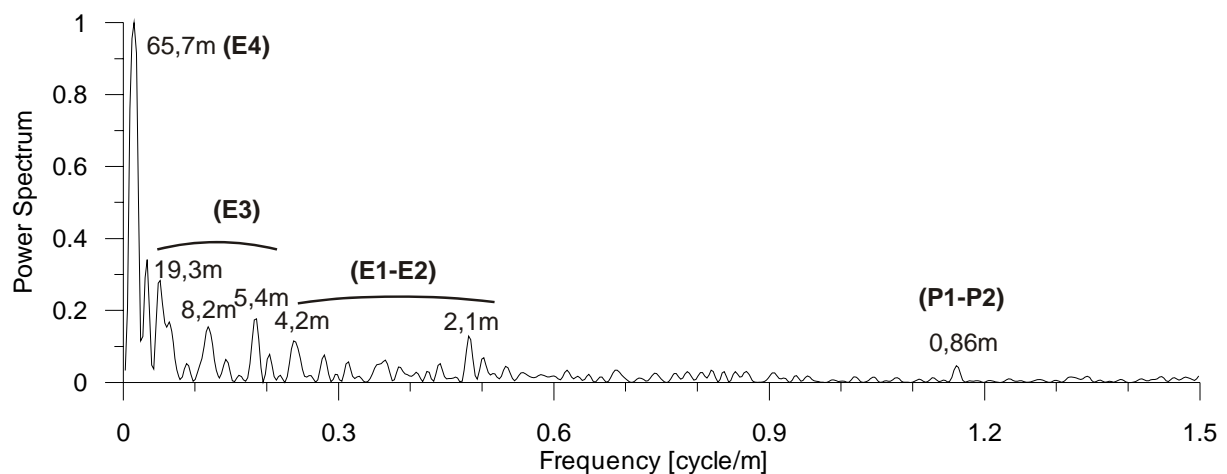


Fig. 124: Power Spectrum of colour data (DE\*Lab) of the outcrops of the Drei Gleichen area showing the Milankovitch cycles with their respective sedimentation rates. Index names in brackets: see fig. 117.

The ESA of the E3 eccentricity (fig. 125) also show the different sedimentation rates depending on the position within the playa system as above. But here the results are contradictory: high sedimentation rates occur within the more central part of the basin and low sedimentation rates occur in the marginal basin. This may be due to local influences that overprint the general trend of the playa system. This is strengthened by the presence of fluvial sandstones within the green/gray sediments, i.e. the more central basin at the Wachsenburg outcrop (see also chapter 3 *Playa Facies*).

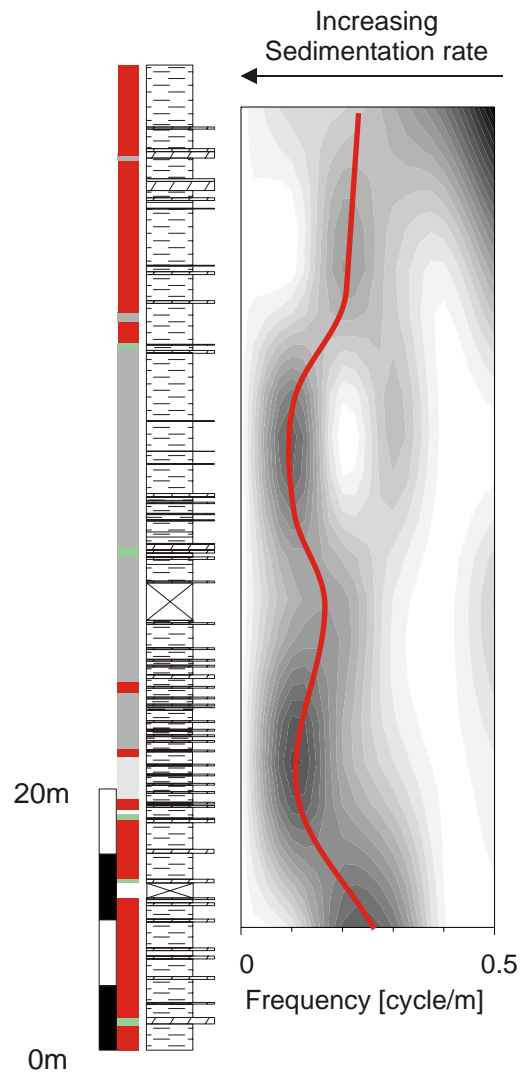


Fig. 125: ESA of colour data (DE\*Lab) from the outcrops of the Drei Gleichen area showing a simplified model for the evolution of cycles related to the eccentricity E3 (red line). Power legend: see fig. 122.

## 6 A Basin Wide Correlation

Based on the stratigraphic correlation (see fig. 8 in the *Introduction* chapter) and the high resolution colour cyclostratigraphy a basin-wide correlation from the N German Basin to the SW German Basin can be provided. Some problems must be considered when correlating colour bundles at a regional scale:

- It is possible to correlate bundles of colours at a local scale (fig. 14, chapter *Methods*). But at regional scale this is not true anymore (fig. 126). This is due to the fact that the facies shows an important shift from red at the marginal basin, i.e. the mudflat, to green/gray (even dark gray) in the central basin. In the present case the outcrops of the Drei Gleichen area (Thuringia) represent the most marginal position within the playa system and the MorsDp52a site represents the most central part of the playa system. Within time slice A5 (L5) core MorsDp52a shows at its base dark gray mudstones (fig. 126). This is also the section where a maximum of gypsum formation is observed at site MorsDp52a. In Thuringia the facies shift toward the red mudstones of the Untere Pedogene Folge (UPF). Then in the SW German Basin (core Malschenberg) the facies change again and green/gray sediments are deposited. This means colours changes are diachronous through the basin. Thus a basin-wide correlation based only on colour bundles (of the same colour) is not possible. A detailed cyclostratigraphy for each site is therefore necessary before starting with the correlation of the different sites. Furthermore, the presence of isochronous marker horizons as basin-wide discordances and marker beds is necessary as background information for the correlation. The background correlation chart used for the colour correlation is based on the work of several authors: BRENNER 1973 (S Germany), KELLNER 1997 (Thuringia), AIGNER & HORNING 1999 (S Germany), NITSCH 2005a (S and N Germany), BEUTLER 2005 (S and N Germany) and BEUTLER (in press; core MorsDp52a).
- Another problem is that local control on sedimentation may overprint the allocyclic control on sedimentation. This can lead to local changes within the colours. Fig. 126 shows the correlation from the N German Basin to the SW German Basin. Whereas time slices A1 (L1), A2 (L2), A5 (L5) and A6 (L6) can be further subdivided and correlated throughout all sections, time slices A3 (L3) and A4 (L4) (both time slices comprises the Mittlere Graue Mergel (MGM) at the site of the Drei Gleiche area) can neither be correlated at a 400kyr scale from site MorsDp52a to the Drei Gleichen area nor from site Malschenberg to the Drei Gleichen area. This coincides with the surprising fact that contrary to the sites MorsDp52a and Malschenberg the sedimentation rates in the Drei Gleichen area are higher within the MGM than in the Untere Bunte Mergel (UBM) and the Obere Bunte Mergel (fig. 125, chapter 6 *Frequency Analysis*). A local control on sedimentation is therefore possible and may overprint the allocyclic control on sedimentation. An interpretation is given in fig.127: locally increased subsidence rate, which may be induced by upcoming salt diapirs of Permian age, could have produced locally important depressions in Thuringia. These depressions were filled up by sediments from the surrounding area. Important local depressions are common in the N German Basin as shown by WALTER (2002, see also chapter 3.2 *Clay Mineralogy*). However, as the lower and upper delimiting marker horizons are well known and the time slices A3 (L3) and A4 (L4) comprise five 400kyr cycles the time of the local influence on sedimentation in the Drei Gleichen area is about 2 Myr.

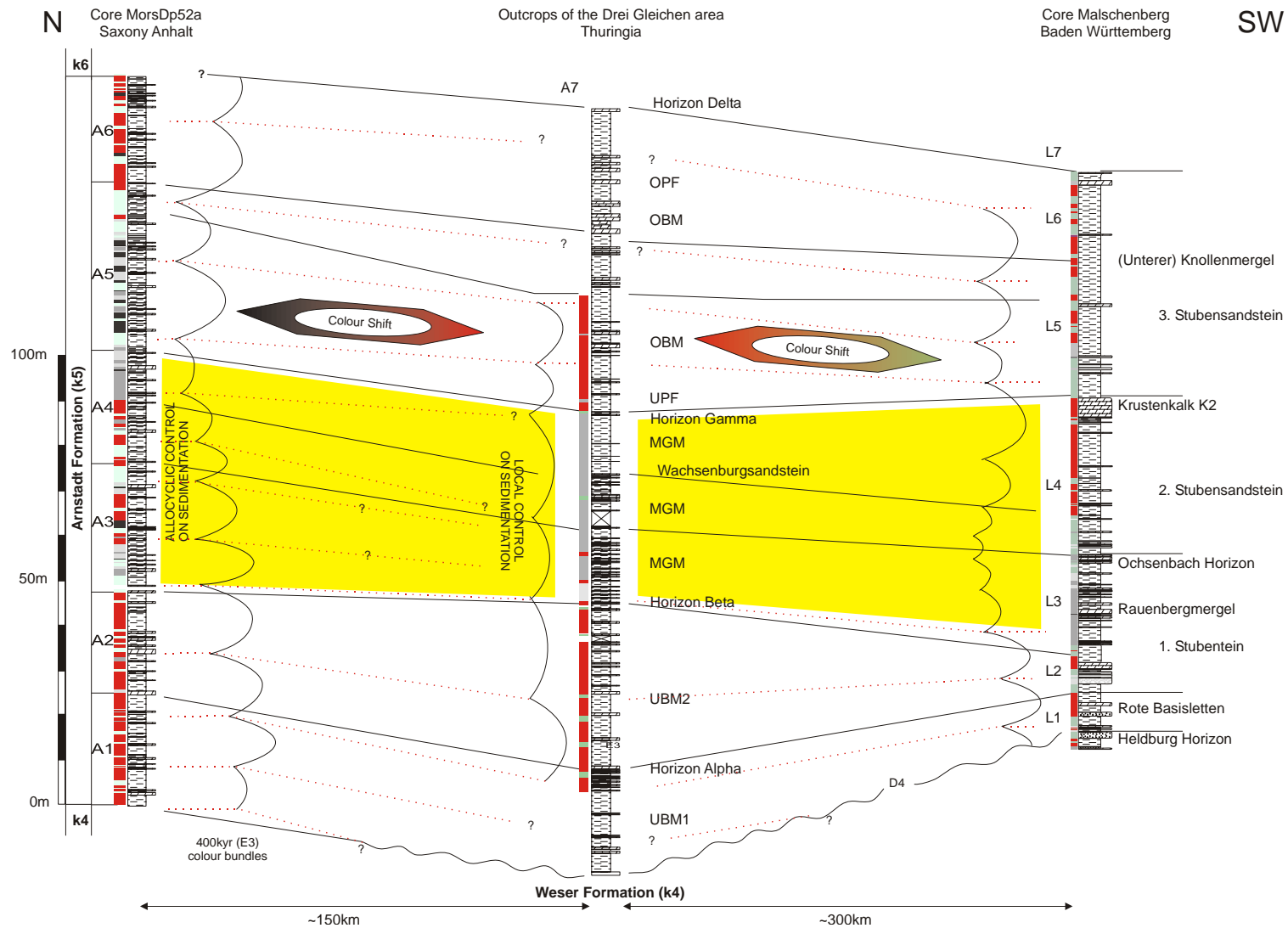


Fig. 126: Stratigraphic correlation based on colour cycles of the German Keuper Basin during k5 (Arnstadt Formation) illustrating the problems which one is faced with when correlating colour cycles. Background correlation chart based on BRENNER 1973 (S Germany), KELLNER 1997 (Thuringia), AIGNER & HORNING 1999 (S Germany), NITSCH 2005a (S and N Germany), BEUTLER 2005 (S and N Germany) and BEUTLER (in press; core MorsDp52a).

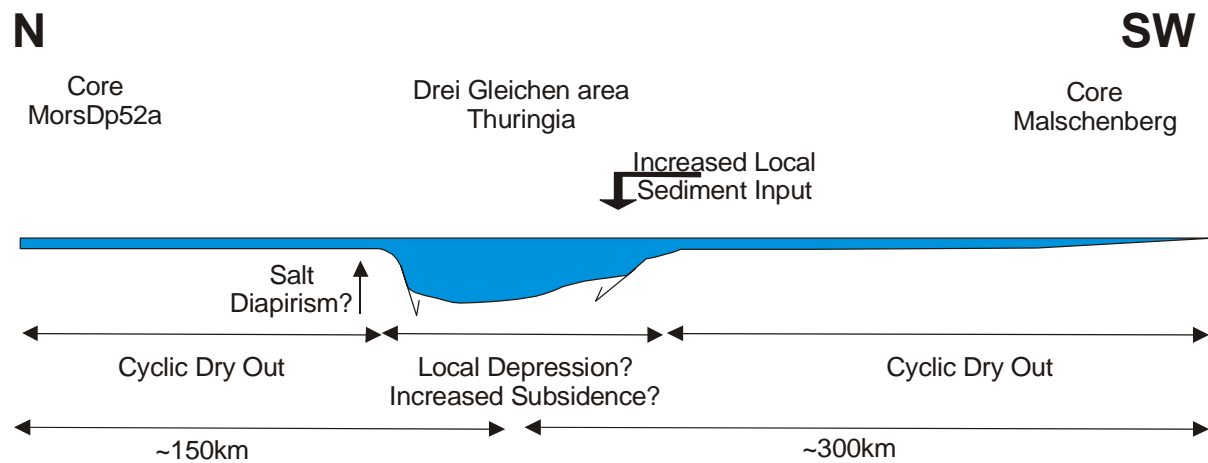


Fig. 127: Simplified sketch illustrating the relation between increased subsidence and local sediment input during A4 (Level of the Wachsenburg Sandstein).

Fig. 128 shows a direct cyclostratigraphic correlation between the N German Basin and the SW German Basin. Then it is also possible to correlate time slice A3 (L3) at 400kyr scale. The correlation suggests also that the each “small cycle” (A1-A7) after NITSCH (2005) is composed of two to three 400kyr cycles. Thus one “small cycle” represents about 800kyr to 1200kyr. A1 is composed of two 400kyr cycles at site MorsDp52a. At the Malschenberg site only both cycles are not present. As it supposed that the basin-wide discordance D4 (BEUTLER 1998) at the top of the Heldburg horizon is not developed at site MorsDp52a (see also chapter 5.2 *Stable Carbon and Oxygen Isotopes*) the cycles onlap on the discordance D4. The top of L3 (A3) is characterized by the presence of the Ochsenbach horizon with a discordance at its top. This makes a further correlation within time slice A4 (L4) impossible at the moment. The remaining time slices A5 (L5) and A6 (L6) again can be correlated at a 400kyr scale. The subsidence rate in the N German Basin is generally somewhat higher than in the S German Basin. This is traduced by generally slightly thicker cycles in the N German Basin.



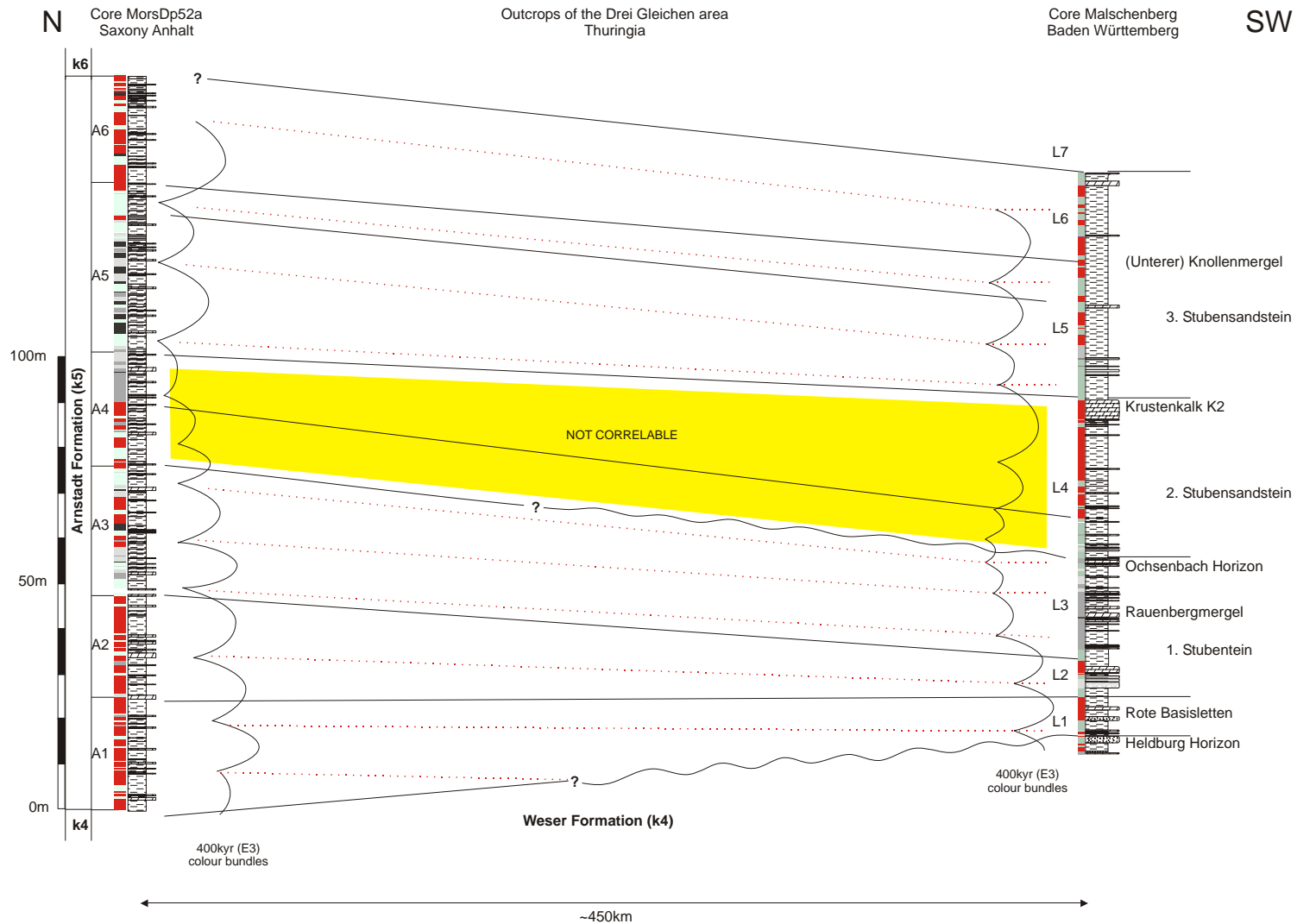


Fig. 128: Stratigraphic correlation based on colour cycles of the German Keuper Basin during k5 (Arnstadt Formation). Background correlation chart based on BRENNER 1973 (S Germany) , KELLNER 1997 (Thuringia), AIGNER & HORNING 1999 (S Germany), NITSCH 2005a (S and N Germany), BEUTLER 2005 (S and N Germany) and BEUTLER (in press; core MorsDp52a).

## 7 Conclusion

1. The Steinmergel Keuper Basin in Germany was located between 20° and 25° within the super continent Pangaea and was strongly influenced by Pangaeian monsoon circulation. The central basin is situated in northern part of the playa system. It displays no sandstones or fewer as it is the case in the marginal basin in S Germany. Investigation of playa cycles based on high resolution sampling of data made it possible to establish an integrated climate model.
2. In the Steinmergel Keuper playa system three different basic cycle types depending on their position within the playa system can be distinguished. The basic gypsum cycle corresponds to the most central part of the playa, and was formed by successive flooding and evaporation events during generally wetter periods. A somewhat more marginal cycle is the wet-dry cycle, reflecting fast changes between dry and humid periods. The most marginal cycle is the dolocrête cycle formed within the dry mudflat. It shows the evolution of evaporating groundwaters.
3. The basic wet-dry cycle could be further divided into two sub-cycles. The first sub-cycle is composed by a succession of dark gray mudstones followed by a dolomite bed. The mudstone was deposited during flooding of the playa and the dolomite was formed during beginning of increased evaporation. In the second sub-cycle a red mudstone with dolocrête at the top was deposited in dry periods by occasional flooding. After seasonal dry-out of the playa the sediments were oxidized and hematite was formed. The dolocrête precipitated because of evaporating groundwaters.
4. Clay mineralogy analysis revealed a cyclic shift from illite to smectite reflecting the aggradation/degradation of illite due to repeated wetting and drying of the playa system. Chlorite and corrensite that were formed in the mudflat are mainly of pedogenetic origin. When they appear in lake sediments they seem to be originated by very early diagenetic processes. The presence of analcime and zeolithe in the lower part of the Steinmergel Keuper playa system suggests the presence of soda lakes. The source of the necessary sodium is probably Permian salt, which came up during the early kimmerian tectonic phase. This is supported by increased chloride content.
5. All cycles are characterized by major elements' chemistry that supports the hypothesis of lake level change. K/Al ratios, for example, reflect the weathering pattern of the hinterlands. Increased chemical weathering of the Vindelician and Bohemian massifs are traduced by lowered K/Al ratios within the dark gray sediments and dolomites, reflecting the presence of a perennial lake. By contrast, in the red mudstones the K/Al ratios are higher, indicating the increased physical weathering of the hinterlands.
6. A major influence of salinity could not be demonstrated despite the extreme setting of the environment. However, smaller variation in salinity can be observed in the wet/dry cycles.

- 
7. Stable oxygen isotopes reflect changing lake level trends within the playa. Lighter values indicate a raising lake level and heavier ratios suggest a lake level fall. This is concordant with changing weathering pattern of the hinterlands, as suggested by the K/Al ratios.
  8. Colours of the Steinmergel Keuper playa system show a striking cyclicity at all scales. The most intriguing cyclicity is shown by changes from green/gray to red, reflecting perfectly the cyclic changes of oxidizing/reducing conditions in the playa system. This is supported by slightly increased Fe/Al ratios on the red mudstone. The red colours are due to the presence of finely dispersed hematite in the mudstone. Lightness varies in function of the dolomite content: the more dolomite is present, the lighter the sediments are.
  9. Spectral analysis suggests a coupling between the monsoonal activity and orbital forcing of the climate changes. Power Spectra indicate that the basic cycles are related to precession (P1+P2) and the sub-cycles are related to the presence of hemi-precessional cycles. Basic cycles are bundled in eccentricity cycles of 100 kyr (E1+E2), which themselves are bundled into eccentricity cycles of 400 kyr (E3). Bundles of E3 cycles form the eccentricity cycle of ~2 Myr (E4), the lowest-frequency climate cycle found in the Steinmergel Keuper playa system. A weak presence of the obliquity signal suggests a probable periodic aeolian input from the north into the playa. ESA further reveals a cyclic variation of the sedimentation rate depending on the position within the playa system. Sedimentation rate is higher in the marginal basin than it is in the central basin.

## 8 Outlook

The presence of hemi-precession-related cycles suggests a lot of interesting questions for further research. Hemi-precessional cycles are related to the passage of the equinoxes through perihelion and aphelion every 10kyr to 11kyr leading to an increased insolation of the earth's equator during these times. The present study showed that the beginning dry out of the playa lake and the deflation of the mudflat are related to these cycles. A crucial question is which climate phenomenon on a yearly scale is responsible for the beginning dry-out of the playa and the deflation of the mudflat.

REUNING (2005, 2006) suggested that there might be a relationship between hemi-precessional cycles and El Niño-like phenomena within Pliocene sediments. He found that during insolation maxima on hemi-precessional timescales the region of Florida experienced increased rainfall and river run-off as consequence of a more El Niño-like state in the East Equatorial Pacific. Otherwise said the frequency of El Niño-like phenomena rises during the passage of the equinoxes through perihelion and aphelion.

As shown in the present work the monsoonal activity during the Upper Triassic produced the hemi-precessional cycles. The relationship between monsoon activity and El Niño-like phenomena is known. In the model put forward here the playa lake started drying out during hemi-precession. This would fit with the findings of REUNING (2005, 2006) that hemi-precessional cycles modulate the frequency of El Niño-like phenomena. It could be possible that the Steinmergel Keuper playa system started drying out with an onset of El Niño-like phenomena induced by the hemi-precession. Increased frequency of El Niño-like phenomena would then cause a decrease of the monsoonal activity over the playa and the lake would begin to dry out. First the dolomite beds would precipitate as long as the lake exists and after dry-out only the mudstones would be deposited by episodic flooding events. After seasonal dry out of the lake the sediment would be under oxidizing conditions and hematite could be formed. Dolomite would be formed only as pedogenetic dolocrête within the dry mudflat. This would be during times of summer in perihelion. With the next hemi-precession the deflation of the mudflats would increase. Then during summer in aphelion the playa system would be flooded again. Whether all facies developed during one precessional cycle also of course depends on the eccentricity.

However, this is only an outlook on the research that can be done. To verify this hypothesis much more research in recent but also in older sediments is necessary. But if it should be true that El Niño-like phenomena existed during the Upper Triassic the next question would be: when did this kind of phenomena appear for the first time?

## 9 References

Adams, A. E., MacKenzie, W. S. (2001): A Colour Atlas of Carbonate Sediments and Rocks Under the Microscope. 180p. Manson Publishing, London.

Aldinger, V. (1965): Zur Petrographie des Kieselsandsteins. Arb. Geol. Paläont. Inst. TH Stuttgart, N. F. 48: 90.

Aigner, T.; Heinz, J.; Hornung, J. & Asprion, U. (1999): A hierarchical process-approach to reservoir heterogeneity: Examples from outcrop analogues. Bull. Centres Rech. Explor. Prod. Elf-Aquitaine, vol. 22, no 1, p. 1-11.

Aigner, T.; Hornung, J.; Junghans, W.-D. & Pöppelreiter, M. (1998): Base level cycles in the Triassic of the South-German Basin: a short progress report. Zbl. Geol. Paläont. Teil I, vol. 7-8, p. 537-544, Stuttgart, Dec. 1999.

Arakel, A.V., Jacobson, G. and Lyons, W. B. (1990): Sediment-water interaction as a control on geochemical evolution of playa lake systems in the Australian arid interior: Hydrobiologia, v. 197, p. 1-12.

Baldschuhn, R. Binot, F. Frisch, U. Kockel F. (1999): Tectonic Atlas of Northwest Germany and the German North Sea Sector. Geologisches Jahrbuch Reihe A, Heft 153. Bundesanstalt für Geowissenschaften und Rohstoffe, Hannover.

Berger, A. (1992): Astronomical theory of paleoclimates and the last glacial-interglacial cycle. In: Methods and concepts in European Quaternary stratigraphy; proceedings of a session of INQUA, Subcommission for European Quaternary Stratigraphy and Long Terrestrial Records Working Group. Quaternary Science Reviews. 11, p. 571-581.

Berger, A. and Loutre, M. F., (1989). Pre-Quaternary Milankovitch frequencies. Nature, 342: 133.

Berger, A. and Loutre, M. F., 1994. Astronomical forcing through geological time. In: P. L. De Boer and D. G. Smith (Eds.), *Orbital Forcing and Cyclic Sequences*. Special Publication. Blackwell, Oxford, pp. 15-24.

Berger, A. and Tricot, C. (1986): Global climatic changes and astronomical theory of paleoclimates. In: Cazenave, A., ed., *Earth Rotation: Solved and Unsolved Problems*, D. Reidel Publ. Company, Dordrecht, Holland, p. 111-129.

Bloemendal, J. (1993): Origin of the sedimentary magnetic record at Ocean Drilling Program sites on the Owen Ridge, Weter Arabian Sea. Journal of Geophysical Research, 98B, 4199-4219.

Bradley, R. S. (1985): Quaternary Paleoclimatology: Methods of Paleoclimatic Reconstruction, Allen & Unwin, 472 p.

- Broecker, W. S & Denton, G. H. (1990): What drives glacial cycles ? *Scientific American*, January 1990, p. 49-56.
- Beutler, G. (1998): Keuper. *Hallesches Jahrb. Geowiss. Reihe B, Beiheft 6*, 45-58. Halle (Saale).
- Beutler, G. (2005): Megasporen In: *Deutsche Stratigraphische Kommission (Hrsg.)*, 2005: Stratigraphie von Deutschland IV - Keuper. Mit Beiträgen von Beutler, G., Dittrich, D., Dockter, J., Ernst, R., Etzold, A., Farrenschon, J., Freudenberger, W., Heunisch, C., Kelber, K.-P., Knapp, G., Lutz, M., Nitsch, E., Oppermann, K., Schubert, J., Schulz, E., Schweizer, V., Seegis, D., Tessin, R. & Vath, U.-- Courier Forschungsinstitut Senckenberg 253:296 S., 64 Abb., 50 Tab., 2 Taf.; Frankfurt am Main.
- Beutler G. & Oppermann, K. (2005): Ostarcoden. In: *Deutsche Stratigraphische Kommission (Hrsg.)*, 2005: Stratigraphie von Deutschland IV - Keuper. Mit Beiträgen von Beutler, G., Dittrich, D., Dockter, J., Ernst, R., Etzold, A., Farrenschon, J., Freudenberger, W., Heunisch, C., Kelber, K.-P., Knapp, G., Lutz, M., Nitsch, E., Oppermann, K., Schubert, J., Schulz, E., Schweizer, V., Seegis, D., Tessin, R. & Vath, U.-- Courier Forschungsinstitut Senckenberg 253:296 S., 64 Abb., 50 Tab., 2 Taf.; Frankfurt am Main.
- Beutler, G. (in press): Erläuterungen zu Blatt Helmstedt (GK 25,     ). Landesamt für Geologie und Bergwesen, Sachsen Anhalt.
- Blatt, H., Middleton, G., Murray, R. (1972): *Origin of sedimentary rocks*. Prentice-Hall Inc., New Jersey.
- Bowler, J. M. (1981). "Australian salt lakes. A paleohydrologic approach." *Hydrobiologia* **82**: 431-444.
- Brenner, K. (1973). *Stratigraphie und Paläogeographie des oberen Mittelkeupers in Südwest-Deutschland*. Arb. Inst. Geol. Paläont. Univ. Stuttgart. Stuttgart, Univ. Stuttgart. **NF 68**: 101-222.
- Brenner, K. (1978a). "Profile aus dem oberen Mittelkeuper Südwest-Deutschlands." *Arb. Inst. Geol. Paläont.* **NF 72**: 103-203.
- Brenner, K. (1978b). "Sammlung und Revision der bis 1978 veröffentlichten Profile aus dem oberen Mittelkeuper Südwest-Deutschlands." *Arb. Inst. Geol. Paläont.* **NF 72**: 205-243.
- Brenner, K., Villinger, E. (1981). "Stratigraphie und Nomenklatur des oberen Mittelkeuper Südwest-Deutschlands." *Jh. des Geol. Landesamt Baden Württemberg* **23**: 45-86.
- Brigatti, M. F. a. P., L. (1984). "Crystal Chemistry Of Corrensite: A Review." *Clays and Clay Minerals* **32(5)**: 391-399.

- Christmann, H., Schweizer, V. and Kiefer, E., 1990. Tonmineralverteilung im oberen Mittelkeuper (Obere Bunte Mergel, Coburg-Folge) bei Stuttgart, ermittelt über röntgenographische Verfahren. Jahresberichte und Mitteilungen des oberrheinischen geologischen Vereins, N. F. 72: 303-314.
- Clemmensen, L. B., Kent, D. V. and Jenkins, F. A., 1998. A late Triassic lake system in East Greenland: facies, depositional cycles and paleoclimate. *Palaeogeography, Palaeoclimatology, Palaeoecology*, 140(1-4): 135-159.
- Crowley, T. J. (1994): *Pangean Climates*. G. D. Klein. Boulder, CO, Geological Society of America, Inc. GSA Special Paper: 25-40.
- De Boer, P. L. and Smith, D. G. (1994): *Orbital Forcing and Cyclic Sequences*. In: P. L. De Boer and D. G. Smith (Eds.), *Orbital Forcing and Cyclic Sequences*. Special Publication. Blackwell, Oxford, pp. 1-14.
- Deconnink, J. F., Strasser, A. & Debrabant, P. (1988): Formation of illitic minerals at surface temperatures in Purbeckian sediments (Lower Berriasian, Swiss and French Jura). – *Clay Menr.* 23, 91-103.
- Droste, J. B. Bhattacharya, N. & Sunderman, J. A. (1962): Clay mineral alteration in some Indiana soils. – *Clays Clay Miner., Proc 9<sup>th</sup> nat. Conf.* 329-342., Pergomon Press, Oxford 1962.
- Dubiel, R. F., Parrish, J. T., Parrish, J. M. and Good, S. C., 1991. The Pangean megamonsoon – evidence from the Upper Triassic Chinle Formation, Colorado Plateau. *Palaios*, 6(4): 347-370.
- Duchrow, H. (1984). *Keuper. Geologie de Osnabrücker Landes*. H. Klassen. Osnabrück, Naturwissenschaftliches Museum Osnabrück: 221-334.
- Etzold, A & Schweizer, V (2005): *Der Keuper in Baden Württemberg*. In: *Deutsche Stratigraphische Kommission (Hrsg.)*, 2005: *Stratigraphie von Deutschland IV - Keuper*. Mit Beiträgen von Beutler, G., Dittrich, D., Dockter, J., Ernst, R., Etzold, A., Fahrenschon, J., Freudenberger, W., Heunisch, C., Kelber, K.-P., Knapp, G., Lutz, M., Nitsch, E., Oppermann, K., Schubert, J., Schulz, E., Schweizer, V., Seegis, D., Tesin, R. & Vath, U.-- Courier Forschungsinstitut Senckenberg 253:296 S., 64 Abb., 50 Tab., 2 Taf.; Frankfurt am Main.
- Eugster, H. P. a. H., L. A. (1978). *Saline Lakes. Lakes - Chemistry, Geology, Physics*. A. Lerman. Berlin, Springer Verlag.
- Fischer, G., (1925): *Zur Kenntnis der Entstehung der Steinmergel im fränkischen bunten Keuper*. N. Jb. Miner. Geol. Paläont., Beil.-Bd. 51 Abt. B: 413-476.
- Flögel, S. (2001): *On The Influence of Precessional Milankovitch Cycles on the Late Cretaceous Climate System: Comparison of GCM-Results, Geochemical, and Sedimentary Proxies for the Western Interior Seaway of North America*. PhD Thesis. Christian-Albrechts-University Kiel. 236p.

Forster, T. and Heller, F. (1997): Magnetic enhancement paths in loess sediments from Tajikistan, China and Hungary. *Geophysical Research Letters*, 24, 17-20.

Harder, H. (1972): The role of magnesium in the formation of smectite minerals. – *Chem. Geol.* 10, 31-39.

Harder, H. (1978): Synthesis of iron layer silicate minerals under natural conditions. – *Chem. Geol.* 14, 241-253.

Hambach, U., Reinhardt, L., Wonik, T., Port, G., Krumsiek, K. and Ricken, W., (1999). Orbital forcing in a low-latitude playa system: evidence from evolutionary spectral analyses (ESA) of geophysical and geochemical data from the Steinmergel-Keuper (Late Triassic, S-Germany). In: ALFRED-WEGENER-STIFTUNG (Editor), *Sediment '99. Terra Nostra. Alfred-Wegener Stiftung, Bremen*, pp. 97-100.

Hammer, U. T. (1981). "Primary production in saline lakes. A review." *Hydrobiologia* **81**: 47-57.

Haunschild, H. (1985). "Der Keuper in der Forschungsbohrung Obernsees." *Geologica Bavaria* **88**: 103-130.

Hay, W. W., DeConto, R. M. & Wold, CH. N. (1997): Climate: Is the past the key to the future ? *Geol. Rundschau* 86, p. 471-491.

Hay, R. L. (1966): Zeolites and zeolitic reactions in sedimentary rocks. *Geol. Soc. Amer. Spec. Paper* 85, 130 pp.

Heim, D. (1990). *Tone und Tonminerale*. Stuttgart, Enke-Verlag.

Herczeg, A. L., Barnes, C. J., Macumber, P. G. and Olley, J. M. (1992). "A stable isotope investigation of groundwater-surface water interactions at Lake Tyrell, Victoria, Australia." *Chemical Geology* **96**: 19-32.

Hines, M. E., Lyons, W. B., Lent, R. M. and Long, D. T. (1992). "Sedimentary biogeochemistry of an acidic, saline groundwater discharge zone in Lake Tyrell, Victoria, Australia." *Chemical Geology* **96**: 53-65.

Hornung, J., (1998): *Dynamische Stratigraphie, Reservoir- und Aquifer-Sedimentologie einer alluvialen Ebene: Der Stubensandstein in Baden-Württemberg (Obere Trias, Mittlerer Keuper)*. Ph.D. Thesis, Eberhard-Karls-Universität, Tübingen, 211 pp.

Hornung, J. & Aigner, T. (1999): Reservoir and aquifer characterization of fluvial architectural elements: Stubensandstein, Upper Triassic, southwest Germany. *Sed. Geol.* 129, 215-280.

Hornung, J. & Aigner, T. (2002a): Reservoir architecture in a terminal alluvial plain: an outcrop analogue study (Upper Triassic, Southern-Germany). Part 1: Sedimentology and petrophysics. *J. Petrol. Geol.*, vol. 25, no.1, p. 3-30.



- Hornung, J. & Aigner, T. (2002b): Reservoir architecture in a terminal alluvial plain: an outcrop analogue study (Upper Triassic, Southern-Germany). Part 2: Cyclicity, models and controls. *J. Petrol. Geol.*, vol. 25, no.2, p. 151-178.
- Hopf, H. a. M., T. (1992). "Erster Nachweis von Dinosaurierresten im Steinmergelkeuper der Drei Gleichen bei Arnstadt - Ein Beitrag zur Fauna des Mittleren Keupers in Thüringen." *Z. geol.Wiss.* **20**: 327-335.
- Imbrie, J., Berger, A., Boyle, E. A., Clemens, S. C., Duffy, A., Howard, W. R., Kukla, G., Kutzbach, J., Martinson, D. G., McIntyre, A., Mix, A. C., B., M., Morley, J. J., Peterson, L. C., Pisias N. G., Prell, W. L., Raymo, M. E., Shackleton, N. J. and Toggweiler, J. R., (1992): On the structure and origin of major glaciation cycles. 1. Linear responses to Milankovitch forcing. *Paleoceanography*, 7(6): 701-738.
- Johnson, L. C. (1964): Occurrence of regularly interstratified chlorite-vermiculate as a weathering product of chlorite in a soil. – *Am. Miner.* 49, 556-572.
- Kellner, A. (1997). Das Typusprofil der Arnstadt-Formation (Steinmergelkeuper, Obere Trias) in Thüringen. Halle/Saale, Martin Luther Universität Halle-Wittenberg: 71 pp.
- Junghans, W.-D., Aigner, T. and Ricken, W., (1997). Fluviale Architektur des Mittleren Stubensandsteins am südwestlichen Schönbuch (Trias, Baden-Württemberg). *Neues Jahrbuch für Geologie und Paläontologie, Abhandlungen*, 204(3): 285-320.
- Kendall, A. C. (1984): Evaporites. In: Walker, R. G. (Ed.) *Facies Model: Geoscience Canada Reprint Series 1*. p. 259-296.
- Kendall, A. C. (1992). Evaporites. *Facies Models. Response to Sea Level Change*. R. G. W. a. N. P. James. ST. John's, Newfoundland, Geological Association of Canada: 375-409.
- Kent, D. V., Olsen, P. E. AND Witte, W. K., 1995. Late Triassic-earliest Jurassic geomagnetic polarity sequence and Paleolatitudes from drill cores in the Newark rift basin, eastern North America. *Journal of Geophysical Research*, 100(B8): 14,965-14,998.
- Kern, A. and Aigner, T. (1997). Faziesmodell für den Kieselsandstein (Keuper, Obere Trias) von SWDeutschland: eine terminale alluviale Ebene. *N. Jb. Geolog. Paläont. Mh(H. 5)*: 267-285.
- Köppen, W. (1931): *Grundriß der Klimakunde*. Walter de Gruyter & Co. Berlin und Leipzig. 389.
- Konstanty, J. C. and Ricken, W., (1997). Genetic Stratigraphy Of Fluvial Deposits: Implications Of Base Level Changes On Stacking Pattern Architecture, Sediment '97. *Terra Nostra*. Alfred-Wegener-Stiftung, Köln, pp. 108-109.
- Kostrewa, R., (1995). Sedimentology of the Stubensandstein Rivers, Mainhardter Wald, Northern Württemberg. unpublished Diploma Thesis Thesis, Eberhardt-Karls-Universität Tübingen, Tübingen, 80+Appendix I-XVIII pp.

Küpper, H. (1978). DuMont's Farbenatlas. Köln, DuMont.

Kutzbach, J. E. (1981): Monsoon climate in the early Holocene: Climatic experiment using the Earth's orbital parameters for 9000 years ago. *Science*, v. 214, p.59-61.

Kutzbach, J. E. (1994). Idealized Pangean climates: Sensitivity to orbital change. Pangea: Paleoclimate, Tectonics, and Sedimentation During Accretion, Zenith, and Breakup of a Supercontinent. G. D. Klein. Boulder, CO, Geological Society of America, Inc. GSA Special Paper: 41-55.

Kutzbach, J. E. a. G., R. G. (1989). "Pangean climates: Megamonsoons of the Megacontinent." *Journal of Geophysical Research* **94(D3)**: 3341-3357.

Last, W. m. (1990). "Lacustrine dolomite - an overview of modern, Holocene, and Pleistocene occurrences." *Earth Science Review* **27**: 221-263.

Lewandowski, J. (1988): Tonminerale im Keuper zwischen Osnabrück und Helmstedt. *N. Jb. Geol. Paläont. Abh.* **176**, 2, 157-185. Stuttgart.

Li, H.-C. a. K., T.-L. (1997). "d13C-d18O covariance as a paleohydrological indicator for closed-basin lakes." *Paleogeography, paleoclimatology, Paleoecology* **133**: 69-80.

Lomb, N. R., (1976). Least-squares frequency analysis of unequally spaced data. *Astrophysics and Space Science*, 39: 447-462.

Lutz, M. (2005): Leitflächen (Allo-)Stratigraphie und ihre Anwendung im Keuper. In: *Deutsche Stratigraphische Kommission (Hrsg.)*, 2005: Stratigraphie von Deutschland IV - Keuper. Mit Beiträgen von Beutler, G., Dittrich, D., Dockter, J., Ernst, R., Etzold, A., Farrenschon, J., Freudenberger, W., Heunisch, C., Kelber, K.-P., Knapp, G., Lutz, M., Nitsch, E., Oppermann, K., Schubert, J., Schulz, E., Schweizer, V., Seegis, D., Tessin, R. & Vath, U.-- Courier Forschungsinstitut Senckenberg 253:296 S., 64 Abb., 50 Tab., 2 Taf.; Frankfurt am Main.

Milankovitch, M. M. (1941): Kanon der Erdbestrahlung. Beograd. Königlich Serbische Akademie, 484 pp.

Müller, S., (1955). Terrestrische Kalke im Stubensandstein (Mittlerer Keuper) Nordwürttembergs im Vergleich mit rezenten Bildungen. *Jh. geol. Landesamt Baden-Württemberg*, 1: 217-232.

Naumann, E. (1911). "Beitrag zur Gliederung des Mittleren Keupers in Thüringen." *Jahrbuch der Preußischen Geologischen Landesanstalt* **28(3)**: 549-580.

Nitsch, E. (1996): Fazies; Diagenese und Stratigraphie der Grabfeld Gruppe Süddeutschlands (Keuper, Trias). 304p. PhD Thesis. Universität Köln.

Nitsch, E. (2005a): Zyklusstratigraphie des Keupers. In: *Deutsche Stratigraphische Kommission (Hrsg.)*, 2005: Stratigraphie von Deutschland IV - Keuper. Mit Beiträgen von Beutler, G., Dittrich, D., Dockter, J., Ernst, R., Etzold, A., Farrenschon, J., Freudenberger, W., Heunisch, C., Kelber, K.-P., Knapp, G., Lutz, M., Nitsch, E., Oppermann, K., Schubert, J., Schulz, E., Schweizer, V., Seegis, D., Tessin, R. & Nitsch, E.

- Courier Forschungsinstitut Senckenberg 253:296 S., 64 Abb., 50 Tab., 2 Taf.; Frankfurt am Main.
- Nitsch, E. (2005b): Paläoböden im süddeutschen Keuper. Jber. Mitt. oberrhein. geol. Ver., N.F. **87**, 135-176, Stuttgart.
- Oldfield, F. (1999): The rock magnetic identification of magnetic mineral and grain size assemblages. In: Walden, J., Oldfield, F. and Smith, J. P. (Eds.). Environmental Magnetism: a practical guide. Technical Guide, No. 6. Quaternary Research association, London. 98-112.
- Olsen, P. E. and Kent, D. V., 1996. Milankovitch climate forcing in the tropics of Pangea during the Late Triassic. *Palaeogeography, Palaeoclimatology, Palaeoecology*, 122(1-4): 1-26.
- Parrish, J. T. (1993). "Climate of the supercontinent Pangea." *The Journal of Geology* **101**: 215-233.
- Peterson, M. N. A. a. V. D. B., C. C. (1965). "Chert: modern inorganic deposition in a carbonate-precipitating locality." *Science* **149** (1501-1503).
- Pimentel, N. L., Wright, V. P. and Azevedo, T. M., (1996). Distinguishing early groundwater alteration effects from pedogenesis in ancient alluvial basins: examples from the Palaeogene of southern Portugal. *Sedimentary Geology*, 105: 1-10.
- Press, W. H., Teukolsky, S. A., Vetterling, W. T. and Flannery, B. P., 1992. *Numerical Recipes in FORTRAN, The Art of Scientific Computing*. Cambridge University Press, Cambridge, New York, Melbourne, 963 pp.
- Rachold, V. E. (1994). *Geochemie der Unterkreide Nordwestdeutschlands: Zyklen und "Events"*. Göttingen, Georg-August-Universität: 94 pp.
- Reinhardt, L., (1994). *Sedimentologie des Stubensandsteins im südlichen Schwäbischen Wald (Teil I). Kartierung nördlich von Unterjesingen (GK 7419) Blatt Herrenberg SE (Teil II)*. unpublished Diploma Thesis Thesis, Eberhard-Karls-Universität, Tübingen, 70+26 pp.
- Reinhardt, L. a. R., W. (1998). The strati-chem record of playa cycles: implications for paleo-climate control (Triassic, Middle Keuper, S-Germany). 15th International Sedimentological Congress. Abstracts. A. M. G. D. C. a. J. S. S. J. C. Canaveras. Alicante, Spain, Publicaciones de la Universidad de Alicante: 653-654.
- Reinhardt, L. & Ricken, W. (2000a). Climate cycles documented in a playa system: comparison of geochemical signatures derived from subbasins (Triassic, Middle Keuper, German Basin). *Zbl. Geol. Paläont. Teil I* 1999 Heft 3-4, p. 315-340; Stuttgart.
- Reinhardt, L. & Ricken, W. (2000b). The Stratigraphic and Geochemical Record of Playa Cycles: Monitoring a Pangaeen Monsoon-like System (Triassic, Middle Keuper, S. Germany). *Palaeogeogr., Palaeoclimatol., Palaeoecol.*, Vol. 161 (1-2), 205-227, Amsterdam.

- Reinhardt, L. (2002). Dynamic stratigraphy and geochemistry of the Steinmergel-Keuper playa system: a record of Pangaeon megamonsoon cyclicity (Triassic, Middle Keuper, Southern Germany). Geologisches Institut Köln. Köln, Universität Köln: 174.
- Reuning, L. (2004): The Origin of Sub-Milankovitch Cycles in Early Pliocene Carbonate Platform Sediment: Bahamas vs. Maldives. PhD Thesis. Christian-Albrecht Universität. Kiel. 114p.
- Lars Reuning, John J. G. Reijmer, Christian Betzler, Axel Timmermann and Silke Steph (2006): Sub-Milankovitch cycles in periplatform carbonates from the early Pliocene Great Bahama Bank. *Paleoceanography*, Vol. 21
- Richter, D. K., (1985a): Composition and genesis of the evaporite- and the dolcrete-playa dolomites in the middle Keuper near Coburg (NE Bavaria). *Neues Jahrbuch für Geologie und Paläontologie, Abhandlungen*, 170: 87-128.
- Richter, D. K., (1985b): Die Dolomite der Evaporit- und der Dolcrete-Playasequenz im mittleren Keuper bei Coburg (NE-Bayern). *Neues Jahrbuch Geologisch Paläontologische Abhandlungen*, 170(1): 87-128.
- Röhling, H.-G., Heunisch, C.: [Klimaentwicklung in der PermoTrias](http://www.bgr.de/bt_klima/index.html). [http://www.bgr.de/bt\\_klima/index.html](http://www.bgr.de/bt_klima/index.html).
- Rosen, M. R. (1994): The importance of Groundwater in Playas: A Review of Playa Classifications and the Sedimentology and Hydrology of Playas. In: Rosen, M. R. (Ed.): *Plaeoclimate and Basin Evolution of Playa Systems..* Boulder, Colorado, Geological Society of America Special Paper 289. 1-18.
- Rosenbaum, J. a. S., S. M. F. (1986). "An isotopic study of siderites, dolomites and ankerites at high temperatures." *Geochimica et Cosmochimica Acta* **50**: 1147-1150.
- Rutherford, S. and D'Hondt, S. (2000): Early Onset and tropical forcing of 100, 000-year Pleistocene glacial cycles. *Nature*, **408**:72-75.
- Scargle, J. D., 1982. Studies in astronomical time series analysis. II. Statistical aspects of spectral analysis of unevenly spaced data. *The Astrophysical Journal*, 263: 835-853.
- Scargle, J. D., 1989. Studies in astronomical time series analysis. III. Fourier transforms, autocorrelation functions, and cross-correlation functions of unevenly spaced data. *The Astrophysical Journal*, 343: 133 874-887.
- Schaaf, M. (1995). Digital Sediment Color Analysis. PhD Thesis. Ruhr Universität Bochum, 243p.
- Schauer, M. (1994). Diplomkartierung. Tübingen, University of Tübingen.
- Schinle, I. (1979): Tonmineralogische Untersuchungen an Keupersedimenten. – Dipl. – Arb. Univ. Stuttgart, 59p.

Schlenker, B. (1971): Petrographische Untersuchung am Gipskeuper und Lettenkeuper von Stuttgart. – Oberrhein. Geol. Abh. 20, 69-102.

Schüle, F. (1974). Petrographische Untersuchungen an des Bunten Mergeln des Mittleren Keupers. Tübingen, Eberhard-Karls-Universität: 81 pp.

Schünke, M. (1984). "Die Gesteinsfarben im Mittleren Keuper von Südwestdeutschland." Arbeiten aus dem Institut für Geologie und Paläontologie der Universität Stuttgart **N. F. 79**: 55-131.

Schulz, E. (1996). "Eine Mikroflora aus dem Steinmergelkeuper vom SW-Hang der Wachsenburg bei Gotha (Thüringen)." Neues Jahrbuch Geologisch Paläontologische Abhandlungen **200(1/2)**: 75-86.

Schwertmann, U. (1976): Die Verwitterung mafischer Chlorite. – Z. Pflanzenernähr. Bodenk. 1976, 27-36.

Scotese, C. R. (2001): Atlas of Earth History, PALEOMAP Project, Arlington, Texas, 52 pp.

Seegis, D. (1997). Die Lehrbergschichten im Mittleren Keuper von Süddeutschland - Stratigraphie, Petrographie, Paläontologie, Genese. Stuttgart, University of Stuttgart: 335 pp.

Seegis, D. (2005): Tetrapoden. In: *Deutsche Stratigraphische Kommission (Hrsg.)*, 2005: Stratigraphie von Deutschland IV - Keuper. Mit Beiträgen von Beutler, G., Dittrich, D., Dockter, J., Ernst, R., Etzold, A., Farrenschon, J., Freudenberger, W., Heunisch, C., Kelber, K.-P., Knapp, G., Lutz, M., Nitsch, E., Oppermann, K., Schubert, J., Schulz, E., Schweizer, V., Seegis, D., Tessin, R. & Vath, U.-- Courier Forschungsinstitut Senckenberg 253:296 S., 64 Abb., 50 Tab., 2 Taf.; Frankfurt am Main.

Seegis, D. (2005): Fische. In: *Deutsche Stratigraphische Kommission (Hrsg.)*, 2005: Stratigraphie von Deutschland IV - Keuper. Mit Beiträgen von Beutler, G., Dittrich, D., Dockter, J., Ernst, R., Etzold, A., Farrenschon, J., Freudenberger, W., Heunisch, C., Kelber, K.-P., Knapp, G., Lutz, M., Nitsch, E., Oppermann, K., Schubert, J., Schulz, E., Schweizer, V., Seegis, D., Tessin, R. & Vath, U.-- Courier Forschungsinstitut Senckenberg 253:296 S., 64 Abb., 50 Tab., 2 Taf.; Frankfurt am Main.

Seegis, D. (2005): Muscheln und weitere Invertebraten. In: *Deutsche Stratigraphische Kommission (Hrsg.)*, 2005: Stratigraphie von Deutschland IV - Keuper. Mit Beiträgen von Beutler, G., Dittrich, D., Dockter, J., Ernst, R., Etzold, A., Farrenschon, J., Freudenberger, W., Heunisch, C., Kelber, K.-P., Knapp, G., Lutz, M., Nitsch, E., Oppermann, K., Schubert, J., Schulz, E., Schweizer, V., Seegis, D., Tessin, R. & Vath, U.-- Courier Forschungsinstitut Senckenberg 253:296 S., 64 Abb., 50 Tab., 2 Taf.; Frankfurt am Main.

Sandford, W. E., and Wood, W. W. (1991): Brine evolution and mineral deposition in hydrologically open evaporite basins. American Journal of Science, v. 291, p. 687-710.

- Seidel, G. (1995). Geologie von Thüringen. Stuttgart, E. Schweizerbart'sche Verlagsbuchhandlung (Nägele u. Obermiller).
- Sengerling, K. (1979): Tonmineralogische Untersuchungen an Keupersedimenten (Bunte Mergel) von einem Aufschluß westlich Welzheim. – Dipl. Arb. Univ. Stuttgart. 40p.
- Srodón, J. & Eberl, D. D. (1984): Illite. In: *Reviews in Mineralogy. Micas* (Ed. Bailey), 495-544. Mineral. Society of America, Publ. 13, Chelsea, Michigan.
- Talbot, M. R. (1990). "A review of the palaeohydrological interpretation of carbon and oxygen isotopic ratios in primary lacustrine carbonates." *Chemical Geology* **80**: 261-279.
- Talbot, M. R., Holm, K. and Williams, M. A. J. (1994). "Sedimentation in low-gradient desert margin systems: a comparison of the Late Triassic of northwest Somerset (England) and the late Quaternary of east-central Australia." *Geological Society of America Special Paper* **289**: 97-117.
- Tougiannidis, N. (2004): Geochemische, Spektrophotometrische und Stratigraphische Untersuchung in Pedogene Folgen des Steinmeregglekeupers (obere Trias) im Thüringer Becken (unpub. Master Thesis). Albert Magnus Universität Köln.
- Thomas, D. S. G., 1997. Arid environments: their nature and extent. In: D. S. G. Thomas (Editor), *Arid Zone Geomorphology (Process, Form and Change in Drylands)*. John Wiley & Sons Ltd., Chichester, pp. 3-12.
- Trauth, M. (2005): *Praktische Statistik und Numerische Methoden. Kompaktkurs für Geowissenschaftler*. Universität Potsdam.
- Tuenter, E. Weber, S. L., Hilgen, F. J., Lourens, L. J. (2003): The response of the African summer monsoon to remote and local forcing due to precession and obliquity. *Global and Planetary Change* **36**, 219-235.
- Van Houten, F. B. (1962): Cyclic sedimentation and the origin of analcime-rich Upper Triassic Lockatong Formation, West-Central New Jersey and adjacent Pennsylvania. *Amer. Jour. Sci.*, **260**, pp. 561-576.
- Vath, U.-- Courier Forschungsinstitut Senckenberg 253:296 S., 64 Abb., 50 Tab., 2 Taf.; Frankfurt am Main.
- Veizer, J. N., Bruckschen, P., Pawellek, F., Diener, A., Podlaha, O. G., Carden, G. A. F., Jasper, T., Korte, C., Strauss, H., Azmy, K. and Ala, D., 1997. Oxygen isotope evolution of Phanerozoic seawater. *Palaeogeography, Palaeoclimatology, Palaeoecology*, **132**: 159-172.
- Velde, B. (1995): *Origin and Mineralogy of Clays*. Springer
- Walter, S. (2002): *Mächtigkeitenuntersuchungen des Steinmergelkeupers im Bereich der Allertal Struktur (Blatt Helmstedt)*. Landesamt für Geologie und Bergwesen, Sachsen Anhalt.

- 
- Warren, J. K. (1989). *Evaporite Sedimentology*. New Jersey, Prentice Hall.
- Warren, J. K. (1999). *Evaporites, Their Evolution and Economics*. Berlin, Blackwell Sciences.
- Wedepohl, K. H. (1971). Environmental influences on the chemical composition of shales and clays. *Physics and chemistry of the Earth*. F. P. L. H. Ahrens, S. K. Run-corn and H. C. Urey. Oxford, Pergamon: 305-333.
- Wedepohl, K. H. (1991). The composition of the upper earth's crust and the natural cycles of selected metals. *Metals in natural raw materials. Natural resources. Metals and their compounds in the environment*. E. Merian. Weinheim, VCH-Verlagsgesellschaft: 3-17.
- Wood, W. W. a. S., W. E. (1990). "Ground-water control of evaporite deposition." *Economic Geology* **85**: 1226-1235.
- Wright, D. T. (1999). "The role of sulfate-reducing bacteria and cyanobacteria in dolomite formation in distal ephemeral lakes of the Coorong region, South Australia." *Sedimentary Geology* **126(1-4)**: 147-157.
- Ziegler, P. A., 1990. *Geological Atlas of Western and Central Europe*. Shell Internationale Petroleum Maatschappij, The Hague.

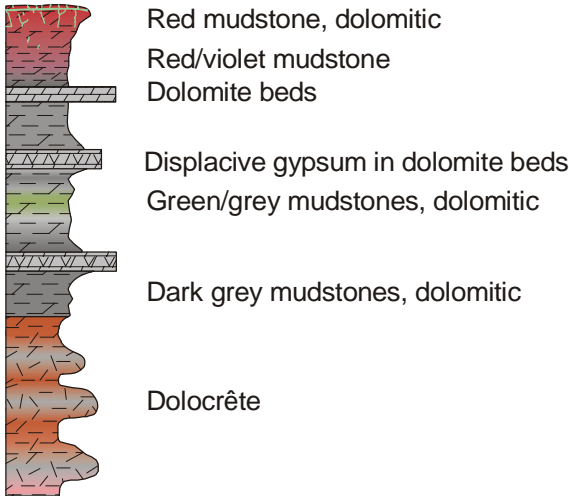
## Appendix

SiO <sub>2</sub> (%)	58.90	Si (%)	27.49	Si /Al	3.1094
TiO <sub>2</sub> (%)	0.78	Ti (%)	0.47	Ti /Al	0.0529
Al <sub>2</sub> O <sub>3</sub> (%)	16.70	Al (%)	8.84	Al /Al	1.0001
MnO (%)	0.09	Mn (%)	0.07	Mn /Al	0.0079
Fe <sub>2</sub> O <sub>3</sub> (%)	6.50	Fe (%)	4.55	Fe /Al	0.5147
MgO (%)	2.60	Mg (%)	1.56	Mg /Al	0.1765
CaO (%)	2.20	Ca (%)	1.57	Ca /Al	0.1778
Na <sub>2</sub> O (%)	1.60	Na (%)	1.19	Na /Al	0.1343
K <sub>2</sub> O (%)	3.60	K (%)	2.99	K /Al	0.3379
P <sub>2</sub> O <sub>5</sub> (%)	0.16	P (%)	0.07	P /Al	0.0079
S (ppm)	2400.00	S (ppm)	2400.00	S /Al	271.4932
Ba (ppm)	580.00	Ba (ppm)	580.00	Ba /Al	65.6109
Ni (ppm)	68.00	Ni (ppm)	68.00	Ni /Al	7.6923
Co (ppm)	19.00	Co (ppm)	19.00	Co /Al	2.1493
Cr (ppm)	90.00	Cr (ppm)	90.00	Cr /Al	10.1810
V (ppm)	130.00	V (ppm)	130.00	V /Al	14.7059
Sr (ppm)	300.00	Sr (ppm)	300.00	Sr /Al	33.9367
Sc (ppm)	13.00	Sc (ppm)	13.00	Sc /Al	1.4706
Cu (ppm)	45.00	Cu (ppm)	45.00	Cu /Al	5.0905
Zn (ppm)	95.00	Zn (ppm)	95.00	Zn /Al	10.7466
Ga (ppm)	19.00	Ga (ppm)	19.00	Ga /Al	2.1493
As (ppm)	10.00	As (ppm)	10.00	As /Al	1.1312
Rb (ppm)	140.00	Rb (ppm)	140.00	Rb /Al	15.8371
Y (ppm)	41.00	Y (ppm)	41.00	Y /Al	4.6380
Zr (ppm)	160.00	Zr (ppm)	160.00	Zr /Al	18.0995
Nb (ppm)	18.00	Nb (ppm)	18.00	Nb /Al	2.0362
Mo (ppm)	2.60	Mo (ppm)	2.60	Mo /Al	0.2941
Cs (ppm)	5.50	Cs (ppm)	5.50	Cs /Al	0.6222
La (ppm)	40.00	La (ppm)	40.00	La /Al	4.5249
Ce (ppm)	95.00	Ce (ppm)	95.00	Ce /Al	0.7466
Nd (ppm)	18.00	Nd (ppm)	18.00	Nd /Al	2.0362
W (ppm)	1.80	W (ppm)	1.80	W /Al	0.2036
Pb (ppm)	20.00	Pb (ppm)	20.00	Pb /Al	2.2624
Th (ppm)	12.00	Th (ppm)	12.00	Th /Al	1.3575
U (ppm)	3.70	U (ppm)	3.70	U /Al	0.4186

Tab. 7: Average composition of shale. From REINHARDT 2000, after WEDEPOHL 1971, 1991.



**Signatures used:**



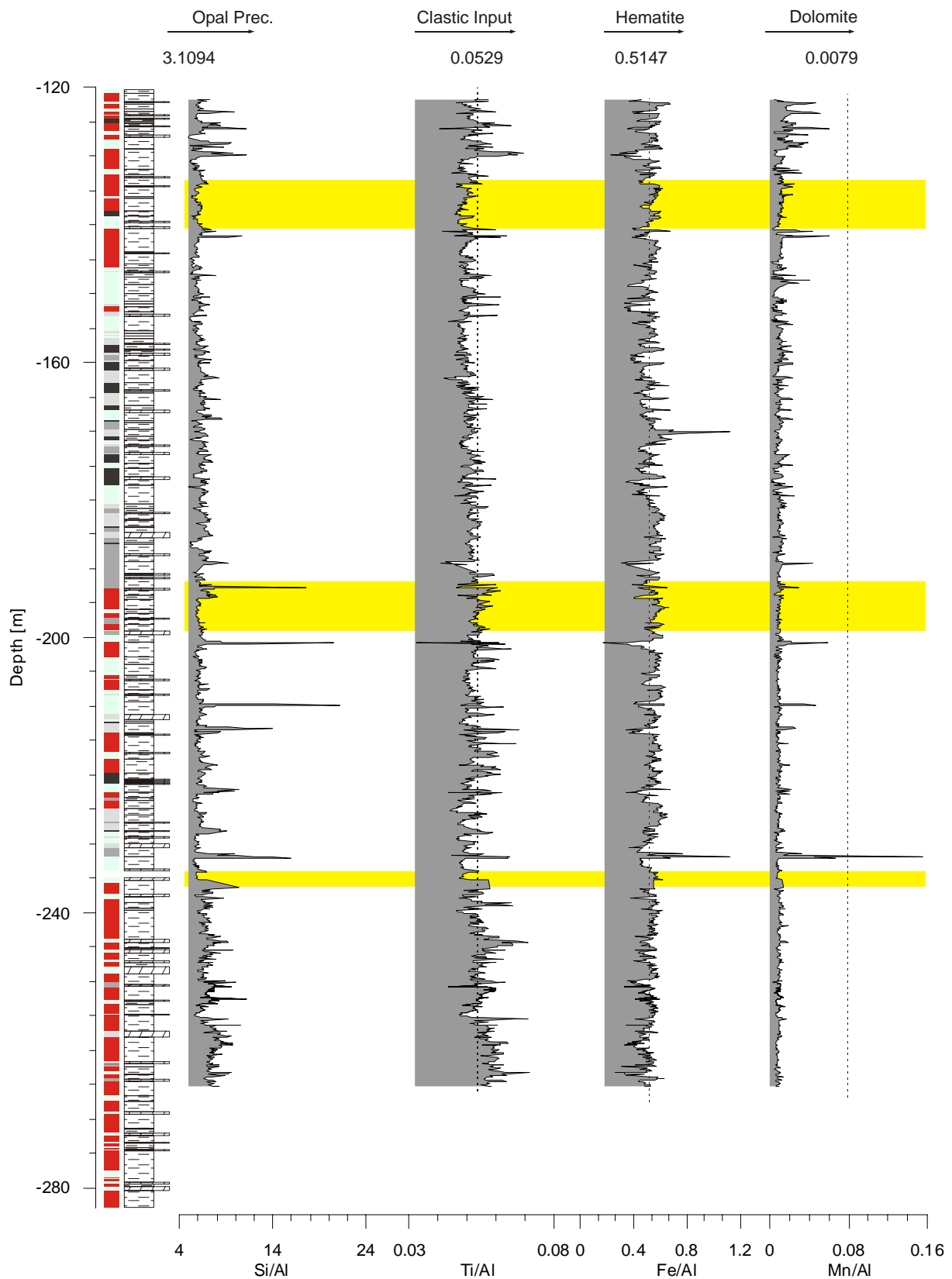


Fig. 129: Long term trends of the element /Al ratios of core MorsDp52a. XRF data by courtesy of H.-G. Röhling NLFb, Hannover.

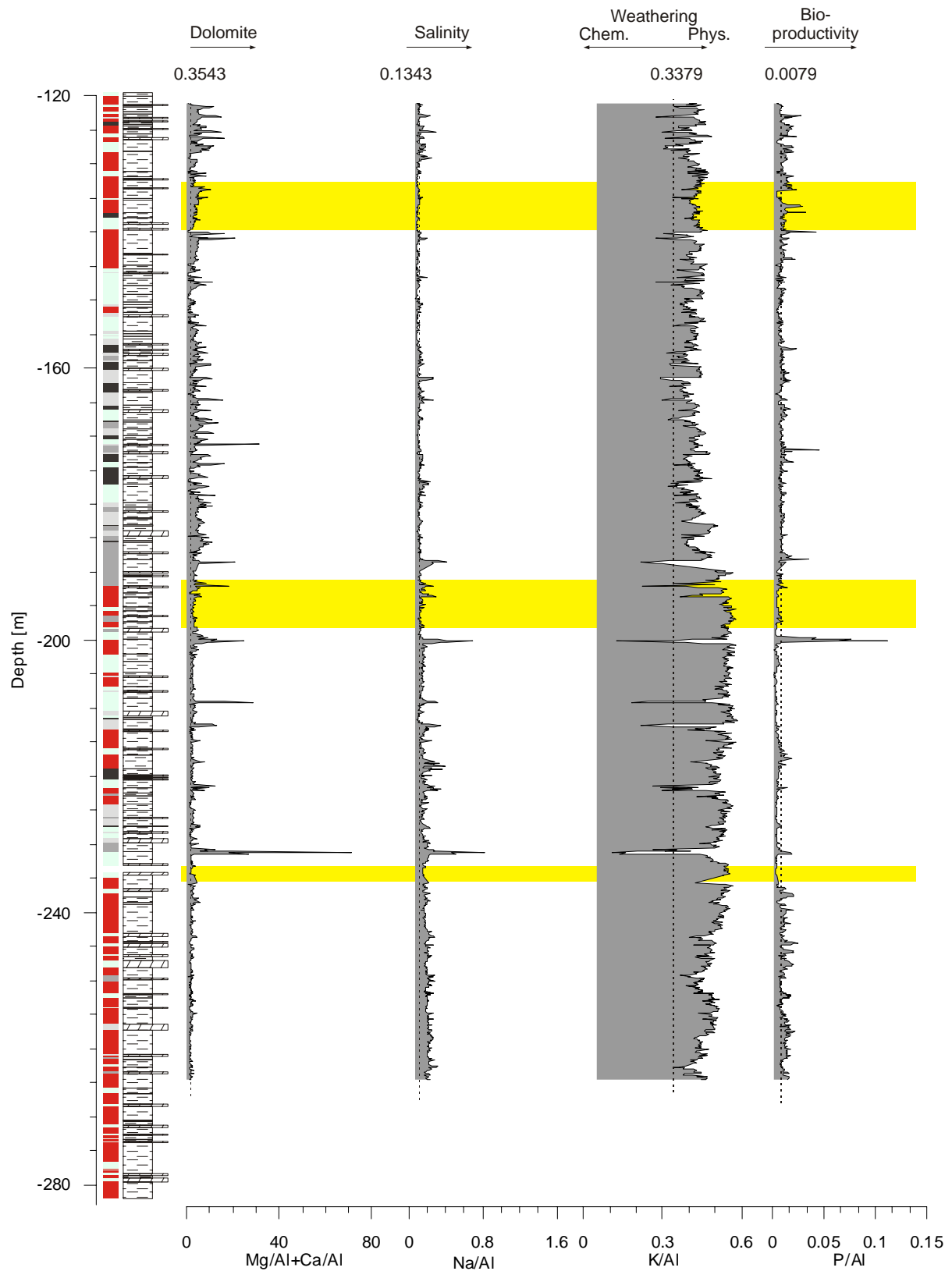


Fig. 129 continued: Long term trends of the element /Al ratios of core MorsDp52a. XRF data by courtesy of H.-G. Röhling NfB, Hannover.

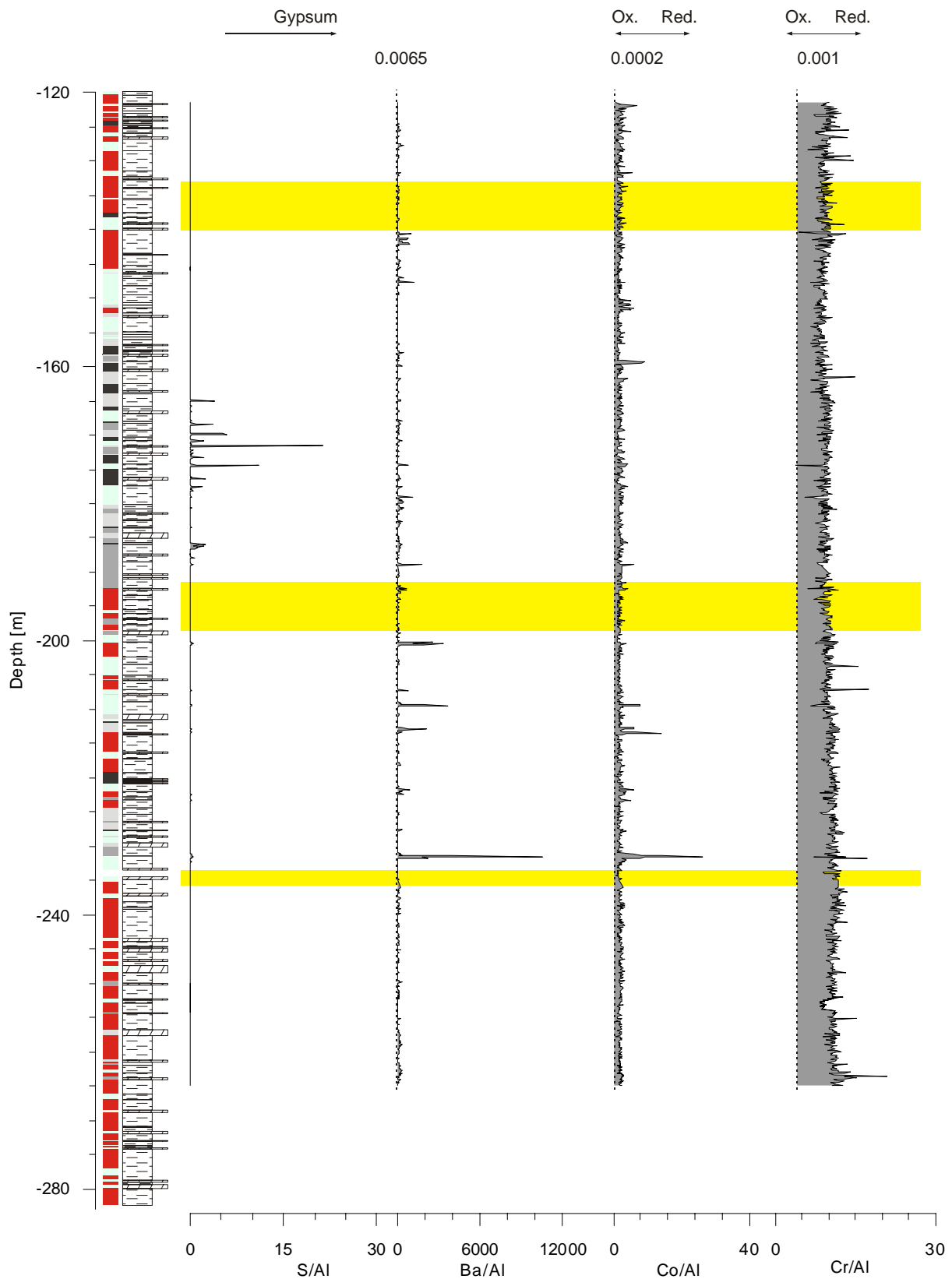


Fig. 129 continued: Long term trends of the element /Al ratios of core MorsDp52a. XRF data by courtesy of H.-G. Röhling NLFb, Hannover.

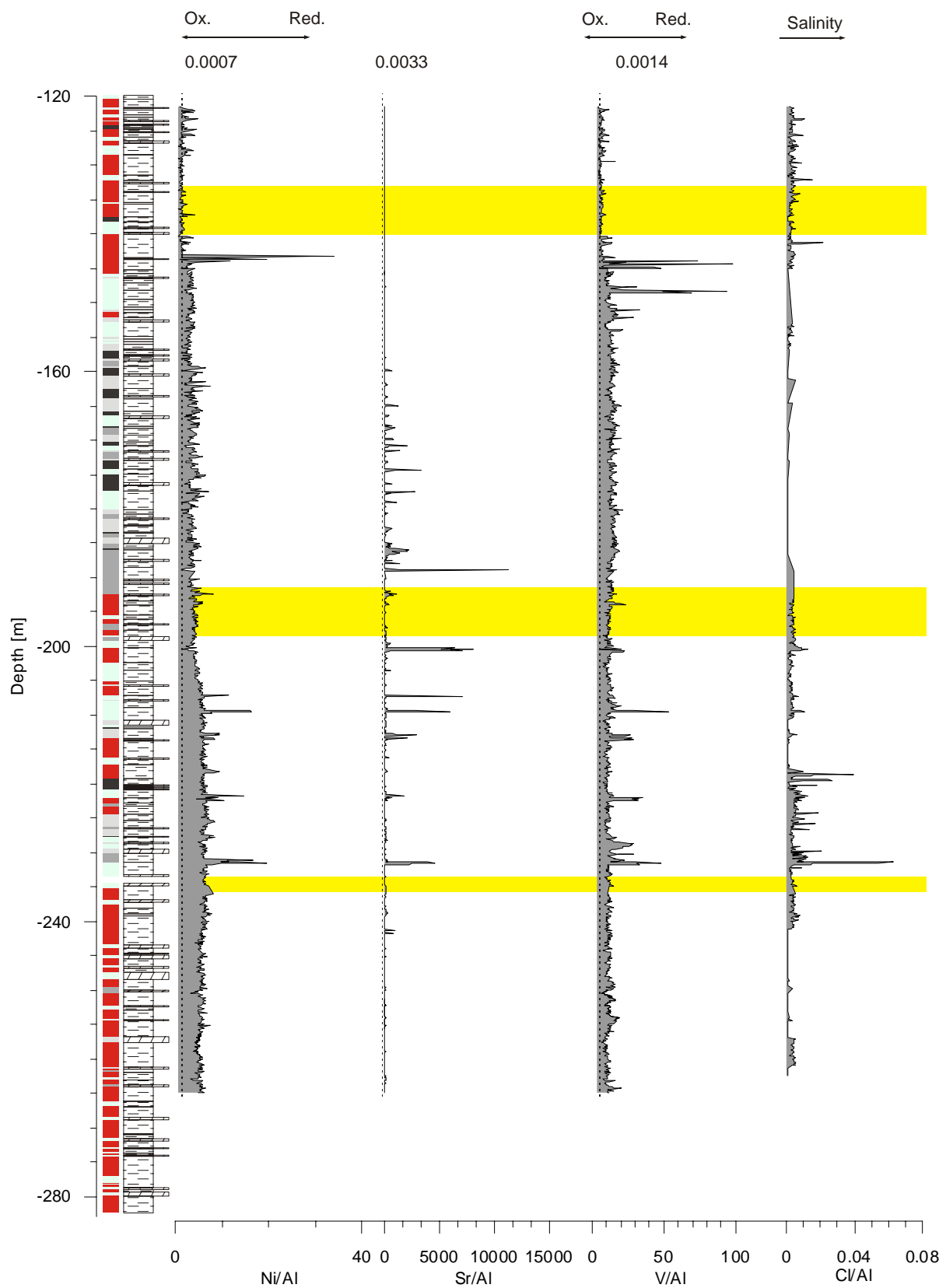


Fig. 129 continued: Long term trends of the element /Al ratios of core MorsDp52a. XRF data by courtesy of H.-G. Röhlting NLFb, Hannover.

## Danksagung

Diese Arbeit wäre ohne die Hilfe von all den Menschen, die mir stets geholfen haben nicht möglich gewesen. Bei allen möchte ich mich von Herzen bedanken.

Bedanken möchte ich mich bei Werner Ricken für die äußerst faszinierende Arbeit, die er mir angeboten hat. Er stand stets für Diskussionen und mit guten Ratschlägen zur Seite. Herr Prof. Klaus Krumsiek war so nett sich als Zweitprüfer zur Verfügung zu stellen. Die DFG war so freundlich dieses Projekt zu finanzieren.

Ganz besonders möchte ich mich bei meiner Frau für ihre großartige Unterstützung bedanken. Sie hat mir immer beigestanden und stets den Rücken frei gehalten. Ein großer Dank geht auch an meine Mutter, meine Geschwister sowie meinen Schwiegereltern, die mich alle stets moralisch unterstützt haben.

Ohne die Hilfe von Nikolaos Tougiannidis und Knut Arends wären die Arbeiten an den Kernen sowie Aufschlüssen nicht so einfach gewesen. Auch ihnen ein herzlichen Dank. Dank auch an Andreas Holzapfel, der mir bei so mancher Arbeit geholfen hat. Bedanken möchte ich mich bei Lutz Reinhardt und Ulrich Hambach. Die sehr kritischen Fragen und Anmerkungen von Lutz Reinhardt waren und sind mir eine wertvolle Hilfe. Ulrich Hambach hat freundlicherweise die Suszeptibilitätsmessungen durchgeführt und war stets zu Diskussionen bereit. Eine weitere wertvolle Hilfe war Uwe Kasper von der Universität Köln, der mich sehr kompetent bei chemischen Fragestellungen beraten hat. Ein ganz herzlicher Dank geht an Michael Weber, der mit seinen Tipps und kritischen Fragen stets ein willkommener Diskussionspartner war. Ein großer Dank geht auch an Gerhard Beutler, der mir mit seiner liebenswürdigen Art immer eine große Hilfe war und stets die Zeit für Diskussionen hatte. Heinz-Gerd Röhling vom NfB war so liebenswürdig mir einen riesigen RFA – Datensatz zur Verfügung zu stellen. Bei Herr Etzold vom LGRB Baden Württemberg bedanke ich mich für den Bohrkern, den er mir für Untersuchungen zur Verfügung gestellt hat. Bei Edgar Nitsch bedanke ich mich für die Tipps, die ich von ihm auf der Keuper Tagung 2003 in Tübingen erhalten habe. Des Weiteren bedanke ich mich beim Bundesamt für Strahlenschutz für die Erlaubnis am Bohrkern MorsDp52a Arbeiten durchführen zu dürfen. Bei Rainer Petschick vom Senckenberg Institut bedanke ich mich für die Tonmineralogie und bei Michael Joachimski von der Universität Erlangen für die Isotopenmessungen. Bei Herr Euler von der Universität Bonn bedanke ich mich für die röntgendiffraktometrische Messungen. Bedanken möchte ich mich auch bei Jens Hornung, Oliver Kempf sowie Rainer Gaupp, die mir auf verschiedenen Sediment – Tagungen nützliche Tipps gaben.

Zuletzt möchte ich mich herzlich bei allen Mitarbeitern/innen des Institutes für Geologie und Mineralogie der Universität Köln sowie bei Heiko Freitag und Markus Hirschfeld für die freundliche Aufnahme und Unterstützung bedanken.

## Curriculum Vitae

### Persönliche Daten:

Name: Thorsten Vollmer  
 Geburtsdatum: 18.05.1969  
 Geburtsort: Leichlingen  
 Nationalität: Deutsch  
 Status: verheiratet  
 Kinder: 1

### Schulausbildung:

1979 – 1987: Wohnhaft in Puerto Ordaz, Venezuela, Besuch einer einheimischen Schule  
 1987 – 1988: Besuch der berufsbildenden Schule Bitburg. Fachrichtung: Elektrotechnik  
 1988 – 1992: Besuch des staatlichen Eifelgymnasiums Neuerburg.

### Dienst:

1992 – 1993: Militärdienst

### Studium:

1993 – 1995: Studium der theoretischen Physik an der TU München  
 1995 – 1997: Studium der Geologie an der TU München.  
 Vordiplom: SS 1997  
 1997 – 1999: Studium der Geowissenschaften an der Université de Montpellier, Frankreich  
 Abschlüsse: 1998: Licence, Science de la Terre  
 1999 : Maîtrise, Science de la Terre  
 Thema der Abschlussarbeit: Etude d'un corps gréseux fluvial dans le Trias de Lodève  
 1999 – 2002 : Studium der Geologie an der Universität Göttingen  
 Abschluss: Februar 2002: Diplom in Geologie/Paläontologie  
 Thema der Diplomarbeit: „Geochemische Untersuchungen an oberdevonischen Karbonat – Seeps des McWhae Ridges, Canning Basin, Western Australia“  
 Oktober 2002 –  
 Oktober 2005: Wiss. Ang. an der Universität Köln im Rahmen einer Promotion bei Prof. Werner Ricken. Titel der Dissertation: „Paleoclimatology of Upper Triassic Playa Cycles: New Insights into Orbital Controlling Factors of a Pangaeon Monsoonal System“.

**Sprachen:**

Deutsch (Muttersprache)  
Spanisch (fließend)  
Französisch (fließend)  
Englisch (sehr gut)

**Hobbies:**

Tanzen (Standard und Latein), Bergwandern, Reisen



# Erklärung

"Ich versichere, dass ich die von mir vorgelegte Dissertation selbständig angefertigt, die benutzten Quellen und Hilfsmittel vollständig angegeben und die Stellen der Arbeit - einschließlich Tabellen, Karten und Abbildungen -, die anderen Werken im Wortlaut oder dem Sinn nach entnommen sind, in jedem Einzelfall als Entlehnung kenntlich gemacht habe; dass diese Dissertation noch keiner anderen Fakultät oder Universität zur Prüfung vorgelegen hat; dass sie - abgesehen von unten angegebenen Teilpublikationen - noch nicht veröffentlicht worden ist sowie, dass ich eine solche Veröffentlichung vor Abschluss des Promotionsverfahrens nicht vornehmen werde. Die Bestimmungen dieser Promotionsordnung sind mir bekannt. Die von mir vorgelegte Dissertation ist von Prof. Dr. Werner Ricken betreut worden."